



National Library  
of Canada

Acquisitions and  
Bibliographic Services Branch

395 Wellington Street  
Ottawa, Ontario  
K1A 0N4

Bibliothèque nationale  
du Canada

Direction des acquisitions et  
des services bibliographiques

395 rue Wellington  
Ottawa (Ontario)  
K1A 0N4

## NOTICE

The quality of this microform is heavily dependent upon the quality of the original thesis submitted for microfilming. Every effort has been made to ensure the highest quality of reproduction possible.

If pages are missing, contact the university which granted the degree.

Some pages may have indistinct print especially if the original pages were typed with a poor typewriter ribbon or if the university sent us an inferior photocopy.

Reproduction in full or in part of this microform is governed by the Canadian Copyright Act, R.S.C. 1970, c. C-30, and subsequent amendments.

## AVIS

La qualité de cette microforme dépend grandement de la qualité de la thèse soumise au microfilmage. Nous avons tout fait pour assurer une qualité supérieure de reproduction.

S'il manque des pages, veuillez communiquer avec l'université qui a conféré le grade.

La qualité d'impression de certaines pages peut laisser à désirer, surtout si les pages originales ont été dactylographiées à l'aide d'un ruban usé ou si l'université nous a fait parvenir une photocopie de qualité inférieure.

La reproduction, même partielle, de cette microforme est soumise à la Loi canadienne sur le droit d'auteur, SRC 1970, c. C-30, et ses amendements subséquents.

Canada

INTERFACIAL SLIP OF A QUARTZ SENSOR IN LIQUID

FRANCESCO FERRANTE

A Thesis  
in  
The Department  
of  
Physics

Presented in Partial Fulfilment of the Requirements  
for the Degree of Master of Science at  
Concordia University  
Montreal, Quebec, Canada

April 1993

© Francesco Ferrante, 1993



National Library  
of Canada

Bibliothèque nationale  
du Canada

Acquisitions and  
Bibliographic Services Branch

Direction des acquisitions et  
des services bibliographiques

395 Wellington Street  
Ottawa, Ontario  
K1A 0N4

395 rue Wellington  
Ottawa (Ontario)  
K1A 0N4

0-315-84669-0

0-315-84669-0

**The author has granted an irrevocable non-exclusive licence allowing the National Library of Canada to reproduce, loan, distribute or sell copies of his/her thesis by any means and in any form or format, making this thesis available to interested persons.**

**L'auteur a accordé une licence irrévocable et non exclusive permettant à la Bibliothèque nationale du Canada de reproduire, prêter, distribuer ou vendre des copies de sa thèse de quelque manière et sous quelque forme que ce soit pour mettre des exemplaires de cette thèse à la disposition des personnes intéressées.**

**The author retains ownership of the copyright in his/her thesis. Neither the thesis nor substantial extracts from it may be printed or otherwise reproduced without his/her permission.**

**L'auteur conserve la propriété du droit d'auteur qui protège sa thèse. Ni la thèse ni des extraits substantiels de celle-ci ne doivent être imprimés ou autrement reproduits sans son autorisation.**

ISBN 0-315-84669-0

**Canada**

## ABSTRACT

### Interfacial Slip of a Quartz Sensor in Liquid

Francesco Ferrante

The interfacial slip parameter is a complex-valued property of the interface between the solid surface of a quartz sensor and the liquid in contact with the sensor surface. It is introduced in the theory of the quartz-liquid system by generalizing the no-slip boundary condition. The interfacial slip parameter is defined as the displacement of a particle of liquid in contact with the sensor surface divided by the displacement of a particle on the surface of the sensor.

The theoretical expression for impedance of the sensor is derived in terms of the interfacial slip parameter. The impedance of the sensor is measured by the network analysis method for hydrophilic and hydrophobic surfaces in water-glycerol solutions. The experimental values of impedance are fitted to the theory by non-linear regression analysis to find the interfacial slip parameter. A mechanical model of interfacial slip is devised which explains the variation of the interfacial slip parameter with viscosity of the liquid. The results indicate that there is considerable slip in low-viscosity liquids, near the viscosity of water, and very little slip in liquids of high viscosity, near that of glycerol.

## ACKNOWLEDGEMENTS

I wish to thank my supervisor, Professor Arlin L. Kipling, for his guidance, patient help and constructive criticism in the course of the research and the preparation of this thesis.

Also, I would like to take this opportunity to thank Professor Michael Thompson, Director of the Chemical Sensors Group, Chemistry Department, University of Toronto, for his many helpful and stimulating discussions, and for his gracious hospitality during my visits to the University of Toronto.

My thanks is also extended to Mr. Mengsu Yang, Ph.D. graduate student in the Chemical Sensors Group, for his assistance in the experimental work which was done at the University of Toronto.

I greatly appreciate the help with graphics and wordprocessing by my good friend, Mario D'Amico.

Last but not least I would like to thank my parents, Antonnieta and Italo Ferrante, for their constant support, encouragement and prayers.

This work was part of the collaborative research project, A DNA Probe Biosensor Based on Acoustic Wave Transmission, conducted by Professors Michael Thompson and Arlin Kipling, and funded by an NSERC Strategic Grant, 1990-93. I received financial support from this grant which I gratefully acknowledge.

## CONTENTS

List of Figures . . . . .	viii
List of Tables . . . . .	xi
CHAPTER 1 INTRODUCTION . . . . .	1-1
CHAPTER 2 THEORY . . . . .	2-1
Introduction . . . . .	2-1
2.1 Elasticity . . . . .	2-2
2.2 Electromagnetism . . . . .	2-7
2.3 Piezoelectricity . . . . .	2-14
2.4 Fluid Mechanics . . . . .	2-30
2.5 Boundary Conditions of Solid-Liquid Model . . . . .	2-34
2.6 Solution of Solid-Liquid Model . . . . .	2-36
2.7 Impedance . . . . .	2-41
CHAPTER 3 EXPERIMENT . . . . .	3-1
Introduction . . . . .	3-1
3.1 Experimental Method . . . . .	3-2
3.1.1 Sensors and Liquid . . . . .	3-2
3.1.2 Experimental Arrangement . . . . .	3-3
3.2 Non-Linear Regression Analysis . . . . .	3-7
3.2.1 Statement of the Non-Linear Regression Analysis Problem . . . . .	3-7
3.2.2 Definition of Sum Of Squares Of Errors, SSE . . . . .	3-7
3.2.3 Condition for SSE to be a Minimum . . . . .	3-8
3.2.4 Definition of Normal Equations . . . . .	3-8
3.2.5 Example . . . . .	3-9
3.3 Fitting of Theory to Experiment in Air . . . . .	3-12
3.4 Fitting of Theory and Experiment in Liquid . . . . .	3-17

3.5	Interfacial Slip Parameter, $\alpha$ . . . . .	3-25
3.5.1	Plots of $\alpha$ . . . . .	3-25
3.5.2	Numerical Computation of the Real Part of $u_{(0)x}$ and $u_x$ . . . . .	3-25
3.5.3	Discussion of the Variation of $\alpha$ versus Low Values of $\nu$ . . . . .	3-26
3.5.4	Discussion of the Variation of $\alpha$ versus High Values of $\nu$ . . . . .	3-29
3.5.5	Variation of $\alpha$ with Mole Fraction, $M_f$ . . . . .	3-30
CHAPTER 4 MODEL . . . . .		4-1
Introduction . . . . .		4-1
4.1	Interfacial Slip Model . . . . .	4-1
4.1.1	Description of Model . . . . .	4-1
4.1.2	Statement of Problem . . . . .	4-3
4.1.3	Derivation of the Equations of Motion for the Interfacial Slip Model . . . . .	4-5
4.2	Numerical Solution of the Equations of Motion . . . . .	4-7
4.2.1	Description of Runge-Kutta's Method . . . . .	4-7
4.2.2	Numerical Solution of Interfacial Slip Model . . . . .	4-9
CHAPTER 5 CONCLUSIONS . . . . .		5-1
APPENDIX 1	Application Software . . . . .	A1-1
APPENDIX 2	Subscript Notation . . . . .	A2-1
APPENDIX 3	Solution of Boundary Value Problem, Macsyma Program ZIN.WP. . . . .	A3-1
APPENDIX 4	Non-linear Regression Analysis, Example of a Series RLC circuit, Mathcad Program DOC1.MCD. . . . .	A4-1
APPENDIX 5	Non-linear Regression Analysis of Sensor in Air, Mathcad Program DOC2.MCD. . . . .	A5-1
APPENDIX 6	Non-linear Regression Analysis of Sensor in Liquid, Mathcad Program DOC3.MCD. . . . .	A6-1
APPENDIX 7	Plots of Interfacial Slip Parameter, Mathcad Program DOC4.MCD. . . . .	A7-1

APPENDIX 8 Particle Displacement of Sensor in  
Liquid, Mathcad Program DOC5.MCD. . . . A8-1

APPENDIX 9 Numerical Solution of Interfacial Slip  
Model, Mathcad Program DOC6.MCD. . . . A9-1

References . . . . . R-1



## LIST OF FIGURES

Figure 2.1	Solid-liquid model showing quantities used to express the five boundary conditions, and showing in brackets the five properties of the solid, the two properties of the liquid and the one property of the interface. . . . .	2-34
Figure 2.2	Total free charge, $Q_f$ , found by surface integration of electric displacement, $D_i$ . . . . .	2-43
Figure 3.1	Sensor in liquid with (a) hydrophilic coating and (b) hydrophobic coating. . .	3-4
Figure 3.2	Experimental arrangement showing (a) the top and side views of the piezoelectric quartz sensor and (b) the sensor in liquid connected to the network analysis system. . . . .	3-5
Figure 3.3	Sum Of Squares Of Errors for a series RLC circuit. . . . .	3-32
Figure 3.4	Magnitude of impedance for a series RLC circuit. . . . .	3-33
Figure 3.5	Phase of impedance for a series RLC circuit. . . . .	3-34
Figure 3.6	Phase of impedance of the hydrophilic sensor in air. . . . .	3-35
Figure 3.7	Magnitude of impedance of the hydrophilic sensor in air. . . . .	3-36
Figure 3.8	Phase of impedance of the hydrophobic sensor in air. . . . .	3-37
Figure 3.9	Magnitude of impedance of the hydrophobic sensor in air. . . . .	3-38
Figure 3.10	Phase of impedance of the hydrophilic sensor in 0.1 molar water-glycerol solution. . . . .	3-39

Figure 3.11	Magnitude of impedance of the hydrophilic sensor in 0.1 molar water-glycerol solution. . . . .	3-40
Figure 3.12	Phase of impedance of the hydrophilic sensor in 0.6 molar water-glycerol solution. . . . .	3-41
Figure 3.13	Magnitude of impedance of the hydrophilic sensor in 0.6 molar water-glycerol solution. . . . .	3-42
Figure 3.14	Phase of impedance of the hydrophobic sensor in 0.1 molar water-glycerol solution. . . . .	3-43
Figure 3.15	Magnitude of impedance of the hydrophobic sensor in 0.1 molar water-glycerol solution. . . . .	3-44
Figure 3.16	Phase of impedance of the hydrophobic sensor in 0.6 molar water-glycerol solution. . . . .	3-45
Figure 3.17	Magnitude of impedance of the hydrophobic sensor in 0.6 molar water-glycerol solution. . . . .	3-46
Figure 3.18	Real part of interfacial slip parameter versus kinematic viscosity for the hydrophilic and hydrophobic sensor in liquid. . . . .	3-47
Figure 3.19	Imaginary part of interfacial slip parameter versus kinematic viscosity for the hydrophilic and hydrophobic sensor in liquid. . . . .	3-48
Figure 3.20	Magnitude of interfacial slip parameter versus kinematic viscosity for the hydrophilic and hydrophobic sensor in liquid. . . . .	3-49
Figure 3.21	Phase of interfacial slip parameter versus kinematic viscosity for the hydrophilic and hydrophobic sensor in liquid. . . . .	3-50
Figure 3.22	Real part of interfacial slip parameter versus mole fraction for the hydrophilic and hydrophobic sensor in liquid. . . .	3-51

Figure 3.23	Imaginary part of interfacial slip parameter versus mole fraction for the hydrophilic and hydrophobic sensor in liquid. . . . .	3-52
Figure 3.24	Magnitude of interfacial slip parameter versus mole fraction for the hydrophilic and hydrophobic sensor in liquid. . . . .	3-53
Figure 3.25	Phase of interfacial slip parameter versus mole fraction for the hydrophilic and hydrophobic sensor in liquid. . . . .	3-54
Figure 3.26	Solid and liquid particle displacement at the solid-liquid interface for the hydrophilic and hydrophobic sensor in liquid. . . . .	3-55
Figure 3.27	Maximum values of solid and liquid particle displacements at the solid-liquid interface for both the hydrophilic and hydrophobic sensor in liquid. . . . .	3-56
Figure 3.28	Kinematic viscosity versus mole fraction for water-glycerol solutions. . . . .	3-57
Figure 4.1	Mechanical model of interfacial slip showing masses, $m_1$ and $m_2$ , connected by a spring of force constant, $k$ . . . . .	4-4
Figure 4.2	Maximum displacement of mass $m_1$ versus the logarithm of the spring constant, $k$ , divided by the mass, $m_1$ , for the mechanical model of interfacial slip. The maximum displacement of mass $m_1$ is unity.. . . .	4-11

## LIST OF TABLES

Table 2.1	Equations of Piezoelectricity . . . . .	2-17
Table 2.2	Physical Quantities of Piezoelectricity . .	2-18
Table 2.3	Material Properties of Piezoelectricity . .	2-18
Table 2.4	Properties of Quartz . . . . .	2-27
Table 3.1	Summary of Results for $e$ , $\eta$ , $h$ , and $A$ . . .	3-16
Table 3.2	Values for $M_f$ , $\nu$ , and $\rho_1$ of Water-glycerol Solutions . . . . .	3-20
Table 3.3	Interfacial Slip Parameter, $\alpha$ , for Hydrophilic Sensor . . . . .	3-22
Table 3.4	Effective Surface Area, $A$ , for Hydrophilic Sensor . . . . .	3-23
Table 3.5	Interfacial Slip Parameter, $\alpha$ , for Hydrophobic Sensor . . . . .	3-24
Table 3.6	Effective Surface Area, $A$ , for Hydrophobic Sensor . . . . .	3-24
Table 4.1	Model and Interface . . . . .	4-3
Table A2.1	Examples of Tensors . . . . .	A2-3
Table A2.2	Examples of Notation . . . . .	A2-3

## CHAPTER 1

### INTRODUCTION

A piezoelectric quartz sensor is used to detect the presence of specific molecules in a gas or liquid. There are basically two types of quartz sensors, bulk acoustic wave (BAW) and surface acoustic wave (SAW) sensors. In this work only the BAW sensor is considered. The BAW sensor is essentially a thin plate of quartz with a very thin metal electrode on each surface of the quartz. This device is used in the communications field to control frequency, where it is called simply a quartz crystal. It is available commercially in the frequency range from about 2 to 50 MHz. Cady (1964) made major contributions to the development of quartz crystals. Bottom (1982) gives an elementary treatment of the theory of the quartz crystal.

The generic name for a device that is used for molecular recognition is a chemical sensor or biosensor. The name, biosensor, is used when the molecules to be detected are biomolecules, that is, carbon-based molecules found in living organisms. The BAW quartz sensor used for molecular recognition is an AT-cut quartz crystal. This particular cut of quartz operates in the transverse shear mode (TSM), meaning that the direction of vibration of the atoms of the quartz is transverse to the direction of propagation of the acoustic wave. In this mode the displacement of the atoms of quartz is

in the plane of the quartz plate and the wave travels in the direction normal to the plane of the plate.

The principle of operation of a chemical sensor or biosensor is simple. A molecule which reacts only with the molecule to be sensed is bound to the surface of the sensor. Then the sensor is immersed in a gas or liquid. If the molecule to be sensed is present in the gas or liquid, it will bind to the molecule on the surface of the sensor. As a consequence, the mass on the surface increases and the properties of the interface change. Electrical measurements are made to detect the changes on the surface.

The network analysis method developed by Kipling and Thompson (1990) is used to completely electrically characterize the BAW quartz sensor. This method can be used when the sensor is in a liquid of any viscosity. The network analysis method replaces the oscillator method which only partially characterizes a BAW quartz sensor and is limited to operation in liquids of low viscosity. A review article by Thompson, Kipling et al (1991) describes both the network analysis method and the oscillator method. The oscillator method is analyzed by Rajaković et al (1991).

The operation of the BAW quartz sensor in the gas phase is well understood. As mass is added to the surface of the sensor, the resonant frequency of the sensor decreases. The decrease of frequency is proportional to the increase of mass on the surface which was first explained quantitatively by

Sauerbrey (1959). When the sensor is in a gas, the acoustic wave in the quartz is completely reflected at the surface of the sensor and therefore all acoustic energy remains in the quartz. The frequency decreases as mass is added because the distance travelled by the acoustic wave from one face of the sensor to the other increases due to the thickness of the layer of added mass.

The operation of the sensor in the liquid phase is not well understood. The resonant frequency change of a sensor in a liquid is not due directly to the mass added to the surface of the sensor. Rather it is due to the change of properties of the interface between the surface of the sensor and the liquid in contact with the sensor. The nature of the interface changes when the molecule to be sensed is present in the liquid because these molecules bind to the surface and therefore this new layer of molecules is in contact with the liquid. When the sensor is in a liquid, only part of the acoustic wave which is incident on the solid-liquid interface from within the quartz is reflected back into the quartz. The rest of the wave is transmitted into the liquid and is dissipated (changes into thermal energy in the liquid). The phase and magnitude of the acoustic wave which is transmitted into the liquid is very sensitive to the properties of the solid-liquid interface. The acoustic wave carries energy and therefore some of the acoustic energy flows out of the quartz into the liquid. This energy is replaced by electrical energy

supplied to the quartz crystal that is converted by the piezoelectric effect into acoustic energy. The change of electrical energy supplied to the sensor changes the electrical characteristics measured at the terminals of the sensor.

The interfacial properties are related to three fundamental attributes of the interface: the type of molecule on the surface of the sensor, the type of molecule in the liquid which is in contact with the sensor surface and the force of attraction between the two sets of molecules. If the force of attraction is relatively strong, the surface is said to be hydrophilic and if relatively weak, the surface is hydrophobic. It is expected that there will be some slip between the molecules on the surface of the sensor and the molecules of the liquid in contact with the surface, especially when the surface is hydrophobic.

The objective of this research is to study the slip at the solid-liquid interface of a quartz sensor. A two-layer model is used, the layers being quartz and the liquid, with the interface characterized by a new property called the interfacial slip parameter. This model allows relative motion between the surface of the sensor and the liquid in contact with the surface. Reed et al (1990) used a two-layer model but with the no-slip boundary condition. Duncan-Hewitt and Thompson (1992) used a four-layer model to account for interfacial effects, where one layer is quartz and the other



three layers are different phases of the liquid, as an alternative to explicitly introducing slip at the interface.

A model of slip has been used for the case of the interface between two elastic media which are imperfectly bonded, Schoenberg (1980). The slip between the two solid regions is postulated to be linearly related to the shear stress at the interface, the slip parameter being the proportionality factor with the dimension of length/stress. In this thesis the interfacial slip parameter is defined differently.

The interfacial slip parameter appears in the theory of the two-layer model in one of the boundary conditions. The theoretical expression for impedance was found, which is a function of the interfacial slip parameter, Chapter 2. Measurements of impedance were made by the network analysis method and the experimental values of impedance were fitted to the theoretical expression for impedance using non-linear regression analysis to find the interfacial slip parameter, Chapter 3. A mechanical model of interfacial slip was devised whose predictions agree with the experimental results, Chapter 4. It is concluded that there is slip at the solid-liquid boundary of a BAW quartz sensor, Chapter 5.

The application software used in the research and in the preparation of this thesis is listed in Appendix 1.

## CHAPTER 2

### THEORY

#### Introduction

The theory of the two-layer model of a piezoelectric quartz sensor is derived in terms of a new property of the interface called the interfacial slip parameter.

The two-layer model is a solid-liquid model which neglects the thickness of two other layers of material between the quartz and liquid: the metal electrode which is attached to the quartz and the chemical coating which is attached to the metal electrode. The theory also assumes that the liquid in contact with surface of the solid has the same properties, that is, it has the same structure, as the bulk liquid. The theory focuses on the interaction between the surface of the solid and the liquid in contact with the solid. The interaction is represented by the interfacial slip parameter which is introduced through one of the boundary conditions.

Three fields of physics are combined in this theory. Elasticity, Section 2.1, and electromagnetism, Section 2.2, constitute the theory of piezoelectricity, Section 2.3. The fundamental equations of elasticity and electromagnetism are coupled by the equations of the piezoelectric material. Fluid mechanics, Section 2.4, is the theory of the liquid. The boundary conditions, Section 2.5, of the solid-liquid

interface connect the equations of the piezoelectric medium and the liquid. The boundary value problem is solved, section 2.6, and then the theoretical expression for impedance is derived, section 2.7.

Subscript notation is used throughout and is described in Appendix 2.

## 2.1 Elasticity

There are three fundamental equations of elasticity and one equation of a viscoelastic material, Eringen (1967) and Eringen and Maugin (1990). The fundamental equations are derived from Newton's second law, conservation of angular momentum and the definition of strain. The material equation is a generalization of Hooke's law. Newton's second law and the definition of strain are non-linear equations due to the terms which are products of the variables. Two approximations are made which remove these terms and make the equations linear.

Newton's second law for a viscoelastic solid of density,  $\rho_m$ , is

$$\frac{D}{Dt} (\rho_m \dot{u}_j) = T_{y,i} + F_{(m)j} \quad (2-1)$$

Equation (2-1) relates the particle displacement,  $u_j$ , to the second-rank stress tensor,  $T_{ij}$ , and the external force  $F_{(m)j}$ . The

symbol,  $D/Dt$ , denotes the material derivative with respect to the time,  $t$ .

The total change of particle velocity,  $\dot{u}_j = \dot{u}_j(x, y, z, t)$ , is the total differential of  $\dot{u}_j$ ,  $d\dot{u}_j = (\partial\dot{u}_j/\partial x)dx + (\partial\dot{u}_j/\partial y)dy + (\partial\dot{u}_j/\partial z)dz + (\partial\dot{u}_j/\partial t)dt$ . Divide both sides by  $dt$  and use the notation,  $D\dot{u}_j/Dt$ , instead of  $d\dot{u}_j/dt$ , for the particle acceleration. Since the components of the particle displacement,  $u_i$ , are  $dx_i$ , when the displacement is infinitely small,  $dx_i/dt$  is  $\dot{u}_i$ , the velocity of the particle.

$$\frac{D\dot{u}_j}{Dt} = \frac{\partial\dot{u}_j}{\partial t} + \frac{\partial\dot{u}_j}{\partial x_i}\dot{u}_i \quad (2-2)$$

The term on the left,  $D\dot{u}_j/Dt$ , is the particle acceleration, the first term on the right,  $\partial\dot{u}_j/\partial t$ , the local acceleration and the last term, the convective acceleration. In the theory of linear viscoelasticity, meaning for small deformations of the viscoelastic medium, the magnitude of the deformation gradient is much less than one, that is,  $|u_{i,j}| \ll 1$ . Therefore from (2-2) the convective term,  $\dot{u}_i \dot{x}_i$ , is much less than the non-convective term,  $\dot{v}_j$  (where  $v_j = \dot{u}_j$ ). Thus for a linear viscoelastic theory, from (2-1), the equation of motion for a medium of uniform mass density,  $\rho_m$ , reduces to

$$\rho_m \ddot{u}_j = T_{ij,i} + F_{(m)j} \quad (2-3)$$

From the law of conservation of angular momentum, at each

point in the medium,  $T_{ij}$  satisfies the following equation.

$$T_{ij} = T_{ji} \quad (2-4)$$

Equation (2-4) states that the stress tensor is symmetric. This is a direct result of the conservation of angular momentum at each point of the medium.

Equation (2-3) constitutes a system of three scalar equations in the twelve dependent variables:  $u_1, u_2, u_3, T_{11}, T_{12}, T_{13}, T_{21}, T_{22}, T_{23}, T_{31}, T_{32},$  and  $T_{33}$ . They are functions of the independent variables: the spatial coordinates,  $x, y, z,$  and the time,  $t$ . Due to the symmetry of  $T_{ij}$ , from (2-4),  $T_{12} = T_{21}, T_{13} = T_{31},$  and  $T_{23} = T_{32}$ . Therefore from (2-4) there are six distinct components of  $T_{ij}$  which are  $T_{11}, T_{12}, T_{13}, T_{22}, T_{23},$  and  $T_{33}$ . Thus the above twelve dependent variables reduce to nine dependent variables given by:  $u_1, u_2, u_3, T_{11}, T_{12}, T_{13}, T_{22}, T_{23},$  and  $T_{33}$ .

For a given deformation of a viscoelastic medium, the general expression relating the second-rank strain tensor,  $S_{ij}$ , to the particle displacement,  $u_j$  is

$$S_{ij} = \frac{1}{2} (u_{ij} + u_{ji} - u_{k,i} u_{k,j}) \quad (2-5)$$

The symmetry of  $S_{ij}$  can be deduced from (2-5). Like the second-rank stress tensor, the second-rank strain tensor is a symmetric tensor, that is,  $S_{ij} = S_{ji}$ . For small deformations,

the magnitude of the product of two deformation gradients is much less than the magnitude of the deformation gradient alone, that is,  $|u_{k,i}u_{k,j}| \ll |u_{i,j} + u_{j,i}|$ . Thus (2-5) reduces to

$$S_{ij} = \frac{1}{2} (u_{i,j} + u_{j,i}) \quad (2-6)$$

Due to the symmetry of  $S_{ij}$ , (2-6) constitutes a system of six scalar equations in the nine dependent variables given by:  $u_1, u_2, u_3, S_{11}, S_{12}, S_{13}, S_{22}, S_{23}$ , and  $S_{33}$ . Equations (2-3) and (2-6), together constitute a system of nine scalar equations in the fifteen dependent variables given by:  $u_1, u_2, u_3, T_{11}, T_{12}, T_{13}, T_{22}, T_{23}, T_{33}, S_{11}, S_{12}, S_{13}, S_{22}, S_{23}$ , and  $S_{33}$ . The above system, does not constitute a complete system of equations. To complete the above system, six additional scalar equations are needed. The completion of the above system of equations is accomplished by the material equation for the viscoelastic medium. For an arbitrary viscoelastic medium, the material equation that relates the stress and strain is

$$T_{ij} = c_{ijkl} S_{kl} + \eta_{ijkl} \dot{S}_{kl} \quad (2-7)$$

Equation (2-7) is the generalized form of Hooke's law for an arbitrary viscoelastic medium, the first term on the right being the elastic term of Hooke's law and the second term, the viscous term. The coefficients  $c_{ijkl}$  and  $\eta_{ijkl}$  are respectively the fourth-rank elastic coefficient tensor and the fourth-rank

viscoelastic coefficient tensor. Equation (2-7) constitutes a system of six scalar equations in no new dependent variables. Thus, (2-3), (2-4), (2-6), and (2-7) constitute a system of fifteen scalar equations in the fifteen dependent variables:  $u_1, u_2, u_3, T_{11}, T_{12}, T_{13}, T_{22}, T_{23}, T_{33}, S_{11}, S_{12}, S_{13}, S_{22}, S_{23},$  and  $S_{33}$ . Therefore (2-3), (2-4), (2-6), and (2-7) constitutes a complete system of equations.

For an arbitrary viscoelastic medium, from the symmetry of both  $T_{ij}$  and  $S_{ij}$ , an inspection of (2-7) reveals that both  $c_{ijkl}$  and  $\eta_{ijkl}$  must satisfy the relations

$$c_{ijkl} = c_{ijlk} = c_{jikl} = c_{klij} \quad (2-8)$$

and

$$\eta_{ijkl} = \eta_{ijlk} = \eta_{jikl} = \eta_{klij} \quad (2-9)$$

The relations for  $c_{ijkl}$  and  $\eta_{ijkl}$  given by (2-8) and (2-9) hold for any viscoelastic medium.

The derivation of the viscoelastic wave equation for a linear viscoelastic material, is obtained by the systematic elimination of the components of the stress and strain from (2-3), (2-6), (2-7), (2-8), and (2-9). The result is the viscoelastic wave equation for  $u_j$ , given by

$$c_{ijkl} u_{k,l} + \eta_{ijkl} \dot{u}_{k,l} + F_{(m)j} = \rho_m \ddot{u}_j \quad (2-10)$$

For the case of plane-wave propagation, (2-10) reduces to

Christoffel's equation.

## 2.2 Electromagnetism

There are four fundamental equations of electromagnetism which are called Maxwell's equations and in general, there are three equations of the material which are the equations for a conductor, a dielectric, and a magnetic material, Lorrain et al (1988).

For a stationary linear medium, Maxwell's four equations are

$$E_{i,i} = \frac{\rho}{\epsilon_0} \quad (2-11)$$

$$B_{i,i} = 0 \quad (2-12)$$

$$\epsilon_{ijk} E_{kj} + \dot{B}_i = 0 \quad (2-13)$$

$$\epsilon_{ijk} B_{kj} - \frac{1}{c^2} \dot{E}_i = \mu_0 J_i \quad (2-14)$$

where  $\epsilon_{ijk}$  is the levi-civita symbol defined in Appendix 2,  $E_i$  is the electric field,  $B_i$  is the magnetic field,  $\rho$  is the total charge density,  $J_i$  is the total current density,  $\epsilon_0$  is the permittivity of free space,  $\epsilon_0 = 8.854 \times 10^{-12}$  F/m,  $\mu_0$  is the



permeability of free space,  $\mu_0 = 4\pi \times 10^{-7}$  H/m and  $c$  is the speed of light,  $c = 2.998 \times 10^8$  m/s.

Equation (2-11) expresses Gauss's law in differential form. Gauss's law, in turn is a consequence of Coulomb's law. Equation (2-12) states the absence of magnetic monopoles. Equation (2-13) is the differential form of Faraday's law for time-dependent magnetic fields. Equation (2-14) is the differential form of Ampère's law for time-dependent electric fields. Maxwell's equations are relations between the fields,  $E_i$  and  $B_i$ , and the sources of the fields,  $\rho$  and  $J_i$ . The sources  $\rho$ , and  $J_i$ , are expressed in terms of the field quantities,  $E_i$  and  $B_i$ , by the equations of the material.

Maxwell's equations constitutes a system of eight scalar equations in the six dependent variables:  $E_1$ ,  $E_2$ ,  $E_3$ ,  $B_1$ ,  $B_2$ , and  $B_3$ . As a result there is some redundancy in the set of equations since there are more equations than unknowns. It is shown in Lorrain et al (1988) that equations (2-11) and (2-12) can be derived from (2-13) and (2-14). The independent variables are the time,  $t$ , and the spatial coordinates,  $x$ ,  $y$  and  $z$ .

The total charge density,  $\rho$ , and the total current density,  $J_i$ , in (2-11) and (2-14) are defined by the two following equations.

$$\rho = \rho_f + \rho_b \quad (2-15)$$

$$J_i = J_f + J_{bi} + J_{Mi} \quad (2-16)$$

The total charge density,  $\rho$ , is divided into two parts: the free charge density,  $\rho_f$  and the bound charge density,  $\rho_b$ . The total current density,  $J_i$ , is divided into three parts: The free charge current density,  $J_{fi}$ , the bound charge current density,  $J_{bi}$ , and the equivalent current density due to the magnetic material,  $J_{Mi}$ , which is due to the motion and spin of charge inside the atom.

The bound charge density in (2-15),  $\rho_b$ , and the current density of bound charge in (2-16),  $J_{bi}$ , are expressed in terms of the polarization,  $P_i$ . The vector,  $P_i$ , is the dipole moment per unit volume. The dipole moment is due to the displacement of positive and negative bound charges, and is defined as  $|q|d$ , where  $d$  is the distance between a positive charge of magnitude,  $|q|$ , and a negative charge of the same magnitude,  $-|q|$ .

The equivalent current density due to a magnetic material,  $J_{Mi}$ , in (2-16) is expressed in terms of the magnetization,  $M_i$ . The vector,  $M_i$ , is the magnetic moment per unit volume. The magnetic moment is due to circulating currents inside an atom or molecule making up the material, and is defined as  $IA$  where  $I$  is the current flowing around a loop of area  $A$ . Equations (2-15) and (2-16) in terms of  $P_i$  and  $M_i$  are

$$\rho = \rho_f - P_{i,i} \quad (2-17)$$

$$J_i = J_{fi} + \dot{P}_i + \epsilon_{ijk} M_{kj} \quad (2-18)$$

In general, there are three equations of the material, one each, for the behaviour of the free charge, the bound charge, and the motion of the charge inside the atom.

(1) Free Charge - Conducting Materials

The material equation for a conducting material of electrical conductivity,  $\sigma$ , is

$$J_{fi} = \sigma E_i \quad (2-19)$$

which is called Ohm's law. The electric field,  $E_i$ , induces the current of free charge,  $J_{fi}$ , and this current is proportional to  $E_i$ , if  $E_i$  is not too large. For an insulator,  $\sigma = 0$ , and therefore  $J_{fi} = 0$ . Also for an insulator, since there are no free charges,  $\rho_f = 0$ .

(2) Bound Charge - Dielectric Materials

The material equation for a dielectric material of electrical susceptibility,  $\chi_e$ , is

$$P_i = \epsilon_0 \chi_e E_i \quad (2-20)$$

The electric field exerts a force on a positive charge in the direction of the field and a force on a negative charge in the

opposite direction. Therefore the electric field displaces positive and negative charges contained in atoms and molecules. If the electric field is not too large, then the displacement of the charges is proportional to the magnitude of the applied electric field. Therefore, the polarization,  $P_i$ , is proportional to the electric field,  $E_i$ . For all materials,  $\chi_e \neq 0$ .

### (3) Atomic Charge - Magnetic Materials

The material equation for a magnetic material of magnetic susceptibility,  $\chi_m$ , is

$$M_i = \frac{\chi_m}{\mu_o (\chi_m + 1)} B_i \quad (2-21)$$

The magnetic field,  $B_i$ , orients current loops in the same direction, that is, the electron orbits and spins inside atoms and molecules are aligned with the magnetic field. The magnetization,  $M_i$ , is proportional to the magnetic field if the magnetic field is not too large, as given by (2-21). For non-magnetic materials,  $\chi_m = 0$ .

The general expressions for  $\rho$  and  $J_i$ , (2-17) and (2-18), in terms of  $E_i$  and  $B_i$  are, from (2-19) to (2-21)

$$\rho = \rho_f - \epsilon_o \chi_e E_{i,i} \quad (2-22)$$

$$J_i = \sigma E_i + \epsilon_o \chi_e \dot{E}_i + \epsilon_{ijk} \frac{\chi_m}{\mu_o (\chi_m + 1)} B_{k,j} \quad (2-23)$$

The material equations for a piezoelectric material are expressed in terms of the electric displacement,  $D_i$ , which is defined as

$$D_i = \epsilon_o E_i + P_i \quad (2-24)$$

The physical significance of  $D_i$  is seen by substituting (2-17) into (2-11); the result is  $(\epsilon_o E_i + P_i)_{,i} = \rho_f$ . Therefore the divergence of  $D_i$ ,  $D_{i,i}$ , is equal to the free charge density,  $\rho_f$ , that is, the free charge is the source of the field,  $D_i$ . For an insulator such as quartz,  $\rho_f = 0$ , and therefore as a result  $D_{i,i} = 0$ .

For a nonconducting ( $\sigma = 0$  and  $\rho_f = 0$ ), nonmagnetic ( $\chi_m = 0$ ) material such as quartz, Maxwell's equations, (2-11) to (2-14), combined with the source equations (2-17) and (2-18) are expressed in terms of the field quantities  $E_i$ ,  $B_i$ , and  $D_i$ , where  $P_i$  is eliminated using (2-24).

$$D_{i,i} = 0 \quad (2-25)$$

$$B_{i,i} = 0 \quad (2-26)$$

$$\epsilon_{ijk} E_{k,j} = -\dot{B}_i \quad (2-27)$$

$$\epsilon_{ijk} B_{j,k} = \mu_o \dot{D}_i \quad (2-28)$$

The relation,  $c^2 = 1/(\mu_0\epsilon_0)$  has been used to obtain (2-28). Maxwell's equations in the form of (2-25) to (2-28) are used in the derivation of the dynamical equations of motion of a viscoelastic piezoelectric material.

The material equation for a dielectric material in terms of  $D_i$  is obtained by combining (2-20) and the definition of  $D_i$ , (2-24).

$$D_i = \epsilon_0 (1 + \chi_e) E_i \quad (2-29)$$

Maxwell's equations, (2-11) to (2-14) can be combined, to yield an equation for  $E_i$  and an equation for  $B_i$ , both of which are wave equations. For the case of a nonmagnetic insulator, substitute (2-22) and (2-23) into (2-11) and (2-14) with  $\rho_f = 0$ ,  $\sigma = 0$ , and  $\chi_m = 0$ . The elimination of  $B_i$  from (2-13) and (2-14), using (2-11) results in the wave equation for  $E_i$  given by

$$E_{i,jj} = \frac{(1 + \chi_e)}{c^2} \ddot{E}_i \quad (2-30)$$

Equation (2-30) constitutes a set of three scalar equations in the three variables:  $E_1$ ,  $E_2$ , and  $E_3$ . By the same token, the elimination of  $E_i$  from (2-13) and (2-14), using (2-12) yields

$$B_{i,j} = \frac{(1 + \chi_e)}{c^2} \ddot{B}_i \quad (2-31)$$

As in (2-30), (2-31) constitutes a set of three scalar equations in the three variables:  $B_1$ ,  $B_2$ , and  $B_3$ .

### 2.3 Piezoelectricity

The equations of motion describing the dynamics of a piezoelectric material such as quartz are obtained by combining the fundamental equations of elasticity with the fundamental equations of electromagnetism together with the material equations of elasticity and electromagnetism generalized for a piezoelectric material, Auld, Volumes I and II (1973), Kinsler et al (1982), and Tiersten (1969). The complete set of equations contains three approximations. Two have already been made when writing the equations of elasticity and one more approximation is made in this section.

One fundamental equation of elasticity is

$$T_{y,i} = \rho_m \ddot{u}_j \quad (2-32)$$

Equation (2-32) is equation (2-3) with  $F_{(m)} = 0$  which is Newton's second law for an arbitrary viscoelastic material. From (2-4),  $T_{ij}$  is symmetric. The second fundamental equation is given by (2-6). From (2-6),  $S_{ij}$  is symmetric.

There is one material equation of elasticity, for a piezoelectric material; it is a generalization of (2-7). For a piezoelectric material with piezoelectric stress coefficient,  $e_{jk}$ , the material equation is

$$T_{ij} = -e_{ijk} E_k + c_{ijkl}^E S_{kl} + \eta_{ijkl}^E \dot{S}_{kl} \quad (2-33)$$

The fundamental equations of electromagnetism for a nonmagnetic insulating material are Maxwell's equations given by (2-25) to (2-28). There is one material equation of electromagnetism for a piezoelectric material. It is a generalization of (2-29). For a material with dielectric strain coefficient,  $\epsilon_{ik}^S$ , and piezoelectric stress coefficient,  $e_{ikl}$ , the equation is

$$D_i = \epsilon_{ik}^S E_k + e_{ikl} S_{kl} \quad (2-34)$$

For a piezoelectric material the two material equations, (2-33) and (2-34), connect (or couple) the fundamental equations of elasticity and electromagnetism, since in both (2-34) and (2-44) there are elastic and electromagnetic variables.

For a nonconducting, nonmagnetic, viscoelastic, piezoelectric material in the absence of external forces, the relevant equations of motion which describe the dynamics of the medium are given by (2-6), (2-25) to (2-28), and (2-32) to (2-34). The above system of equations constitutes a system of twenty-six scalar equations in the twenty-four variables:  $u_i$ ,



$u_2, u_3, T_{11}, T_{12}, T_{13}, T_{22}, T_{23}, T_{33}, S_{11}, S_{12}, S_{13}, S_{22}, S_{23}, S_{33}, E_1, E_2, E_3, B_1, B_2, B_3, D_1, D_2,$  and  $D_3$ . The number of equations exceeds the number of variables by two, due to the redundancy of Maxwell's equations, Lorrain et al (1988); (2-25) and (2-26) can be derived from (2-27) and (2-28). Thus upon the exclusion of (2-25) and (2-26), the above set of equations constitutes a set of twenty-four scalar equations and twenty-four variables. Since the number of equations equals the number of variables, then the system is complete. The system of coupled wave equations interrelating  $u$ , to  $E$ , is derived from this complete set of equations, by eliminating all other variables.

The complete set of the equations of piezoelectricity are given in Table 2.1. The physical quantities of piezoelectricity are given in Table 2.2. The material properties in the equations of piezoelectricity are given in Table 2.3.

Table 2.1 Equations of Piezoelectricity

Type	Category	Name	Equation	Number
Elastic	Fundamental	Newton's second law	$T_{ij,i} = \rho_m \ddot{u}_j$	3
		Definition of strain	$S_{ij} = \frac{1}{2}(u_{i,j} + u_{j,i})$	6
	Material	Hooke's law	$T_{ij} = -e_{ijk} E_k + c_{ijkl}^E S_{kl} + \eta_{ijkl}^E \dot{S}_{kl}$	6
Electromagnetic	Fundamental	Gauss's law	$D_{i,i} = 0$	1
		No magnetic monopoles	$B_{i,i} = 0$	1
		Faraday's law	$\epsilon_{ijk} E_{k,j} = -\dot{B}_i$	3
		Ampère's law	$\epsilon_{ijk} B_{j,k} = \mu_o \dot{D}_i$	3
	Material	Dielectric equation	$D_i = \epsilon_{ik}^S E_k + e_{ikl} S_{kl}$	3

Table 2.2 Physical Quantities of Piezoelectricity

Type	Name	Symbol	Components	Units
Elastic	particle displacement	$u_i$	3	m
	stress	$T_{ij}$	6	$N/m^2$
	strain	$S_{ij}$	6	m/m
Electromagnetic	electric field	$E_i$	3	$N/C$
	magnetic field	$B_i$	3	$V \cdot s/m^2$
	electric displacement	$D_i$	3	$C/m^2$

Table 2.3 Material Properties of Piezoelectricity

Type	Name	Symbol	Units
Elastic	density	$\rho_m$	$kg/m^3$
	elastic coefficient	$c_{ijkl}^E$	$N/m^2$
	viscoelastic coefficient	$\eta_{ijkl}^E$	$N \cdot s/m^2$
Electromagnetic	dielectric strain coefficient	$\epsilon_{ik}^S$	$C/V \cdot m$
Piezoelectric	piezoelectric stress coefficient	$e_{ijk}$	$C/m^2$

In (2-34),  $\epsilon_{ik}^S$ , denotes the second-rank dielectric strain coefficient tensor. The superscript 'S' refers to the measurement of  $\epsilon_{ik}^S$  under conditions of constant strain. Also in (2-34),  $e_{k1}$ , denotes the third-rank piezoelectric stress coefficient tensor. The piezoelectric stress coefficient tensor,  $e_{k1}$ , and the second-rank dielectric strain coefficient tensor,  $\epsilon_{ik}^S$ , satisfy the following symmetry relations as a consequence of the symmetry of  $S_{kl}$ ;  $S_{kl} = S_{lk}$ .

$$e_{k1} = e_{lk} \quad (2-35)$$

$$\epsilon_{ik}^S = \epsilon_{ki}^S \quad (2-36)$$

From (2-35),  $e_{k1}$ , is symmetric with respect to the indices  $l$  and  $k$ , while,  $\epsilon_{ik}^S$ , is symmetric with respect to the indices  $i$  and  $k$ .

The form of the material equations for a piezoelectric material, (2-33) and (2-34), are derived as follows. For an anisotropic material, the electric susceptibility of the medium,  $\chi_e$ , generalizes to the second-rank electric susceptibility coefficient tensor,  $\chi_{ij}^{(e)}$ . Physically the tensor character of  $\chi_e$  is due to the fact that in an anisotropic medium,  $\chi_e$  has different values for different directions. From (2-20), the material equation relating  $P_i$  to  $E_i$ , in an anisotropic medium generalizes to, Auld, Volume I (1973),

$$P_i = \epsilon_o \chi_{ij}^{(e)} E_j + d_{yk} T_{jk} \quad (2-37)$$

where  $d_{ijk}$  is the third-rank strain coefficient tensor.

In (2-37) the first term on the right,  $\epsilon_0 \chi^{(e)} E_j$ , is the only term in (2-20). It is the part of the polarization,  $P_i$ , that is produced by the electric field,  $E_i$ . The second term,  $d_{ijk} T_{jk}$ , represents the other part of the polarization that is produced under the action of an applied stress,  $T_k$ .

The material equation relating the strain,  $S_y$ , to the electric field,  $E_k$ , and the stress,  $T_{kl}$ , is a generalization of (2-7) Auld, Volume I (1973).

$$S_y = d_{yk} E_k + s_{ykl}^E T_{kl} \quad (2-38)$$

In (2-38), the first term,  $d_{yk} E_k$  represents part of the strain that is produced under the action of an applied electric field,  $E_k$ . The second term,  $s_{ykl}^E T_{kl}$ , represents the other part of the strain that is produced under the action of an applied stress,  $T_{kl}$ . The coefficient,  $s_{ykl}^E$ , is the fourth-rank compliance coefficient tensor, a property of the material, which is a measure of the deformation of the material materials under the action of an applied stress,  $T_{kl}$ . The superscript, E on  $s_{ykl}^E$ , indicates that the measurement of  $s_{ijkl}^E$  is made under conditions of constant electric field,  $E_i$ .

Using (2-24) and (2-37), the expression for the electric displacement,  $D_i$ , in terms of  $E_i$  and  $T_{ij}$  is

$$D_i = \epsilon_y^T E_j + d_{yjk} T_{jk} \quad (2-39)$$

where

$$\epsilon_{ij}^T = \epsilon_o (\delta_{ij} + \chi_{ij}^{(e)}) \quad (2-40)$$

where  $\delta_{ij}$  is the kronecker delta defined in Appendix 2.

Equation (2-40) is the definition of the second-rank dielectric stress coefficient tensor,  $\epsilon_{ij}^T$ . The superscript, T, denotes that  $\epsilon_{ij}^T$  is measured under conditions of constant stress. From (2-38) and (2-39) the expressions relating  $T_{ij}$  and  $D_i$  to  $E_i$  and  $S_{ij}$  are

$$T_{ij} = -e_{ijk} E_k + c_{ijkl}^E S_{kl} \quad (2-41)$$

$$D_i = \epsilon_{ik}^S E_k + e_{ikl} S_{kl} \quad (2-42)$$

where  $c_{ijkl}^E$  is the reciprocal of  $s_{ijkl}^E$ , that is,  $c_{ijkl}^E = (s_{ijkl}^E)^{-1}$ , and

$$e_{ijk} = c_{ijkl}^E d_{klk} \quad (2-43)$$

$$\epsilon_{ik}^S = \epsilon_{ik}^T - d_{ij} c_{ijkl}^E d_{klk} \quad (2-44)$$

$$e_{ikl} = d_{ij} c_{ijkl}^E \quad (2-45)$$

Equations (2-43) and (2-45), are the defining equations for the third-rank piezoelectric stress coefficient tensor,  $e_{ijk}$ . Equation (2-44) expresses the relationship between  $\epsilon_{ik}^T$  and  $\epsilon_{ik}^S$ . Equation (2-41) is true for an elastic material and is generalized for a viscoelastic material by adding a viscous term to give the viscoelastic equation, (2-33). Equation (2-42) is one of the two piezoelectric material equations stated

earlier, (2-34). From this point forward, the superscripts 'E' and 'S' on  $c_{ijkl}^E$  and  $\epsilon_{ik}^S$  respectively will be dropped, so as to simplify the notation.

In the following discussion, the system of coupled wave equations for a linear viscoelastic piezoelectric material, relating  $u_i$  to  $E_i$ , will be derived from the complete set of equations for a linear viscoelastic piezoelectric material: (2-6), (2-25) to (2-28) and (2-32) to (2-34). In addition the symmetry equations (2-8) and (2-9) are required. From (2-6), (2-8), (2-9), and (2-33), (2-32) reduces to

$$-e_{ijk} E_{k,i} + c_{ijkl} u_{k,li} + \eta_{ijkl} \dot{u}_{k,li} = \rho_m \ddot{u}_j \quad (2-46)$$

From (2-27) and (2-28), after elimination of  $B_i$ ,

$$E_{j,y} - E_{i,ij} = -\mu_o \ddot{D}_i \quad (2-47)$$

From (2-6) and (2-34), (2-47) reduces to

$$E_{j,y} - E_{i,ij} = -\mu_o \left[ \epsilon_{ik} \ddot{E}_k + \frac{1}{2} e_{i\ell} (\ddot{u}_{k,l} + \ddot{u}_{l,k}) \right] \quad (2-48)$$

Equations (2-46) and (2-48) constitute a system of coupled wave equations for a linear viscoelastic piezoelectric material which interrelates  $u_i$  to  $E_i$ . The above system constitutes a complete system of six scalar equations in the six variables (unknowns):  $u_1$ ,  $u_2$ ,  $u_3$ ,  $E_1$ ,  $E_2$ , and  $E_3$ . For the case of a non-piezoelectric viscoelastic medium,  $e_{ijk} = 0$ , thus (2-46) and (2-48) reduce to

$$c_{ijkl} u_{k,l} + \eta_{ijkl} \dot{u}_{k,l} = \rho_m \ddot{u}_j \quad (2-49)$$

$$E_{j,y} - E_{i,w} = -\mu_o \epsilon_{ik} \ddot{E}_k \quad (2-50)$$

In the absence of external forces, (2-49) is identical to (2-10). Since  $e_{ijk} = 0$ , then from (2-43) and (2-45),  $d_{ijk} = 0$ . Thus from (2-44),  $\epsilon_{ik}^S = \epsilon_{ik}^T = \epsilon_o (\delta_{ik} + \chi^{(e)}_{ik})$ . Since the viscoelastic material is non-piezoelectric, then by necessity, the material must be isotropic. Thus for an isotropic viscoelastic material,  $\delta_{ij} = 1$ ,  $\chi^{(e)}_{ij} \rightarrow \chi_c$ , and  $\epsilon_{ik}^S \rightarrow \epsilon_o (1 + \chi_c)$ , and hence (2-50) reduces to (2-30). Therefore, for an isotropic viscoelastic material,  $u_i$  and  $E_i$  decouple and the resulting equations reduce to those of an isotropic viscoelastic material.

The vector potential,  $A_i$ , is defined by the following equation.

$$B_i = \epsilon_{ijk} A_{k,j} \quad (2-51)$$

In vector notation, (2-51) is  $\mathbf{B} = \nabla \times \mathbf{A}$ . Equation (2-12),  $\nabla \cdot \mathbf{B} = 0$ , implies that  $\mathbf{B} = \nabla \times \mathbf{A}$  since  $\nabla \cdot (\nabla \times \mathbf{A}) = 0$ . In general the electric field,  $E_i$ , is expressed as the sum of two potentials: one scalar, and the other vector. In terms of the scalar potential,  $\varphi$ , and the vector potential,  $A_i$ , the expression for  $E_i$  is

$$E_i = -\varphi_{,i} - \dot{A}_i \quad (2-52)$$

The general form of  $E_i$ , given by (2-52) is a consequence of (2-13).



For an anisotropic viscoelastic material such as quartz, the frequency of elastic vibrations is many orders of magnitude greater than the corresponding frequency of pure electromagnetic vibrations. Due to the low value of piezoelectric coupling in quartz, the electromagnetic field is essentially decoupled from the elastic field. Thus the magnitude of the second term in (2-52) is much less than the magnitude of the first term in (2-52). The inequality  $\|\dot{A}_i\| \ll \|\varphi_{,i}\|$  is called the quasi-static approximation. Equation (2-52) becomes

$$E_i = -\varphi_{,i} \quad (2-53)$$

In the quasi-static approximation, the equations of motion relating  $u_i$  to  $\varphi$ , are derived from the following equations: (2-35), (2-46), (2-48), and (2-53). From (2-53), (2-46) reduces to

$$e_{ijk} \varphi_{,ki} + c_{ijkl} u_{k,l} + \eta_{ijkl} \dot{u}_{k,li} = \rho_m \ddot{u}_j \quad (2-54)$$

Differentiating (2-48) with respect to the spatial coordinate,  $x_i$ , (2-48) reduces to

$$\epsilon_{ik} \ddot{E}_{k,i} + \frac{1}{2} e_{ikl} (\ddot{u}_{k,li} + \ddot{u}_{l,ki}) = 0 \quad (2-55)$$

From (2-35) and (2-53), (2-55) reduces to

$$e_{ikl} \ddot{u}_{k,li} - \epsilon_{ik} \ddot{\varphi}_{,ki} = 0 \quad (2-56)$$

From (2-6), (2-25), (2-34), (2-35), and (2-53), (2-25) reduces

to

$$e_{ikl} u_{k,li} - \epsilon_{ik} \varphi_{,ki} = 0 \quad (2-57)$$

From an inspection of (2-56) and (2-57), (2-56) is simply (2-57) differentiated twice with respect to the time,  $t$ . Thus in the quasi-static approximation, (2-54) and (2-57) are the dynamical equations of motion for a linear viscoelastic piezoelectric material interrelating  $u_i$  and  $\varphi$ . The above system of equations constitutes a complete system of four scalar equations in the four variables:  $u_x$ ,  $u_y$ ,  $u_z$ , and  $\varphi$ .

An AT-cut quartz crystal, is a rotated Y-cut quartz crystal, which has been rotated through an angle of  $\theta = 35.25^\circ$  about the X-axis. It operates in the transverse shear mode, as will be explained. The XYZ-coordinate system refers to the crystal axis coordinate system.

The rotation of the XYZ-coordinate system into the xyz-coordinate system through an angle  $\theta$ , about the X-axis is given by the following rotation matrix,  $a_{ij}$ ,

$$a_{ij} = \begin{bmatrix} 1 & 0 & 0 \\ 0 & \cos\theta & \sin\theta \\ 0 & -\sin\theta & \cos\theta \end{bmatrix} \quad (2-58)$$

In the following the prime refers to the XYZ-coordinate system. The components of the elastic coefficient tensor,  $c'_{ijkl}$ , with respect to the XYZ-coordinate system are related to the components of  $c_{ijkl}$  with respect to the xyz-coordinate system

by the following transformation.

$$c_{ijkl} = a_{im} a_{jn} a_{ko} a_{lp} c'_{mnop} \quad (2-59)$$

By the same token, the components of  $\eta'_{ijkl}$  are related to the components of  $\eta_{ijkl}$  by

$$\eta_{ijkl} = a_{im} a_{jn} a_{ko} a_{lp} \eta'_{mnop} \quad (2-60)$$

The components of the piezoelectric stress coefficient tensor,  $e'_{ijk}$ , with respect to the XYZ-coordinate system are related to the components of  $e_{ijk}$  with respect to the xyz-coordinate system by the following transformation.

$$e_{ijk} = a_{im} a_{jn} a_{ko} e'_{mno} \quad (2-61)$$

The components of the dielectric tensor,  $\epsilon'_{ij}$ , with respect to the XYZ-coordinate system are related to the components of  $\epsilon_{ij}$  with respect to the xyz-coordinate system by the following transformation.

$$\epsilon_{ij} = a_{im} a_{jn} \epsilon'_{mn} \quad (2-62)$$

For an AT-cut quartz crystal, the values for:  $c_{ijkl}$ ,  $e_{ijk}$ , and  $\epsilon_{ij}$  with respect to the xyz-coordinate system are given in Table 2.4, Tiersten (1969).

Table 2.4 Properties of Quartz

$c_{ijkl}$ Elastic Coefficient		$e_{ijk}$ Piezoelectric Stress Coefficient		$\epsilon_{ik}$ Dielectric Strain Coefficient	
Components	Values $10^9$ (N/m <sup>2</sup> )	Components	Values C/m <sup>2</sup>	Components	Values C/V · m
$c_{1111}$	86.74	$e_{111}$	0.171	$\epsilon_{11}$	39.21
$c_{1112}$	0.0	$e_{112}$	0.0	$\epsilon_{12}$	0.0
$c_{1113}$	0.0	$e_{113}$	0.0	$\epsilon_{13}$	0.0
$c_{1122}$	-8.25	$e_{122}$	-0.152	$\epsilon_{22}$	39.82
$c_{1123}$	-3.66	$e_{123}$	0.067	$\epsilon_{23}$	0.68
$c_{1133}$	27.15	$e_{133}$	-0.0187	$\epsilon_{33}$	40.42
$c_{1212}$	29.01	$e_{211}$	0.0		
$c_{1312}$	2.53	$e_{212}$	-0.095		
$c_{1313}$	68.81	$e_{213}$	0.108		
$c_{2212}$	0.0	$e_{222}$	0.0		
$c_{2213}$	0.0	$e_{223}$	0.0		
$c_{2222}$	129.77	$e_{233}$	0.0		
$c_{2223}$	5.7	$e_{311}$	0.0		
$c_{2233}$	-7.42	$e_{312}$	0.067		
$c_{2312}$	0.0	$e_{313}$	-0.0761		
$c_{2313}$	0.0	$e_{322}$	0.0		
$c_{2323}$	38.61	$e_{323}$	0.0		
$c_{3312}$	0.0	$e_{333}$	0.0		
$c_{3313}$	0.0				
$c_{3323}$	9.92				
$c_{3333}$	102.83				

From (2-59) to (2-62), using Table 2.4, the equations of motion for the thickness shear wave solution of an AT-cut quartz material are

$$c_{1212} \frac{\partial^2 u_x}{\partial y^2} + \eta_{1212} \frac{\partial^3 u_x}{\partial y^2 \partial t} + e_{212} \frac{\partial^2 \varphi}{\partial y^2} = \rho_q \frac{\partial^2 u_x}{\partial t^2} \quad (2-63)$$

$$c_{2322} \frac{\partial^2 u_z}{\partial y^2} + \eta_{2322} \frac{\partial^3 u_z}{\partial y^2 \partial t} + c_{2222} \frac{\partial^2 u_y}{\partial y^2} + \eta_{2222} \frac{\partial^3 u_y}{\partial y^2 \partial t} = \rho_q \frac{\partial^2 u_y}{\partial t^2} \quad (2-64)$$

$$c_{2323} \frac{\partial^2 u_z}{\partial y^2} + \eta_{2323} \frac{\partial^3 u_z}{\partial y^2 \partial t} + c_{2322} \frac{\partial^2 u_y}{\partial y^2} + \eta_{2322} \frac{\partial^3 u_y}{\partial y^2 \partial t} = \rho_q \frac{\partial^2 u_z}{\partial t^2} \quad (2-65)$$

$$e_{212} \frac{\partial^2 u_x}{\partial y^2} - \epsilon_{22} \frac{\partial^2 \varphi}{\partial y^2} = 0 \quad (2-66)$$

where  $c_{1312}$  is a component of the elastic coefficient tensor,  $e_{213}$  is a component of the piezoelectric stress coefficient tensor,  $\eta_{1312}$ , is a component of the viscoelastic coefficient tensor, and  $\epsilon_{23}$  is a component of the dielectric strain coefficient tensor, all given in Table 2.4.

In (2-63) to (2-66),  $u_x$ ,  $u_y$ , and  $u_z$  are the x, y and z components of the particle displacement in the quartz material of mass density,  $\rho_q$ , and  $\varphi$  is the potential. The four scalar equations (2-63) to (2-66) relate the four variables  $u_x$ ,  $u_y$ ,  $u_z$ , and  $\varphi$ . The quantities  $u_x$  and  $\varphi$  appear only in (2-63) and (2-66), while the quantities  $u_y$  and  $u_z$  appear only in (2-64)

and (2-65). Therefore  $u_y$  and  $u_z$  are decoupled from  $\varphi$ , while  $u_x$  is coupled to  $\varphi$ . Furthermore the dependent variables  $u_x$ ,  $u_y$ ,  $u_z$ , and  $\varphi$  are functions of the independent variables  $y$  and  $t$  only. From (2-66) if  $\varphi = 0$ , then from (2-63) and (2-66)  $u_x = 0$ , after some mathematical reasoning. If  $\varphi \neq 0$ , then  $u_x \neq 0$  and so  $\varphi$  causes the displacement,  $u_x$ , which is a function of  $y$  and  $t$  only. Therefore the wave propagates in the  $y$ -direction, with the associated particle displacement in the  $x$ -direction and so the wave is a transverse wave. The AT-cut quartz is also called transverse-shear-mode (TSM) quartz for this reason. Since  $u_y$  and  $u_z$  are decoupled from  $\varphi$ , then if  $u_y$  and  $u_z$  are zero at some time, then they will be zero for all time.

Let  $c = c_{1212}$ ,  $\eta = \eta_{1212}$ ,  $e = e_{212}$ , and  $\epsilon = \epsilon_{22}$ , and denote partial differentiation with respect to  $y$  by a prime and with respect to  $t$  by a dot. Then (2-63) and (2-66) become.

$$c u_x'' + \eta \dot{u}_x'' + e \varphi'' = \rho_q \ddot{u}_x \quad (2-67)$$

$$e u_x'' - \epsilon \varphi'' = 0 \quad (2-68)$$

Equations (2-67) and (2-68) are the coupled linear partial differential equations for the thickness shear-wave solution relating the particle displacement,  $u_x$ , to the potential,  $\varphi$ , in the quartz.

The thickness shear-wave viscoelastic wave equation for the particle displacement,  $u_x$ , is obtained by eliminating the

potential,  $\varphi$ , from (2-67) and (2-68). The thickness shear-wave viscoelastic wave equation is

$$\bar{c} u_x'' + \eta \dot{u}_x'' = \rho_q \ddot{u}_x \quad (2-69)$$

where  $\bar{c}$  is called the stiffened elastic constant of quartz, and is defined as

$$\bar{c} = c + \frac{e^2}{\epsilon} \quad (2-70)$$

From (2-6), (2-8), (2-9), (2-33), (2-34), (2-35), (2-36) and from Table 2.1, the components of  $T_y$  and  $D_i$  in quartz are

$$T_{yx} = c u_x' + \eta \dot{u}_x' + e \varphi' \quad (2-71)$$

$$T_{zx} = c_{1312} u_x' + \eta_{1312} \dot{u}_x' + e_{213} \varphi' \quad (2-72)$$

$$T_{xx} = T_{yy} = T_{yz} = T_{zz} = 0 \quad (2-73)$$

$$D_x = 0 \quad (2-74)$$

$$D_y = e u_x' - \epsilon \varphi' \quad (2-75)$$

$$D_z = e_{213} u_x' - \epsilon_{23} \varphi' \quad (2-76)$$

## 2.4 Fluid Mechanics

There are two fundamental equations of fluid mechanics, the equation of continuity and Newton's second law applied to a liquid, Hughes and Brighton (1967), Landau and Lifshitz

(1987), and Yuan (1967). There is one equation of the material which gives the general linear relationship between the stress in the liquid medium and the corresponding deformation of the liquid medium arising from the action of the stress.

The equation of continuity for a liquid medium of mass density,  $\rho_l$  is.

$$\dot{\rho}_l + (\rho_l v_{(0)i})_{,i} = 0 \quad (2-77)$$

In (2-77),  $v_{(0)i}$ , denotes the  $i$ -th component of the particle velocity in the liquid medium. The general linear expression for the relation between the stress components of the liquid medium,  $T_{(0)ij}$ , and the components of the liquid particle velocity,  $v_{(0)i}$ , for a liquid medium is

$$T_{(0)ij} = -p \delta_{ij} + \mu (v_{(0)i,j} + v_{(0)j,i} - \frac{2}{3} \delta_{ij} v_{(0)k,k}) + \zeta \delta_{ij} v_{(0)k,k} \quad (2-78)$$

In (2-78),  $p$ , denotes the liquid pressure at a point in the liquid medium,  $\mu$ , denotes the dynamic viscosity of the liquid medium, and  $\zeta$ , denotes the second coefficient of viscosity of the liquid medium. The second coefficient of viscosity,  $\zeta$ , is a measure of the viscosity of the liquid medium that arises when turbulent effects are present. From Newton's second law, the equation of motion for a liquid medium is

$$T_{(0)ij,i} + F_{(0)j} = \rho_l (\dot{v}_{(0)j} + v_{(0)i} v_{(0)j,i}) \quad (2-79)$$

For an incompressible liquid medium, the liquid mass density,  $\rho_l$  is considered to be constant, that is, the same at



all points. For an incompressible liquid medium, (2-77) reduces to

$$v_{(0),i,i} = 0 \quad (2-80)$$

From (2-80), with liquid pressure neglected, (2-78) reduces to

$$T_{(0)ij} = \mu (v_{(0)ij} + v_{(0),i,j}) \quad (2-81)$$

In an incompressible liquid medium, physical effects due to turbulence, such as convection, are negligible in comparison to the translatory motion of the liquid medium. Thus the convective term in (2-79),  $v_{(0)i} v_{(0),i,j}$ , is negligible in comparison to the non-convective term  $\dot{v}_{(0),j}$ . Thus for an incompressible liquid medium with constant dynamic viscosity,  $\mu$ , and mass density,  $\rho_l$ , in the absence of all external forces, from (2-80) and (2-81), (2-79) reduces to

$$\nu v_{(0),ii} = \dot{v}_{(0),j} \quad (2-82)$$

where  $\nu$  is called the kinematic viscosity and is defined as

$$\nu = \frac{\mu}{\rho_l} \quad (2-83)$$

Equation (2-82) constitutes a complete system of three scalar equations in the three variables:  $v_x$ ,  $v_y$ , and  $v_z$ . Equation (2-82) is the Navier-Stokes equation for an incompressible liquid medium.

Let the surface of the liquid be in contact with the plane surface of a solid material undergoing transverse oscillations in a direction parallel to the surface of the

liquid. The transverse vibratory motion of the solid will be transmitted to the surface of the liquid in contact with the solid, via contact forces, which are attractive forces between surface liquid particles and surface solid particles. A cartesian coordinate system is chosen, such that, the surface of the liquid lies in the  $xz$ -plane, with the  $y$ -axis directed into the liquid medium. The transverse motion of the solid surface in the  $x$ -direction, will produce a transverse motion of the liquid in the  $x$ -direction, with each component of the particle displacement of the liquid being a function of the spatial coordinate,  $y$ , and the time,  $t$ , only. That is:  $u_{(0)x} = u_{(0)x}(y,t)$ ,  $u_{(0)y} = 0$  and  $u_{(0)z} = 0$ . The  $x$ -component of the particle displacement of the liquid,  $u_{(0)x}$ , is the only non-vanishing component. Since  $v_{(0)i} = \dot{u}_{(0)i}$ , then:  $v_{(0)x} = v_{(0)x}(y,t)$ ,  $v_{(0)y} = 0$  and  $v_{(0)z} = 0$ . Therefore (2-82) reduces to one scalar equation in the variable,  $v_{(0)x}$ .

$$\nu v_{(0)x}'' = \dot{v}_{(0)x} \quad (2-84)$$

There is also only one non-vanishing stress component of the liquid medium,  $T_{(0)yx}$ , from (2-81) and as a result (2-81) reduces to one scalar equation, given by

$$T_{(0)yx} = \mu v_{(0)x}' \quad (2-85)$$

## 2.5 Boundary Conditions of Solid-Liquid Model

There are five boundary conditions for the solid-liquid two-layer system shown in Figure 2.1. Two of the boundary conditions are applied at the solid-air interface, and the other three are applied at the solid-liquid interface. Figure 2.1 depicts a liquid-loaded sensor with quantities at the two interfaces,  $y = 0$  and  $y = h$ , which appear in the following five boundary conditions.

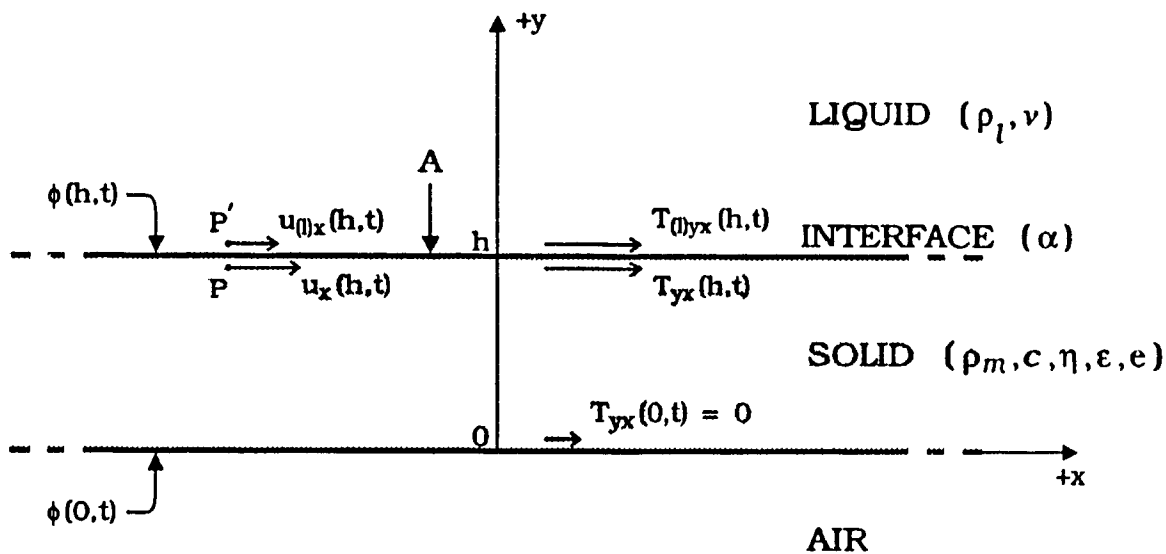


Figure 2.1 Solid-liquid model showing quantities used to express the five boundary conditions, and showing in brackets the five properties of the solid, the two properties of the liquid and the one property of the interface.

(1) Shear Stress At  $y = 0$  (Stress-free boundary condition at solid-air interface)

$$T_{yx}(0,t) = 0 \quad (2-86)$$

Equation (2-86) states that at the solid-air interface, the air in contact with the surface of the sensor at  $y = 0$  produces a negligible shear stress on the solid surface.

(2) Shear Stress At  $y = h$  (Continuity of stress boundary condition at solid-liquid interface)

$$T_{yx}(h,t) = T_{(0)yx}(h,t) \quad (2-87)$$

Equation (2-87) is the stress-continuity boundary condition at the solid-liquid interface. Physically the stress must be continuous at all points along the solid-liquid interface, that is, there can only be one value of stress at each point along the solid-liquid interface.

(3) Particle Displacement At  $y = h$  (Slip boundary condition at solid-liquid interface)

$$u_{(0)x}(h,t) = \alpha u_x(h,t) \quad (2-88)$$

The boundary condition, (2-88), defines the interfacial slip parameter,  $\alpha$ . The interfacial slip parameter,  $\alpha$ , is a measure of the relative displacement between two points, P in the solid at the interface and P' in the liquid at the interface. In general  $\alpha$  is a complex-valued quantity, which accounts for the phase difference between the displacements,  $u_{(0)x}$  and  $u_x$ . The relative displacement between P and P', is a measure of the strength of the interaction that arises between P and P'.

Thus  $\alpha$ , may be viewed as that parameter which is a measure of the strength of the interaction between P and P'. Figure 2.1 shows points P and P', and their respective displacements.

(4) Potential At  $y = 0$  (Potential boundary condition at solid-air interface)

$$\varphi(0,t) = -\varphi_o e^{j\omega t} \quad (2-89)$$

Equation (2-89) specifies the value of the potential at the bottom electrode of the sensor.

(5) Potential At  $y = h$  (Potential boundary condition at solid-liquid interface)

$$\varphi(h,t) = +\varphi_o e^{j\omega t} \quad (2-90)$$

Equation (2-90) specifies the values of the potential at the top electrode of the sensor.

## 2.6 Solution Of Solid-Liquid Model

The following is a list of the equations needed for the solution of the boundary value problem. There are three equations of quartz: (2-67), (2-68) and (2-71). There are two equations of the liquid: (2-84) and (2-85). The quartz and liquid equations are combined with the five boundary conditions: (2-86), (2-87), (2-88), (2-89), and (2-90). In particular, two of the boundary conditions connect the quartz equations with the liquid equations: the continuity of stress boundary condition, (2-87), and the slip boundary condition,

(2-88).

From (2-69), the general plane-wave solution to the viscoelastic wave equation is

$$u_x = (a_1 e^{jk_q y} + a_2 e^{-jk_q y}) e^{j\omega t} \quad (2-91)$$

where

$$k_q = \omega \left[ \frac{\rho_q}{c + \omega \eta j} \right]^{1/2} \quad (2-92)$$

In (2-91),  $a_1$  and  $a_2$  are complex-valued constants. The quantity,  $k_q$ , in (2-92) is complex-valued and is called the wave number for quartz.

The general plane-wave solution to (2-84) is

$$v_{(0)x} = (a_5 e^{-jk_l y} + a_6 e^{jk_l y}) e^{j\omega t} \quad (2-93)$$

where

$$k_l = \left[ \frac{\omega}{j\nu} \right]^{1/2} \quad (2-94)$$

In (2-93)  $a_5$  and  $a_6$  denote complex-valued constants. The quantity,  $k_l$ , in (2-94) is the complex-valued wave number of the liquid medium. From (2-93) as  $y \rightarrow \infty$ ,  $\exp(-jk_l y) \rightarrow 0$ , and  $\exp(jk_l y) \rightarrow \infty$ . Since  $\exp(jk_l y) \rightarrow \infty$ , then,  $v_{(0)x} \rightarrow \infty$ . Physically this is not possible, since for all  $y$ ,  $v_{(0)x}$  must be finite. Therefore in order for  $v_{(0)x}$  to be finite,  $a_6 = 0$ . Hence (2-93) reduces to

$$v_{(0)x} = a_5 e^{-\gamma_1 y} e^{j\omega t} \quad (2-95)$$

From (2-68) and (2-91), the expression for the potential,  $\varphi$ , is

$$\varphi = \frac{e}{\epsilon} u_x + (a_3 y + a_4) e^{j\omega t} \quad (2-96)$$

In (2-96),  $a_3$  and  $a_4$  are complex-valued constants.

The boundary value problem to be solved consists of the five boundary conditions which relate the five unknowns:  $a_1$ ,  $a_2$ ,  $a_3$ ,  $a_4$ , and  $a_5$ .

(1) Stress-free boundary condition: (2-86)

Using (2-71), (2-91), and (2-96), the first algebraic equation is

$$a_3 e - (a_2 - a_1) \delta k_q = 0 \quad (2-97)$$

(2) Continuity of stress boundary condition: (2-87)

Using (2-71), (2-85), (2-91), (2-95), and (2-96), the second algebraic equation is

$$-\frac{\delta(a_2 \gamma_1^2 - a_1) k_q - a_3 e \gamma_1}{\gamma_1} = \frac{a_5 k_1 \nu \omega \rho_1}{\gamma_2} \quad (2-98)$$

(3) Slip boundary condition: (2-88)

Using  $v_x = \dot{u}_x$  and  $v_{(0)x} = \dot{u}_{(0)x}$ , with (2-91) and (2-95), the third algebraic equation is

$$\frac{a_3}{\gamma_2} = \frac{\alpha(a_1 + \gamma_1^2 a_2)}{\gamma_1} \quad (2-99)$$

(4) Potential boundary condition: (2-89)

Using (2-91) and (2-96), the fourth algebraic equation is

$$\frac{e}{\epsilon}(a_1 + a_2) + a_4 = -\varphi_o \quad (2-100)$$

(5) Potential boundary condition: (2-90)

Using (2-91) and (2-96), the fifth and final algebraic equation is

$$\frac{e(a_1 + a_2 \gamma_1^2) + \epsilon \gamma_1 (h a_3 + a_4)}{\epsilon \gamma_1} = \varphi_o \quad (2-101)$$

In (2-100) and (2-101),  $\varphi_o$ , is the amplitude of the applied source voltage. From (2-97) to (2-101), the complex-valued quantities  $\gamma_1$ ,  $\gamma_2$ , and  $\delta$  are defined as

$$\gamma_1 = e^{j h k} \quad (2-102)$$

$$\gamma_2 = e^{j h k} \quad (2-103)$$

$$\delta = \eta \omega - j \bar{c} \quad (2-104)$$

The algebraic solution to (2-97) to (2-101), is found by the Macsyma program, ZIN.WP. The Macsyma program ZIN.WP is given in Appendix 3. The solution to the above system of algebraic equations follows.



$$a_1 = \frac{\alpha b_{12} + b_{11}}{\alpha b_{14} + b_{13}} \quad (2-105)$$

$$a_2 = \frac{\alpha b_{22} + b_{21}}{\alpha b_{24} + b_{23}} \quad (2-106)$$

$$a_3 = \frac{(\alpha b_{32} + b_{31}) \varphi_o}{\alpha b_{34} + b_{33}} \quad (2-107)$$

$$a_4 = \frac{\alpha b_{42} + b_{41}}{\alpha b_{44} + b_{43}} \quad (2-108)$$

$$a_5 = \frac{\alpha b_{52} + b_{51}}{\alpha b_{54} + b_{53}} \quad (2-109)$$

where

$$b_{11} = -2 \delta e \epsilon (\gamma_1 - 1) \gamma_1 k_q \varphi_o \quad (2-110)$$

$$b_{12} = -2 e \epsilon \gamma_1^2 k_l \nu \omega \varphi_o \rho_l \quad (2-111)$$

$$b_{13} = \delta (\gamma_1 - 1) k_q (\delta \epsilon (\gamma_1 + 1) h k_q + 2 e^2 (\gamma_1 - 1)) \quad (2-112)$$

$$b_{14} = k_l (\delta \epsilon (\gamma_1^2 + 1) h k_q + e^2 (\gamma_1 - 1) (\gamma_1 + 1)) \nu \omega \rho_l \quad (2-113)$$

$$b_{21} = 2 \delta e \epsilon (\gamma_1 - 1) k_q \varphi_o \quad (2-114)$$

$$b_{22} = 2 e \epsilon k_l \nu \omega \rho_l \varphi_o \quad (2-115)$$

$$b_{23} = b_{13} \quad (2-116)$$

$$b_{24} = b_{14} \quad (2-117)$$

$$b_{31} = 2\delta^2\epsilon(\gamma_1 - 1)(\gamma_1 + 1)k_q^2 \quad (2-118)$$

$$b_{32} = 2\delta\epsilon(\gamma_1^2 + 1)k_1k_q\nu\rho_1\omega \quad (2-119)$$

$$b_{33} = b_{13} \quad (2-120)$$

$$b_{34} = b_{14} \quad (2-121)$$

$$b_{41} = -\delta^2\epsilon(\gamma_1 - 1)(\gamma_1 + 1)hk_q^2\varphi_o \quad (2-122)$$

$$b_{42} = -k_1(\delta\epsilon(\gamma_1^2 + 1)hk_q - e^2(\gamma_1 - 1)(\gamma_1 + 1))\nu\rho_1\omega\varphi_o \quad (2-123)$$

$$b_{43} = b_{13} \quad (2-124)$$

$$b_{44} = b_{14} \quad (2-125)$$

$$b_{51} = 0 \quad (2-126)$$

$$b_{52} = 2\delta e\epsilon(\gamma_1 - 1)^2\gamma_2k_q\varphi_o \quad (2-127)$$

$$b_{53} = b_{13} \quad (2-128)$$

$$b_{54} = b_{14} \quad (2-129)$$

## 2.7 Impedance

The theoretical complex-valued expression for the impedance,  $Z$ , will be used in the analysis of the experimental results which is presented in Chapter 3. The impedance of the

sensor is defined as the voltage across the sensor,  $v$ , divided by the current through the sensor,  $i$ , shown in Figure 2.2.

The current through the sensor,  $i$ , is the time rate of change of total free charge on an electrode of the sensor. Let the total free charge on one electrode be  $Q_f$ . Then the current,  $i$ , through the sensor is, by definition

$$i = \frac{dQ_f}{dt} \quad (2-130)$$

The free charge density,  $\rho_f$ , is found by combining equation (2-11),  $E_{i,s} = \rho/\epsilon_0$ , equation (2-17),  $\rho = \rho_f - P_{i,s}$ , and the definition of the electric displacement, equation (2-24),  $D_s = \epsilon_0 E_s + P_s$ . The result is

$$D_{i,s} = \rho_f \quad (2-131)$$

The total free charge,  $Q_f$ , is obtained by integrating (2-131) over the volume,  $V$ , of the dashed region shown in Figure 2.2. This region is a very thin box that encloses the interface between the quartz and the metal electrode. All of the free charge on the metal electrode is at the interface side of the electrode, the row of plus signs for the polarity of  $v$  which is indicated.

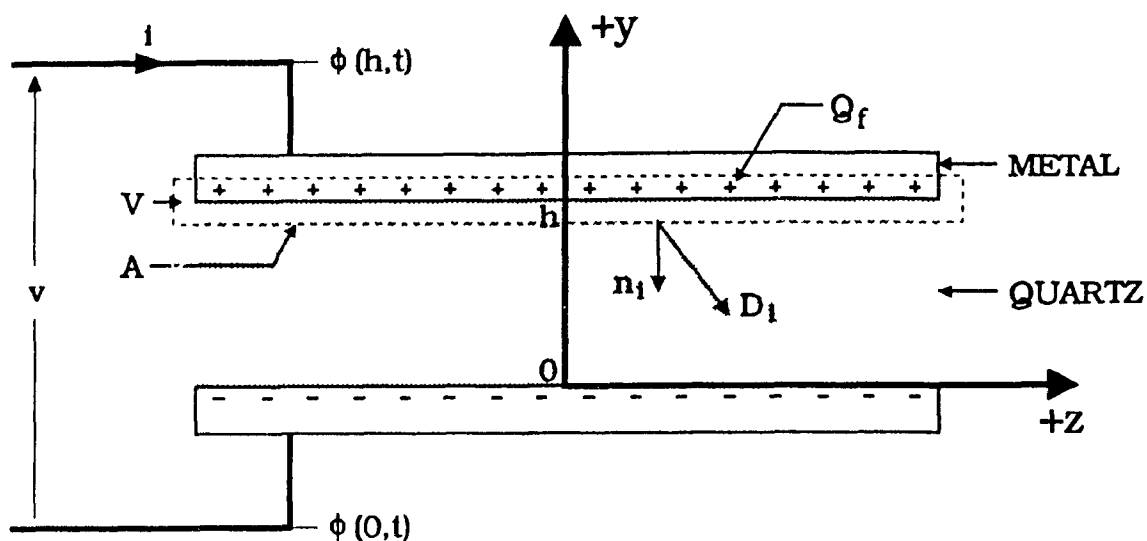


Figure 2.2 Total free charge,  $Q_f$ , found by surface integration of the electric displacement,  $D_i$ .

The result of the integration of (2-131) is

$$\int_V D_{i,i} dV = \int_V \rho_f dV \quad (2-132)$$

where the right side of (2-132) is the total free charge on the electrode,  $Q_f$ . The left side of (2-132) is converted to a surface integral over the area,  $A$ , of the region in Figure 2.2 by the application of the divergence theorem. The total free charge,  $Q_f$ , from (2-132) is

$$Q_f = \int_A D_i n_i dA \quad (2-133)$$

From (2-74) to (2-76),  $D_i$  lies in the  $yz$ -plane as shown in Figure 2.2. Furthermore there is only a flux of  $D_i$  through the bottom surface of the region, the surface which is in the quartz. There is no  $D_i$  in the metal electrode. The unit

normal,  $n_1$ , of the bottom surface points downward since the the unit normal points outward from the region. Therefore the components of  $n_i$  are  $n_x = 0$ ,  $n_y = -1$  and  $n_z = 0$ . From (2-75), (2-91), and (2-96), (2-133) reduces to

$$Q = \epsilon A a_3 e^{j\omega t} \quad (2-134)$$

From (2-130) and (2-134), the current,  $i$ , flowing through the quartz sensor is

$$i = \frac{dQ_f}{dt} = j\omega \epsilon A a_3 e^{j\omega t} \quad (2-135)$$

The voltage across the sensor,  $v$ , is the potential at the top electrode minus the potential at the bottom electrode, Figure 2.2. Using (2-89) and (2-90),

$$v = \varphi(h, t) - \varphi(0, t) = 2\varphi_0 e^{j\omega t} \quad (2-136)$$

The impedance of the sensor,  $Z$ , is defined as

$$Z = \frac{v}{i} \quad (2-137)$$

Substitute for  $i$  from (2-135) and  $v$  from (2-136).

$$Z = \frac{2\varphi_0}{j\omega \epsilon A a_3} \quad (2-138)$$

Using (2-107), (2-138) reduces to the final form for the impedance,  $Z$ , given by

$$Z = -\frac{2j}{A \omega \epsilon} \left[ \frac{\alpha b_{34} + b_{33}}{\alpha b_{32} + b_{31}} \right] \quad (2-139)$$

The impedance is a function of five properties of quartz, ( $\rho_q, c, \eta, \epsilon, e$ ), two properties of the liquid ( $\rho_l, \nu$ ), one property of the interface ( $\alpha$ ), two geometrical properties ( $A$  and  $h$ ) and the angular frequency ( $\omega$ ). In the next chapter the interfacial slip parameter,  $\alpha$ , will be determined by fitting the theoretical complex-valued expression for the impedance,  $Z$ , to the corresponding experimental values of  $Z$ .

## CHAPTER 3

### EXPERIMENT

#### Introduction

The interfacial slip parameter is found for sensors with hydrophilic and hydrophobic coatings in water-glycerol solutions. This is done by fitting the experimental values of impedance measured by the network analysis method to the theoretical expression for the impedance derived in the last chapter.

The experimental method, Section 3.1, is the network analysis method developed by Kipling and Thompson (1990). A piezoelectric quartz sensor is completely characterized by this method by repeatedly measuring the magnitude and phase of the impedance over the resonant region of the sensor. Non-linear regression analysis, Section 3.2, is used to fit the complex-valued experimental values of impedance to the theoretical expression for impedance. The experimental data for the sensors in air are fitted to theory, Section 3.3, and the piezoelectric coefficient,  $e$ , the viscoelastic coefficient,  $\eta$ , thickness of the sensor,  $h$ , and effective area of the sensor,  $A$ , are found. Then the experimental data for the sensors in water-glycerol solutions are fitted to theory, Section 3.4, and the interfacial slip parameter,  $\alpha$ , is found as well as the effective area of the sensor,  $A$ . The

interfacial slip parameter is presented and discussed in terms of the kinematic viscosity and mole fraction of the water-glycerol solutions, Section 3.5.

### 3.1 Experimental Method

#### 3.1.1 Sensors and Liquid

##### Hydrophilic Sensor

The hydrophilic sensor, consists of a silver (Ag) plated AT-cut 9-MHz quartz crystal unit coated with a hydrophilic (water-loving) chemical coating whose chemical formula is  $\text{COOH}(\text{CH}_2)_{10}\text{SH}$  and name is 1-mercapto undecanoic acid. This molecule is a chain,  $\text{COOH}-\text{CH}_2-\dots-\text{CH}_2-\text{SH}$ , with the SH strongly bonded to the silver surface and the COOH end in contact with the liquid. The COOH is polar and therefore attracts the water molecules which are also polar. Figure 3.1(a) shows the sensor with the hydrophilic coating. This sensor is designated 9AgLic.

##### Hydrophobic Sensor

The hydrophobic sensor, consists of a silver (Ag) plated AT-cut 9-MHz quartz crystal unit coated with a hydrophobic (water-fearing) chemical coating whose chemical formula is  $\text{CH}_3(\text{CH}_2)_{15}\text{SH}$  and name is n-hexadecane thiol (or 1-mercapto hexadecane). This molecule is a chain,  $\text{CH}_3-\text{CH}_2-\dots-\text{CH}_2-\text{SH}$ , with the SH strongly bonded to the silver surface and  $\text{CH}_3$  in contact with the liquid. Unlike the hydrophilic molecule, the



$\text{CH}_3$  is non-polar and therefore interacts weakly with the water molecules. Figure 3.1(b) shows the sensor with the hydrophobic coating. This sensor is designated 9AgBic.

### **Liquid**

The liquid used in the experiment consists of water-glycerol solutions of varying concentrations ranging from pure water to pure glycerol in steps of 0.1 mole fraction of glycerol in water.

#### **3.1.2 Experimental Arrangement**

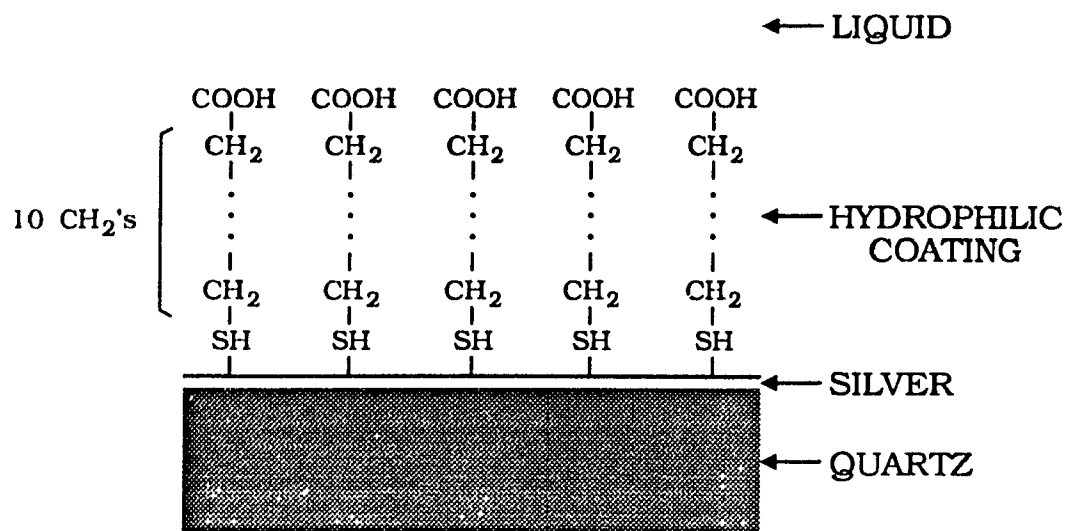
The following equipment, was used in the measurement of the magnitude and phase of the impedance,  $Z$ , for both the hydrophilic and hydrophobic sensors. Figure 3.2(a) shows the structure of the piezoelectric quartz sensor, not drawn to scale. The sensor is a thin disk of quartz with a very thin metal electrode on each surface in the shape shown in the figure. Figure 3.2(b) shows the sensor with a chemical coating attached to one of the electrodes and a liquid in contact with the coating. The network analysis system consists of the following equipment:

HP-4195A Network Spectrum Analyzer

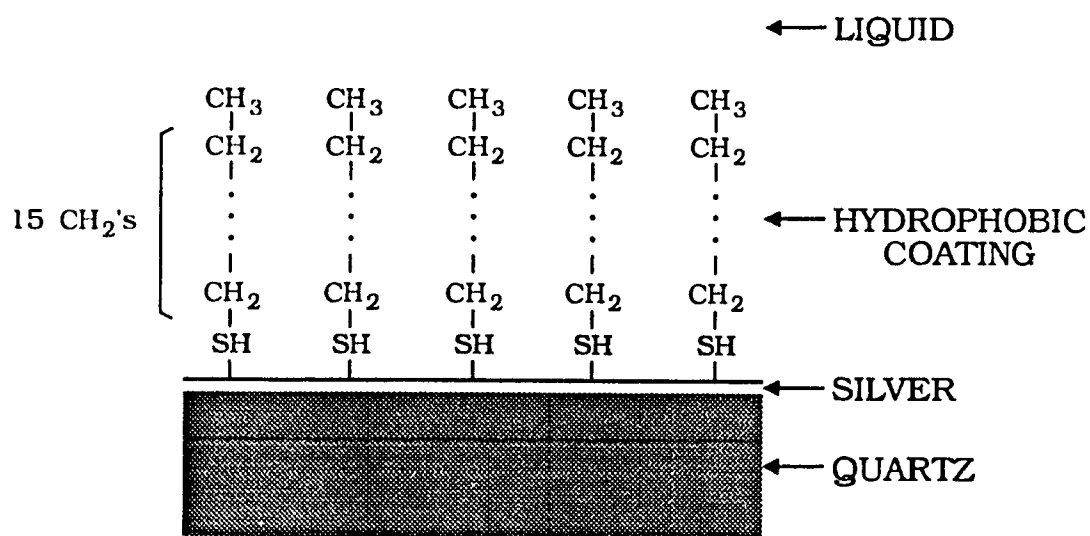
HP-41951A Impedance Test Kit

HP-16092A Spring Clip Fixture

The sensors are installed in an assembly not shown in Figure 3.2(b) and the assembly is connected to the Spring Clip Fixture.



(a)



(b)

Figure 3.1 Sensor in liquid with (a) hydrophilic coating and (b) hydrophobic coating.

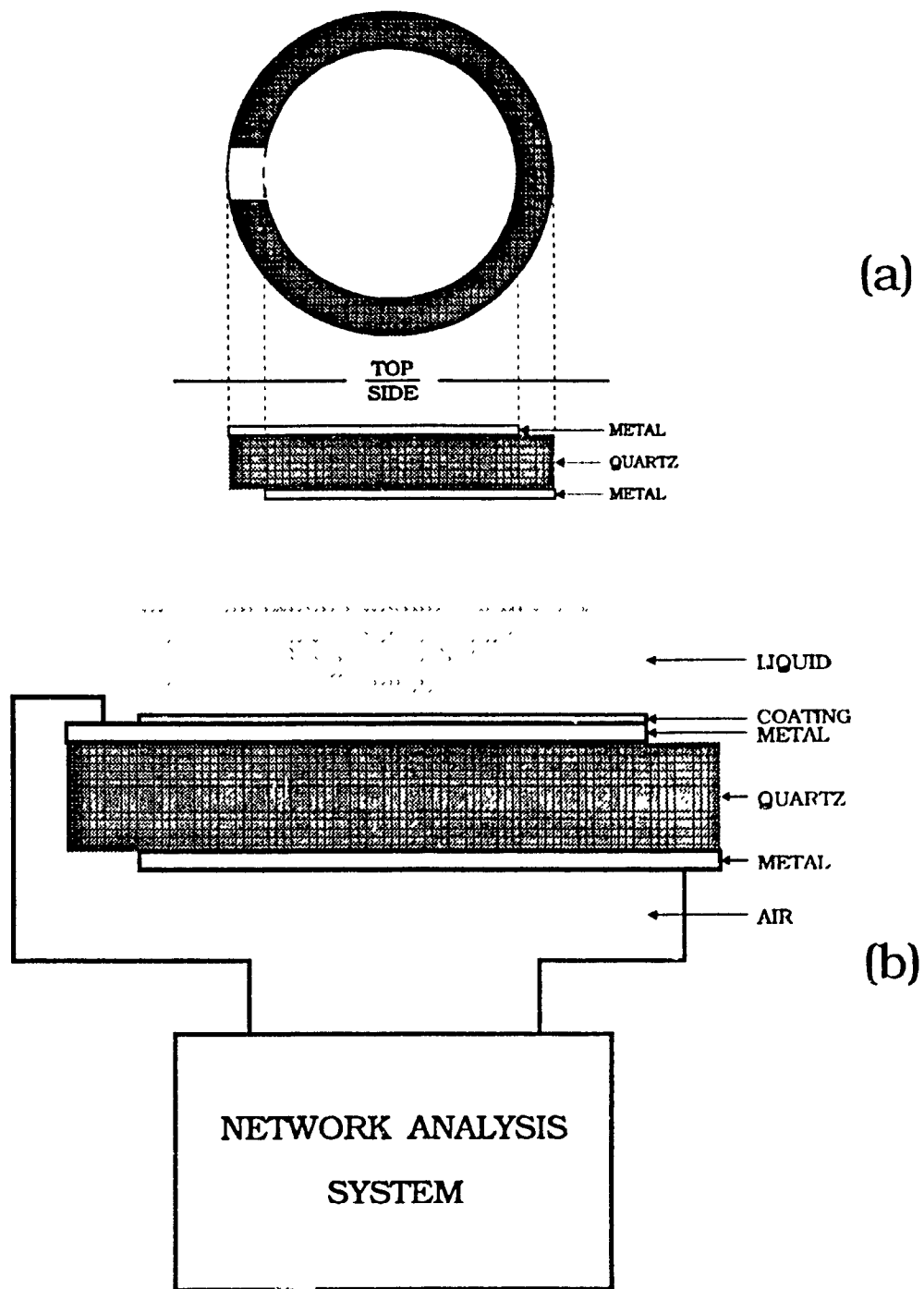


Figure 3.2 Experimental arrangement showing (a) the top and side views of the piezoelectric quartz sensor and (b) the sensor in liquid connected to the network analysis system.

The experimental measurement process consists of two parts: measurement in air and measurement in liquid.

#### **Air**

The magnitude,  $|Z|$ , and phase,  $\theta_z$ , of the impedance,  $Z$ , for both 9AgLic and 9AgBic were measured in air. The measurement of  $|Z|$  and  $\theta_z$ , was carried out over the closed frequency interval  $I = [f_0, f_1]$ . The closed interval,  $I$ , consists of  $N = 401$  equally spaced frequency points, in the stepsize of,  $\Delta f = (f_1 - f_0)/N$ . The nominal resonant frequency,  $f_0$ , is midway between  $f_0$  and  $f_1$ . The difference between  $f_1$  and  $f_0$  is called the frequency span. The nominal resonant frequency is  $f_0 = 9$  MHz and the typical frequency span is 80 kHz.

#### **Liquid**

The magnitude,  $|Z|$ , and the phase,  $\theta_z$ , of the impedance were measured for both sensors in water-glycerol solutions of varying concentrations, ranging from pure water to pure glycerol in steps of 0.1 mole fraction. At each concentration, the closed interval  $I$  was modified, that is, the frequency span was either increased or decreased so as to ensure that measurements were made over the complete resonant region.

The preparation of the water-glycerol solutions was done 24 hours in advance so as to ensure that the solution would be in its equilibrium state. The water-glycerol solution is said to be in equilibrium when there is no diffusitory action

between water and glycerol. The liquid solution may be considered to a very good approximation to be in its equilibrium state, that is, the water-glycerol solution is homogenous throughout.

### 3.2 Non-Linear Regression Analysis

#### 3.2.1 Statement of the Non-Linear Regression Analysis Problem

Given a complex-valued function  $F(p_1, \dots, p_n, \omega)$  of  $n$  complex-valued parameters,  $p_1, \dots, p_n$  and angular frequency,  $\omega$ , determine  $p_1, \dots, p_n$  such that the function  $F(p_1, \dots, p_n, \omega)$  is a good fit to the experimental data.

#### 3.2.2 Definition of Sum Of Squares Of Errors, SSE

The optimization of  $F(p_1, \dots, p_n, \omega)$ , with respect to the experimental data,  $\{\omega_i, y_i\}$  ( $i = 1, \dots, N$ ,  $N =$  the number of experimental data points), is achieved by minimizing the "Sum Of Squares Of Errors",  $SSE(p_1, \dots, p_n)$  defined by

$$SSE(p_1, \dots, p_n) = \frac{1}{N} \sum_{i=1}^N |y_i - F(p_1, \dots, p_n, \omega_i)|^2 \quad (3-1)$$

In general, the experimental data is considered to be complex-valued, that is,  $y_i \in \mathbb{C}$  (where  $\mathbb{C}$  denotes the field of complex numbers) for each  $i = 1, \dots, N$ . Physically the quantity,  $|y_i - F(p_1, \dots, p_n, \omega_i)|^2$  represents the square of the

distance between the two complex numbers  $y_i$  and  $F(p_1, \dots, p_n, \omega_i)$  in the complex plane  $\mathbb{C}$  for each  $i = 1, \dots, N$ . Thus the function, SSE, is simply the sum of the squares of the distances between  $y_i$  and  $F(p_1, \dots, p_n, \omega_i)$  ( $i = 1, \dots, N$ ). Since  $SSE(p_1, \dots, p_n) \geq 0$  for all  $p_k \in \mathbb{C}^n$ , where,  $p_k = (p_1, \dots, p_n)$ . Then  $SSE(p_1, \dots, p_n)$  has an absolute minimum at some point,  $p_{k_0} \in \mathbb{C}^n$ . The point,  $p_{k_0} = (p_{01}, \dots, p_{0n})$  is called the "best-fit point". The  $n$  coordinates,  $p_{01}, \dots, p_{0n}$  are called the " $n$  best-fit parameters". Thus at  $p_k = p_{k_0}$ ,  $SSE(p_{k_0}) = SSE(p_{01}, \dots, p_{0n}) = 0$ .

### 3.2.3 Condition for SSE to be a Minimum

At  $p_k = p_{k_0}$ ,  $SSE(p_k)$  as an absolute minimum. To determine the best fit point  $p_k = p_{k_0}$ , take the total differential of  $SSE(p_k)$ .

$$dSSE(p_1, \dots, p_n) = \frac{1}{N} \sum_{i=1}^N \frac{\partial SSE(p_1, \dots, p_n)}{\partial p_i} dp_i \quad (3-2)$$

The condition for  $SSE(p_1, \dots, p_n)$  to be a minimum is given by

$$dSSE(p_1, \dots, p_n) = 0 \quad (3-3)$$

### 3.2.4 Definition of Normal Equations

Using condition (3-3), and the fact that the  $dp_i$  for each  $i = 1, \dots, n$  are all independent of each other, the normal equations from condition (3-3) are given by

$$\frac{\partial SSE(p_1, \dots, p_n)}{\partial p_i} = 0, \quad i = 1, \dots, n \quad (3-4)$$

The above system of normal equations, constitutes a system of  $n$  non-linear algebraic equations in the  $n$  unknowns,  $p_1, \dots, p_n$ . The numerical solution to the above non-linear algebraic system, yields the desired best fit point  $p_k = p_{k^*}$ , that is

$$\frac{\partial SSE(p_{1^*}, \dots, p_{n^*})}{\partial p_i} = 0, \quad i = 1, \dots, n \quad (3-5)$$

### 3.2.5 Example

In Appendix 4, Mathcad program DOC1.MCD demonstrates non-linear regression analysis. A simple example is used to show how Mathcad's **Minerr** function is used to perform a non-linear curve-fitting procedure to a non-linear multi-valued complex-valued function denoted by  $Z$ . The function  $Z$  models the electrical impedance of a series RLC circuit. Thus the function,  $Z = Z(R, L, C, \omega)$ , depends on three parameters,  $R$ ,  $L$ , and  $C$ , which, denote respectively the resistance, inductance and the capacitance of the series RLC circuit, and the angular frequency,  $\omega$ , which is defined as  $\omega = 2\pi f$  where  $f$  is the frequency. The impedance,  $Z$ , is given by

$$Z = R + j\left(\omega L - \frac{1}{\omega C}\right) \quad (3-6)$$

The resonant frequency,  $f$ , is defined as the frequency at which  $Z$  is real, or equivalently, the frequency at which the phase of  $Z$  is zero. The resonant frequency,  $f$ , is given by

$$f = \frac{1}{2\pi} \frac{1}{\sqrt{LC}} \quad (3-7)$$

The function  $Z = Z(R, L, C, \omega)$ , is fitted to the complex-valued data consisting of  $Z_i = Z(R, L, C, \omega_i)$ , where  $R$  and  $L$  are given arbitrary values of 10.0 k $\Omega$  and 10.0 mH respectively. The value for  $C$  was computed from equation (3-7) using  $f = 9.0$  MHz. Given that  $L = 10.0$  mH, the value of  $C$  is,  $C = 0.031$  pF. The function  $Z$  is computed over the closed frequency interval,  $I = [8.0 \text{ MHz}, 10.0 \text{ MHz}]$  and then randomized using Mathcad's `rnd` function. The exact data for  $Z$  is randomized so as to simulate an experimental data set. The interval  $I$ , is chosen, so that the centre frequency of  $I$ , corresponds to the resonant frequency of the series RLC circuit.

The non-linear curve-fitting procedure, implemented by Mathcad's `Minerr` function, implements the Levenberg-Marquardt method. The Levenberg-Marquardt method, a quasi-Newton method, is a variation of the gradient method. In Newton's method, each entry of the jacobian is computed via a numerical differentiation procedure. In contrast, in the quasi-Newton method, each entry of the jacobian is replaced by an appropriate finite-difference approximation. The Levenberg-



Marquardt algorithm uses a down-hill search method (gradient method) to obtain an initial estimate of the parameters in question. Once an initial estimate of the parameters have been made, the algorithm then uses the quasi-Newton method to refine the initial estimates of the parameters to the desired accuracy.

Mathcad's non-linear curve-fitting procedure is effectuated by providing both the function  $SSE(L)$  and the appropriate guess value  $L$  denoted by  $L_{guess}$ . Once the appropriate guess value for  $L$  as been given, the best fit value for  $L$  denoted by  $L_{fit}$  is obtained by minimizing  $SSE(L)$  via Mathcad's **Minerr** function. The value of  $L_{fit}$  is 10.002 mH.

From Figure 3.3,  $SSE(L)$  has only one absolute minimum in the interval [1.0 mH, 20.0 mH]. The absolute minimum of  $SSE(L)$  occurs at  $L = 10.0$  mH. Since  $SSE$  has only one absolute minimum in the interval [1.0 mH, 20.0 mH], then any value for  $L$  within the above mentioned interval can serve as an appropriate guess value for  $L$ .

Figures 3.4 and 3.5 give the magnitude and phase, respectively, of the impedance of the RLC series circuit, and show the simulated experimental data produced by the Mathcad **rnd** function and the fitted curve.

### 3.3 Fitting of Theory to Experiment in Air

In Section 2.6 of Chapter 2, the expression for the impedance,  $Z$ , of the coated sensor in air is given by

$$Z_a = \frac{\zeta_a}{A} \quad (3-8)$$

where

$$\zeta_a = \zeta_a(e, \eta, h, \omega) = 2j \frac{b_{33}}{b_{31}} \quad (3-9)$$

with

$$b_{31} = \delta (\gamma_1 - 1) k_q (\delta \epsilon (\gamma_1 + 1) h k_q + 2 e^2 (\gamma_1 - 1)) \quad (3-10)$$

and

$$b_{33} = 2 \delta^2 \epsilon (\gamma_1 - 1) (\gamma_1 + 1) k_q^2 \quad (3-11)$$

where  $\gamma_1 = \exp(jhk_q)$  and  $\delta = \eta\omega - jc$

with

$$k_q = k_q(e, \eta, \omega) = \omega \left[ \frac{\rho_q}{c(e) + j\omega\eta} \right]^{1/2} \quad (3-12)$$

and

$$\bar{c} = \bar{c}(e) = c + \frac{e^2}{\epsilon} \quad (3-13)$$

From an examination of (3-9) to (3-13),  $\zeta_a$  is a complex-valued function which is independent of the effective surface area, A.  $\zeta_a$  in terms of rectangular coordinates in the complex plane is expressed as

$$\zeta_a = \zeta_{Re} + j \zeta_{Im} \quad (3-14)$$

From (3-9) the magnitude of Z,  $|Z|$ , is

$$|Z| = \frac{1}{A} \sqrt{\zeta_{Re}^2 + \zeta_{Im}^2} \quad (3-15)$$

and the phase of Z,  $\theta_z$ , is

$$\theta_z = \arctan \left( \frac{\zeta_{Im}}{\zeta_{Re}} \right) \quad (3-16)$$

Note that  $|Z|$  is inversely proportional to A and  $\theta_z$  is independent of A.

Appendix 5 is Mathcad program DOC2.MCD which fits theory to experiment in air. The theoretical complex-valued expression for the impedance, Z, of the hydrophilic and hydrophobic coated sensor in air is fitted to the corresponding experimental data for the impedance, Z, via a

three-step process. The three steps are:

- (1) The Fitting Of  $\theta_z$  To Experiment In Air
- (2) The Fitting Of  $|Z|$  To Experiment In Air
- (3) The Fitting Of  $Z$  To Experiment In Air

In air the theoretical complex-valued expression for the impedance,  $Z$ , is given by

$$Z_a = Z_a(c, e, \epsilon, \eta, \rho_q, h, A, \omega) \quad (3-17)$$

The values for the elastic constant of quartz,  $c$ , the dielectric stress constant of quartz,  $\epsilon$ , and the mass density of quartz,  $\rho_q$ , are, from Tiersten (1969),

$$c = 29.01 \cdot 10^9 \text{ N/m}^2$$

$$\epsilon = 39.82 \cdot 10^{-12} \text{ C/V m}$$

$$\rho_q = 2649 \text{ kg/m}^3$$

The fitting of (3-17) to the experimental data is achieved by varying four parameters: the piezoelectric stress constant of quartz,  $e$ , the visco-elastic constant of quartz,  $\eta$ , the thickness of the coated sensor,  $h$ , and the effective surface area of the sensor,  $A$ . The variation of the parameters  $e$ ,  $\eta$ ,  $h$ , and  $A$  is achieved by the implementation of Mathcad's **Minerr** function, via Mathcad's Solve Block facility. Below is the outline of the three-step process.

In step 1, the appropriate guess values for the piezoelectric stress constant,  $e$ , the visco-elastic constant,  $\eta$ , and the thickness,  $h$ , denoted respectively by  $e_{\text{guess}}$ ,  $\eta_{\text{guess}}$ , and  $h_{\text{guess}}$  are chosen. Then the starting values for

$e$ ,  $\eta$ , and  $h$ , denoted respectively by  $e_{start}$ ,  $\eta_{start}$ , and  $h_{start}$ , are determined by minimizing the Sum Of Squares Of Errors,  $SSE1(e, \eta, h)$ , via Mathcad's `Minerr` function.

The values for  $e_{start}$ ,  $\eta_{start}$ ,  $h_{start}$ , and the guess value for the effective surface area  $A$ , denoted by  $A_{guess}$  are used in step 2 to determine the starting value for  $A$ , denoted by  $A_{start}$ . The determination of  $A_{start}$  is achieved by minimizing the Sum Of Squares Of Errors,  $SSE2(A)$ , via Mathcad's `Minerr` function.

Finally in step 3, using the values  $e_{start}$ ,  $\eta_{start}$ ,  $h_{start}$ , and  $A_{start}$ , best-fit values for  $e$ ,  $\eta$ ,  $h$ , and  $A$  denoted respectively by  $e_{fit}$ ,  $\eta_{fit}$ ,  $h_{fit}$ , and  $A_{fit}$ , are determined by minimizing the Sum Of Squares Of Errors,  $SSE3(e, \eta, h, A)$ , via Mathcad's `Minerr` function.

For the hydrophilic coated sensor in air, the best-fit values for  $e$ ,  $\eta$ ,  $h$ , and  $A$ , are denoted respectively by  $e_{1fit}$ ,  $\eta_{1fit}$ ,  $h_{1fit}$ , and  $A_{1fit}$ . For the hydrophobic coated sensor in air, the best-fit values for  $e$ ,  $\eta$ ,  $h$ , and  $A$ , are denoted respectively by,  $e_{2fit}$ ,  $\eta_{2fit}$ ,  $h_{2fit}$ , and  $A_{2fit}$ . Table 3.1 summarizes the final results for  $e$ ,  $\eta$ ,  $h$ , and  $A$ .

The piezoelectric stress coefficient,  $e$ , is found experimentally because if the value of  $e$  from the literature is used, it is not possible to fit the theoretical expression for  $\theta_z$  to the experimental data. From Tiersten (1969), page 60, the piezoelectric stress coefficient is  $e_{26} = -0.095 \text{ C/m}^2$  and from Table 3.1 the best-fit value of  $e$  is  $-0.0798 \text{ C/m}^2$ .

It is presumed that the value of  $e$  in the literature is incorrect. The value of the viscoelastic coefficient,  $\eta$ , was not found in the literature and therefore it was necessary to measure it.

**Table 3.1 Summary of Results for  $e$ ,  $\eta$ ,  $h$ , and  $A$**

Physical Properties	Hydrophilic Surface (Air)			Hydrophobic Surface (Air)		
	guess values	starting values	fitted values	guess values	starting values	fitted values
$e$ (C/m <sup>2</sup> )	-0.079	-0.07979	-0.07980	-0.079	-0.07979	-0.07980
$\eta$ (N·m/s <sup>2</sup> )	0.011	0.01187	0.008376	0.24	0.2438	0.2344
Geometrical Properties						
$h$ ( $\mu$ m)	183.87	183.878	183.879	183.98	183.986	183.979
$A$ (cm <sup>2</sup> )	0.28	0.2698	0.2984	0.25	0.2533	0.2575

Figures 3.6 through 3.9 are the plots of the experimental and fitted curves for  $|Z|$  and  $\theta_z$  for both the hydrophilic and hydrophobic coated sensors in air.

From Figures 3.6 through 3.9 the curves for the phase and magnitude of  $Z$  for the hydrophilic sensor in air, are less damped than the corresponding curves of the phase and

magnitude of  $Z$  for the hydrophobic sensor in air. The greater damping of the phase and magnitude of  $Z$  in the case of the hydrophobic sensor, is consistent with the results in Table 3.1. In Table 3.1 the value of  $\eta$  for the hydrophobic sensor in air is greater than the corresponding value of  $\eta$  for the hydrophilic sensor in air. The greater value of  $\eta$  for the case of the hydrophobic sensor in air, results in the damping effect of both the phase and magnitude of  $Z$ . Also the molecular weight of  $\text{CH}_3(\text{CH}_2)_{15}\text{SH}$  (258 g/mol), the hydrophobic coating, is greater than the molecular weight of  $\text{COOH}(\text{CH}_2)_{10}\text{SH}$  (218 g/mol). Thus a sensor coated with  $\text{CH}_3(\text{CH}_2)_{15}\text{SH}$  is expected to exhibit greater damping than a similar sensor coated with  $\text{COOH}(\text{CH}_2)_{10}\text{SH}$ . However, the viscoelastic coefficient of the sensors were not measured before they were coated and so it is possible that the higher  $\eta$  for the hydrophobic sensor, Table 3.1, is due, in part or in total, to the mechanical characteristics of the sensor.

#### 3.4 Fitting of Theory and Experiment in Liquid

In Section 2.6 of Chapter 2, the expression for the impedance,  $Z$ , of the liquid-loaded sensor is given by

$$Z_l = \frac{\zeta_l}{A} \quad (3-18)$$

For a liquid-loaded sensor, the expression for  $\zeta_1$ , equation (3-9), generalizes to

$$\zeta_1 = 2j \frac{\alpha b_{34} + b_{33}}{\alpha b_{32} + b_{31}} \quad (3-19)$$

where  $\alpha$  denotes the interfacial slip parameter which is a complex-valued property of the solid-liquid interface. The interfacial slip parameter,  $\alpha$ , expressed in rectangular coordinates of the complex plane, is

$$\alpha = \alpha_{Re} + j\alpha_{Im} \quad (3-20)$$

It is also instructive to express  $\alpha$  in terms of the polar coordinates in the complex plane,  $|\alpha|$  and  $\theta_\alpha$ , which are called the magnitude and phase of  $\alpha$ , respectively.

$$\alpha = |\alpha| e^{j\theta_\alpha} \quad (3-21)$$

The polar coordinates,  $|\alpha|$  and  $\theta_\alpha$ , expressed in terms of the rectangular coordinates,  $\alpha_{Re}$  and  $\alpha_{Im}$ , are

$$|\alpha| = \sqrt{\alpha_{Re}^2 + \alpha_{Im}^2} \quad (3-22)$$

and

$$\theta_\alpha = \arctan \left( \frac{\alpha_{Im}}{\alpha_{Re}} \right) \quad (3-23)$$



The expressions for  $b_{33}$  and  $b_{31}$  are given by (3-10) and (3-11) respectively. The quantities  $b_{32}$  and  $b_{34}$  are

$$b_{32} = 2 \delta \epsilon (\gamma_1^2 + 1) k_l k_q \nu \rho_l \omega \quad (3-24)$$

and

$$b_{34} = k_l (\delta \epsilon (\gamma_1^2 + 1) h k_q + e^2 (\gamma_1 - 1) (\gamma_1 + 1)) \nu \omega \rho_l \quad (3-25)$$

where

$$k_l = k_l(\nu, \omega) = \left[ \frac{\omega}{J \nu} \right]^{1/2} \quad (3-26)$$

The expressions for  $|Z|$  and  $\theta_z$  are given by equations which correspond to (3-15) and (3-16), respectively.

Appendix 6 is Mathcad program DOC3.MCD which fits theory to experiment in liquid. Using the values for  $e$ ,  $\eta$ ,  $h$ , and  $A$  found in air, the theoretical complex-valued expression for the impedance,  $Z$ , of the hydrophilic and hydrophobic coated sensor immersed in water-glycerol solutions of varying concentrations ranging from pure water to pure glycerol in steps of 0.1 mole fraction, is fitted to the corresponding experimental data for the impedance,  $Z$ .

In liquid, the theoretical complex-valued expression for the impedance,  $Z$ , is given by

$$Z_i = Z_i(c, e, \epsilon, \eta, \rho_q, \rho, \nu, \alpha, h, A, \omega) \quad (3-27)$$

In (3-27) the same values are used for  $c$ ,  $\epsilon$ , and  $\rho_q$  as used in  $Z_a$ , (3-17). In addition the values of the kinematic viscosity,  $\nu$ , and mass density,  $\rho_i$ , for each solution of water-glycerol which were used, are from the CRC Handbook of Chemistry and Physics, Lide (1990-91). Table 3.2 shows the values of  $\nu$  and  $\rho_i$ , for each mole fraction,  $M_f$ , used in the experiments.

Table 3.2 Values for  $M_f$ ,  $\nu$ , and  $\rho_i$  of Water-glycerol Solutions

Mole Fraction, $M_f$ of Glycerol in Water	Kinematic Viscosity $\nu$ (cS)	Mass Density $\rho_i$ (kg/L)
0.0 (Water)	1.002	0.9980
0.1	2.867	1.088
0.2	7.365	1.142
0.3	16.97	1.177
0.4	39.06	1.201
0.5	67.43	1.218
0.6	142.1	1.231
0.7	330.9	1.241
0.8	572.1	1.249
0.9	986.5	1.256
1.0 (Glycerol)	1398.	1.261

The parameters that are varied in the fitting of (3-27)

to the experimental data are the interfacial slip factor,  $\alpha$ , and the effective surface area,  $A$ . The above fitting is done for both the hydrophilic and hydrophobic coated sensors immersed in the water-glycerol solution.

For the hydrophilic coated sensor immersed in a water-glycerol solution, the guess and fitted values for  $\alpha$  and  $A$  are summarized by the following two expressions,  $(\alpha_{\text{guess}_{k_{\text{lic}}}}, A_{\text{guess}_{k_{\text{lic}}}})$  and  $(\alpha_{\text{fit}_{k_{\text{lic}}}}, A_{\text{fit}_{k_{\text{lic}}}})$ , for each  $k_{\text{lic}} = 1, \dots, 11$ . The subscripted variable,  $k_{\text{lic}}$ , takes on integral values from 1 to 11 inclusive, with  $k_{\text{lic}} = 1$  representing pure water and  $k_{\text{lic}} = 11$  representing pure glycerol. For the hydrophobic coated sensor immersed in a water-glycerol solution, the guess and fitted values for  $\alpha$  and  $A$  are summarized by the following two expressions,  $(\alpha_{\text{guess}_{k_{\text{bic}}}}, A_{\text{guess}_{k_{\text{bic}}}})$  and  $(\alpha_{\text{fit}_{k_{\text{bic}}}}, A_{\text{fit}_{k_{\text{bic}}}})$  for each  $k_{\text{bic}} = 1, \dots, 7$ . The subscripted variable  $k_{\text{bic}}$ , takes on integral values from 1 to 7 inclusive, with  $k_{\text{bic}} = 1$  representing pure water and  $k_{\text{bic}} = 7$  representing pure glycerol. For the case of the hydrophobic coated sensor immersed in the water-glycerol solution, four of the eleven data files for the magnitude and phase of  $Z$ , were corrupted, likely due to a poor electrical connection during the measurement process.

For the hydrophilic sensor immersed in the water-glycerol solution, for each,  $k_{\text{lic}} = 1, \dots, 11$ , the determination of the best-fit values for  $\alpha$  and  $A$  denoted by  $(\alpha_{\text{fit}_{k_{\text{lic}}}}, A_{\text{fit}_{k_{\text{lic}}}})$ , is achieved by minimizing the Sum Of Squares Of Errors,

SSElic( $\alpha_{klic}$ ,  $A_{klic}$ ,  $klic$ ) via Mathcad's **Minerr** function. For the hydrophobic sensor immersed in the water-glycerol solution, for each,  $kbic = 1, \dots, 7$ , the determination of the best-fit values for  $\alpha$  and  $A$  denoted by ( $\alpha_{fit_{kbic}}$ ,  $A_{fit_{kbic}}$ ), is achieved by minimizing the Sum Of Squares Of Errors, SSEbic( $\alpha_{kbic}$ ,  $A_{kbic}$ ,  $kbic$ ) via Mathcad's **Minerr** function. Tables 3.3 through 3.6 summarize the results for the guess and fitted values of  $\alpha$  and  $A$  for both the hydrophilic and hydrophobic coated sensors in water-glycerol solutions.

**Table 3.3 Interfacial Slip Parameter,  $\alpha$ , for Hydrophilic Sensor**

	Interfacial Slip Parameter, $\alpha$ Hydrophilic Sensor				
	guess values	fitted values			
Mole Fraction, $M_f$ of Glycerol in Water		$\alpha_{Rc}$	$\alpha_{lm}$	$ \alpha $	$\theta_\alpha$ (deg)
0.0 (Water)	3.76+2.30j	3.774	2.299	4.419	31.35
0.1	2.6+1.3j	2.631	1.246	2.911	25.34
0.2	1.9+0.6j	1.914	0.6510	2.022	18.79
0.3	1.6+0.4j	1.680	0.4000	1.727	13.39
0.4	1.4+0.2j	1.432	0.2130	1.447	8.461
0.5	1.3+0.1j	1.316	0.1180	1.321	5.110
0.6	1.1+0.07j	1.172	0.06900	1.174	3.393
0.7	0.92+0.01j	0.9370	0.01600	0.9370	1.000
0.8	0.8-0.003j	0.8930	-0.004000	0.8930	-0.2850
0.9	0.8-0.04j	0.8420	-0.04800	0.8440	-3.234
1.0 (Glycerol)	0.8-0.06j	0.8300	-0.06600	0.8320	-4.556

Table 3.4 Effective Surface Area, A, for Hydrophilic Sensor

Mole Fraction, $M_f$ of Glycerol in Water	Effective Surface Area, A (cm <sup>2</sup> ) Hydrophilic Sensor	
	guess values	fitted values
0.0 (Water)	0.4	0.4115
0.1	0.39	0.3911
0.2	0.34	0.3494
0.3	0.34	0.3509
0.4	0.34	0.3433
0.5	0.33	0.3316
0.6	0.32	0.3271
0.7	0.33	0.3255
0.8	0.32	0.3242
0.9	0.32	0.3236
1.0 (Glycerol)	0.32	0.3221

Table 3.5 Interfacial Slip Parameter,  $\alpha$ , for Hydrophobic Sensor

	Interfacial Slip Parameter, $\alpha$ Hydrophobic Sensor				
	guess values	fitted values			
Mole Fraction, $M_f$ of Glycerol in Water		$\alpha_{Re}$	$\alpha_{Im}$	$ \alpha $	$\theta_\alpha$ (deg)
0.0 (Water)	4.9+2.3j	5.003	2.290	5.503	24.60
0.1	3.2+1.2j	3.268	1.256	3.501	21.03
0.2	2.3+0.7j	2.346	0.6910	2.446	16.42
0.4	1.3+0.1j	1.398	0.1490	1.405	6.086
0.6	1.1+0.00093j	1.176	0.003000	1.176	0.1420
0.8	0.8-0.05j	0.8670	-0.04300	0.8680	-2.855
1.0 (Glycerol)	0.7-0.11j	0.8150	-0.1170	0.8230	-8.202

Table 3.6 Effective Surface Area,  $A$ , for Hydrophobic Sensor

Mole Fraction, $M_f$ of Glycerol in Water	Effective Surface Area, $A$ (cm <sup>2</sup> ) Hydrophobic Sensor	
	guess values	fitted values
0.0 (Water)	0.36	0.3681
0.1	0.37	0.3731
0.2	0.35	0.3584
0.4	0.34	0.3409
0.6	0.35	0.3526
0.8	0.33	0.3346
1.0 (Glycerol)	0.32	0.3399

Figures 3.10 to 3.17 are plots of the experimental and fitted curves for  $\theta_z$  and  $|Z|$  versus frequency,  $f$ .

### 3.5 Interfacial Slip Parameter, $\alpha$

#### 3.5.1 Plots of $\alpha$

Figures 3.18 to 3.25 plot the variation of the real part of  $\alpha$ ,  $\alpha_{Re}$ , the imaginary part of  $\alpha$ ,  $\alpha_{Im}$ , the magnitude of  $\alpha$ ,  $|\alpha|$ , and the phase of  $\alpha$ ,  $\theta_\alpha$ , versus kinematic viscosity,  $\nu$ , and mole fraction,  $M_f$ . In Appendix 7, Mathcad program DOC4.MCD performs a non-linear curve-fitting procedure to the experimental data consisting of  $\alpha_{Re}$ ,  $\alpha_{Im}$ ,  $|\alpha|$ , and  $\theta_\alpha$ , versus  $\nu$  and  $M_f$  by fitting the experimental data to the power law model,  $F(a,b,c,x) = ax^b + c$ , for the case of  $\alpha_{Re}$ ,  $\alpha_{Im}$ ,  $|\alpha|$ ,  $\theta_\alpha$  versus  $\nu$  and to the exponential law model,  $G(a,b,c,x) = ae^{bx} + c$ , for the case of  $\alpha_{Re}$ ,  $\alpha_{Im}$ ,  $|\alpha|$ ,  $\theta_\alpha$  versus  $M_f$ .

#### 3.5.2 Numerical Computation of the Real Part of $u_{(0)x}$ and $u_x$

Appendix 8 is Mathcad program DOC5.MCD which numerically computes the real part of  $u_{(0)x}$  and  $u_x$ . Using the values for  $\rho_q$ ,  $c$ ,  $e$ ,  $\epsilon$ ,  $\eta$ ,  $h$ , and  $A$  for the hydrophilic and hydrophobic sensor in air and the values for  $\alpha$  and  $A$  corresponding to the different mole fractions of glycerol in water for the hydrophilic and hydrophobic sensor in the water-glycerol solution, the real part of  $u_x$  and  $u_{(0)x}$  is computed over the time interval  $[t_s, t_f]$  in time steps of  $\Delta t$  for each  $klic = 1, \dots, 11$  for the case of the hydrophilic sensor and for each  $kbic =$

1, ..., 7 for the case of the hydrophobic sensor. The maximum displacement of the real part of  $u_x$  and  $u_{(0)x}$  for the case of the hydrophilic and hydrophobic sensor was computed by Mathcad's **max** function. The resulting data for the maximum displacement of the real part of  $u_x$  and  $u_{(0)x}$  versus  $\nu$  was then fitted to the power law model  $F(a,b,c,x)$  by Mathcad's **Minerr** function for both the hydrophilic and hydrophobic sensor.

### 3.5.3 Discussion of the Variation of $\alpha$ versus Low Values of $\nu$

In the plots shown in Figures 3.18 and 3.20 at low viscosity values, for the case of the hydrophilic coated sensor immersed in pure water, both  $\alpha_{kc}$  and  $|\alpha|$  are approximately equal to 3.8 and 4.4, respectively. For the case of the hydrophobic coated sensor immersed in pure water, both  $\alpha_{kc}$  and  $|\alpha|$  are approximately equal to 5.0 and 5.5, respectively.

The results at low viscosities for the hydrophilic and hydrophobic surfaces can be interpreted in terms of the greater strength of electrical attraction between a water molecule and a hydrophilic molecule than between a water molecule and a hydrophobic molecule. As the force between the water molecule and the surface molecule increases, the motion of the water molecule will more closely follow the motion of the molecule on the surface, that is,  $|\alpha|$  will approach 1. From Figure 3.20, this is indeed the case;  $|\alpha|$  for the hydrophilic sensor is closer to 1 than  $|\alpha|$  for the hydrophobic



sensor. From Figure 3.21 the sign of the phase,  $\theta_n$ , for both the hydrophilic and hydrophobic sensors means that the liquid particle displacement  $u_{(l)x}$ , leads the quartz particle displacement  $u_x$ , at the interface. Because  $u_{(l)x}$  leads  $u_x$ ,  $u_{(l)x}$  will achieve its maximum displacement at an earlier time than  $u_x$ . Figure 3.26 depicts the time variation of the real part of  $u_x$  and  $u_{(l)x}$  both for the hydrophilic and hydrophobic sensor immersed in pure water. Notice that for both the hydrophilic and hydrophobic sensor, the real part of  $u_{(l)x}$  leads the real part of  $u_x$ . Also from Figure 3.26 the maximum displacement of the real part of  $u_{(l)x}$  for the case of the hydrophilic sensor is greater than the maximum displacement of the real part of  $u_{(l)x}$  for the case of the hydrophobic sensor. By the same token the maximum displacement of the real part of  $u_x$  for the case of the hydrophilic sensor is greater than the maximum displacement of the real part of  $u_x$  for the case of the hydrophobic sensor. This result is to be expected, since for the case of the hydrophobic sensor, the molecular weight of the hydrophobic coating is greater than the molecular weight of the hydrophilic coating in the case of the hydrophilic sensor. The greater molecular weight of the hydrophobic coating induces a greater mass-loading effect than that induced by the hydrophilic coating. A greater mass-loading effect in the case of the hydrophobic sensor, means that for a given input voltage drop across the sensor, the electric field generated, will produce a transverse particle

displacement inversely proportional to the mass of the coating in question. Thus in the case of the hydrophobic sensor the maximum displacement of the real part of the transverse particle displacement,  $u_x$  will be less than the corresponding maximum displacement of the real part of  $u_x$  for the case of the hydrophilic sensor.

Also from Figures 3.18 and 3.20, at low viscosity values, the fact that  $|u_{(0)x}| \neq |u_x|$  at the solid-liquid interface, implies that there is slip between the top surface of the coating in contact with the bottom surface of the liquid. Thus at low viscosity values, the interfacial slip parameter,  $\alpha$ , satisfies the slip condition given by

$$\alpha \neq 1 \qquad (3-28)$$

Figure 3.27 depicts the plots of the maximum displacement of the real part of  $v_x$  and  $u_{(0)x}$  versus  $\nu$  for both the hydrophilic and hydrophobic sensor. From Figure 3.27, for low values of viscosity  $\nu$ , the maximum displacement of the real part of  $u_{(0)x}$  for the case of the hydrophilic sensor is greater than the maximum displacement of the real part of  $u_{(0)x}$  for the case of the hydrophobic sensor. Again this result is expected, since for the case of pure water, the hydrophilic interaction that occurs at the solid-liquid interface is greater than the corresponding hydrophobic interaction. The traction force between the wheels of a car and a dry road

produces a greater displacement of the car, than the displacement that would occur if the wheels of the same car were in contact with an icy road. In much the same way, the greater strength of the hydrophilic interaction between the hydrophilic surface and the water molecules at the solid-liquid interface will produce a greater displacement of the water molecules in the vicinity of the interface than the displacement that would occur if the interaction at the solid-liquid interface were hydrophobic in character. Thus the displacement of the water molecules in the vicinity of a hydrophobic interface is less than the displacement of the water molecules in the vicinity of a hydrophilic interface.

#### 3.5.4 Discussion of the Variation of $\alpha$ versus High Values of $\nu$

From Figures 3.18 and 3.20, as the kinematic viscosity,  $\nu$ , increases towards higher values of viscosity, both  $\alpha_{Rc}$  and  $|\alpha|$  approach unity for both the hydrophilic and hydrophobic coated surfaces. However from Figure 3.19 as  $\nu$  increases towards higher values of viscosity,  $\alpha_{lm}$  approaches zero. This is to be expected, since the strength of the interaction at the solid-liquid interface between water molecules in contact with the coating molecules at the interface, increases as  $\nu$  increases towards higher values of viscosity. For values of  $\nu \gg 1$ , from Figures 3.18, 3.19, and 3.20,  $\alpha_{Rc} \approx 1$ ,  $\alpha_{lm} \approx 0$ , and  $|\alpha| \approx 1$  respectively. From Figure 3-21 as  $\nu$  increases towards higher values of viscosity,  $\theta_\alpha$  decreases until, at some

critical value for kinematic viscosity,  $\nu = \nu_c$ ,  $\theta_\alpha = 0$ . From (3-23)  $\theta_\alpha = 0$  when  $\alpha_{lm} = 0$ . As noted above, from Figure 3.20, for high values of kinematic viscosity,  $\nu$ , the  $|\alpha| = 1$ , which implies that  $|u_{(0)x}| = |u_x|$ , which in turn implies that  $u_{(0)x} = u_x$ . The condition,  $u_{(0)x} = u_x$  implies that at the solid-liquid interface, there is no slip. The no slip condition is given by

$$\alpha = 1 \quad (3-29)$$

From Figure 3.27 over the entire viscosity range from pure water to pure glycerol the maximum displacement of the real part of  $u_{(0)x}$  for the case of the hydrophilic sensor is greater than the maximum displacement of the real part of  $u_{(0)x}$  for the case of the hydrophobic sensor. The same holds true for the maximum displacement of the real part of  $u_x$ . This is to be expected since the strength of the interaction of a hydrophilic surface in contact with a water-glycerol solution at the interface, on the average will be greater than the strength of the interaction between a hydrophobic surface and the water-glycerol solution in question.

### 3.5.5 Variation of $\alpha$ with Mole Fraction, $M_f$

The results for  $\alpha_{Re}$ ,  $\alpha_{Im}$ ,  $|\alpha|$ , and  $\theta_\alpha$  versus mole fraction,  $M_f$ , plotted in Figures 3.22 through 3.25 are the same as the results for  $\alpha_{Re}$ ,  $\alpha_{Im}$ ,  $|\alpha|$ , and  $\theta_\alpha$  versus kinematic viscosity,  $\nu$ , as plotted in Figures 3.18 through 3.21. The fact that the

above two results are the same can be seen from Figure 3.28. From Figure 3.28, low values of mole fraction correspond to low values of kinematic viscosity, whereas high values of mole fraction correspond to high viscosity values. From Figure 3.28,  $M_f = 0$  corresponds to pure water with a viscosity value of  $\nu = 1.00$  cS, and  $M_f = 1$  corresponds to pure glycerol with a viscosity value of  $\nu = 1400$  cS. Thus the variation between  $\nu$  and  $M_f$  as plotted in Figure 3.28, is such that the variation of  $\alpha_{Re}$ ,  $\alpha_{Im}$ ,  $|\alpha|$ , and  $\theta_\alpha$  versus  $M_f$  and  $\nu$  are similar.

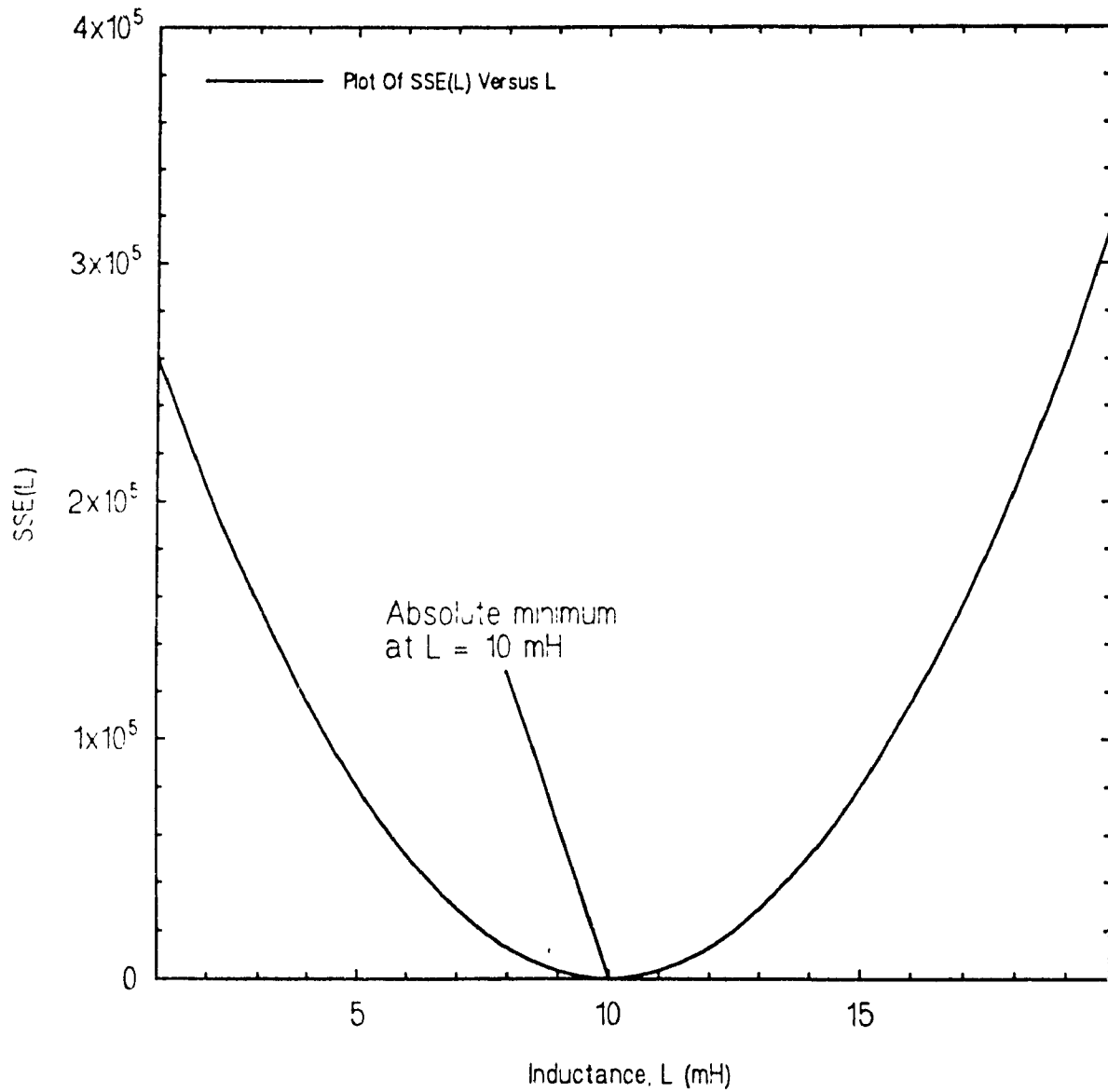


Figure 3.3 Sum Of Squares Of Errors for a series RLC circuit.

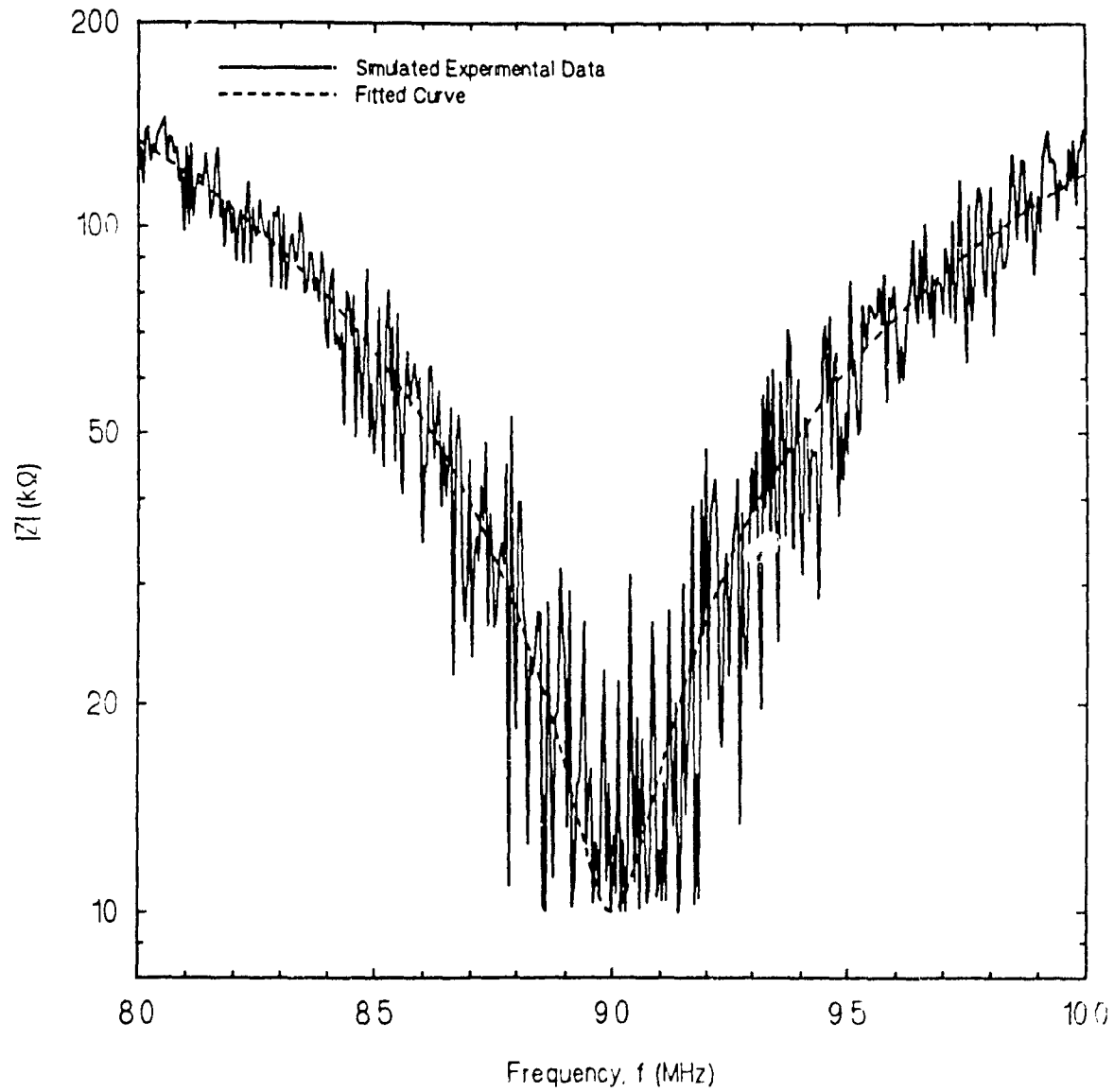


Figure 3.4 Magnitude of impedance for a series RLC circuit.

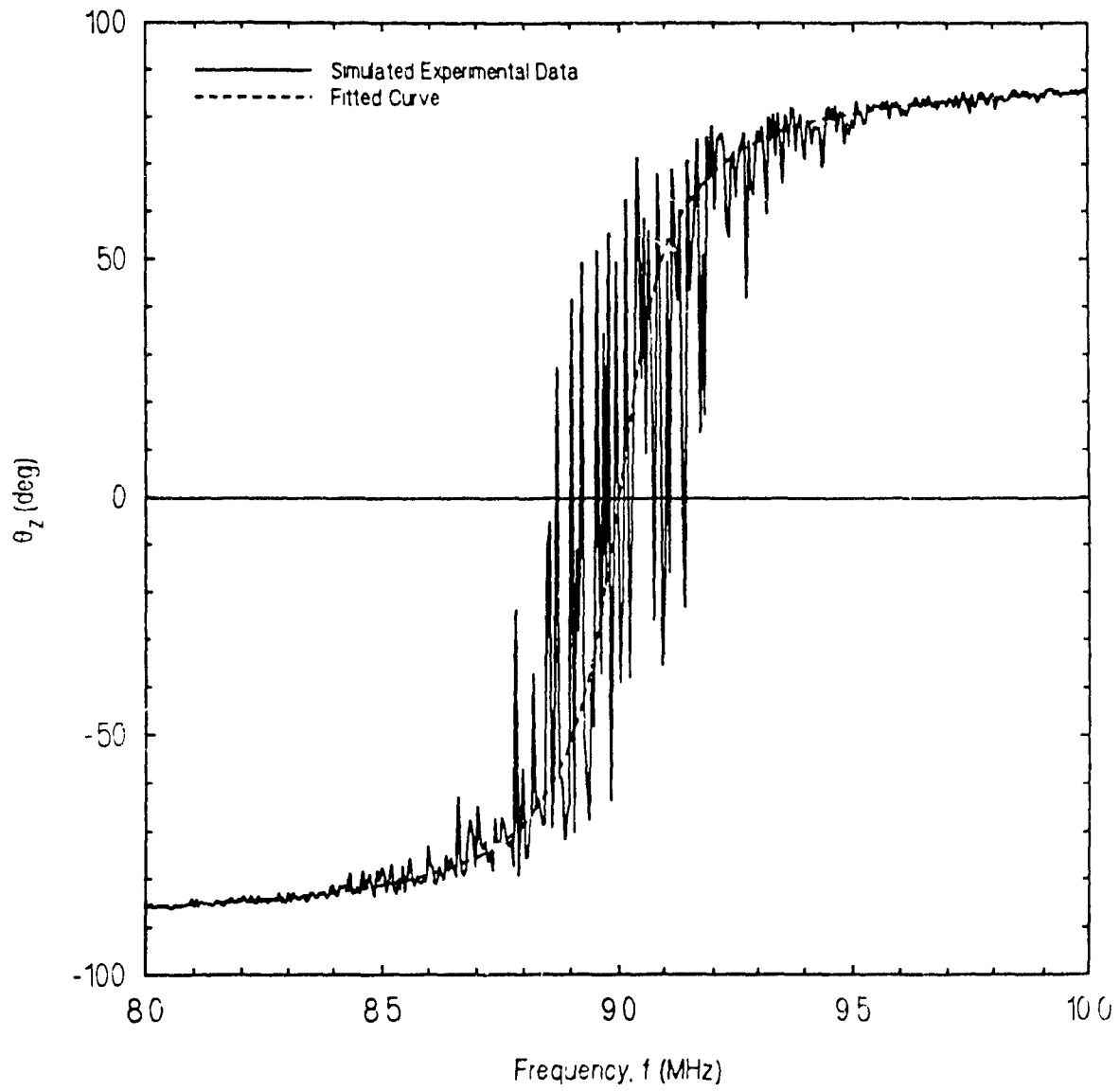


Figure 3.5 Phase of impedance for a series RLC circuit.



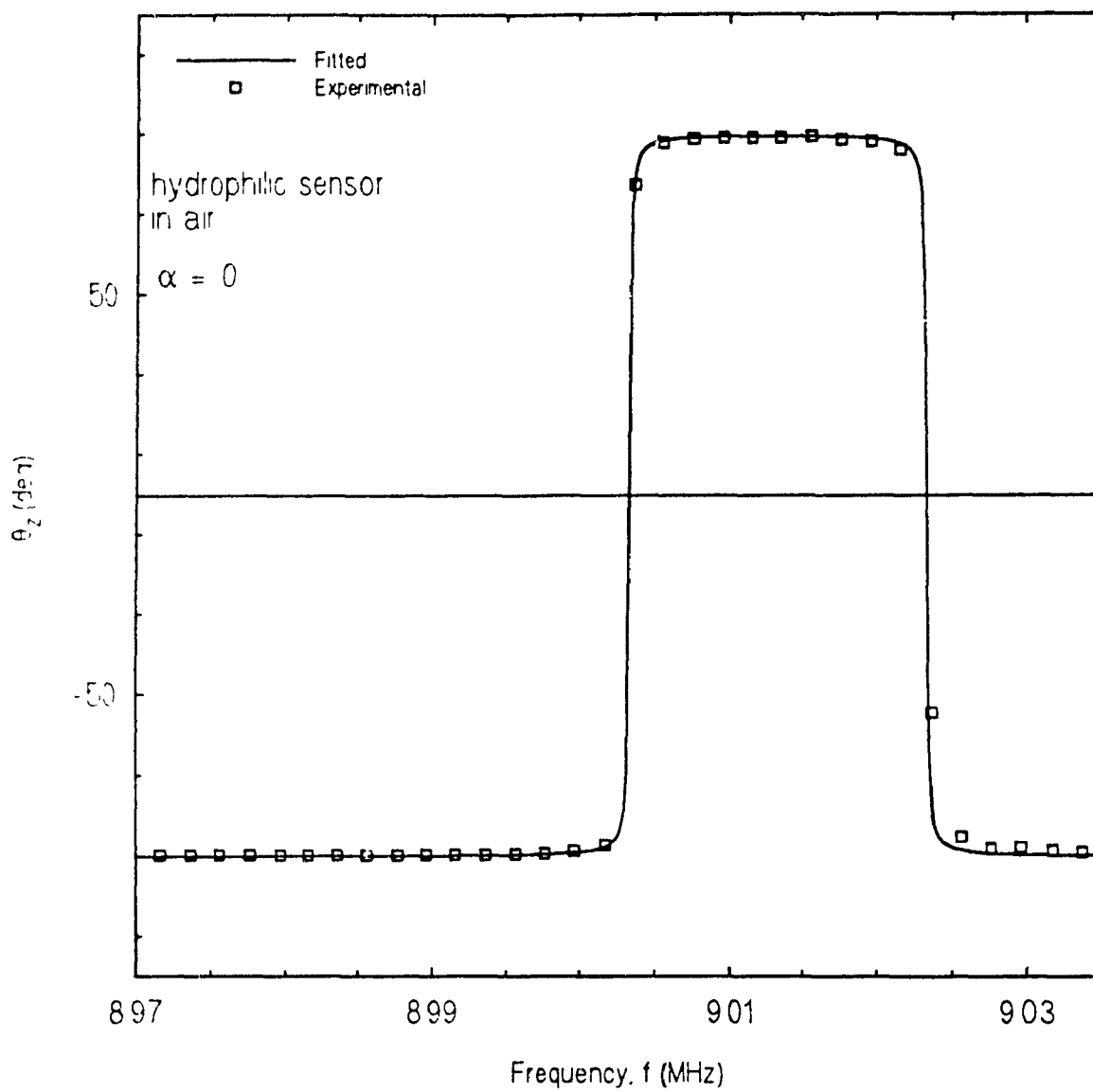


Figure 3.6 Phase of impedance of the hydrophilic sensor in air.

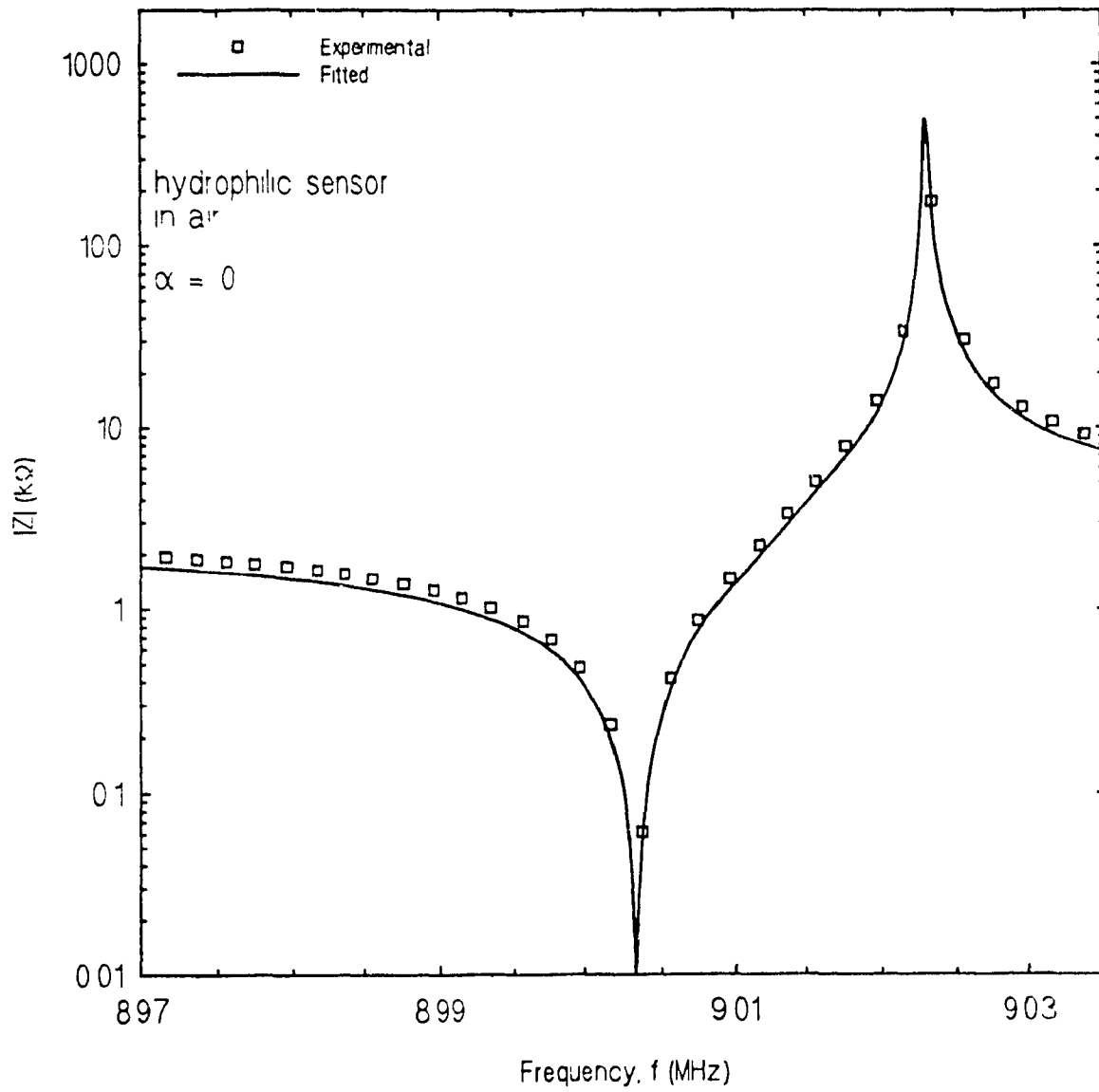


Figure 3.7 Magnitude of impedance of the hydrophilic sensor in air.

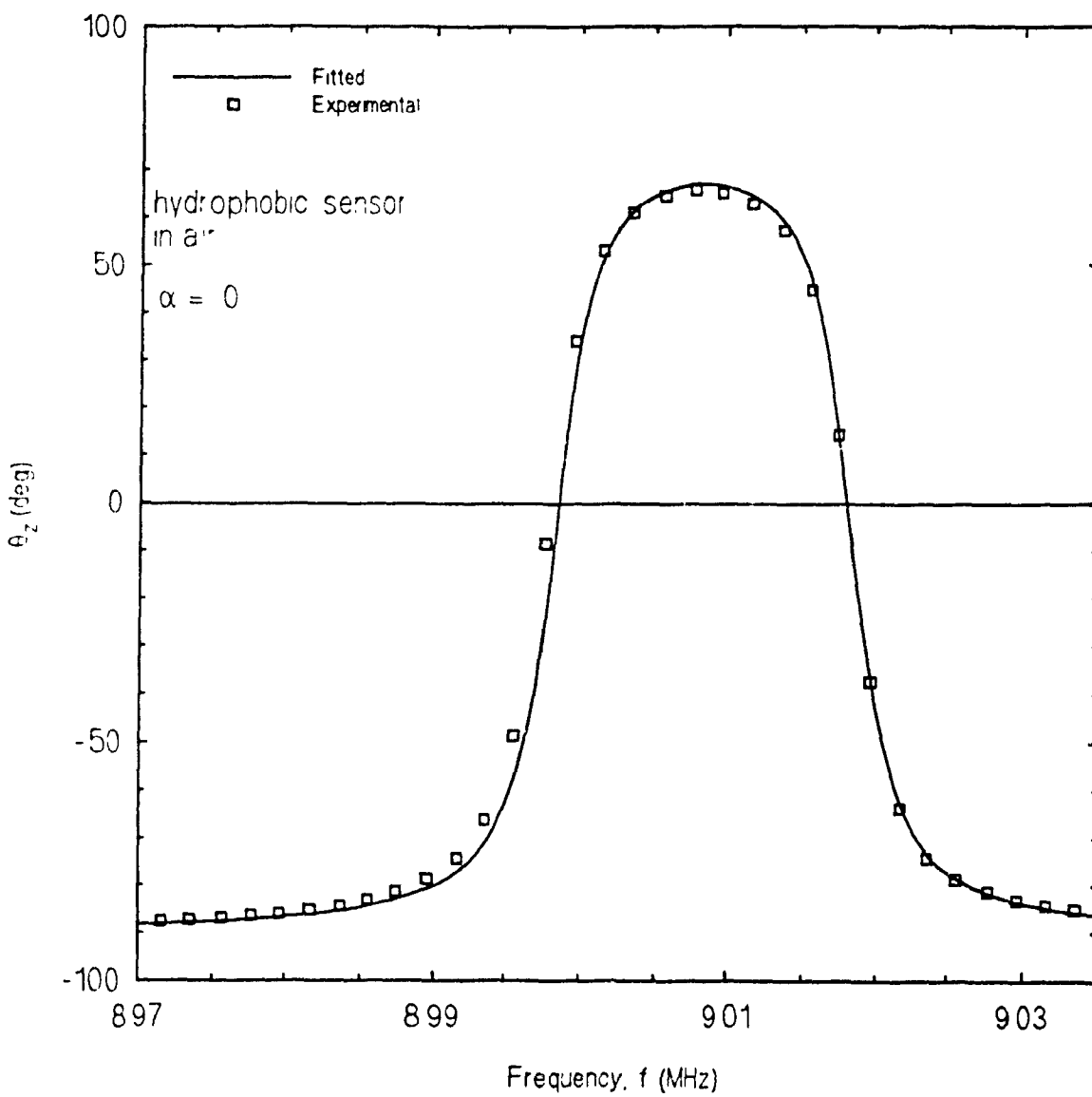


Figure 3.8 Phase of impedance of the hydrophobic sensor in air.

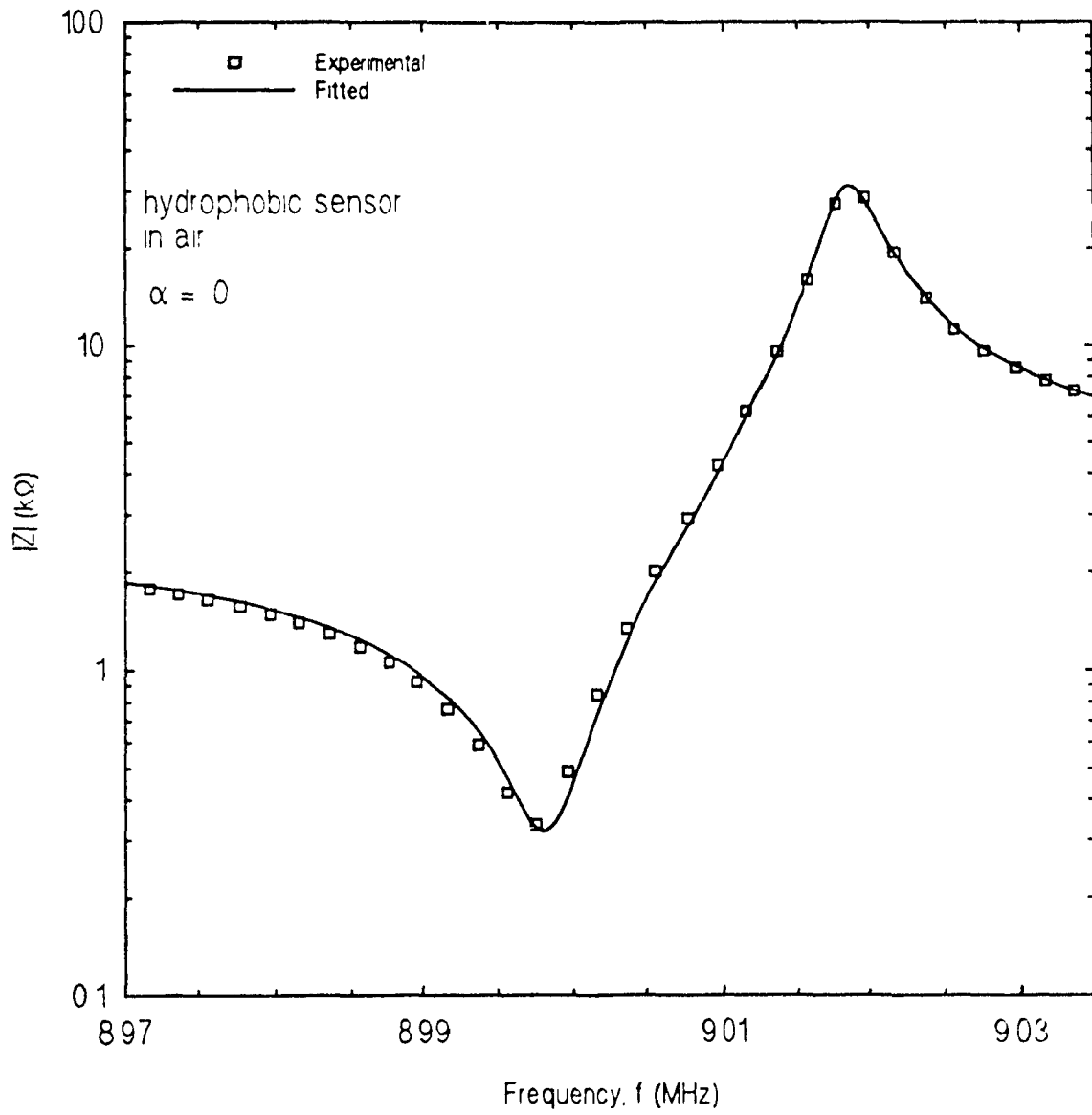


Figure 3.9 Magnitude of impedance of the hydrophobic sensor in air.

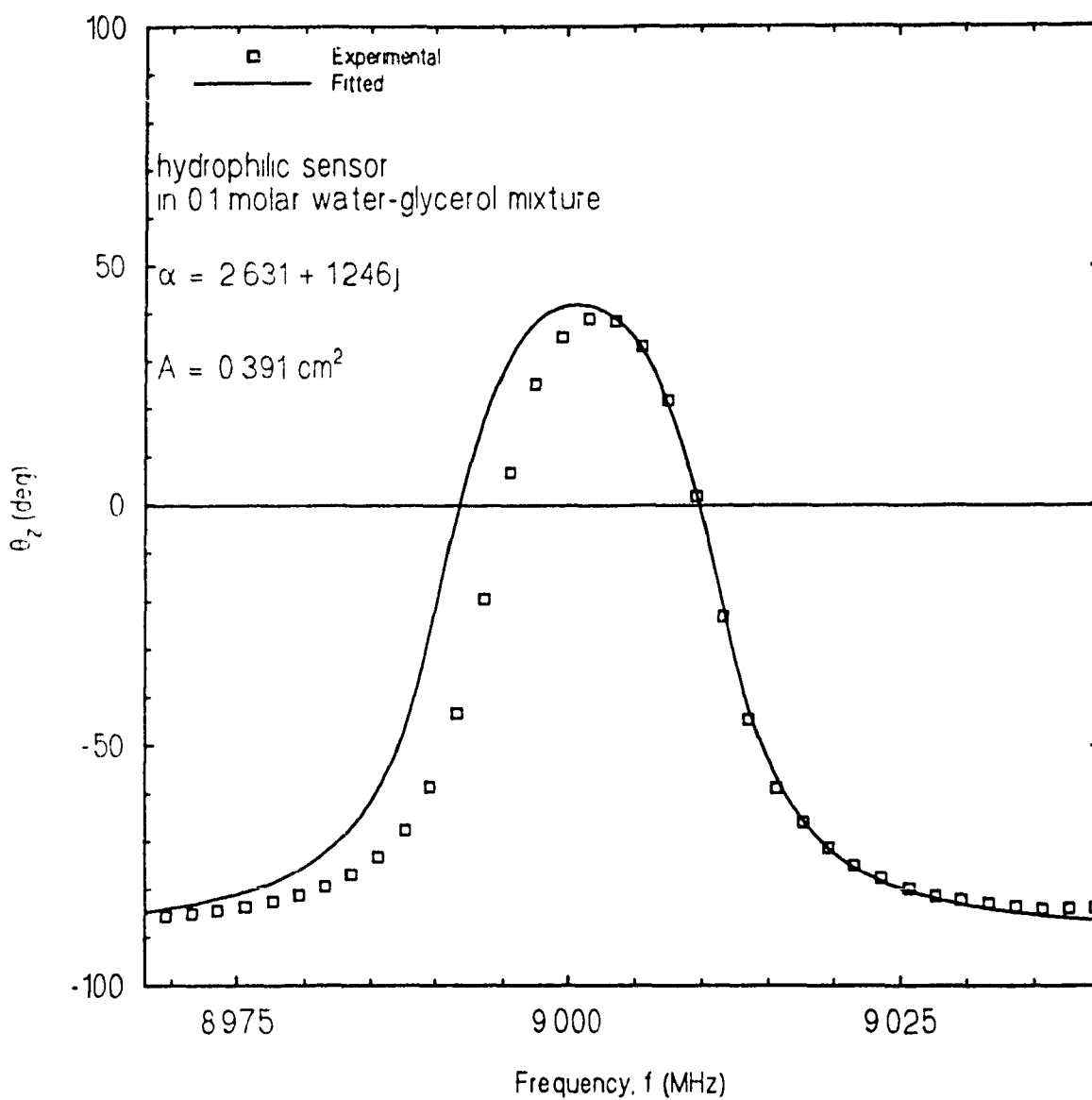


Figure 3.10 Phase of impedance of the hydrophilic sensor in 0.1 molar water-glycerol solution.

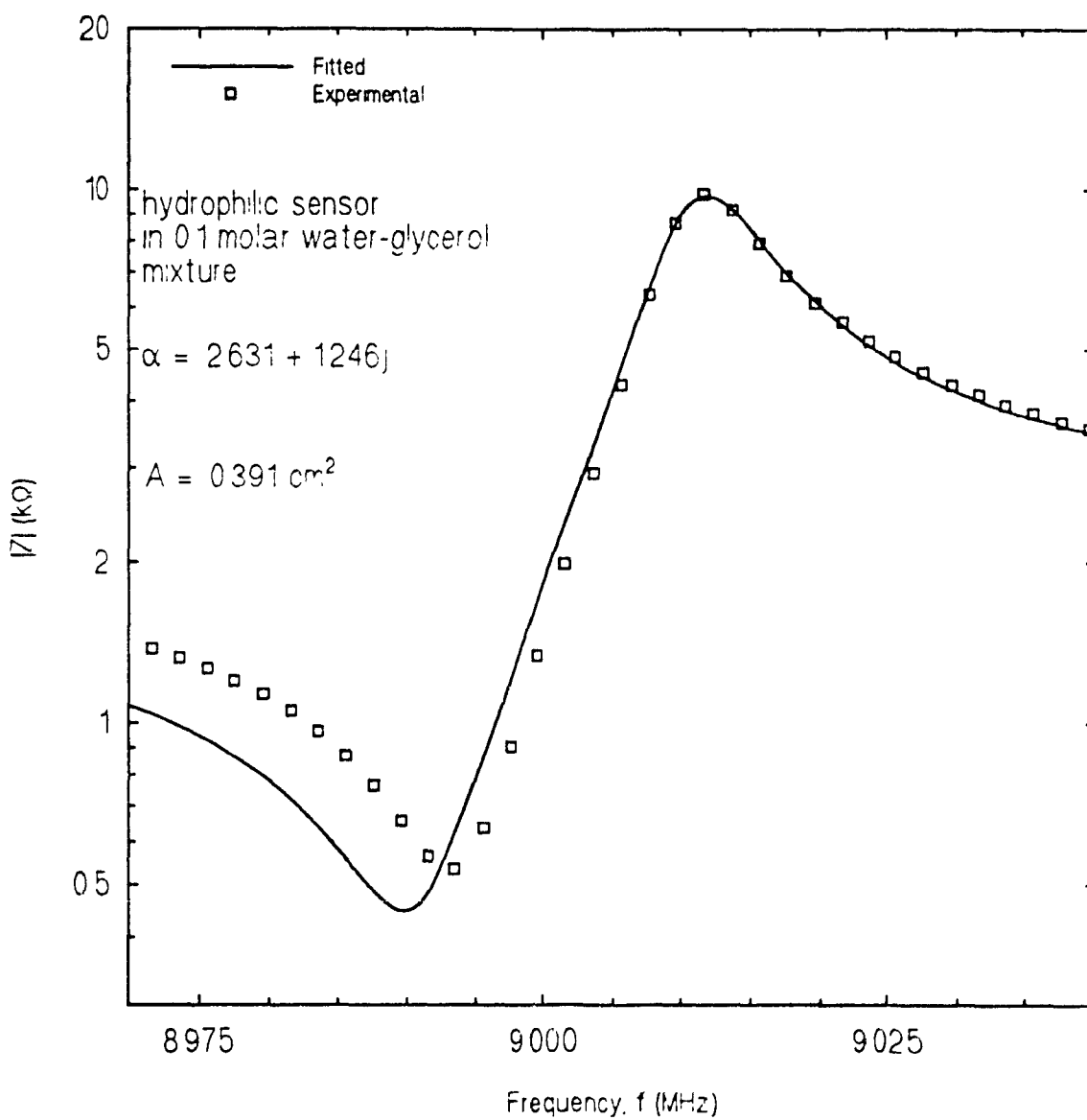


Figure 3.11 Magnitude of impedance of the hydrophilic sensor in 0.1 molar water-glycerol solution.

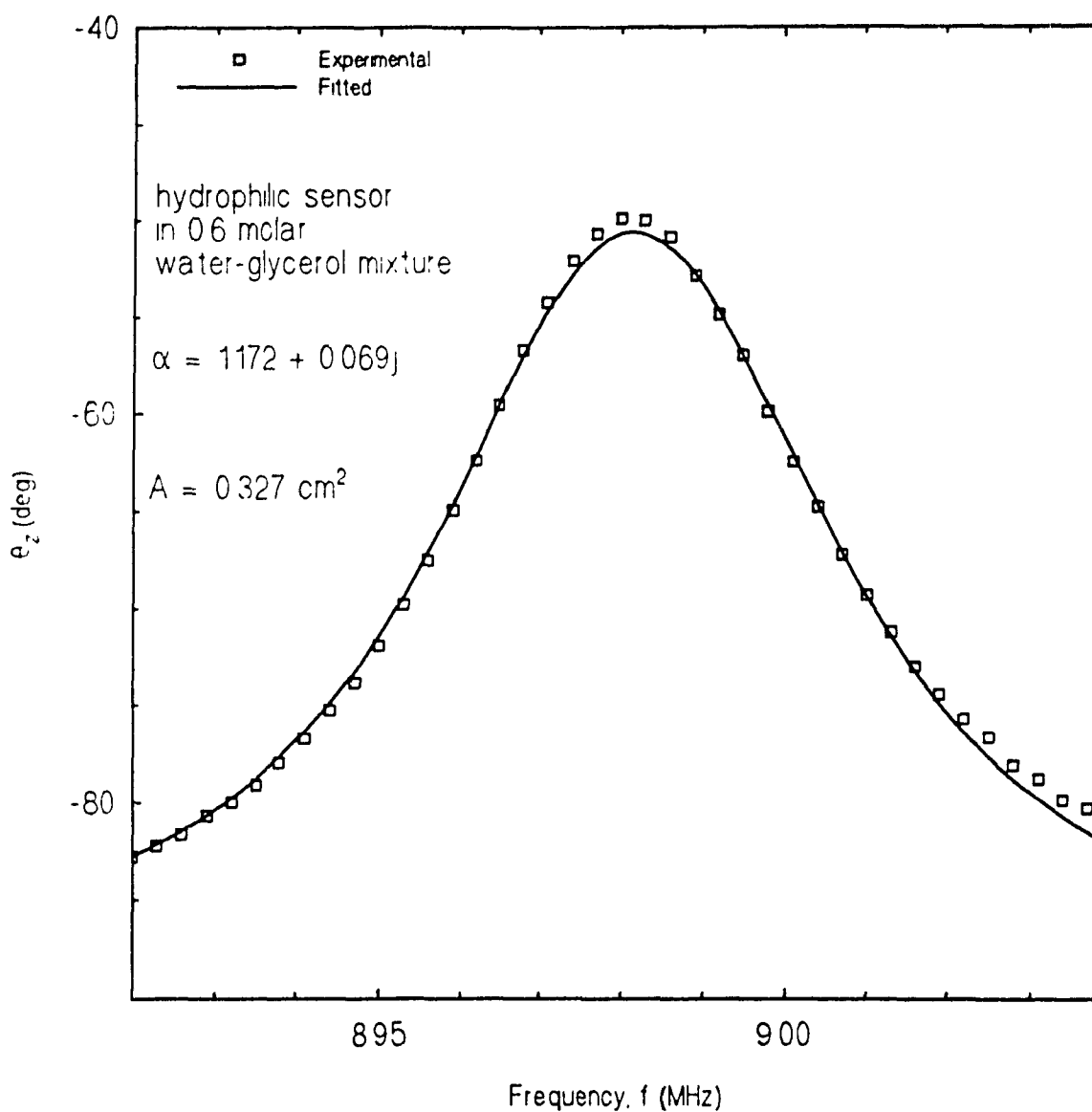


Figure 3.12 Phase of impedance of the hydrophilic sensor in 0.6 molar water-glycerol solution.

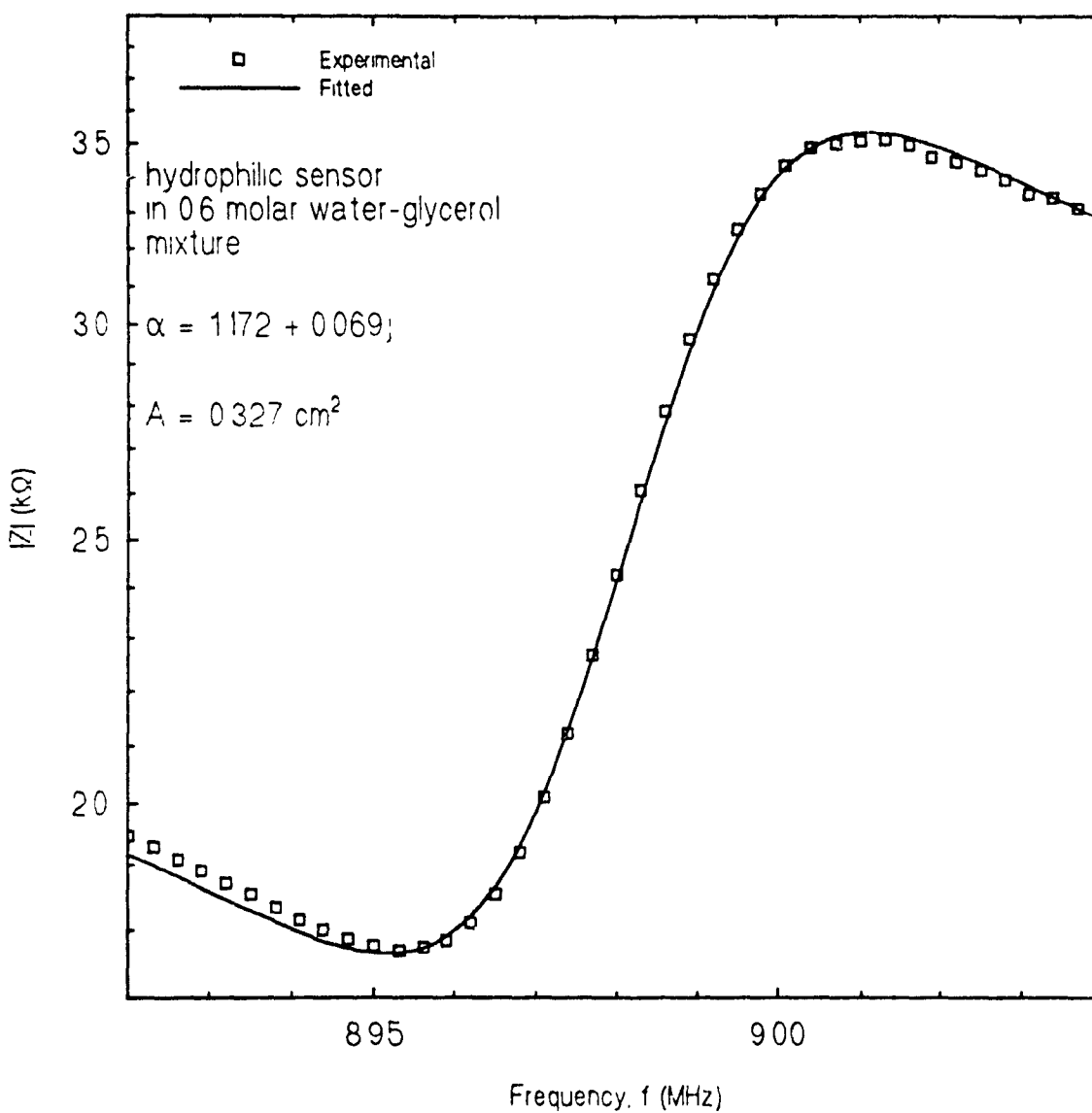


Figure 3.13 Magnitude of impedance of the hydrophilic sensor in 0.6 molar water-glycerol solution.



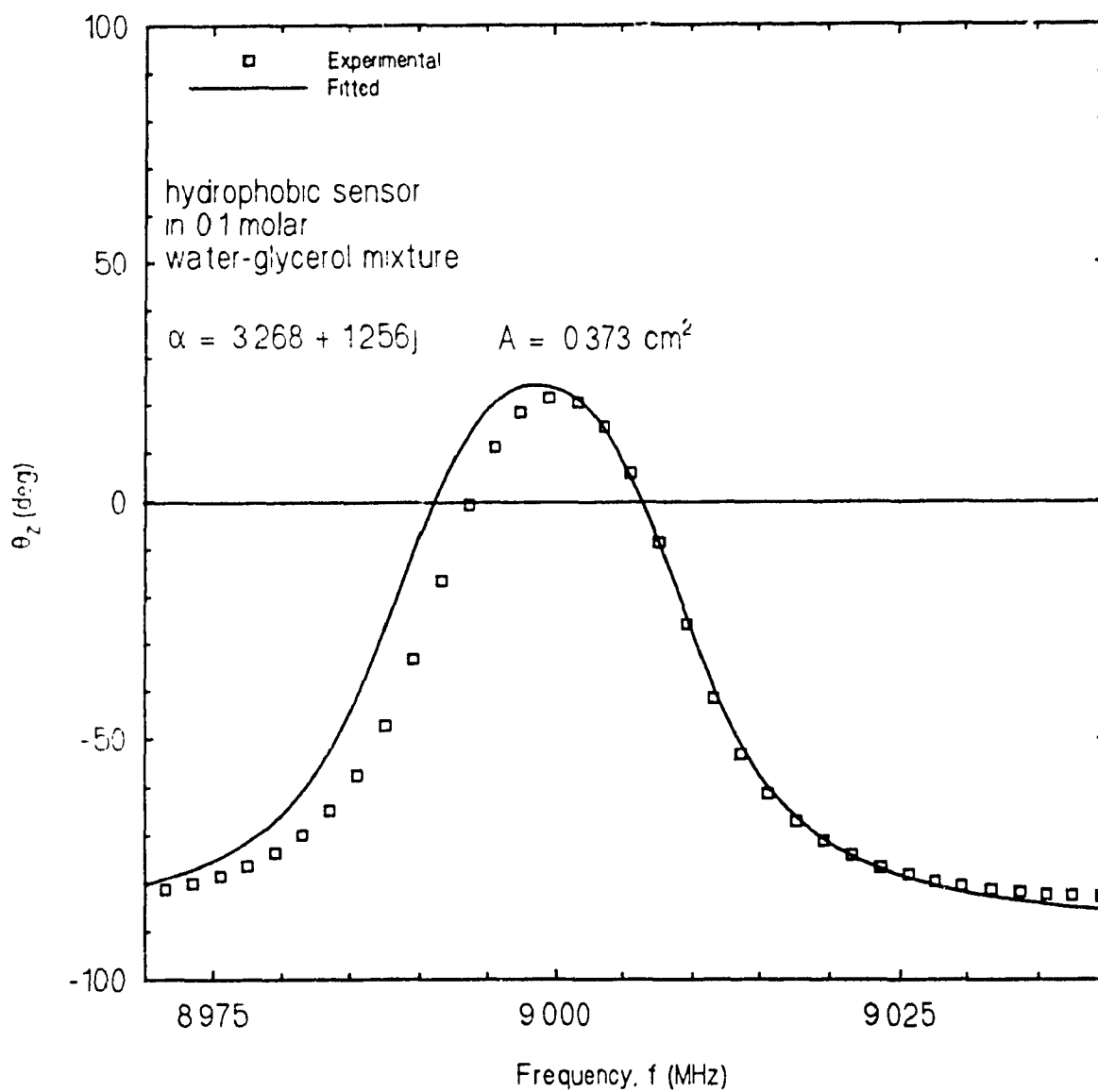


Figure 3.14 Phase of impedance of the hydrophobic sensor in 0.1 molar water-glycerol solution.

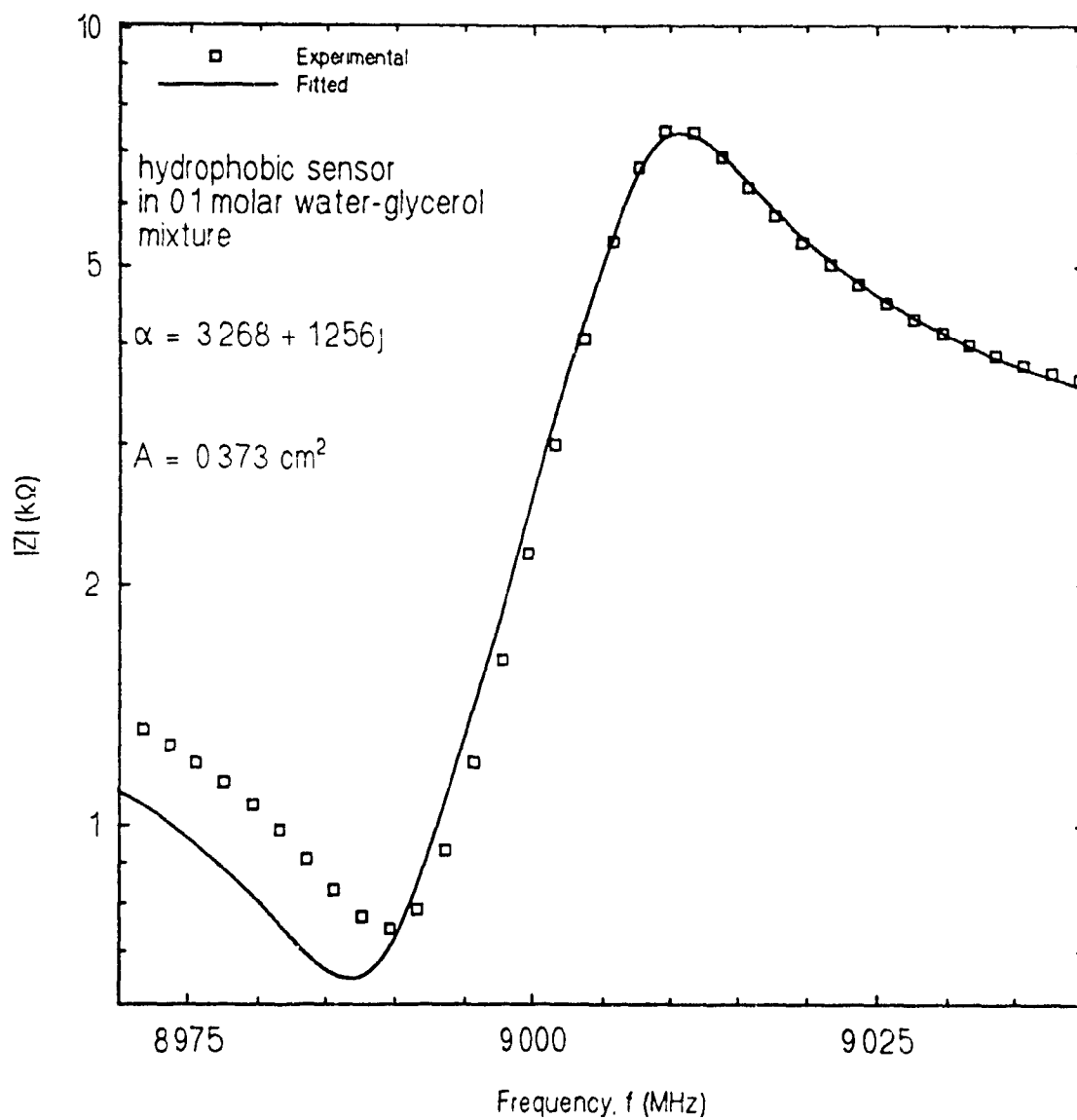


Figure 3.15 Magnitude of impedance of the hydrophobic sensor in 0.1 molar water-glycerol solution.

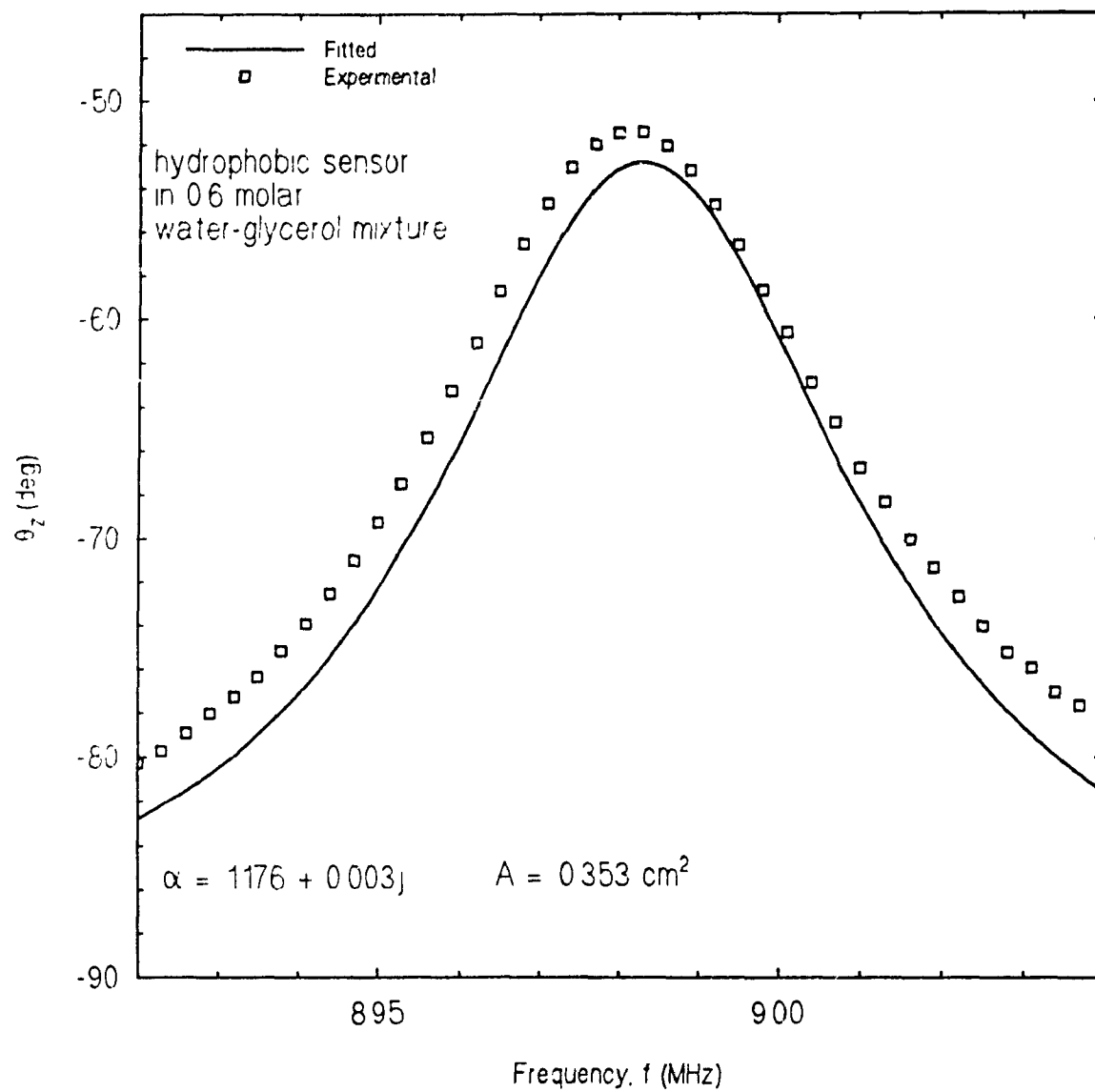


Figure 3.16 Phase of impedance of the hydrophobic sensor in 0.6 molar water-glycerol solution.

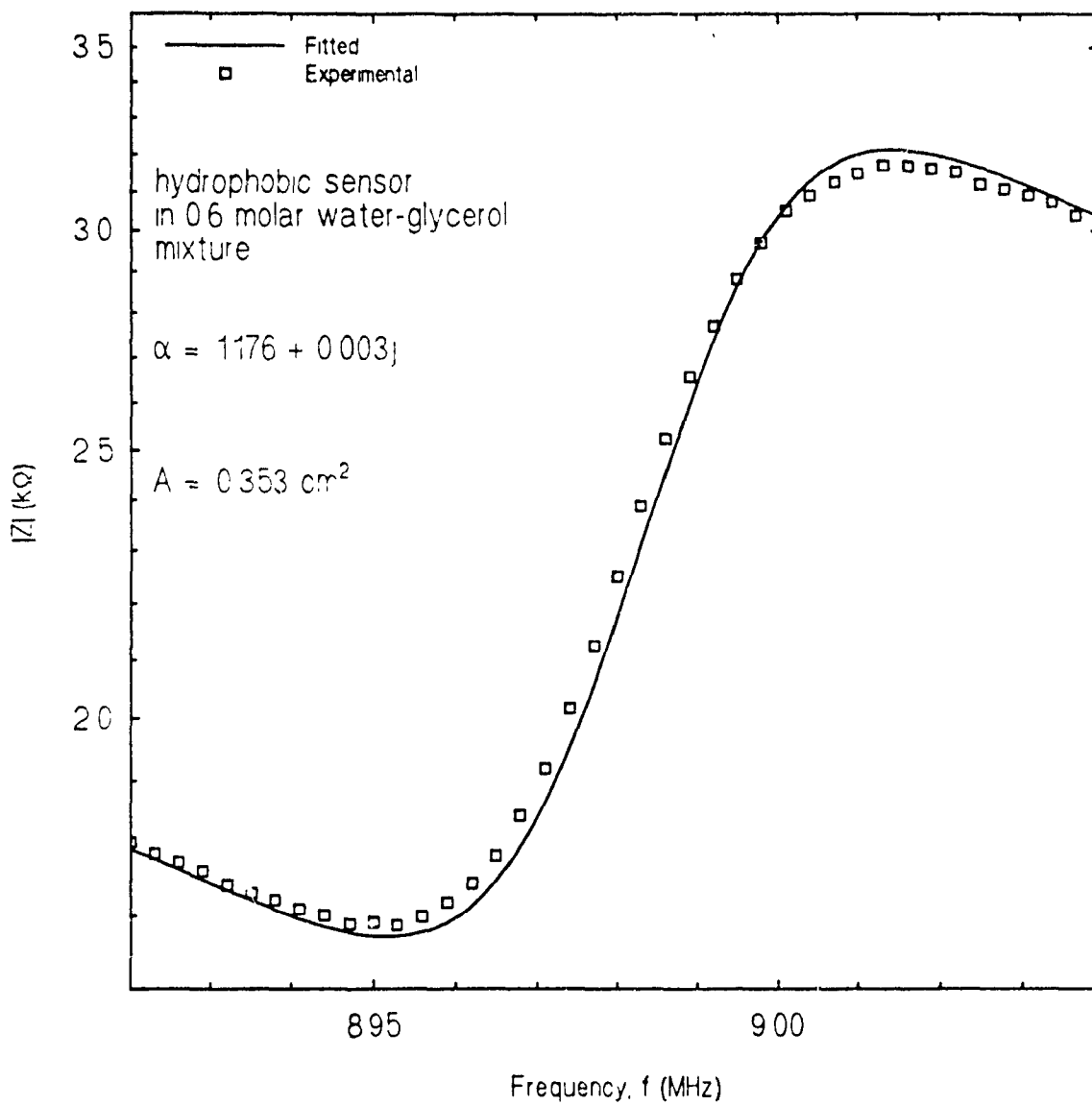


Figure 3.17 Magnitude of impedance of the hydrophobic sensor in 0.6 molar water-glycerol solution.

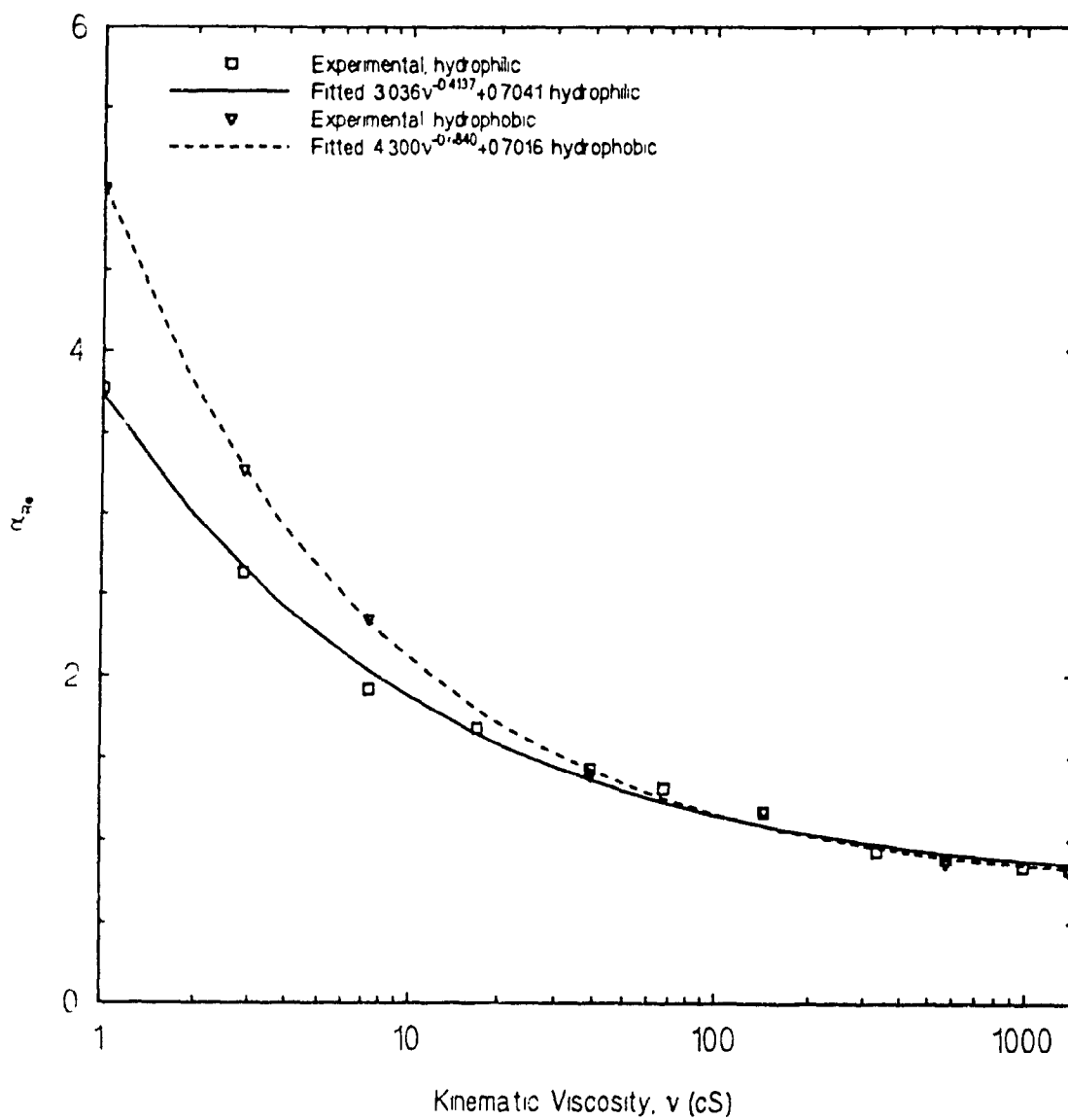


Figure 3.18 Real part of interfacial slip parameter versus kinematic viscosity for the hydrophilic and hydrophobic sensor in liquid.

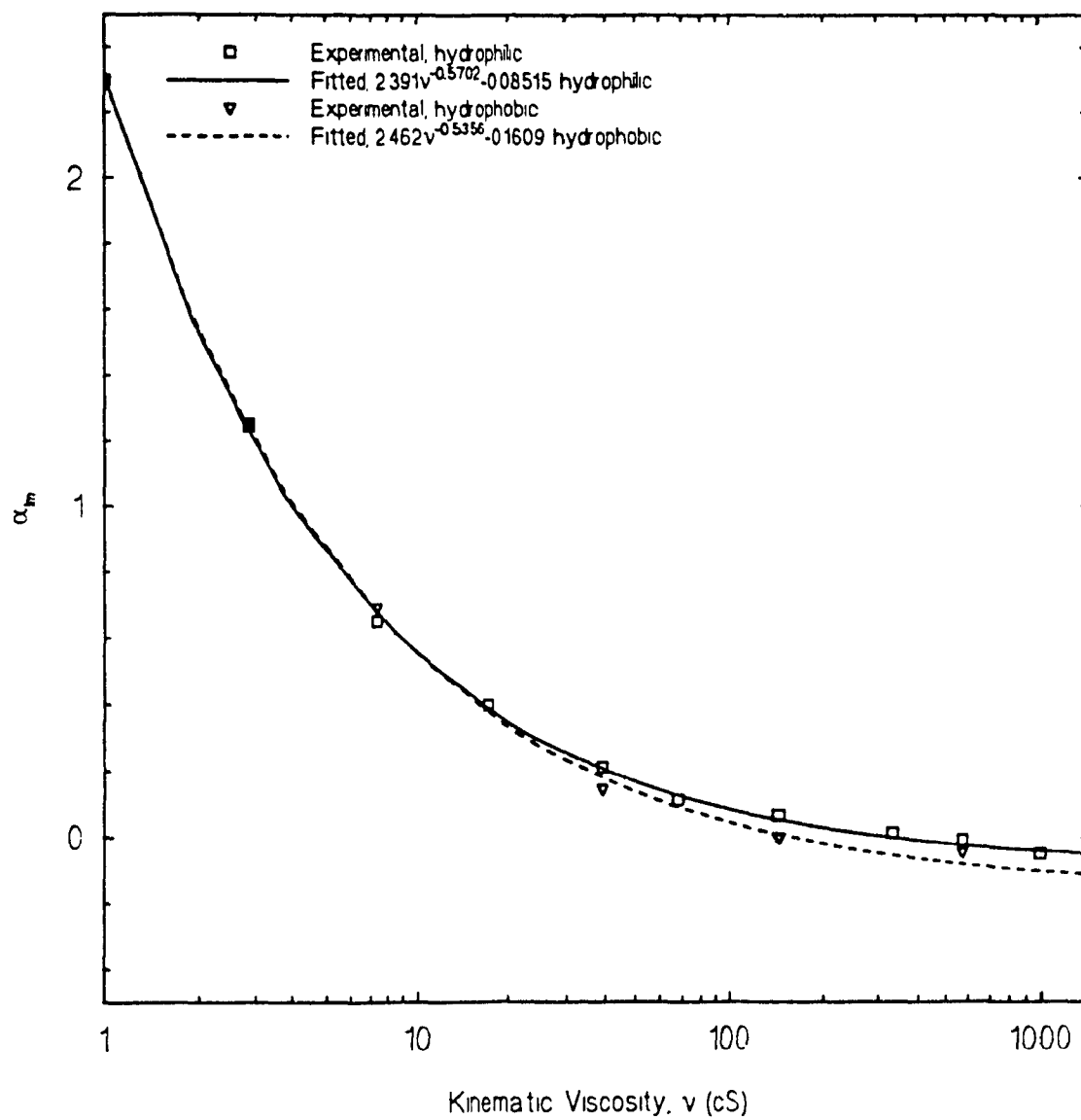


Figure 3.19 *Imaginary part of interfacial slip parameter versus kinematic viscosity for the hydrophilic and hydrophobic sensor in liquid.*

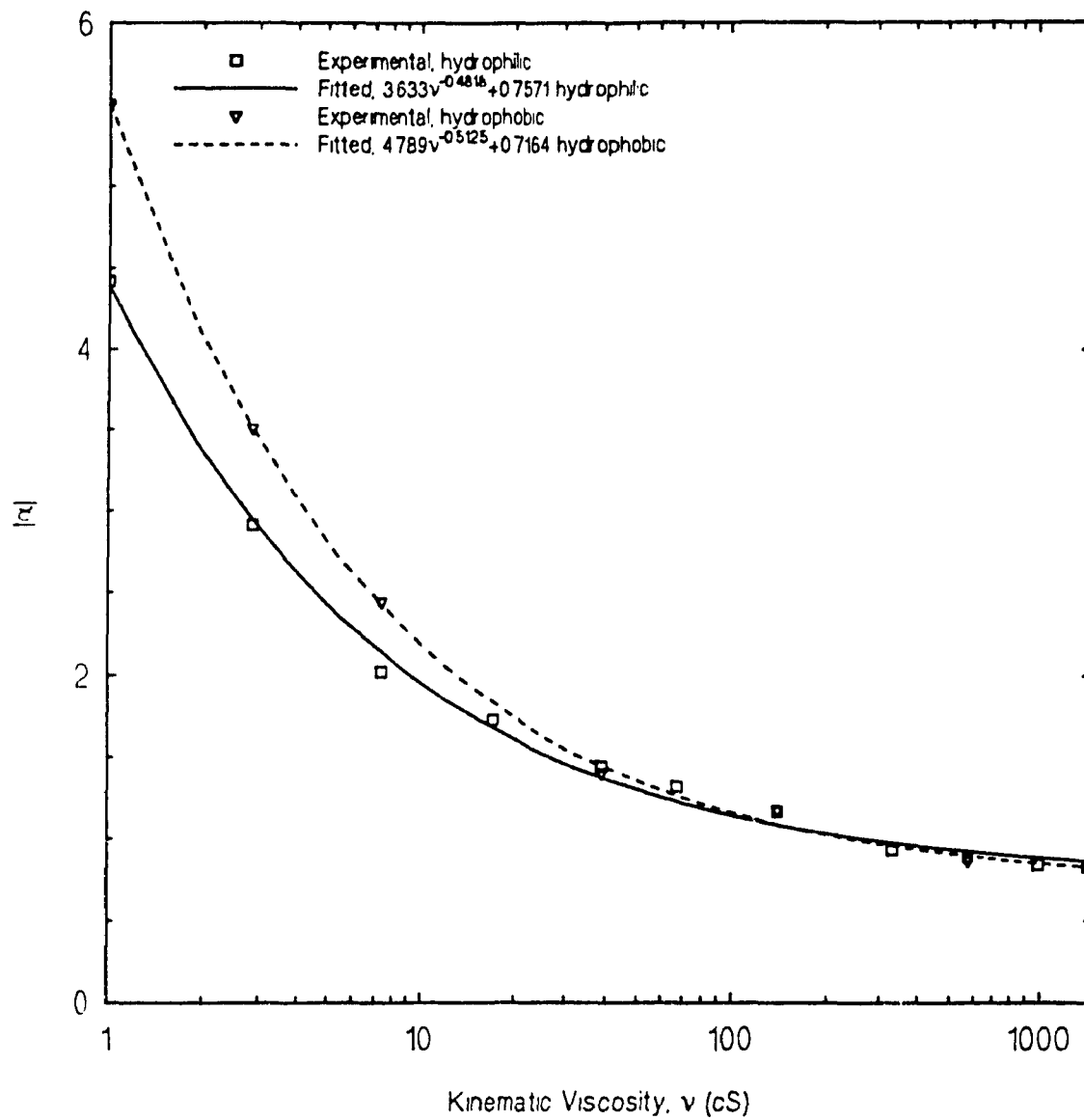


Figure 3.20 Magnitude of interfacial slip parameter versus kinematic viscosity for the hydrophilic and hydrophobic sensor in liquid.

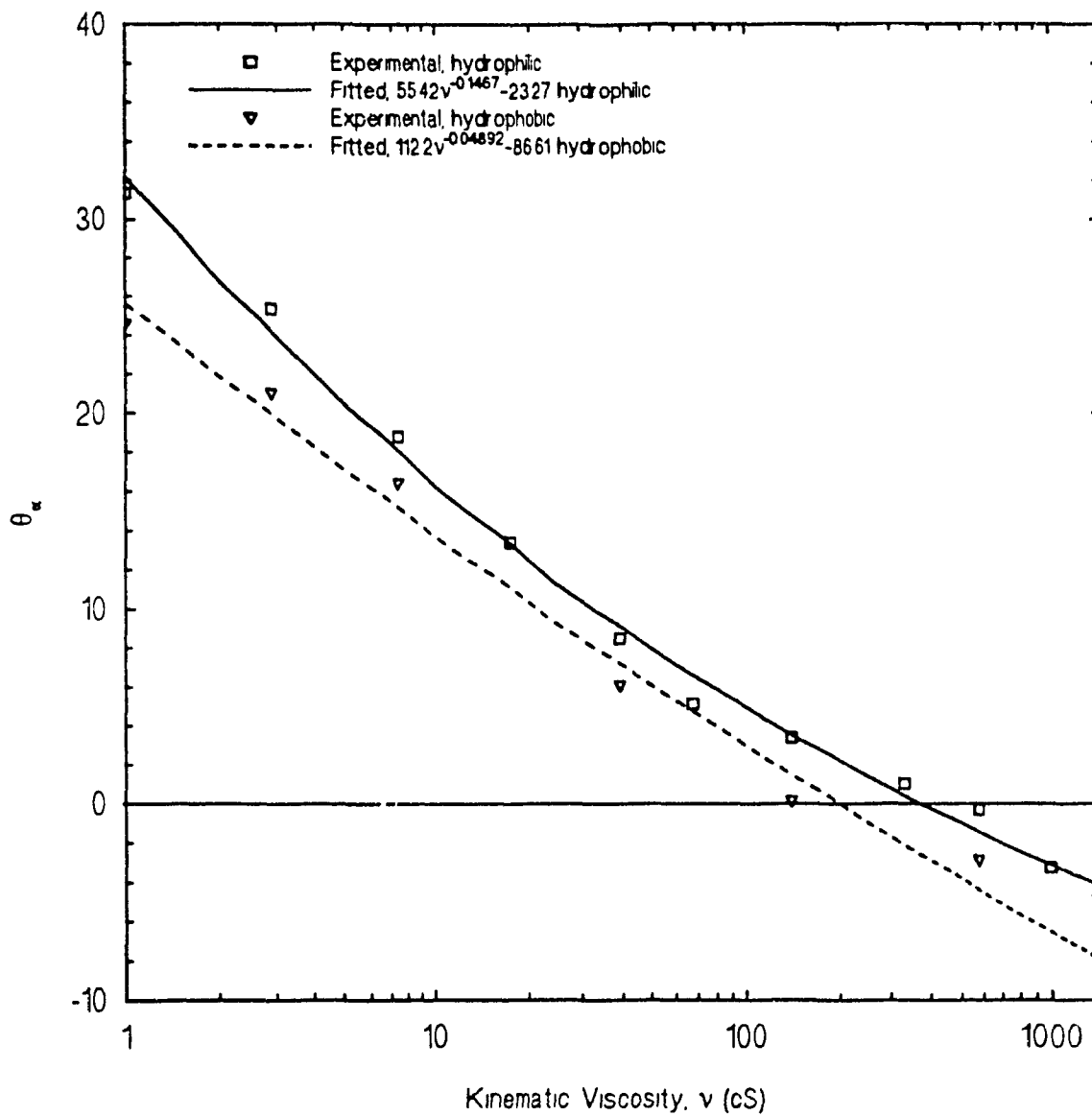


Figure 3.21 Phase of interfacial slip parameter versus kinematic viscosity for the hydrophilic and hydrophobic sensor in liquid.



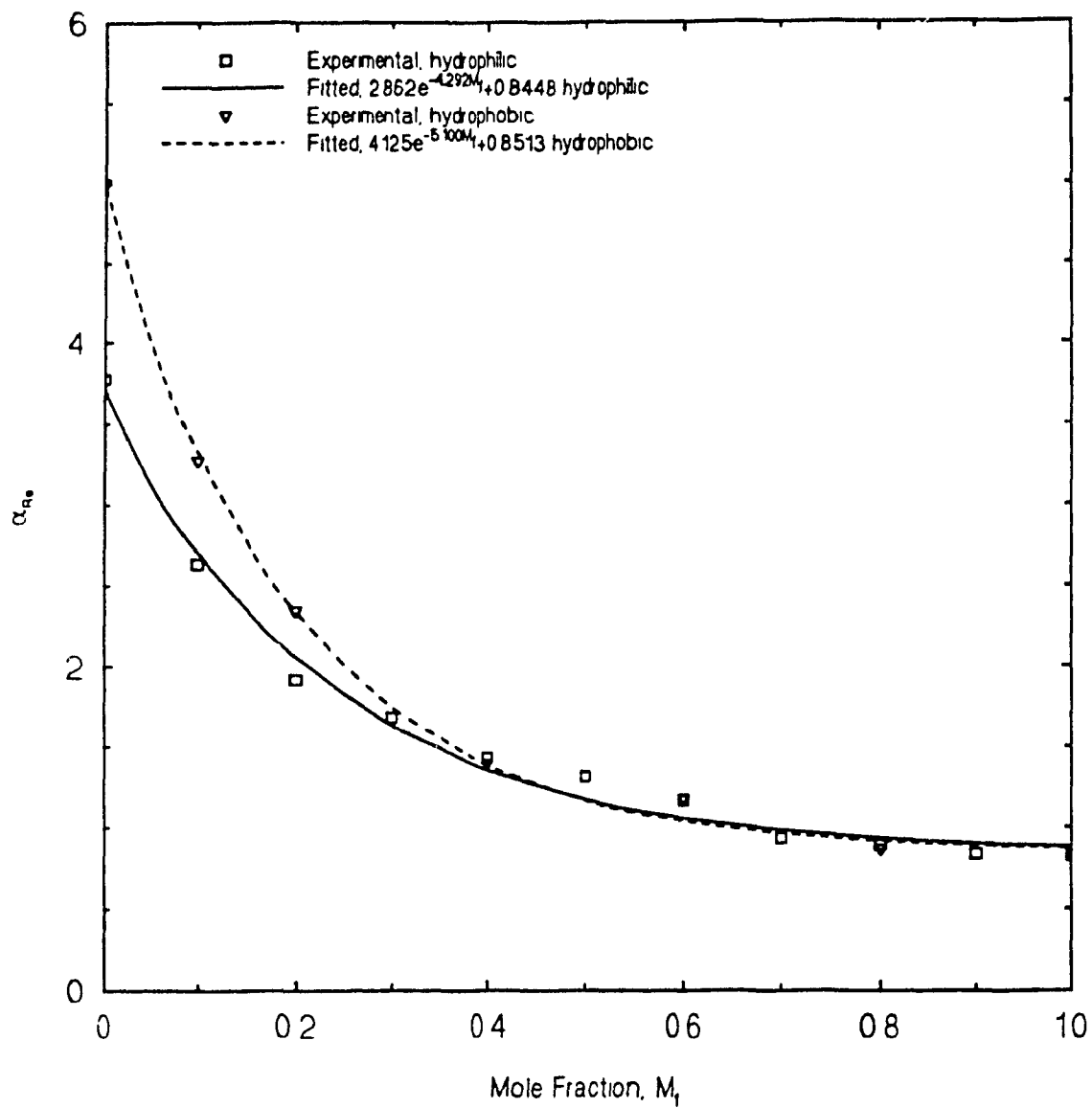


Figure 3.22 Real part of interfacial slip parameter versus mole fraction for the hydrophilic and hydrophobic sensor in liquid.

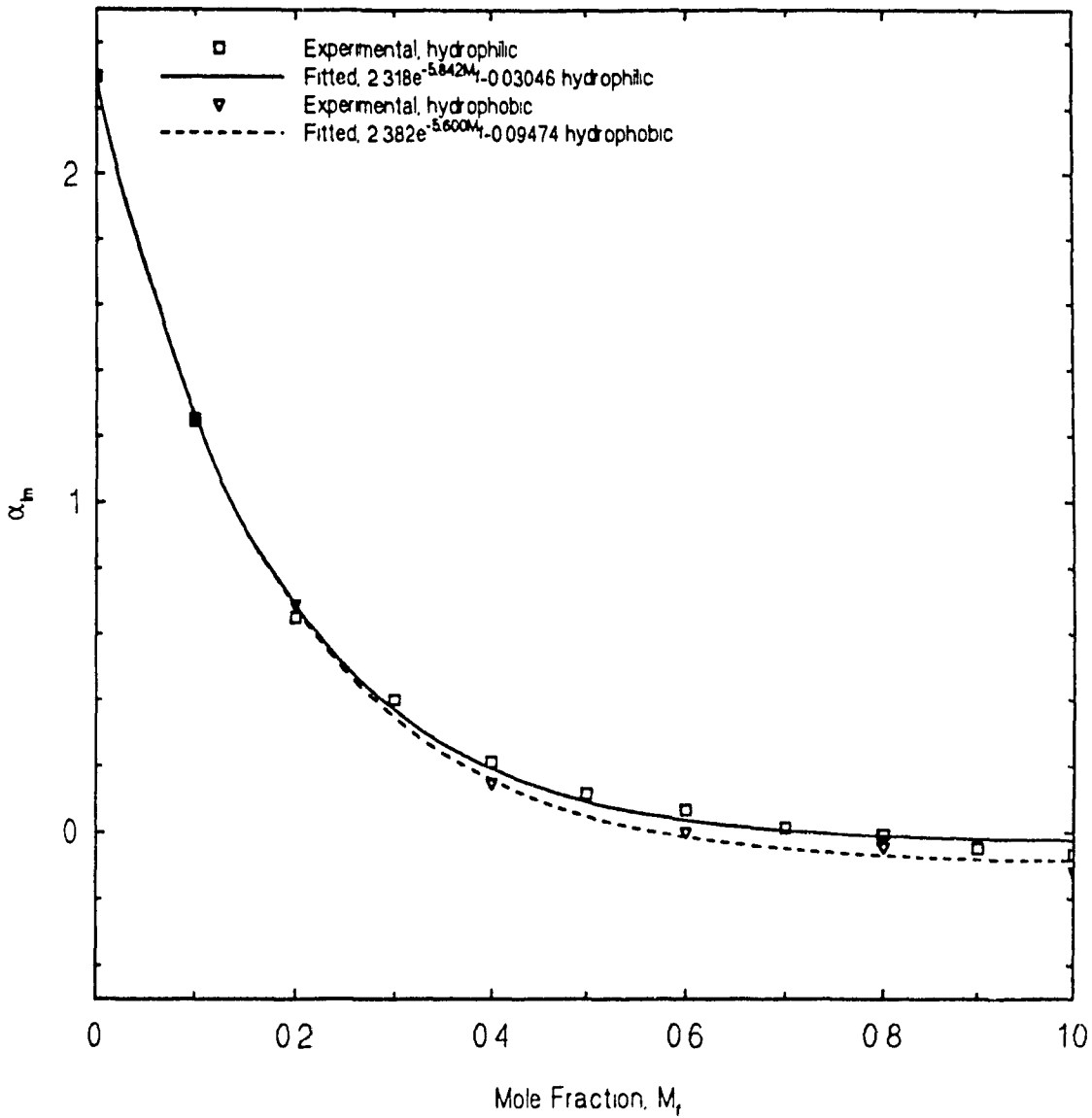


Figure 3.23 *Imaginary part of interfacial slip parameter versus mole fraction for the hydrophilic and hydrophobic sensor in liquid.*

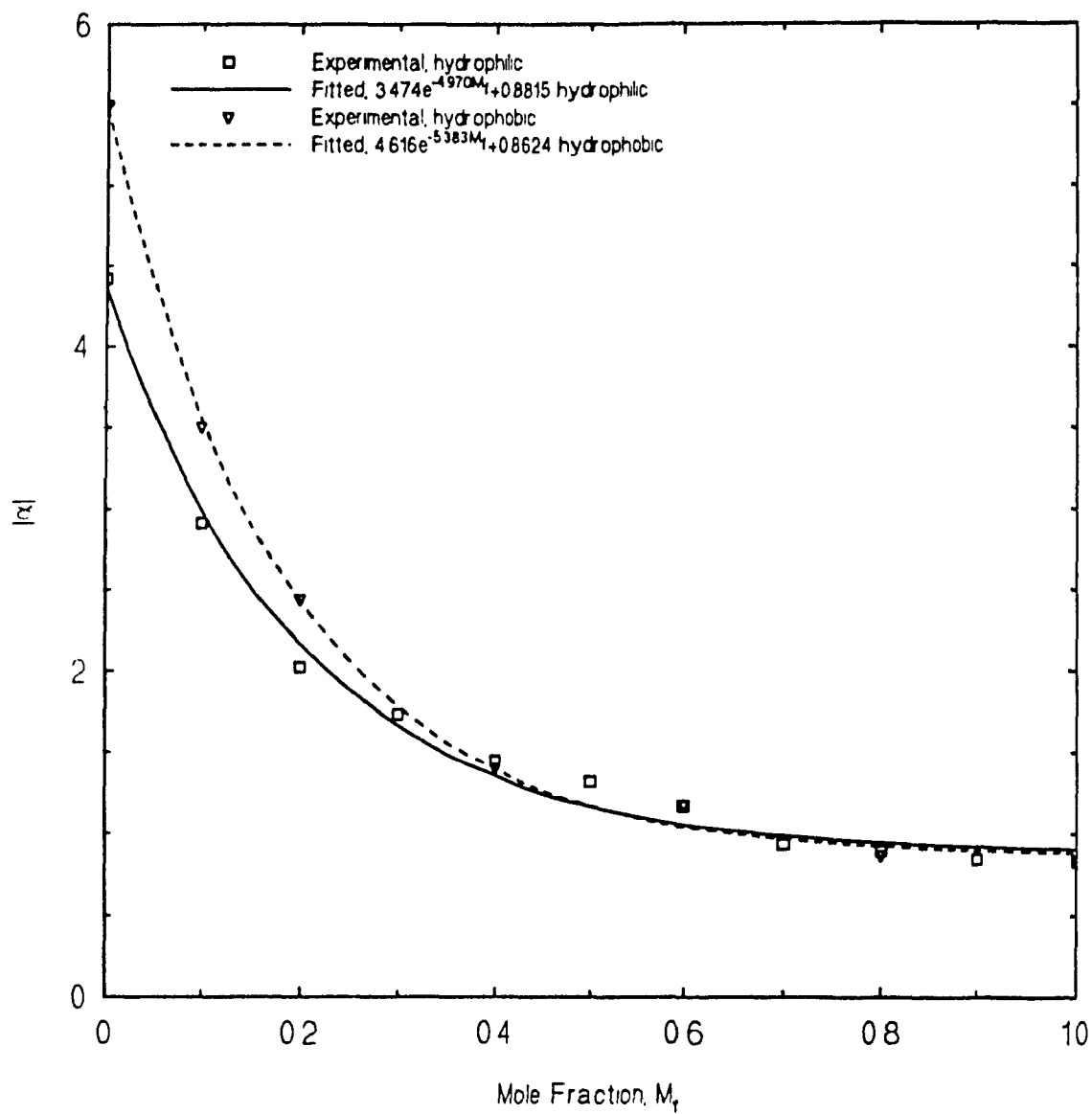


Figure 3.24 Magnitude of interfacial slip parameter versus mole fraction for the hydrophilic and hydrophobic sensor in liquid.

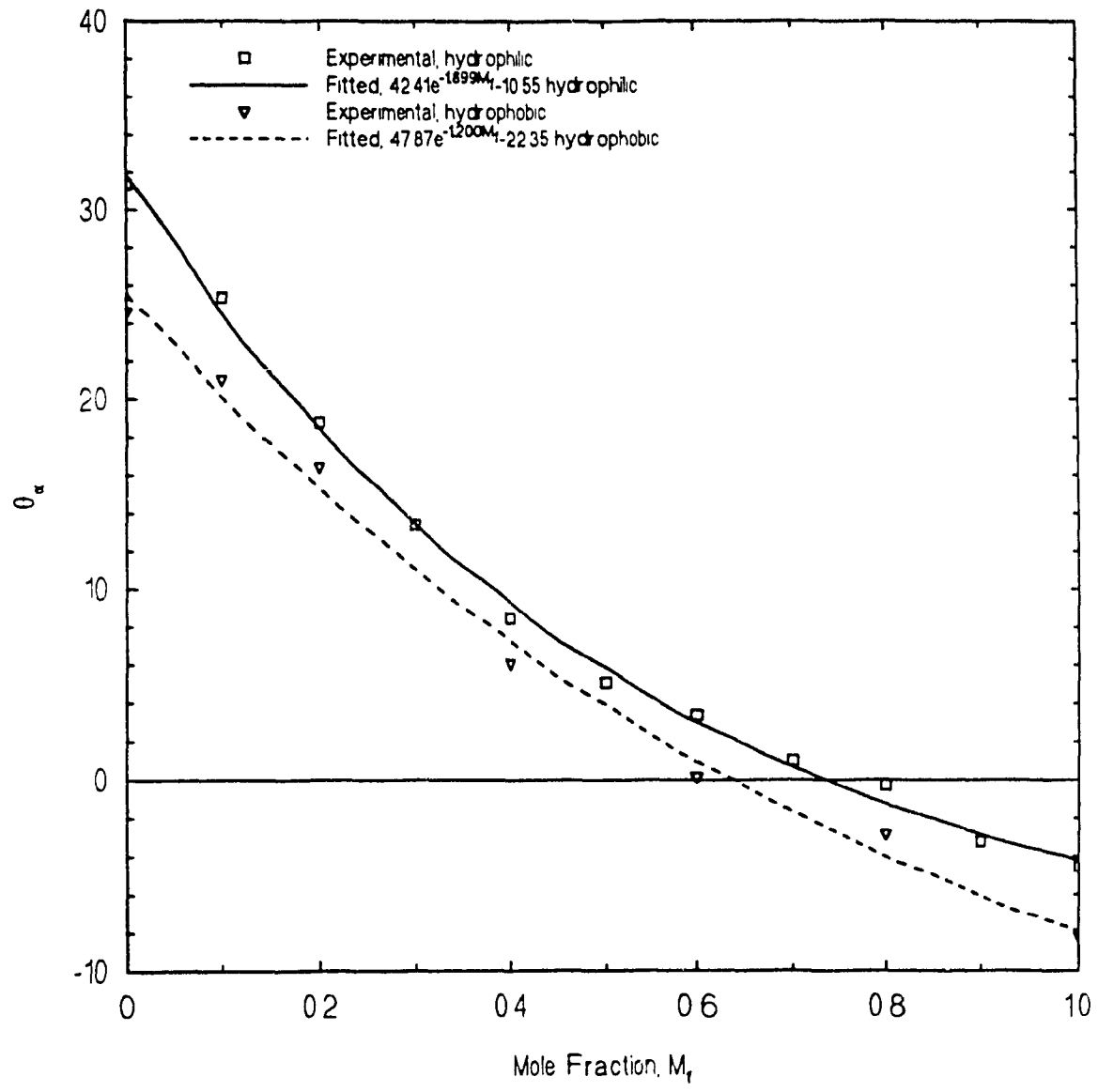


Figure 3.25 Phase of interfacial slip parameter versus mole fraction for the hydrophilic and hydrophobic sensor in liquid.

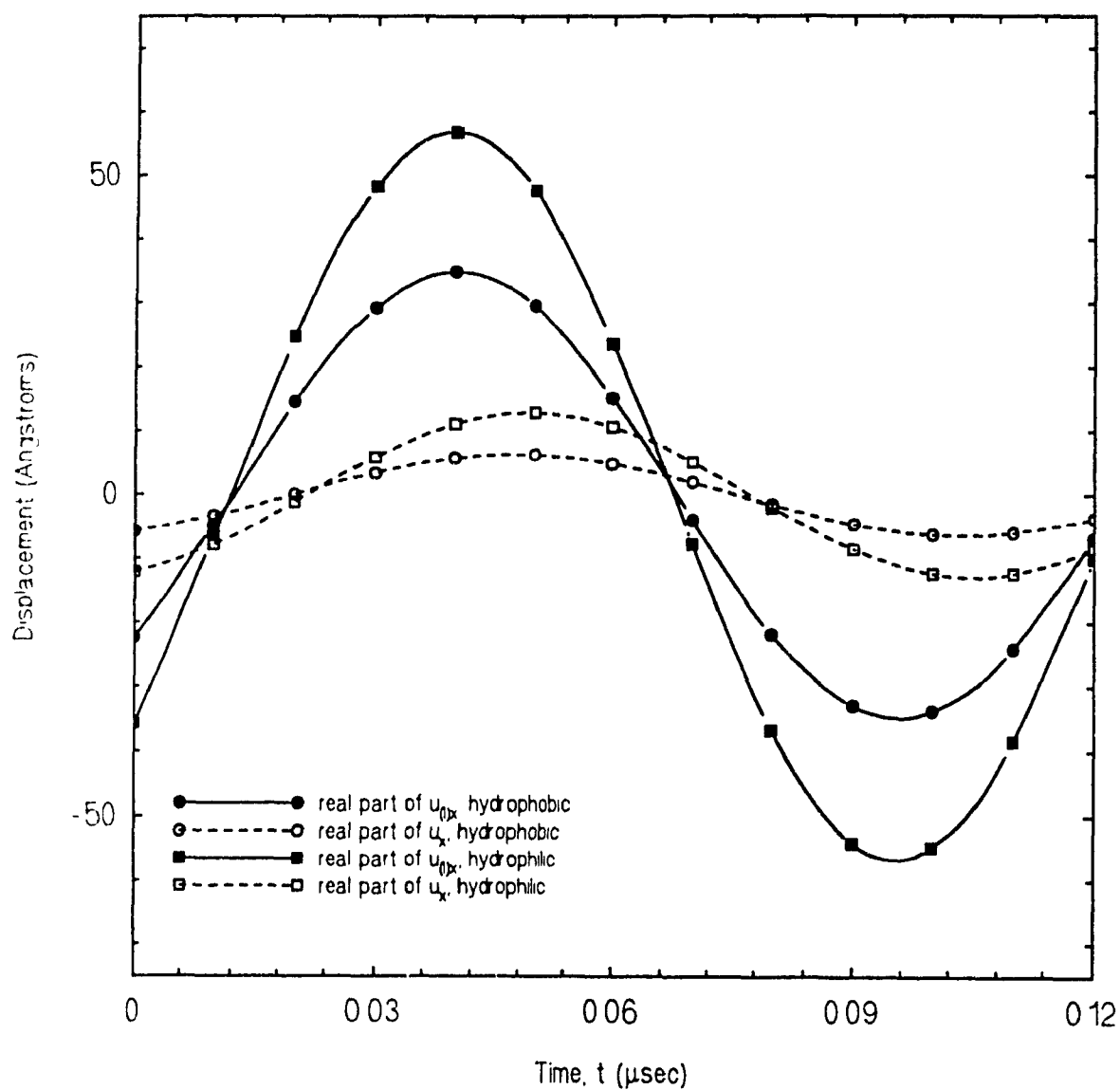


Figure 3.26 Solid and liquid particle displacement at the solid-liquid interface for the hydrophilic and hydrophobic sensor in liquid.

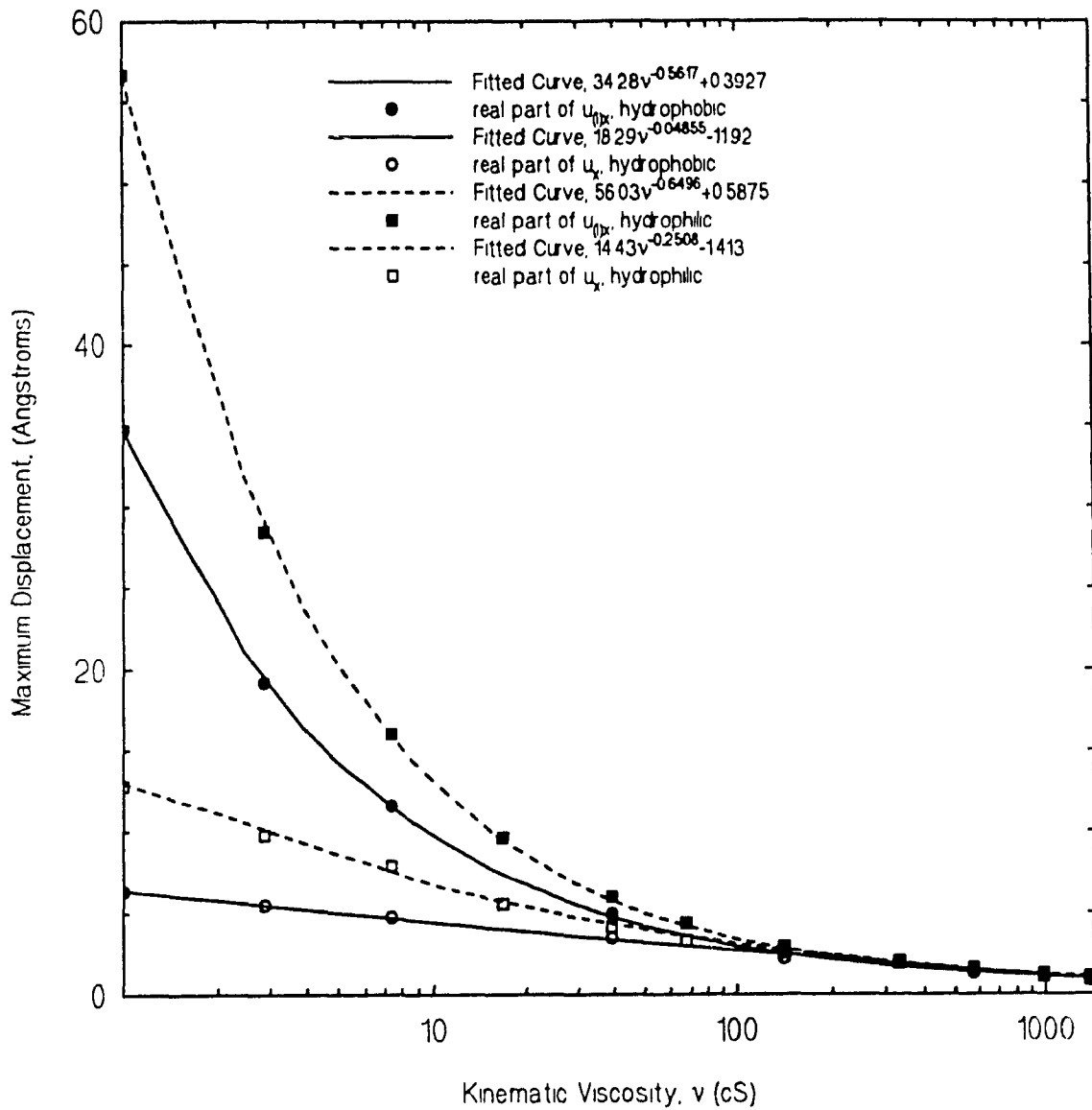


Figure 3.27 Maximum values of solid and liquid particle displacements at the solid-liquid interface for both the hydrophilic and hydrophobic sensor in liquid.

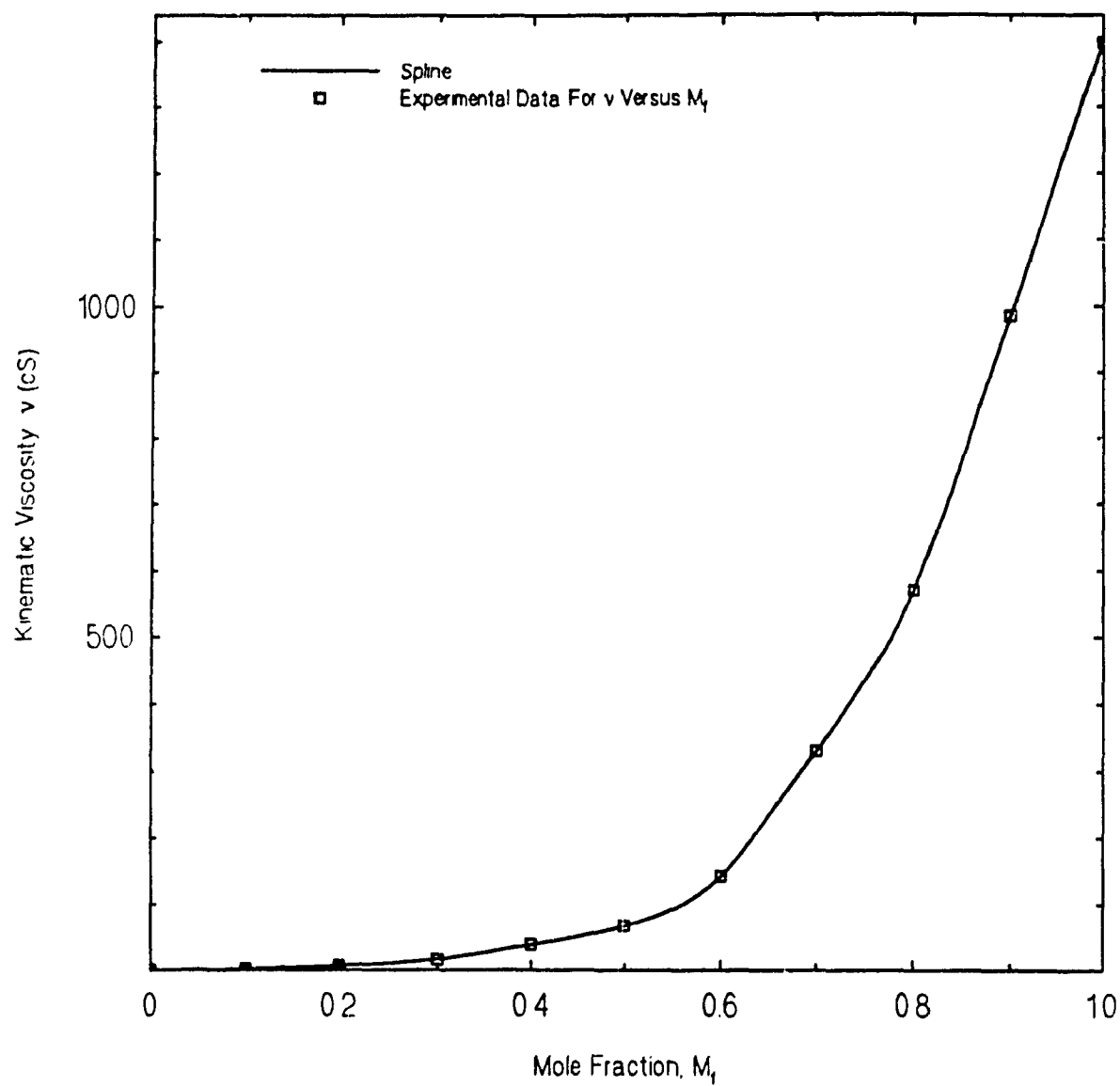


Figure 3.28 Kinematic viscosity versus mole fraction for water-glycerol solution.

## CHAPTER 4

### MODEL

#### Introduction

A mechanical model of slip at the solid-liquid interface of a quartz sensor has been devised. A parameter of the model corresponds to the interfacial slip parameter which was found by fitting experiment and theory in the last chapter.

The mechanical model of interfacial slip is defined and the equation of motion of the system is found by writing the Lagrangian of the system, Section 4.1. The equation of motion of the system cannot be solved analytically since it is nonlinear. Therefore it is necessary to solve the equation by a numerical procedure, Section 4.2.

#### 4.1 Interfacial Slip Model

##### 4.1.1 Description of Model

The interfacial slip is modeled by a spring-mass system consisting of two masses  $m_1$  and  $m_2$ , and a spring of force constant,  $k$ , connecting the two masses as shown in Figure 4.1. The two masses  $m_1$  and  $m_2$  are constrained to move along the  $x$ -direction, which lies in the plane of the spring-mass system.

In the interfacial slip model, mass,  $m_1$ , represents the mass of a liquid particle, in contact with the top surface of



the sensor, while mass,  $m_2$ , represents the mass of a solid particle on the surface of the sensor. The motion of the masses in the x-direction corresponds to the transverse shear mode (TSM) of AT-cut quartz. The spring connecting masses  $m_1$  and  $m_2$  represents the force of interaction that occurs between the liquid molecules and the solid molecules which are in contact at the top surface of the sensor. The quantity,  $k$ , represents the strength of the force of interaction that occurs at the solid-liquid interface. The interaction that occurs at the solid-liquid interface arises primarily due to electromagnetic forces that occur between liquid molecules in contact with solid molecules at the top surface of the sensor coating. This model is the first step in the understanding of the experimental variation of  $\alpha_{Re}$ ,  $\alpha_{Im}$ ,  $|\alpha|$  and  $\alpha_\theta$  versus kinematic viscosity,  $\nu$ , and mole fraction,  $M_f$ .

The relation between the elements of the mechanical model and the solid-liquid interface is summarized in Table 4.1.

**Table 4.1 Model and Interface**

Mechanical Model	Solid-liquid Interface
$m_1$	mass of liquid particle
$m_2$	mass of solid particle
$k$	force of attraction between solid and liquid particles
motion in x-direction	transverse shear mode (TSM)

#### 4.1.2 Statement of Problem

The displacement of mass,  $m_2$ , is  $x_2 = x_2(t) = A \cos(\omega t + \phi)$ , with  $A$ ,  $\omega$ , and  $\phi$  denoting respectively the amplitude, the angular frequency, and the phase angle of the displacement. It is required to find the displacement of mass  $m_1$ , given by,  $x_1 = x_1(t)$ , at any time,  $t$ . The quantities  $x_1(t)$  and  $x_2(t)$  are shown in Figure 4.1.

In Figure 4.1,  $l$  and  $l'$  denote respectively the nonextended length of the spring at time = 0, and the extended length of the spring at time =  $t$ . At time = 0 the motion of masses  $m_1$  and  $m_2$  start from rest, at their respective equilibrium positions.

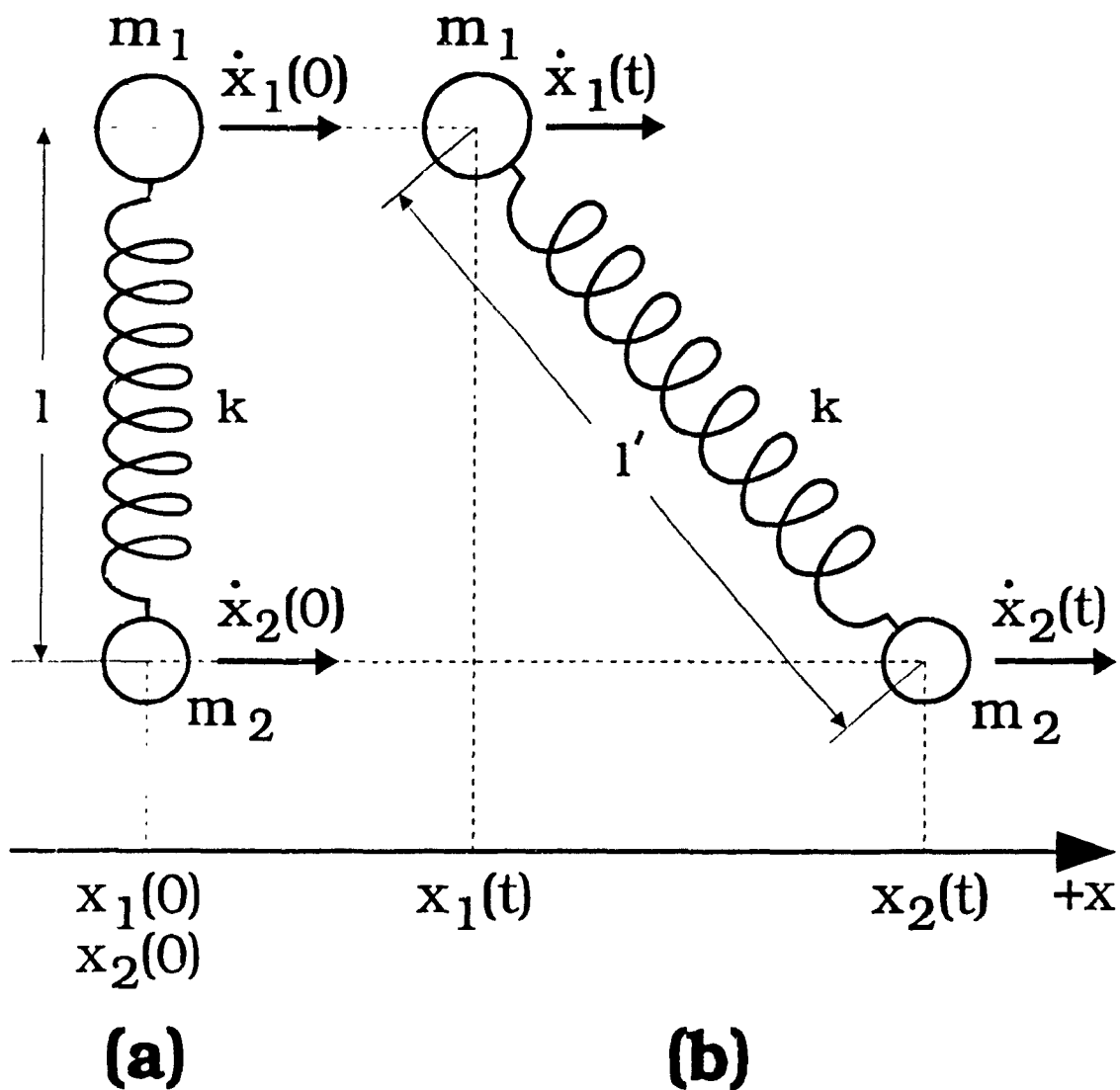


Figure 4.1 Mechanical model of interfacial slip showing masses  $m_1$  and  $m_2$  connected by a spring of force constant,  $k$ , at (a) time = 0 and (b) time =  $t$ .

### 4.1.3 Derivation of the Equations of Motion for the Interfacial Slip Model

The equation of motion for mass,  $m_1$ , is obtained from the Lagrangian,  $\mathcal{L}$ , of the spring-mass system at time =  $t$ . From Figure 4.1, the elongation,  $s = l' - l$ , of the spring at time =  $t$ , is given by

$$s = \sqrt{l^2 + (x_2 - x_1)^2} - l \quad (4-1)$$

The potential energy,  $V$ , and the kinetic energy,  $T$ , of the spring-mass system at time =  $t$ , are given by

$$V = \frac{1}{2}ks^2 = \frac{1}{2}k(\sqrt{l^2 + (x_2 - x_1)^2} - l)^2 \quad (4-2)$$

$$T = \frac{1}{2}(m_1\dot{x}_1^2 + m_2\dot{x}_2^2) \quad (4-3)$$

The spring in the model, has zero mass since it represents the electrical force between masses  $m_1$  and  $m_2$ . The Lagrangian,  $\mathcal{L}$ , of the spring mass system is given by

$$\begin{aligned} \mathcal{L} = T - V = & \frac{1}{2}(m_1\dot{x}_1^2 + m_2\dot{x}_2^2) \\ & - \frac{1}{2}k(\sqrt{l^2 + (x_2 - x_1)^2} - l)^2 \end{aligned} \quad (4-4)$$

Given that  $x_2 = x_2(t) = A \cos(\omega t + \phi)$ , equation (4-4) reduces to

$$\mathcal{L} = \frac{1}{2} (m_1 \dot{x}_1^2 + m_2 A^2 \omega^2 \sin^2(\omega t + \phi)) - \frac{1}{2} k (\sqrt{l^2 + (A \cos(\omega t + \phi) - x_1)^2} - l)^2 \quad (4-5)$$

Lagrange's equation of motion for mass,  $m_1$ , is given by

$$\frac{d}{dt} \frac{\partial \mathcal{L}}{\partial \dot{x}_1} = \frac{\partial \mathcal{L}}{\partial x_1} \quad (4-6)$$

From equations (4-5) and (4-6), the equation of motion for mass  $m_1$  is given in terms of  $\gamma$  which is defined as  $\gamma = x_2 - x_1 = A \cos(\omega t + \phi) - x_1$ .

$$\ddot{x}_1 = \frac{k}{m_1} \frac{(\sqrt{l^2 + \gamma^2} - l) \gamma}{\sqrt{l^2 + \gamma^2}} \quad (4-7)$$

Note that (4-7) is a second-order differential equation which is highly non-linear.

## 4.2 Numerical Solution of the Equations of Motion

### 4.2.1 Description of Runge-Kutta's Method

The fourth-order Runge-Kutta method, is used to solve equation (4-7) numerically for  $x_1$  as a function of the time,  $t$ . A system of  $n$  first-order differential equations in  $n$  unknowns  $u_0, \dots, u_n$  is given by

$$\dot{u}_i = F_i(u_i, t) \quad (4-8)$$

For each  $j = 0, 1, \dots, N - 1$  where  $N$ , is the number of time steps, the following four functions  $K_1, K_2, K_3$ , and  $K_4$  implement the fourth-order Runge-Kutta method of stepsize,  $h$ . In the four equations below,  $u_y = u_i(t_j)$ .

$$K_{1y} = hF_i(t_j, u_y) \quad (4-9)$$

$$K_{2y} = hF_i(u_y + \frac{1}{2}K_{1y}, t_j + \frac{h}{2}) \quad (4-10)$$

$$K_{3y} = hF_i(u_y + \frac{1}{2}K_{2y}, t_j + \frac{h}{2}) \quad (4-11)$$

$$K_{4y} = hF_i(u_y + K_{3y}, t_{j+1}) \quad (4-12)$$

For each  $i = 0, 1, \dots, n$  and  $j = 0, 1, \dots, N - 1$  the following recursive procedure, performs a weighted average.

$$u_{i,j+1} = u_{ij} + \frac{1}{6} (K_{1ij} + 2K_{2ij} + 2K_{3ij} + K_{4ij}) \quad (4-13)$$

Equation (4-7), may be rewritten as a first-order system consisting of two equations in the two unknowns  $u_0, u_1$ . Let

$$u_0 = x_1 \quad (4-14)$$

$$u_1 = \dot{x}_1 \quad (4-15)$$

$$\dot{u}_1 = \ddot{x}_1 \quad (4-16)$$

The following set of two equations will be solved by Mathcad. The first equation is obtained by substituting (4-14) into (4-15). The second equation is (4-7) written using (4-14) and (4-16).

$$\begin{aligned} \dot{u}_0 &= u_1 \\ \dot{u}_1 &= \frac{k}{m_1} \frac{(\sqrt{l^2 + \gamma^2} - 1) \gamma}{\sqrt{l^2 + \gamma^2}} \end{aligned} \quad (4-17)$$

The system of two equations, (4-17), are solved numerically by

the Mathcad program described in the next subsection.

#### 4.2.2 Numerical Solution of Interfacial Slip Model

In Appendix 9, Mathcad document DOC6.MCD implements the fourth-order Runge-Kutta method for the numerical solution of the equation of motion of mass,  $m_1$ . The displacement,  $x_1$ , of mass,  $m_1$ , is computed over five periods of the motion, that is, the closed time interval  $I = [0, 5/f]$ , for several values of the ratio,  $k/m_1$ , starting with a numerical value of 1 and ending with a numerical value of  $10^9$  metric units. In the interval,  $I$ , the frequency,  $f = 9.0$  MHz, is the oscillating frequency of mass,  $m_2$ . Mass,  $m_2$ , starts its motion from rest, with an amplitude,  $A$ , of one metric unit, and a phase angle,  $\phi$ , of  $-\pi/2$  radians. The motion of masses  $m_1$  and  $m_2$  both start at time  $t = 0$ . The displacement,  $x_1$ , of mass,  $m_1$ , was computed over the closed interval,  $I$ , in time steps of,  $\Delta t = 0.001 \mu\text{s}$ . The total number of points computed was  $N = 555$ . At each value of  $k/m_1$ , the maximum displacement,  $x_{1\text{max}}$ , was computed over the closed interval,  $I$ , using Mathcad's **max** function. The maximum displacement,  $x_{1\text{max}}$ , is defined as the greatest displacement of mass,  $m_1$ , over the closed interval,  $I$ . A two-dimensional data vector of data pairs, with each pair consisting of the  $\log(k/m_1)$  versus  $x_{1\text{max}}$ , was created in a semi-interactive manner using Mathcad's **WRITEPRN** and **APPENDPRN** functions. The data file **X1MAX.PRN**, which is a result of applying the functions **WRITEPRN** and **APPENDPRN**, contains the data pairs consisting of  $\log(k/m_1)$  versus  $x_{1\text{max}}$ . Figure 4.2



shows the variation of the maximum displacement of mass  $m_1$  versus the  $\log(k/m_1)$ . From Figure 4.2 at a certain critical value of  $k/m_1$ , the maximum displacement of mass  $m_1$  achieves its maximum value, therefore the spring-mass system is in resonance at this value.

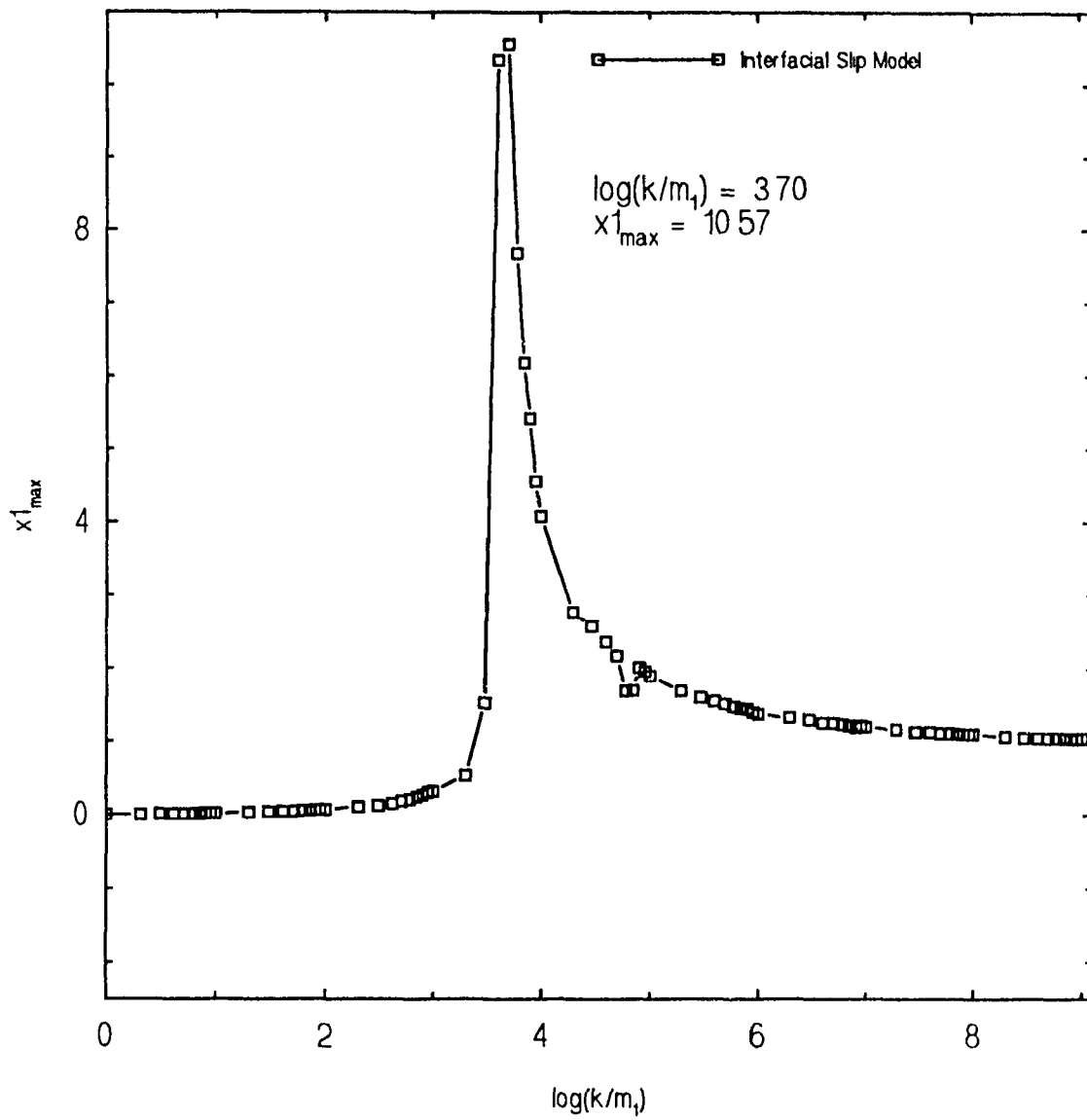


Figure 4.2 Maximum displacement of mass  $m_1$  versus the logarithm of the spring constant,  $k$ , divided by the mass,  $m_1$ , for the mechanical model of interfacial slip. The maximum displacement of mass  $m_2$  is unity.

## CHAPTER 5

### CONCLUSIONS

A new property of the interface called the interfacial slip parameter was introduced in the theory of the sensor in order to account for the slip between the surface of a sensor vibrating in the transverse shear mode and a liquid which is in contact with the surface of the sensor. The theoretical expression for the impedance was derived which is a function of the interfacial slip parameter. The impedance of sensors with hydrophilic and hydrophobic coatings was measured in water-glycerol solutions using the network analysis method. Then the interfacial slip parameter was found by fitting the experimental values of impedance to the theoretical expression for impedance using non-linear regression analysis.

The interfacial slip parameter,  $\alpha$ , is defined as  $\alpha = u_{(0)x}/u_x$ , where  $u_{(0)x}$  is the displacement of a liquid particle in contact with the solid surface of the sensor and  $u_x$  is the displacement of a solid particle on the surface of the sensor. If the force between the liquid particle and solid particle is very strong, their displacements will be the same and so  $\alpha = 1$ . In this case there is no slip at the interface between the solid and liquid. At the other extreme, if the force between the liquid and solid is zero, then there is no connection between the solid and liquid. In this case when the solid particles on the surface of the sensor move, the liquid

particles do not move, that is,  $\alpha = 0$ . Intuitively, one expects that the magnitude of  $\alpha$  should be between 0 and 1.

The measurements of impedance were made for the sensors in both air and liquid, and the experimental values of impedance were fitted to the theoretical expression for impedance using nonlinear regression analysis. In air,  $\alpha$  was set equal to zero since the connection between the molecules on the surface of the solid and the molecules in air is very weak. Two properties of the quartz were found by fitting theory and experiment in air: the piezoelectric stress coefficient,  $e$ , and the viscoelastic coefficient,  $\eta$ . The value of  $e$  found for both the hydrophilic and hydrophobic sensors is the same:  $e = -0.0798 \text{ C/m}^2$ , from Table 3.1. This is significantly different than the value of  $e$  in the literature:  $e = -0.095 \text{ C/m}^2$ . Since 401 measurements of impedance, each at a different frequency, were used to find  $e$ , and the value of  $e$  was the same for both sensors, it is speculated that the value of  $e$  in the literature is incorrect. The value of  $\eta$  for quartz was also found by fitting theory and experiment in air since  $\eta$  was not found in the literature. The value of  $\eta$  was not the same for both sensors.

The interfacial slip parameter,  $\alpha$ , was found by fitting the experimental values of impedance found in water-glycerol solutions with the theoretical expression for impedance. The magnitude of  $\alpha$ ,  $|\alpha|$ , is plotted versus kinematic viscosity of water-glycerol solutions in Figure 3.20 for hydrophilic and

hydrophobic sensors. At high viscosities, where the interaction between the solid surface and the liquid is strong,  $|\alpha|$  is near 1, as expected. At low viscosities, however, the magnitude of  $\alpha$  is larger than 1, not less than 1 as expected when the interaction at the interface is weak. Furthermore, at low viscosities,  $|\alpha|$  for the hydrophobic surface is greater than  $|\alpha|$  for the hydrophilic surface, as seen from the left side of Figure 3.20. This means that the amplitude of the liquid particle is greater when the interaction between the liquid particle and solid particle is smaller.

This behaviour is explained by a mechanical model which was invented to represent the interaction between particles on the surface of the sensor and particles of the liquid in contact with the surface. The model is drawn in Figure 4.1. Two masses connected by a spring are constrained to move transversely. One mass,  $m_2$ , represents a solid particle on the sensor surface which moves sinusoidally with time at a constant frequency and at constant amplitude, which is chosen as unity. The other mass,  $m_1$ , represents a liquid particle in contact with the solid particle. The spring, with spring constant,  $k$ , represents the force of attraction between the two particles. The system was analyzed to find the displacement of the liquid particle in terms of its mass,  $m_1$ , and the spring constant,  $k$ .

The variation of maximum displacement (the amplitude) of

the liquid particle in the model as a function of the log of the (spring constant)/(mass of liquid particle) is given in Figure 4.2. As expected, as the spring constant approaches zero, the amplitude of the liquid particle approaches zero. At this extreme, the liquid particle and solid particle are disconnected. As the spring constant becomes very large, the amplitude of the liquid particle becomes 1, the same as the solid particle. This is the other extreme where the liquid and solid particles are rigidly connected together. In between the two extremes there is a resonant region of the spring-mass system. The amplitude of the liquid-particle mass is a maximum at a particular value of the ratio of the spring constant,  $k$ , and the mass of the liquid particle,  $m_1$ . In Figure 4.2 the frequency is 9.0 MHz and  $k/m_1$  is expressed in metric units. The mass of the solid particle,  $m_2$ , does not influence the motion of  $m_1$  in this model because it is driven (forced to oscillate) at a constant unit amplitude.

The amplitude of the liquid-particle in Figure 4.2 is numerically equal to the magnitude of the interfacial slip parameter in Figure 3.20, since the amplitude of the solid-particle is unity. The spring constant,  $k$ , in Figure 4.2 corresponds to the kinematic viscosity of the liquid in contact with the surface of the sensor in Figure 3.20. The mass,  $m_1$ , in Figure 2 corresponds to the mass of the liquid particle in contact with the sensor surface. In Figure 4.2 the log of  $k/m_1$  is plotted and in Figure 3.20 the kinematic

viscosity is plotted on a log scale.

It is clear from the results of the analysis of the mechanical model given in Figure 3.20 that an increase of  $k$ , say by a factor of two, has exactly the same effect as a decrease of  $m_1$  by the same factor of two. In the experiments, various water-glycerol solutions were in contact with the sensor surface, starting with pure water and ending with pure glycerol. The viscosity of water is 1 cS and the viscosity of glycerol is 1400 cS which corresponds to the spring constant,  $k$ , in the model. But as the water is replaced by the glycerol, the mass of the liquid molecules in contact with the sensor surface also increases, corresponding to the mass,  $m_1$ , in the model. The molecular weight of water,  $H_2O$ , is 18 and the molecular weight of glycerol,  $C_3H_8O_3$ , is 92. As the solution changes from water to glycerol, the viscosity increases by a factor of 1400 whereas the molecular weight increases by only a factor of about 5. So the increase of viscosity is offset somewhat by the mass of the liquid molecules. However, when comparing Figure 3.20 and Figure 4.2, the mass of the liquid particles can be regarded as constant.

The shape of the curve to the right of the resonant peak of the model in Figure 4.2 is the same as the shape of the curve of the experimental results in Figure 3.20. In Figure 3.20,  $|\alpha| \approx 5$  for kinematic viscosity = 1 and  $|\alpha| \approx 1$  for kinematic viscosity  $\approx 10^3$ . In Figure 4.2,  $x_{1_{max}}$  (which is

numerically the same as  $|\alpha|$ ) has the value of 5 at  $k/m_1 \approx 10^4$ , and  $x_{1_{\max}}$  drops to about 1 at  $k/m_1 \approx 10^7$ . So very roughly, a kinematic viscosity of 1 corresponds to a  $k/m_1$  of  $10^4$  and the two quantities are roughly proportional to each other.

The separation of the curves for the hydrophilic and hydrophobic sensors in Figure 3.20 can also be interpreted in terms of the model of Figure 4.2. At low viscosity  $|\alpha|$  for the hydrophobic sensor is larger than  $|\alpha|$  for the hydrophilic sensor. At a given viscosity, that is, for a given water-glycerol solution in the experiments, the force of interaction between the liquid and a hydrophobic surface is less than between the same liquid and a hydrophilic surface. Therefore the value of  $k$  in Figure 4.2 is lower and so the value of  $x_{1_{\max}}$  (which equals  $|\alpha|$ ) is larger, which is in agreement with the larger  $|\alpha|$  in Figure 3.20. Effectively, the hydrophobic sensor surface corresponds to a region of Figure 4.2 which is to the left of the region for the hydrophilic sensor surface.

In summary, there is good qualitative agreement between the experimental results and the predictions of the mechanical model of interfacial slip. For both the hydrophilic and hydrophobic sensors, there is considerable slip when the liquid in contact with the surface is water (low viscosity) and very little slip when the liquid is glycerol (high viscosity).



## APPENDIX 1      Application Software

The application software that was used to do the research and prepare the thesis is listed below. IBM-compatible 386 and 486 computers were used to run the software. The computer used in the Physics research laboratory is an IBM-compatible 486DX, 33 MHz with 32 MB of RAM. It is connected to a Hewlett-Packard LaserJet III printer which was used to print the thesis. The application software is the following.

- (1) Windows 3.1
- (2) WordPerfect 5.1 for Windows
- (3) CoreDraw 2.0 for Windows
- (5) EasyPlot for DOS
- (4) Mathcad 3.1 for Windows
- (6) Macsyma 417.125 for Windows

Windows 3.1 is the operating system.

WordPerfect 5.1 is a word processing program. The text was typed, and the equations and tables were made with WordPerfect. WordPerfect was also used as described below.

CorelDraw 2.0 is a graphics (or drawing) program. The diagrams were made with CorelDraw and then the .cdr files were exported to .tif files using File/Export in CorelDraw. A WordPerfect macro was used to add the diagrams to WordPerfect files by using Graphics/Figure/Retrieve and then formatting the diagrams by Graphics/Figure/Position and then setting, Anchor to: Character and Size: Auto Both.

EasyPlot is a plotting (or presentation) program. The graphs were made by EasyPlot from text files of the data from the network analyzer. The graphs were plotted by EasyPlot. Then the captions and page numbers were printed on the graphs by WordPerfect.

Mathcad 3.1 is a numerical mathematics program. The Mathcad programs were printed by Mathcad. Then the titles and page numbers were printed on the Mathcad pages by WordPerfect.

Macsyma 417.125 is a symbolic mathematics program. The source code and the output of the Macsyma program are text files which were printed by WordPerfect.

## APPENDIX 2      Subscript Notation

Subscript (also called tensor) notation is used instead of symbolic (also called vector) notation because the equations of piezoelectricity include tensor quantities of rank two and greater. Although symbolic notation can be used to state the equations, the equations cannot be easily manipulated using this notation.

The conventions of the notation for cartesian tensors are stated, the kronecker delta and levi-civita symbol are defined, and examples of tensor quantities and notation are given.

### Conventions

The numbers 1, 2 and 3 label the x, y and z directions, respectively. The coordinates of a point (x,y,z) are written  $(x_1, x_2, x_3)$ . The components of a vector, the particle displacement for example,  $(u_x, u_y, u_z)$  are written  $(u_1, u_2, u_3)$ . The indices i,j,k . . . are used to represent the x, y and z directions and they take the values 1, 2 and 3.

- (1) Range Convention: single subscript  
Subscript i that occurs once in a term takes all three values of 1,2,3. For example,

$$u_i \text{ means } u_1, u_2, u_3$$

- (2) Summation Convention: repeated subscript  
Subscript i that occurs twice (or more) in a term is summed over 1,2,3. For example,

$$a_{ij} u_j \text{ means } \sum_{j=1}^3 a_{ij} u_j$$

- (3) Partial derivative convention: subscript comma  
Subscript ,i denotes partial differentiation with respect to the ith coordinate,  $x_i$ . For example,

$$u_{i,j} \text{ means } \frac{\partial u_i}{\partial x_j}$$

**Kronecker Delta,  $\delta_{ij}$** 

The kronecker delta by definition is

$$\delta_{ij} = \begin{cases} 1 & \text{if } i = j \\ 0 & \text{if } i \neq j \end{cases}$$

For example,  $\delta_{11} = 1$  and  $\delta_{12} = 0$ .

**Levi-civita Symbol,  $\epsilon_{ijk}$** 

The levi-civita symbol, also called the permutation symbol, by definition is

$$\epsilon_{ijk} = \begin{cases} 1 & \text{if } (ijk) \text{ is an even permutation of } (123) \\ -1 & \text{if } (ijk) \text{ is an odd permutation of } (123) \\ 0 & \text{if any two indices are equal} \end{cases}$$

For example,  $\epsilon_{123} = 1$ ,  $\epsilon_{213} = -1$  and  $\epsilon_{113} = 0$ .

The levi-civita symbol is related to the kronecker delta by the following identity.

$$\epsilon_{ijk} \epsilon_{ipq} = \delta_{jp} \delta_{kq} - \delta_{jq} \delta_{kp}$$

The following two relations are a consequence of the identity above.

$$\epsilon_{ijk} \epsilon_{ijl} = 2 \delta_{kl}$$

$$\epsilon_{ijk} \epsilon_{ijk} = 3!$$

### Examples

The examples of tensors in Table A2.1 are from the equations of piezoelectricity. The rank of a tensor quantity is equal to the number of subscripts on the quantity.

**Table A2.1 Examples of Tensors**

Tensor		Quantity	
Rank	Name	Symbol	Name
0	scalar	$\varphi$	scalar potential
1	vector	$E_i$	electric field
		$u_i$	particle displacement
2		$T_{ij}$	stress
		$S_{ij}$	strain
		$\epsilon_{ik}$	dielectric strain coefficient
3		$e_{ijk}$	piezoelectric stress coefficient
4		$C_{ijkl}$	elastic coefficient

The examples of notation in Table A2.2 are from the equations of piezoelectricity. In the symbolic notation, a single dot indicates summation over a single subscript and a double dot, summation over two subscripts. The symbolic notation does not indicate the rank of the tensor. This is the symbolic notation used by Auld, Volume I (1973).

**Table A2.2 Examples of Notation**

Name	Symbolic Notation	Subscript Notation
gradient	$\nabla\varphi$	$\varphi_{,i}$
divergence	$\nabla \cdot \mathbf{E}$	$E_{i,i}$
curl	$\nabla \times \mathbf{E}$	$\epsilon_{ijk} E_{k,j}$
	$\nabla u$	$u_{,i}$
	$\nabla \cdot \mathbf{T}$	$T_{ij,i}$
	$\mathbf{e} \cdot \mathbf{E}$	$e_{ij} E_j$
	$\mathbf{e} : \mathbf{S}$	$e_{,ij} S_{ji}$

APPENDIX 3      Solution of Boundary Value Problem,  
Macsyma Program ZIN.WP

MACSYMA SOURCE CODE

```
(clearscreen(),kill(all),fancy_display:false)$

/* Determine the electrical input impedance Zin for
the liquid loaded AT-Cut

quartz sensor... */

/* establish dependencies for uq,ul, and vl. */

(ratfac:true,
 depends([uq,ul,vl.phi],[y,t]),
 depends([f1,f2,f3],y),
 assume(nu>0,omega>0))$

/* The equation of motion for the transverse particle
displacement uq in the quartz sensor
is
given by...*/

eq1:cbar*difff(uq,y,2) + eta*difff(uq,y,2,t,1) -
rhoq*difff(uq,t,2) = 0;

/* The potential phi and the transverse particle
displacement uq are related to each
other by the following relation...*/

eq2:e*difff(uq,y,2) - epsilon*difff(phi,y,2) = 0;

/* Let uq = f1(y)*exp(%i*omega*t) and phi =
f2(y)*exp(%i*omega*t), equation eq1
reduces to...*/

(expr1:ev(eq1,uq =
f1*exp(%i*omega*t),diff,ratsimp)/exp(%i*omega*t),
 expr1:ratsimp(expr1,difff(f1,y,2)),
 disp(expr1))$

/* Let f1 = exp(%i*r*y), the general solution to
equation eq1 is given by...*/

(expr1:factor(ev(expr1,f1 =
exp(%i*r*y),diff,ratsimp)/exp(%i*r*y)),
 soll:solve(expr1,r),
 disp("The christoffel equation to equation eq1 is
given by...",
 expr1,
 "The solution to the above christoffel equation
```

```

is given by..."
      sol1))$

      /* Let kq denote the complex wave number for the quartz
sensor, kq is defined as
follows...*/

      cwq:kq = rhs(sol1[2]);

      /* The general solution to equation eq1 is given
by...*/

      (sol1:subst(kq,rhs(sol1[2]),sol1),
      gen_sol1:uq =
sum(concat(a,i)*exp(%i*rhs(sol1[i])*y),i,1,2)*exp(%i*omega*t
),
      disp(gen_sol1))$

      /* From equation eq2 the potential phi is given by...*/

      (expr2:expand(ev(eq2,[phi =
f2*exp(%i*omega*t),gen_sol1],diff,ratsimp)/exp(%i*omega*t)),
      expr2:ode(expr2,f2,y),
      expr2:subst(a3,%k2,expr2),
      expr2:rhs(expand(subst(a4,%k1,expr2))),
      gen_sol2:ev(phi = expr2*exp(%i*omega*t),sol2),
      disp(gen_sol2))$

/* Perform a check to determine if gen_sol1 and gen_sol2
satisfy equations eq1 and
      eq2...*/

      (check1:ev([eq1,eq2],[gen_sol1,gen_sol2],diff,ratsimp),
      check1:ev(check1,cwq,ratsimp),
      map(disp,check1))$

      /* The equation of motion for the transverse particle
velocity v1 in the liquid medium is
      given by...*/

      eq3:mu*diff(v1,y,2) - rho1*diff(v1,t,1) = 0;

      /* With mu = nu*rho1 and v1 = diff(u1,t,1), then
equation eq3 reduces to...*/

      eq3:expand(ev(eq3,[mu = nu*rho1,v1 =
diff(u1,t,1)],diff)/rho1);

      /* Let u1 = f3(y)*exp(%i*omega*t), then equation eq3

```

reduces to...\*/

```
    expr3:factor(ev(eq3,u1 =
f3*exp(%i*omega*t),diff,ratsimp)/exp(%i*omega*t));
```

/\* Let  $f3 = \exp(i*r*y)$ , then the general solution to equation eq3 is given by...\*/

```
    (expr3:factor(ev(expr3,f3 =
exp(%i*r*y),diff,ratsimp)/exp(%i*r*y)),
    sol3:solve(expr3,r),
    disp("The christoffel equation to equation eq3 is
given by...",
        expr3,
        "The solution to the above christoffel equation
is given by...",
        sol3))$
```

/\* Let  $k1$  denote the complex wave number for the liquid-medium,  $k1$  is defined as follows...\*/

```
    cw1:k1 = rhs(sol3[2]);
```

/\* The general solution equation eq3 is given by...\*/

```
    (sol3:subst(k1,rhs(sol3[2]),sol3),
    gen_sol3:u1 =
sum(concat(a,i+4)*exp(%i*rhs(sol3[i])*y),i,1,2)*exp(%i*omega
*t),
    disp(gen_sol3))$
```

/\* Perform a check to determine if gen\_sol3 satisfies equation eq3...\*/

```
    (check3:ev(eq3,gen_sol3,diff,ratsimp),
    check3:ev(check3,cw1,ratsimp),
    disp(check3))$
```

/\* Physically as  $y \rightarrow \text{infinity}$ ,  $u1 \rightarrow 0$ , therefore consider the limit as  $y \rightarrow \text{infinity}$  of each of the two terms  $\exp(i*k1*y)$  and  $\exp(-i*k1*y)$  seperately...\*/

```
    (term1:exp(%i*k1*y),
    term1:ev(term1,cw1,ratsimp),
    term1:factor(rectform(term1)),
```

```

disp(term1))$

/* take the limit of the magnitude of the above
expression as y -> infinity...*/

(term1:trigsimp(cabs(term1)),
 limit1:'limit(term1,y,inf) = limit(term1,y,inf));

(term2:exp(-%i*k1*y),
 term2:ev(term2,cw1,ratsimp),
 term2:factor(rectform(term2)),
 disp(term2))$

/* take the limit of the magnitude of the above
expression as y -> infinity...*/

(term2:trigsimp(cabs(term2)),
 limit2:'limit(term2,y,inf) = limit(term2,y,inf));

/* As y -> infinity exp(%i*k1*y) -> infinity while
exp(-%i*k1*y) -> 0.
Therefore in order for u1 to remain finite for all y
a6 must be set to zero.
Thus for finite u1, a6=0. */

gen_sol3:ev(gen_sol3,a6=0,ratsimp);

/* The shear stresses Tq and Tl are given by... */

(Tq:c*diff(uq,y,1)+eta*diff(uq,y,1,t,1)+e*diff(phi,y,1),
 Tl:mu*diff(vl,y,1),
 Tl:ev(Tl,[vl = diff(u1,t,1),mu = nu*rhol],diff),
 display(Tq,Tl))$

/* Substituting gen_sol1,gen_sol2, and gen_sol3 into
the expression for Tq and Tl.
Tq and Tl reduce down to...*/

(Tq:ev(Tq,[gen_sol1,gen_sol2],diff,ratsimp),
 Tq:factorsum(ratsimp(ratsubst(cbar,c+e^2/epsilon,Tq))),
 Tl:factorsum(ev(Tl,gen_sol3,diff,ratsimp)),
 display(Tq,Tl))$

/* Implement the boundary conditions...*/

/* Stress free boundary condition: Tq(0,t) = 0 */

```



```
BC1:ratsimp(ev(Tq=0,y=0,ratsimp)/exp(%i*omega*t),a1,a2,a3,a4,
,a5,kq,kl);
```

```
/* continuity of stress across interface: Tq(h,t) =
T1(h,t) */
```

```
BC2:ratsimp(ev(Tq =
T1,y=h,ratsimp)/exp(%i*omega*t),a1,a2,a3,a4,a5,kq,kl);
```

```
/* Potential at bottom surface of quartz sensor:
phi(0,t) = -phi0*exp(%i*omega*t) */
```

```
(phi:rhs(gen_sol2),
BC3:ratsimp(ev(phi =
-phi0*exp(%i*omega*t),y=0,ratsimp)/exp(%i*omega*t),a1,a2,a3,
a4,a5,kq,kl));
```

```
/* Potential at top surface of quartz sensor: phi(h,t)
= phi0*exp(%i*omega*t) */
```

```
BC4:ratsimp(ev(phi =
phi0*exp(%i*omega*t),y=h,ratsimp)/exp(%i*omega*t),a1,a2,a3,a
4,a5,kq,kl);
```

```
/* slip boundary condition: ul(h,t) = alpha*uq(h,t) */
```

```
(uq:rhs(gen_sol1),
ul:rhs(gen_sol3),
BC5:ratsimp(ev(ul = alpha*uq, y=h,
ratsimp)/exp(%i*omega*t),a1,a2,a3,a4,a5,kq,kl));
(pause(),
clearscreen(),
disp("Let",gamma1 = exp(%i*h*kq), gamma2 =
exp(%i*h*kl), delta =
eta*omega-%i*cbar),
pause(),
clearscreen()))$
```

```
(BC:expand([BC1,BC2,BC3,BC4,BC5]),
BC:ratsubst(gamma1,exp(%i*h*kq),BC),
BC:ratsubst(gamma2,exp(%i*h*kl),BC),
BC:ratsimp(ratsubst(delta, eta*omega-%i*cbar,BC)),
map(dispatch,BC),
pause(),
```

```

clearscreen())$

/* The solution to the above boundary value problem is
given by...*/

(solBC:linsolve(BC,[a1,a2,a3,a4,a5]),
 solBC1:rhs(solBC[1]),
 solBC2:rhs(solBC[2]),
 solBC3:rhs(solBC[3]),
 solBC4:rhs(solBC[4]),
 solBC5:rhs(solBC[5]),
 solBC1num:num(solBC1),
 solBC1denom:denom(solBC1),
 solBC2num:num(solBC2),
 solBC2denom:denom(solBC2),
 solBC3num:num(solBC3),
 solBC3denom:denom(solBC3),
 solBC4num:num(solBC4),
 solBC4denom:denom(solBC4),
 solBC5num:num(solBC5),
 solBC5denom:denom(solBC5),
 pause(),
 clearscreen(),
 disp("Let",
      b11 = factorsum(ratcoef(solBC1num,alpha,0)),
      b12 = factorsum(ratcoef(solBC1num,alpha,1)),
      b13 = factorsum(ratcoef(solBC1denom,alpha,0)),
      b14 = factorsum(ratcoef(solBC1denom,alpha,1)),
      "Therefore...",
      a1 = (b11 + alpha*b12)/(b13 + alpha*b14)),
 pause(),
 clearscreen(),
 disp("Let",
      b21 = factorsum(ratcoef(solBC2num,alpha,0)),
      b22 = factorsum(ratcoef(solBC2num,alpha,1)),
      b23 = factorsum(ratcoef(solBC2denom,alpha,0)),
      b24 = factorsum(ratcoef(solBC2denom,alpha,1)),
      "Therefore...",
      a2 = (b21 + alpha*b22)/(b23 + alpha*b24)),
 pause(),
 clearscreen(),
 disp("Let",
      b31 =
factorsum(ratcoef(ratcoef(solBC3num,alpha,0),phi0)),
      b32 =
factorsum(ratcoef(ratcoef(solBC3num,alpha,1),phi0)),
      b33 = factorsum(ratcoef(solBC3denom,alpha,0)),
      b34 = factorsum(ratcoef(solBC3denom,alpha,1)),
      "Therefore...",
      a3 = ((b31 + alpha*b32)*phi0)/(b33 + alpha*b34)),
 pause(),

```

```

clearscreen(),
disp("Let",
      b41 = factorsum(ratcoef(solBC4num,alpha,0)),
      b42 = factorsum(ratcoef(solBC4num,alpha,1)),
      b43 = factorsum(ratcoef(solBC4denom,alpha,0)),
      b44 = factorsum(ratcoef(solBC4denom,alpha,1)),
      "Therefore...",
      a4 = (b41 + alpha*b42)/(b43 + alpha*b44)),
pause(),
clearscreen(),
disp("Let",
      b51 = factorsum(ratcoef(solBC5num,alpha,0)),
      b52 = factorsum(ratcoef(solBC5num,alpha,1)),
      b53 = factorsum(ratcoef(solBC5denom,alpha,0)),
      b54 = factorsum(ratcoef(solBC5denom,alpha,1)),
      "Therefore...",
      a5 = (b51 + alpha*b52)/(b53 + alpha*b54))$

/* The electric displacement D in the quartz sensor is
given by... */

(D:e*diff('uq,y,1) - epsilon*diff('phi,y,1),
 display(D))$

/* Substituting uq and phi into D we get... */

(D:ev(D,diff,ratsimp),
 display(D))$

/* The total surface charge Q of the quartz sensor is
given by... */

Q:D*A;

/* The instataneous current i is given by... */

i:diff(Q,t,1);

/* The electrical input impedance of the liquid-loaded
AT-cut quartz sensor is given by...
*/

(Zin:(-phi0*exp(%i*omega*t) - phi0*exp(%i*omega*t))/i,
 a3:((b31 + alpha*b32)*phi0)/(b33 + alpha*b34),
 Zin:ratsimp(ev(Zin)),
 display(Zin))$

```

## MACSYMA OUTPUT

```
>> Executing: D:\MACSYMA\MACSYMA.EXE D:\MACSYMA\MACSYMA.CLO
This is Macsyma 417.125 for Intel 80386/486 Series
Computers.
Copyright (c) 1982 - 1992 Macsyma Inc. All rights reserved.
Portions copyright (c) 1982 Massachusetts Institute of
Technology.
All rights reserved.
Type "DESCRIBE(TRADE_SECRET);" to see important legal
notices.
Type "HELP();" for more information.
```

```
D:\macsyma\system\init.lsp being loaded.
←|$LABEL(-1,15,Times New Roman,)Batching the file
D:\macsyma\mac-init.mac
Batchload done.
(c1) display2d:false$
(c2) batch("D:\\MACSYMA\\ZIN.TXT");

(c3) (clearscreen(),kill(all),fancy_display:false)$

(c1) /* Determine the electrical input impedance Zin for
the liquid loaded AT-Cut

    quartz sensor... */

/* establish dependencies for uq,ul, and vl. */

(ratfac:true,
 depends([uq,ul,vl,phi],[y,t]),
 depends([f1,f2,f3],y),
 assume(nu>0,omega>0))$

(c2) /* The equation of motion for the transverse particle
displacement uq in the quartz sensor is
given by...*/

eq1:cbar*diff(uq,y,2) + eta*diff(uq,y,2,t,1) -
rhoq*diff(uq,t,2) = 0;

(D2)
cbar*'DIFF(uq,y,2)-rhoq*'DIFF(uq,t,2)+eta*'DIFF(uq,t,1,y,2)
= 0

(c3) /* The potential phi and the transverse particle
displacement uq are related to each
other by the following relation...*/

eq2:e*diff(uq,y,2) - epsilon*diff(phi,y,2) = 0;

(D3) e*'DIFF(uq,y,2)-epsilon*'DIFF(phi,y,2) = 0
```

```
(c4) /* Let  $u_q = f_1(y) \exp(i\omega t)$  and  $\phi = f_2(y) \exp(i\omega t)$ , equation eq1 reduces to...*/
```

```
(expr1:ev(eq1,uq =
f1*exp(i*omega*t),diff,ratsimp)/exp(i*omega*t),
expr1:ratsimp(expr1,diff(f1,y,2)),
disp(expr1))$
```

$$f_1 \omega^2 \rho_0 + \text{DIFF}(f_1, y, 2) * (i \eta \omega + \bar{c}) = 0$$

```
(c5) /* Let  $f_1 = \exp(i r y)$ , the general solution to equation eq1 is given by...*/
```

```
(expr1:factor(ev(expr1,f1 =
exp(i*r*y),diff,ratsimp)/exp(i*r*y)),
sol1:solve(expr1,r),
disp("The christoffel equation to equation eq1 is given
by..."),
expr1,
"The solution to the above christoffel equation is
given by..."),
sol1))$
```

"The christoffel equation to equation eq1 is given by..."

$$\omega^2 \rho_0 - i \eta \omega r^2 - \bar{c} r^2 = 0$$

"The solution to the above christoffel equation is given by..."

```
[r = -omega*sqrt(rho0/(i*eta*omega+cbar)),r =
omega*sqrt(rho0/(i*eta*omega
+cbar))]
```

```
(c6) /* Let  $k_q$  denote the complex wave number for the quartz sensor,  $k_q$  is defined as follows...*/
```

```
cwq:kq = rhs(sol1[2]);
```

```
(D6)  $k_q = \omega \sqrt{\rho_0 / (i \eta \omega + \bar{c})}$ 
```

```
(c7) /* The general solution to equation eq1 is given
by...*/
```

```
(sol1:subst(kq,rhs(sol1[2]),sol1),
gen_sol1:uq =
sum(concat(a,i)*exp(i*rhs(sol1[i])*y),i,1,2)*exp(i*omega*t
```

```

),
  disp(gen_sol1))$
uq = %e^(%i*omega*t)*(a2*%e^(%i*kq*y)+a1*%e^-(%i*kq*y))

(c8) /* From equation eq2 the potential phi is given by...*/
(expr2:expand(ev(eq2,[phi =
f2*exp(%i*omega*t),gen_sol1],diff,ratsimp)/exp(%i*omega*t)),
  expr2:ode(expr2,f2,y),
  expr2:subst(a3,%k2,expr2),
  expr2:rhs(expand(subst(a4,%k1,expr2))),
  gen_sol2:ev(phi = expr2*exp(%i*omega*t),sol2),
  disp(gen_sol2))$
D:\macsyma\ode\ode.fas being loaded.
D:\macsyma\ode\odeaux.fas being loaded.
D:\macsyma\ode\ode2.fas being loaded.

phi =
%e^(%i*omega*t)*(a2*e*%e^(%i*kq*y)/epsilon+a1*e*%e^-(%i*kq*y)
)/epsilon
+a3*y+a4)

(c9) /* Perform a check to determine if gen_sol1 and
gen_sol2 satisfy equations eq1 and eq2...*/

(check1:ev([eq1,eq2],[gen_sol1,gen_sol2],diff,ratsimp),
  check1:ev(check1,cwq,ratsimp),
  map(disp,check1))$

0 = 0

0 = 0

(c10) /* The equation of motion for the transverse particle
velocity v1 in the liquid medium is
given by...*/

eq3:mu*diff(v1,y,2) - rho1*diff(v1,t,1) = 0;

(D10) mu*'DIFF(v1,y,2)-rho1*'DIFF(v1,t,1) = 0

(c11) /* With mu = nu*rho1 and v1 = diff(u1,t,1), then
equation eq3 reduces to...*/

eq3:expand(ev(eq3,[mu = nu*rho1,v1 =
diff(u1,t,1)],diff)/rho1);

```

```

(D11) nu*'DIFF(u1,t,1,y,2) - 'DIFF(u1,t,2) = 0

(c12) /* Let u1 = f3(y)*exp(%i*omega*t), then equation eq3
reduces to...*/

expr3:factor(ev(eq3,u1 =
f3*exp(%i*omega*t),diff,ratsimp)/exp(%i*omega*t));

(D12) omega*(f3*omega+%i*'DIFF(f3,y,2)*nu) = 0

(c13) /* Let f3 = exp(%i*r*y), then the general solution to
equation eq3 is given by...*/

(expr3:factor(ev(expr3,f3 =
exp(%i*r*y),diff,ratsimp)/exp(%i*r*y)),
sol3:solve(expr3,r),
disp("The christoffel equation to equation eq3 is given
by...",
expr3,
"The solution to the above christoffel equation is
given by...",
sol3))$

"The christoffel equation to equation eq3 is given by..."

-omega*(%i*nu*r^2-omega) = 0

"The solution to the above christoffel equation is given
by..."

[r = -sqrt(-%i)*sqrt(omega)/sqrt(nu),r =
sqrt(-%i)*sqrt(omega)/sqrt(nu)]

(c14) /* Let k1 denote the complex wave number for the
liquid-medium, k1 is defined as follows...*/

cwl:k1 = rhs(sol3[2]);

(D14) k1 = sqrt(-%i)*sqrt(omega)/sqrt(nu)

(c15) /* The general solution equation eq3 is given by...*/

(sol3:subst(k1,rhs(sol3[2]),sol3),
gen_sol3:ul =
sum(concat(a,i+4)*exp(%i*rhs(sol3[i])*y),i,1,2)*exp(%i*omega
*t),

```

```

disp(gen_sol3))$

u1 = %e^(%i*omega*t)*(a6*%e^(%i*k1*y)+a5*%e^-(%i*k1*y))

(c16) /* Perform a check to determine if gen_sol3 satisfies
equation eq3...*/

(check3:ev(eq3,gen_sol3,diff,ratsimp),
 check3:ev(check3,cw1,ratsimp),
 disp(check3))$

0 = 0

(c17) /* Physically as y -> infinity, u1 -> 0, therefore
consider the limit as y -> infinity of
each of the two terms exp(%i*k1*y) and exp(-%i*k1*y)
seperately...*/

(term1:exp(%i*k1*y),
 term1:ev(term1,cw1,ratsimp),
 term1:factor(rectform(term1)),
 disp(term1))$

%e^(sqrt(omega)*y/(sqrt(2)*sqrt(nu)))*(%i*sin(sqrt(omega)*y/
(sqrt(2)*sqrt(nu)
))) + cos(sqrt(omega)*y/(sqrt(2)*sqrt(nu)))

(c18) /* take the limit of the magnitude of the above
expression as y -> infinity...*/

(term1:trigsimp(cabs(term1)),
 limit1:'limit(term1,y,inf) = limit(term1,y,inf));
D:\macsyms\share\trigsimp.fas being loaded.

(D18) 'limit(%e^(sqrt(omega)*y/(sqrt(2)*sqrt(nu))),y,inf) =
inf

(c19) (term2:exp(-%i*k1*y),
 term2:ev(term2,cw1,ratsimp),
 term2:factor(rectform(term2)),
 disp(term2))$

-%e^-(sqrt(omega)*y/(sqrt(2)*sqrt(nu)))*(%i*sin(sqrt(omega)*
y/(sqrt(2)*sqrt
(nu)))-cos(sqrt(omega)*y/(sqrt(2)*sqrt(nu))))

(c20) /* take the limit of the magnitude of the above
expression as y -> infinity...*/

```



```

(term2:trigsimp(cabs(term2)),
 limit2:'limit(term2,y,inf) = limit(term2,y,inf));

(D20) 'limit(%e^-(sqrt(omega)*y/(sqrt(2)*sqrt(nu))),y,inf) =
0

(c21) /* As y -> infinity exp(%i*kl*y) -> infinity while
exp(-%i*kl*y) -> 0.
Therefore in order for ul to remain finite for all y a6
must be set to zero.
Thus for finite ul, a6=0. */

gen_sol3:ev(gen_sol3,a6=0,ratsimp);

(D21) ul = a5*%e^(%i*omega*t-%i*kl*y)

(c22) /* The shear stresses Tq and Tl are given by... */

(Tq:c*diff(uq,y,1)+eta*diff(uq,y,1,t,1)+e*diff(phi,y,1),
 Tl:mu*diff(vl,y,1),
 Tl:ev(Tl,[vl = diff(ul,t,1),mu = nu*rhol],diff),
 display(Tq,Tl))$

tq = c*'DIFF(uq,y,1)+eta*'DIFF(uq,t,1,y,1)+e*'DIFF(phi,y,1)

t1 = nu*rhol*'DIFF(ul,t,1,y,1)

(c23) /* Substituting gen_sol1,gen_sol2, and gen_sol3 into
the expression for Tq and Tl.
Tq and Tl reduce down to...*/

(Tq:ev(Tq,[gen_sol1,gen_sol2],diff,ratsimp),
 Tq:factorsum(ratsimp(ratsubst(cbar,c+e^2/epsilon,Tq))),
 Tl:factorsum(ev(Tl,gen_sol3,diff,ratsimp))),
 display(Tq,Tl))$

tq =
-(kq*(eta*omega-%i*cbar)*(a2*%e^(2*%i*kq*y)-a1)-a3*e*%e^(%i*
kq*y))*%e^
(%i*omega*t-%i*kq*y)

t1 = a5*kl*nu*omega*rhol*%e^(%i*omega*t-%i*kl*y)

(c24) /* Implement the boundary conditions...*/

/* Stress free boundary condition: Tq(0,t) = 0 */

BC1:ratsimp(ev(Tq=0,y=0,ratsimp)/exp(%i*omega*t),a1,a2,a3,a4

```

```

,a5,kq,kl);

(D24)
a3*e-kq*(a2*(eta*omega-%i*cbar)+a1*(%i*cbar-eta*omega)) = 0

(c25) /* continuity of stress across interface: Tq(h,t) =
Tl(h,t) */

BC2:ratsimp(ev(Tq =
Tl,y=h,ratsimp)/exp(%i*omega*t),a1,a2,a3,a4,a5,kq,kl);

(D25)
-%e^-(%i*h*kq)*(kq*(a2*(eta*e^(2*%i*h*kq)*omega-%i*cbar*e^
(2*%i*h*kq))+a1*
(%i*cbar-eta*omega))-a3*e*e^(%i*h*kq)) =
a5*kl*e^-(%i*h*kl)*nu*omega*rhol

(c26) /* Potential at bottom surface of quartz sensor:
phi(0,t) = -phi0*exp(%i*omega*t) */

(phi:rhs(gen_sol2),
BC3:ratsimp(ev(phi =
-phi0*exp(%i*omega*t),y=0,ratsimp)/exp(%i*omega*t),a1,a2,a3,
a4,a5,kq,kl)));

(D26) (a4*epsilon+a2*e+a1*e)/epsilon = -phi0

(c27) /* Potential at top surface of quartz sensor: phi(h,t)
= phi0*exp(%i*omega*t) */

BC4:ratsimp(ev(phi =
phi0*exp(%i*omega*t),y=h,ratsimp)/exp(%i*omega*t),a1,a2,a3,a
4,a5,kq,kl);

(D27)
%e^-(%i*h*kq)*(a2*e*e^(2*%i*h*kq)+a3*epsilon*h*e^(%i*h*kq)
+a4*epsilon*e^
(%i*h*kq)+a1*e)/epsilon = phi0

(c28) /* slip boundary condition: ul(h,t) = alpha*uq(h,t)
*/

(uq:rhs(gen_sol1),
ul:rhs(gen_sol3),
BC5:ratsimp(ev(ul = alpha*uq, y=h,
ratsimp)/exp(%i*omega*t),a1,a2,a3,a4,a5,kq,kl)));

(D28) a5*e^-(%i*h*kl) =
alpha*e^-(%i*h*kq)*(a2*e^(2*%i*h*kq)+a1)

```

```
(c29) (pause(),
clearscreen(),
disp("Let",gamma1 = exp(%i*h*kq), gamma2 = exp(%i*h*kl),
delta = eta*omega-%i*cbar),
pause(),
clearscreen())$
Pausing. Press Enter to continue.
```

"Let"

$$\gamma_1 = e^{(i h k q)}$$

$$\gamma_2 = e^{(i h k l)}$$

$$\Delta = \eta \omega - i \bar{c}$$

Pausing. Press Enter to continue.

```
(c30) (BC:expand([BC1,BC2,BC3,BC4,BC5]),
BC:ratsubst(gamma1,exp(%i*h*kq),BC),
BC:ratsubst(gamma2,exp(%i*h*kl),BC),
BC:ratsimp(ratsubst(delta, eta*omega-%i*cbar,BC)),
map(dispatch,BC),
pause(),
clearscreen())$
```

$$a_3 e^{-(a_2 - a_1) \Delta k q} = 0$$

$$\frac{-((a_2 \Delta \gamma_1^2 - a_1 \Delta) k q - a_3 e \gamma_1) / \gamma_1 = a_5 k l \nu \omega}{\rho / \gamma_2}$$

$$(a_4 \epsilon + (a_2 + a_1) e) / \epsilon = -\phi_0$$

$$\frac{(a_3 \epsilon \gamma_1^h + a_2 e \gamma_1^2 + a_4 \epsilon \gamma_1 + a_1 e) / (\epsilon \gamma_1)}{=} \phi_0$$

$$a_5 / \gamma_2 = \alpha (a_2 \gamma_1^2 + a_1) / \gamma_1$$

Pausing. Press Enter to continue.

(c31) /\* The solution to the above boundary value problem is given by...\*/

```
(solBC:linsolve(BC,[a1,a2,a3,a4,a5]),
 solBC1:rhs(solBC[1]),
 solBC2:rhs(solBC[2]),
 solBC3:rhs(solBC[3]),
 solBC4:rhs(solBC[4]),
 solBC5:rhs(solBC[5]),
 solBC1num:num(solBC1),
 solBC1denom:denom(solBC1),
 solBC2num:num(solBC2),
 solBC2denom:denom(solBC2),
 solBC3num:num(solBC3),
 solBC3denom:denom(solBC3),
 solBC4num:num(solBC4),
 solBC4denom:denom(solBC4),
 solBC5num:num(solBC5),
 solBC5denom:denom(solBC5),
 pause(),
 clearscreen(),
 disp("Let",
      b11 = factorsum(ratcoef(solBC1num,alpha,0)),
      b12 = factorsum(ratcoef(solBC1num,alpha,1)),
      b13 = factorsum(ratcoef(solBC1denom,alpha,0)),
      b14 = factorsum(ratcoef(solBC1denom,alpha,1)),
      "Therefore...",
      a1 = (b11 + alpha*b12)/(b13 + alpha*b14)),
 pause(),
 clearscreen(),
 disp("Let",
      b21 = factorsum(ratcoef(solBC2num,alpha,0)),
      b22 = factorsum(ratcoef(solBC2num,alpha,1)),
      b23 = factorsum(ratcoef(solBC2denom,alpha,0)),
      b24 = factorsum(ratcoef(solBC2denom,alpha,1)),
      "Therefore...",
      a2 = (b21 + alpha*b22)/(b23 + alpha*b24)),
 pause(),
 clearscreen(),
 disp("Let",
      b31 =
factorsum(ratcoef(ratcoef(solBC3num,alpha,0),phi0)),
      b32 =
factorsum(ratcoef(ratcoef(solBC3num,alpha,1),phi0)),
      b33 = factorsum(ratcoef(solBC3denom,alpha,0)),
      b34 = factorsum(ratcoef(solBC3denom,alpha,1)),
      "Therefore...",
      a3 = ((b31 + alpha*b32)*phi0)/(b33 + alpha*b34)),
 pause(),
 clearscreen(),
 disp("Let",
      b41 = factorsum(ratcoef(solBC4num,alpha,0)),
```

```

        b42 = factorsum(ratcoef(solBC4num,alpha,1)),
        b43 = factorsum(ratcoef(solBC4denom,alpha,0)),
        b44 = factorsum(ratcoef(solBC4denom,alpha,1)),
        "Therefore...",
        a4 = (b41 + alpha*b42)/(b43 + alpha*b44)),
pause(),
clearscreen(),
disp("Let",
      b51 = factorsum(ratcoef(solBC5num,alpha,0)),
      b52 = factorsum(ratcoef(solBC5num,alpha,1)),
      b53 = factorsum(ratcoef(solBC5denom,alpha,0)),
      b54 = factorsum(ratcoef(solBC5denom,alpha,1)),
      "Therefore...",
      a5 = (b51 + alpha*b52)/(b53 + alpha*b54)))$
Pausing. Press Enter to continue.

"Let"

b11 = -2*delta*e*epsilon*(gamma1-1)*gamma1*kq*phi0

b12 = -2*e*epsilon*gamma1^2*kl*nu*omega*phi0*rhol

b13 =
delta*(gamma1-1)*kq*(delta*epsilon*(gamma1+1)*h*kq+2*e^2*(gamma1-1))

b14 =
kl*(delta*epsilon*(gamma1^2+1)*h*kq+e^2*(gamma1-1)*(gamma1+1))
*nu*omega
*rhol

"Therefore..."

a1 = (alpha*b12+b11)/(alpha*b14+b13)
Pausing. Press Enter to continue.

"Let"

b21 = 2*delta*e*epsilon*(gamma1-1)*kq*phi0

b22 = 2*e*epsilon*kl*nu*omega*phi0*rhol

```

```

b23 =
delta*(gamma1-1)*kq*(delta*epsilon*(gamma1+1)*h*kq+2*e^2*(gamma1-1))

```

```

b24 =
k1*(delta*epsilon*(gamma1^2+1)*h*kq+e^2*(gamma1-1)*(gamma1+1))
*nu*omega
*rhol

```

"Therefore..."

```

a2 = (alpha*b22+b21)/(alpha*b24+b23)

```

Pausing. Press Enter to continue.

"Let"

```

b31 = 2*delta^2*epsilon*(gamma1-1)*(gamma1+1)*kq^2

```

```

b32 = 2*delta*epsilon*(gamma1^2+1)*k1*kq*nu*omega*rhol

```

```

b33 =
delta*(gamma1-1)*kq*(delta*epsilon*(gamma1+1)*h*kq+2*e^2*(gamma1-1))

```

```

b34 =
k1*(delta*epsilon*(gamma1^2+1)*h*kq+e^2*(gamma1-1)*(gamma1+1))
*nu*omega
*rhol

```

"Therefore..."

```

a3 = (alpha*b32+b31)*phi0/(alpha*b34+b33)

```

Pausing. Press Enter to continue.

"Let"

```

b41 = -delta^2*epsilon*(gamma1-1)*(gamma1+1)*h*kq^2*phi0

```

```

b42 =
-k1*(delta*epsilon*(gamma1^2+1)*h*kq-e^2*(gamma1-1)*(gamma1+
1))*nu
*omega*phi0*rhol

```

```

b43 =
delta*(gamma1-1)*kq*(delta*epsilon*(gamma1+1)*h*kq+2*e^2*(ga
mma1-1))

```

```

b44 =
k1*(delta*epsilon*(gamma1^2+1)*h*kq+e^2*(gamma1-1)*(gamma1+1
))*nu*omega
*rhol

```

"Therefore..."

```

a4 = (alpha*b42+b41)/(alpha*b44+b43)

```

Pausing. Press Enter to continue.

"Let"

```

b51 = 0

```

```

b52 = 2*delta*e*epsilon*(gamma1-1)^2*gamma2*kq*phi0

```

```

b53 =
delta*(gamma1-1)*kq*(delta*epsilon*(gamma1+1)*h*kq+2*e^2*(ga
mma1-1))

```

```

b54 =
k1*(delta*epsilon*(gamma1^2+1)*h*kq+e^2*(gamma1-1)*(gamma1+1
))*nu*omega
*rhol

```

"Therefore..."

```

a5 = (alpha*b52+b51)/(alpha*b54+b53)

```

(c32) /\* The electric displacement D in the quartz sensor is given by... \*/

```
(D:e*diff('uq,y,1) - epsilon*diff('phi,y,1),
 display(D))$
```

```
d = e*'DIFF(uq,y,1)-epsilon*'DIFF(phi,y,1)
```

(c33) /\* Substituting uq and phi into D we get... \*/

```
(D:ev(D,diff,ratsimp),
 display(D))$
```

```
d = -a3*epsilon*e^(%i*omega*t)
```

(c34) /\* The total surface charge Q of the quartz sensor is given by... \*/

```
Q:D*A;
```

```
(D34) -a*a3*epsilon*e^(%i*omega*t)
```

(c35) /\* The instantaneous current i is given by... \*/

```
i:diff(Q,t,1);
```

```
(D35) -%i*a*a3*epsilon*omega*e^(%i*omega*t)
```

(c36) /\* The electrical input impedance of the liquid-loaded AT-cut quartz sensor is given by... \*/

```
(Zin:(-phi0*exp(%i*omega*t) - phi0*exp(%i*omega*t))/1,
 a3:((b31 + alpha*b32)*phi0)/(b33 + alpha*b34),
 Zin:ratsimp(ev(Zin)),
 display(Zin))$
```

```
zin =
-2*i*(alpha*b34+b33)/(a*(alpha*b32+b31)*epsilon*omega)
```

(c37) /\* 6:25PM 1/9/93 \*/



## APPENDIX 4      Non-linear Regression Analysis Example of a Series RLC circuit, Mathcad program DOC1.MCD

Non-linear regression analysis of the theoretical complex-valued expression of the impedance for a series RLC-circuit.

### Introduction

The following is a demonstration of how Mathcad's **Minerr** function can be used to perform a non-linear regression analysis procedure on a multi-valued non-linear complex-valued function,  $Z$ . Mathcad's **Minerr** function implements a modified version of the Levenberg-Marquardt method. The the Levenberg-Marquardt method, a quasi-Newton method, is a variation of the gradient method.

Given a system of  $n$  non-linear algebraic equations in  $n$  unknowns, at each step in the iterative procedure Newton's method computes the jacobian of the non-linear system. Each component of the jacobian is computed by a numerical differentiation procedure. On the other hand, in the quasi-Newton method, each component of the jacobian is replaced by an appropriate finite-difference approximation.

Mathcad's Levenberg-Marquardt algorithm was obtained from the public-domain MINPACK algorithms developed and published by the Argonne National Laboratory in Argonne, Illinois

### Complex-Valued Function

The impedance,  $Z$ , of a series RLC circuit is chosen as the multi-valued non-linear complex-valued function. The expression for the impedance,  $Z$ , in terms of the resistance,  $R$ , the inductance,  $L$ , the capacitance,  $C$ , and the angular frequency,  $\omega$ , is

$$(1) \quad Z(R,L,C,\omega) = R + j \cdot \left( \omega L - \frac{1}{\omega C} \right)$$

The resonant frequency,  $f$ , of the series RLC circuit, is given by

$$(2) \quad f = \frac{1}{2 \cdot \pi} \cdot \frac{1}{\sqrt{L \cdot C}}$$

Let the resonant frequency,  $f$ , be 9.0 MHz.       $f = 9.0 \cdot \text{MHz}$

Let the inductance,  $L$ , be 10.0 mH.       $L_{\text{exact}} = 10.0 \cdot \text{mH}$

From equation (2), the numerical value for the capacitance, C, is.

$$(3) \text{ Cexact} = \frac{1}{4 \text{ Lexact} \pi^2 \cdot f^2}$$

$$\text{Cexact} = 0.031 \cdot \text{pF}$$

Let the numerical value of the resistance, R<sub>exact</sub>, be 10.0 kΩ. R<sub>exact</sub> = 10.0 kΩ

#### Procedure

A simulated set of N experimental data points of the form ( $\omega_1$ , Z<sub>exp<sub>1</sub></sub>) is generated from (1) via Mathcad's **rnd** function. The best fit value for L denoted by L<sub>fit</sub>, is determined by fitting the theoretical complex-valued expression for the impedance,  $Z = Z(R, L, C, \omega)$  to the simulated experimental data, Z<sub>exp<sub>1</sub></sub>. The fitting of Z to Z<sub>exp<sub>1</sub></sub> is achieved by minimizing the Sum Of Squares Of Errors, SSE(L) via Mathcad's **Minerr** function.

Enter number of experimental data points N = 401

Enter the closed interval, I = [f<sub>s</sub>, f<sub>t</sub>]

Enter numerical value for f<sub>s</sub> f<sub>s</sub> = 8.0 MHz

Enter numerical value for f<sub>t</sub> f<sub>t</sub> = 10.0 MHz

Compute step size  $\Delta f$   $\Delta f = \frac{f_t - f_s}{N}$   $\Delta f = 4.988 \cdot \text{kHz}$   $f_1 = f_s$  ; 1 N

$$f_{i+1} = f_i + \Delta f \quad f'_i = f_i$$

Using Mathcad's **rnd** function generate a set of N experimental data points using the theoretical complex-valued expression for Z. The experimental data Z<sub>exp<sub>i</sub></sub> is generated by perturbing the value of L<sub>exact</sub> at each of the N = 401 data points. The perturbation of L<sub>exact</sub> is done by Mathcad's **rnd** function. Mathcad's random function, **rnd(x)**, generates uniformly distributed random numbers between 0 and x inclusive.

The perturbation of L<sub>exact</sub> is accomplished by the expression below.

$$(4) \text{ L\_perturbed}_i = \frac{(\text{Lexact} + \text{rnd}(1) \cdot \text{mfl}) + (\text{Lexact} - \text{rnd}(1) \cdot \text{mfl})}{2}$$

Using values for  $R_{exact}$ ,  $L_{exact}$ , and  $C_{exact}$ , compute the exact values for the impedance,  $Z$ , for each of the  $N = 401$  data points.

$$(5) \quad Z_{exact_i} = Z(R_{exact}, L_{exact}, C_{exact}, 2 \cdot \pi \cdot f_i)$$

Using the perturbed values for  $L_{exact}$ , and the values for  $R_{exact}$  and  $C_{exact}$ , compute the simulated experimental data for the impedance  $Z$ .

$$(6) \quad Z_{exp_i} = Z(R_{exact}, L_{perturbed_i}, C_{exact}, 2 \pi f_i)$$

From equations (5) and (6) compute the magnitude and phase of both  $Z_{exact}$  and  $Z_{exp}$  versus frequency  $f$ .

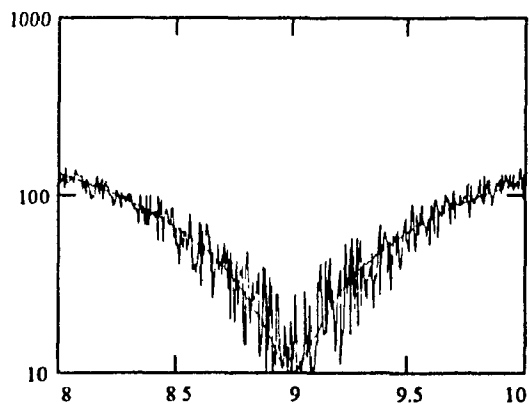
$$(7) \quad MZ_{exact_i} = |Z_{exact_i}|$$

$$(8) \quad MZ_{exp_i} = |Z_{exp_i}|$$

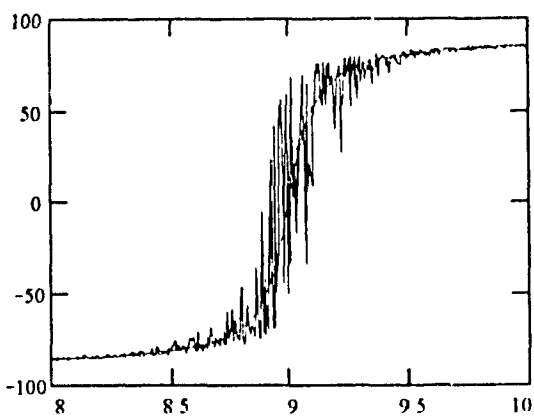
$$(9) \quad \theta Z_{exact_i} = \arg(Z_{exact_i})$$

$$(10) \quad \theta Z_{exp_i} = \arg(Z_{exp_i})$$

Plot the magnitude and phase of both  $Z$  and  $Z_{exp}$  versus frequency  $f$ .



---  $|Z_{exact}|$  versus  $f$   
 —  $|Z_{exp}|$  versus  $f$



-- |Zexact| versus f  
 — |Zexp| versus f

Generate data files of the magnitude and phase of both Zexact and Zexp versus frequency f.

- The data for the magnitude of Zexact versus frequency f is stored in the data file MZEXACT.PRN.
- The data for the magnitude of Zexp versus frequency f is stored in the data file MZEXP.PRN.
- The data for the phase of Zexact versus frequency f is stored in the data file THEXACT.PRN.
- The data for the phase of Zexp versus frequency f is stored in the data file THEXP.PRN.

$$(11) \text{ WRITEPRN(MZEXACT)} = \text{augment} \left( \begin{array}{c} \text{f} \\ \text{MHz} \end{array}, \begin{array}{c} \text{M/Zexact} \\ \text{k}\Omega \end{array} \right) \square$$

$$(12) \text{ WRITEPRN(MZEXP)} = \text{augment} \left( \begin{array}{c} \text{f} \\ \text{MHz} \end{array}, \begin{array}{c} \text{M/Zexp} \\ \text{k}\Omega \end{array} \right) \square$$

$$(13) \text{ WRITEPRN(THEXACT)} = \text{augment} \left( \begin{array}{c} \text{f} \\ \text{MHz} \end{array}, \begin{array}{c} \theta/\text{Zexact} \\ \text{deg} \end{array} \right) \square$$

$$(14) \text{ WRITEPRN(THEXP)} = \text{augment} \left( \begin{array}{c} \text{f} \\ \text{MHz} \end{array}, \begin{array}{c} \theta/\text{Zexp} \\ \text{deg} \end{array} \right) \square$$

The Sum Of Squares Of Errors, SSE(L) is given by

$$(15) \quad SSE(L) = \frac{1}{N} \sum_1 \left( \left| \frac{Z_{exp_1}}{k\Omega} - \frac{Z(R_{exact,L}, C_{exact}, 2\pi f_1)}{k\Omega} \right| \right)^2$$

Compute SSE(L) over the closed interval [1.0 mH, 200.0 mH] in steps of  $\Delta L = 0.1$  mH

Enter numerical value for  $\Delta L$      $\Delta L = 0.1$  mH

Enter numerical value for  $L_{initial}$      $L_{initial} = 1.0$  mH

Enter numerical value for  $L_{terminal}$      $L_{terminal} = 200$  mH

From the values for  $\Delta L$ ,  $L_{initial}$ , and  $L_{terminal}$ , compute the number of interval subdivisions, NL. The expression for NL is

$$(16) \quad NL = \text{floor} \left( \frac{L_{terminal} - L_{initial}}{\Delta L} \right)$$

The value of NL is     $NL = 190$

The variable k takes on integral values from 1 to NL     $k = 1 \dots 190$  inclusive.

$$(17) \quad L_1 = L_{initial}$$

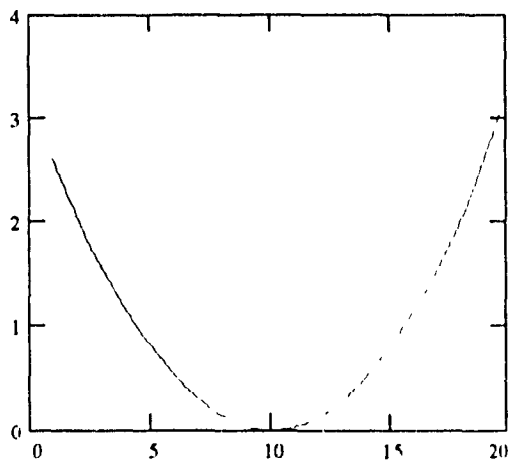
$$(18) \quad L_{k+1} = L_k + \Delta L \quad L_{NL} = L_k$$

Expression (18) generates NL equally spaced subinterval for the above closed interval.

For each  $k = 1, \dots, NL$ , compute SSE(L) for each  $L_k$ . The data for SSE(L) is stored in the one dimensional array,  $SSE\_exp_k$ .

$$(19) \quad SSE\_exp_k = SSE(L_k)$$

Plot the data for SSE(L) versus L



— SSE(L) versus L.

Store the data for SSE(L) versus L in the data file SSEL.PRN

$$(20) \quad \text{WRITEPRN}(SSEL) = \text{augment} \left( \begin{array}{c} 11. \\ \vdots \\ n \end{array}, SSE\_exp \right)$$

From the above plot of SSE(L) versus L, SSE as an absolute minimum in the closed interval [1.0 mH, 20.0 mH]. The absolute minimum of SSE(L) occurs when L = 10.0 mH. Since SSE(L) has only one absolute minimum in the above closed interval, then any value in the above closed interval may be used as a guess value for L. In fact, any value outside the above closed interval will serve as a guess value for L.

In view of the above, to implement MathCAD's Minerr function via MathCAD's Solve Block facility, enter any positive guess value for L.

Enter numerical value for Lguess. Lguess = 15.0 mH

----- Mathcad Solve Block -----

Given

$$(21) \text{ SSE}(\text{Lguess})=0$$

$$(22) \text{ Lfit} = \text{Minerr}(\text{Lguess})$$

-----

The result of the Solve Block, Lfit is given by

$$\text{Lfit} = 10.02 \cdot \text{mH}$$

Compute the residual error, ERR, given by  $\text{ERR} = \text{SSE}(\text{Lfit})$

$$\text{ERR} = 135.515$$

Using the values for Rexact, Lfit, and Cexact, compute the best fit values for Z denoted by Zfit.

$$(23) \text{ Zfit}_1 = \text{Z}(\text{Rexact}, \text{Lfit}, \text{Cexact}, 2\pi f_1)$$

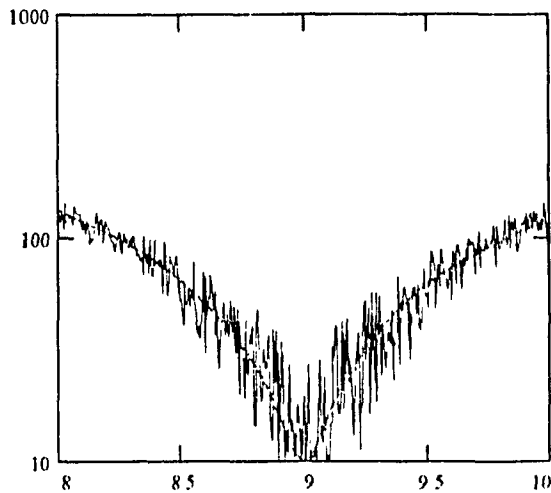
From equation (23) compute the magnitude and phase of Zfit.

$$(24) \text{ MZfit}_1 = |\text{Zfit}_1|$$

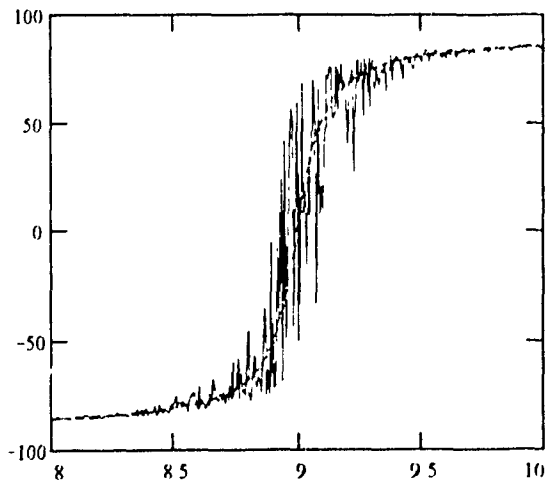
$$(25) \theta \text{Zfit}_1 = \arg(\text{Zfit}_1)$$

Plot the magnitude and phase of Zexp, Zexact, and Zfit versus frequency f.

Plot the magnitude and phase of  $Z_{exp}$ ,  $Z_{exact}$ , and  $Z_{fit}$  versus frequency  $f$ .



—  $|Z_{exp}|$  versus  $f$   
 —  $|Z_{exact}|$  versus  $f$   
 -  $|Z_{fit}|$  versus  $f$



—  $|Z_{exp}|$  versus  $f$   
 —  $|Z_{exact}|$  versus  $f$   
 -  $|Z_{fit}|$  versus  $f$



**APPENDIX 5 Non-linear Regression Analysis of Sensor in Air, Mathcad Program DOC2.MCD**

**Non-linear Regression Analysis of the Theoretical Complex-Valued Expression of the Impedance for the Hydrophilic and Hydrophobic Sensor in Air.**

The best-fit values for  $\epsilon, \eta, h,$  and  $A$  will be determined by fitting the theoretical complex-valued expression of the impedance,  $Z,$  to the corresponding experimental data for the hydrophilic and hydrophobic sensor in air. The fitting is done by using the THREE STEP PROCEDURE, which is outlined below.

In step 1 the starting values for  $\epsilon, \eta,$  and  $h$  are determined by fitting the theoretical expression of the phase of  $Z, \theta_Z,$  to the corresponding experimental data.

In step 2 the starting values for  $\epsilon, \eta,$  and  $h$  found in step 1 will be used to determine the starting value for the effective surface area,  $A,$  by fitting the theoretical expression of the magnitude of  $Z, |Z|,$  to the corresponding experimental data.

In step 3 the starting values for  $\epsilon, \eta, h$  and  $A$  found in steps 1 and 2 will be used to determine the best-fit values of  $\epsilon, \eta, h$  and  $A$  by fitting the theoretical complex-valued expression of  $Z$  to the corresponding experimental data.

The impedance,  $Z,$  of an AT-cut quartz sensor in air is given in terms of the following nine expressions.

$$\bar{c}(\epsilon) = \epsilon + \frac{\epsilon^2}{\epsilon}$$

$$\delta(\epsilon, \eta, \omega) = \eta \omega - j \bar{c}(\epsilon)$$

$$kq(\epsilon, \eta, \omega) = \omega \cdot \frac{\rho q}{\sqrt{\bar{c}(\epsilon) + j \cdot \omega \eta}}$$

$$\gamma l(\epsilon, \eta, h, \omega) = \exp(j h kq(\epsilon, \eta, \omega))$$

$$\lambda 1(\epsilon, \eta, h, \omega) = \gamma l(\epsilon, \eta, h, \omega) - 1$$

$$\lambda 2(\epsilon, \eta, h, \omega) = \gamma l(\epsilon, \eta, h, \omega) + 1$$

$$b31(\epsilon, \eta, h, \omega) = 2 \delta(\epsilon, \eta, \omega)^2 \cdot \epsilon \lambda 1(\epsilon, \eta, h, \omega) \lambda 2(\epsilon, \eta, h, \omega) kq(\epsilon, \eta, \omega)^2$$

$$b33(e, \eta, h, \omega) = \delta(e, \eta, \omega) \lambda 1(e, \eta, h, \omega) \cdot kq(e, \eta, \omega) \left( \delta(e, \eta, \omega) \varepsilon \lambda 2(e, \eta, h, \omega) h kq(e, \eta, \omega) \right. \\ \left. + 2 \cdot e^2 \lambda 1(e, \eta, h, \omega) \right)$$

$$\xi_a(e, \eta, h, \omega) = -\frac{2j}{\omega \varepsilon} \frac{b33(e, \eta, h, \omega)}{b31(e, \eta, h, \omega)}$$

The expression of the impedance,  $Z_a$ , is

$$Z_a(e, \eta, h, A, \omega) = \frac{1}{A} \xi_a(e, \eta, h, \omega)$$

The expression of the magnitude of  $Z_a$ ,  $|Z_a|$ , is

$$MZ_a(e, \eta, h, A, \omega) = |Z_a(e, \eta, h, A, \omega)|$$

The expression of the phase of  $Z_a$ ,  $\theta_{Z_a}$ , is

$$\theta_{Z_a}(e, \eta, h, \omega) = \text{atan} \left( \frac{\text{Im}(\xi_a(e, \eta, h, \omega))}{\text{Re}(\xi_a(e, \eta, h, \omega))} \right)$$

Enter the number of experimental data points  $N$ .  $N = 401$

The range variable,  $i$ , iterates through the  $N$  experimental data points.

$$i = 1 \text{ } N$$

To start the three-step procedure, read in the experimental data for  $|Z|$  and  $\theta_Z$  in air for the hydrophilic and hydrophobic sensors.

#### Experimental Data for Hydrophilic Sensor in Air

Read in data array  $flicAir$  for frequency,  $f$ , an array of 401 values of  $f$ .

$$flicAir = \text{READPRN}(\text{FLICAIR}) \text{ MHz}$$

Read in data array  $MZlicAir$  for the magnitude of  $Z$ ,  $|Z|$ , an array of 401 values of  $|Z|$ .

$$MZlicAir = \text{READPRN}(\text{ZLICAIR}) \text{ k}\Omega$$

Read in data array  $\theta ZlicAir$  for the phase of  $Z$ ,  $\theta_Z$ , an array of 401 values of  $\theta_Z$ .

$$\theta ZlicAir = \text{READPRN}(\text{THLICAIR})$$

Experimental Data for Hydrophobic Sensor in Air

Read in data array fbicAir for frequency, f, an array of 401 values of f.

$$fbicAir = READPRN(FBICAIR) \cdot \text{MHz}$$

Read in data array MZbicAir for the magnitude of Z, |Z|, an array of 401 values of |Z|.

$$MZbicAir = READPRN(ZBICAIR) \cdot k\Omega$$

Read in data array 0ZbicAir for the phase of Z,  $\theta_Z$ , an array of 401 values of  $\theta_Z$ .

$$\theta ZbicAir = READPRN(\theta BICAIR)$$

Using the above frequency data flicAir and fbicAir, compute the corresponding angular frequency data  $\omega licAir$  and  $\omega bicAir$ .

$$\omega licAir = 2 \cdot \pi \cdot flicAir$$

$$\omega bicAir = 2 \cdot \pi \cdot fbicAir$$

Using the experimental data for |Z| and  $\theta_Z$ , for each  $i = 1, \dots, N$  compute the corresponding experimental data for ZlicAir and ZbicAi, using the exponential form for the complex number  $Z = |Z| \exp(j\theta_Z)$ .

$$ZlicAir_i = MZlicAir_i \cdot \exp(j \theta ZlicAir_i \cdot \text{deg})$$

$$ZbicAir_i = MZbicAir_i \cdot \exp(j \theta ZbicAir_i \cdot \text{deg})$$

The above experimental data for |Z| and  $\theta_Z$  consists of 401 points measured at 401 equally spaced frequencies. The resonant region of the quartz sensor is chosen as the frequency interval.

Enter numerical value for the mass density of quartz.

$$\rho_q = 2649 \frac{\text{kg}}{\text{m}^3}$$

Enter numerical value for the elastic constant of quartz.

$$c = 29.01 \cdot 10^9 \frac{\text{newton}}{\text{m}^2}$$

Enter numerical value for the dielectric constant of quartz.

$$\epsilon = 39.82 \cdot 10^{12} \frac{\text{coul}}{\text{volt m}}$$

### Non-Linear Regression Analysis of Hydrophilic Sensor in Air.

**Step 1.** Determine starting values for  $e$ ,  $\eta$  and  $h$  using the experimental data for  $\theta_2$ .

To perform Step 1, define the Sum Of Squares Of Errors,  $SSE1\_1(e, \eta, h)$ .

$$SSE1\_1(e, \eta, h) = \frac{1}{N} \sum_1 \left( \theta_{2lcAir_1} - \frac{\theta_{2a}(e, \eta, h, \omega_{lcAir_1})}{deg} \right)^2$$

To start the non-linear curve-fitting procedure,, enter guess values for  $e$ ,  $\eta$  and  $h$ .

$$e1\_guess = -0.079 \frac{\text{coul}}{\text{m}^2}$$

$$\eta1\_guess = 0.011 \text{ newton} \frac{\text{sec}}{\text{m}^2}$$

$$h1\_guess = 183.87 \mu\text{m}$$

Use Mathcad's Minerr function to perform the non-linear curve fitting procedure.

----- Mathcad Solve Block -----

Given

$$SSE1\_1(e1\_guess, \eta1\_guess, h1\_guess) = 0$$

$$1 = 1$$

$$1 = 1$$

$$\begin{pmatrix} e1\_start \\ \eta1\_start \\ h1\_start \end{pmatrix} = \text{Minerr}(e1\_guess, \eta1\_guess, h1\_guess)$$

-----

In the above Mathcad Solve Block, Mathcad needs two dummy equations,  $1 = 1$ , to form a complete system of three non-linear algebraic equations in the three unknowns  $e$ ,  $\eta$  and  $h$ .

The result of the Solve Block,  $e1\_start$ ,  $\eta1\_start$  and  $h1\_start$  is.

$$e1\_start = -0.0798 \cdot \frac{\text{coul}}{\text{m}^2}$$

$$\eta1\_start = 0.0119 \cdot \text{newton} \frac{\text{sec}}{\text{m}^2}$$

$$h1\_start = 183.878 \cdot \mu\text{m}$$

Compute the residual error, ERR, given by  $ERR = SSE1\_1(e1\_start, \eta1\_start, h1\_start)$ .

$$ERR = 1.945$$

**Step 2.** Use  $e1\_start$ ,  $\eta1\_start$ ,  $h1\_start$  and the experimental data for  $|Z|$  to determine the starting value for the effective surface area,  $A$ .

To perform Step 2, define the Sum Of Squares Of Errors,  $SSE1\_2(A)$ .

$$SSE1\_2(A) = \frac{1}{N} \sum_i \left( \frac{MZicAir_i}{k\Omega} - \frac{MZA(e1\_start, \eta1\_start, h1\_start, A, \omega icAir_i)}{k\Omega} \right)^2$$

To start the non-linear curve-fitting procedure, enter the guess value for  $A$ .

$$A1\_guess = 0.28 \cdot \text{cm}^2$$

Use Mathcad's Minerr function to perform the non-linear curve-fitting procedure.

----- Mathcad Solve Block -----  
Given

$$SSE1\_2(A1\_guess) = 0$$

$$A1\_start = \text{Minerr}(A1\_guess)$$

-----

The result of the Solve Block,  $A1\_start$ , is.

$$A1\_start = 0.2701 \cdot \text{cm}^2$$

Compute the residual error, ERR, given by  $SSE1\_2(A1\_start)$ .

$$ERR = 110.993$$

**Step 3.** Use  $e1\_start$ ,  $\eta1\_start$ ,  $h1\_start$ ,  $A1\_start$  and the experimental data for  $Z$  to compute best-fit values for  $e$ ,  $\eta$ ,  $h$  and  $A$ .

To perform Step 3, define the Sum Of Squares Of Errors,  $SSE1\_3(e, h, \eta, A)$ . The quantity summed, is the product of a complex number and its conjugate.

$$SSE1\_3(e, \eta, h, A) = \frac{1}{N} \sum_i \left( \left| \frac{Z1cAir_i}{k\Omega} - \frac{Za(e, \eta, h, A, \omega1cAir_i)}{k\Omega} \right| \right)^2$$

Use Mathcad's Minerr function to perform the non-linear curve-fitting procedure.

----- Mathcad Solve Block -----

Given

nested solve block

$$SSE1\_3(e1\_start, \eta1\_start, h1\_start, A1\_start) = 0$$

$$l = 1$$

$$l = 1$$

$$l = 1$$

$$\begin{bmatrix} e1\_fit \\ \eta1\_fit \\ h1\_fit \\ A1\_fit \end{bmatrix} = \text{Minerr}(e1\_start, \eta1\_start, h1\_start, A1\_start)$$

-----

The result of the Solve Block,  $e1\_fit$ ,  $\eta1\_fit$ ,  $h1\_fit$  and  $A1\_fit$  is.

$$e1\_fit = -0.0798 \frac{\text{coul}}{\text{m}^2}$$

$$\eta1\_fit = 0.0084 \frac{\text{newton} \cdot \text{sec}}{\text{m}^2}$$

$$h1\_fit = 183.879 \cdot \mu\text{m}$$

$$A1\_fit = 0.2985 \cdot \text{cm}^2$$

Compute the residual error, ERR, given by  $ERR = SSE1\_3(e1\_start, \eta1\_start, h1\_start, A1\_start)$ .

$$ERR = 60.727$$

### Non-Linear Regression Analysis of Hydrophobic Sensor in Air.

For the hydrophilic sensor the value for  $e$  is the same as the value that is used for the hydrophobic sensor. On physical grounds, the value of  $e$  is expected to be independent of the type of chemical coating that is placed on the surface of the sensor. Therefore the value of  $e$  for the hydrophilic and hydrophobic sensor is the same.

**Step 1.** Determine starting values for  $\eta$  and  $h$  using the experimental data for  $\theta_z$ .

To perform Step 1, define the following Sum Of Squares Of Errors  $SSE2_1(\eta, h)$ .

$$SSE2_1(\eta, h) = \frac{1}{N} \sum_1 \left( \theta Z_{bicAir_i} - \frac{\theta Z_a(e1_{fit}, \eta, h, \omega_{bicAir_i})}{deg} \right)^2$$

To start the non-linear curve-fitting procedure, enter guess values for  $\eta$  and  $h$ .

$$\eta_{2\_guess} = 0.24 \cdot \text{newton} \cdot \frac{\text{sec}}{\text{m}^2}$$

$$h_{2\_guess} = 183.98 \mu\text{m}$$

Use Mathcad's Minerr function to perform the non-linear curve-fitting procedure.

----- Mathcad Solve Block -----

Given

$$SSE2_1(\eta_{2\_guess}, h_{2\_guess}) = 0$$

$$l = 1$$

$$\begin{pmatrix} \eta_{2\_start} \\ h_{2\_start} \end{pmatrix} = \text{Minerr}(\eta_{2\_guess}, h_{2\_guess})$$

-----  
The result of the Solve Block,  $\eta_{2\_start}$  and  $h_{2\_start}$  is.

$$\eta_{2\_start} = 0.2439 \cdot \text{newton} \cdot \frac{\text{sec}}{\text{m}^2}$$

$$h_{2\_start} = 183.986 \mu\text{m}$$

Compute the residual error, given by  $ERR = SSE2_1(e1_{fit}, \eta_{2\_start}, h_{2\_start})$ .

$$ERR = 5.351$$

**Step 2.** Use  $\eta_{2\_start}$ ,  $h_{2\_start}$  and the experimental data for  $|Z|$  to determine the starting value for the effective surface area,  $A$ .

To perform Step 2, define the Sum Of Squares Of Errors,  $SSE2\_2(A)$ .

$$SSE2\_2(A) = \frac{1}{N} \sum_i \left( \frac{MZb_{ic}Air_i}{k\Omega} - \frac{MZa(e_{l\_fit}, \eta_{2\_start}, h_{2\_start}, A, \omega_{b_{ic}Air_i})}{k\Omega} \right)^2$$

To start the non-linear curve-fitting procedure, enter the guess value for  $A$ .

$$A2\_guess = 0.25 \text{ cm}^2$$

Use Mathcad's Minerr function to perform the non-linear curve-fitting procedure.

----- Mathcad Solve Block -----  
Given

$$SSE2\_2(A2\_guess) = 0$$

$$A2\_start = \text{Minerr}(A2\_guess)$$

-----  
The result of the Solve Block,  $A2\_start$ , is.

$$A2\_start = 0.2533 \cdot \text{cm}^2$$

Compute the residual error,  $ERR$ , given by  $SSE2\_2(A2\_start)$ .

$$ERR = 0.311$$



**Step 3.** Use  $h2\_start$ ,  $\eta2\_start$ ,  $A2\_start$  and the experimental data for  $Z$  to compute best-fit values for  $\eta$ ,  $h$  and  $A$ .

To perform Step 3, define the Sum Of Squares Of Errors,  $SSE2\_3(\eta, h, A)$ . The quantity summed, is the product of a complex number and its conjugate.

$$SSE2\_3(\eta, h, A) = \frac{1}{N} \sum_i \left( \left| \frac{Z_{bicAir_i}}{k\Omega} - \frac{Z_a(e1\_fit, \eta, h, A, \omega_{bicAir_i})}{k\Omega} \right| \right)^2$$

Use Mathcad's Minerr function to perform the non-linear curve-fitting procedure.

----- Mathcad Solve Block -----  
Given

$$SSE2\_3(\eta2\_start, h2\_start, A2\_start) = 0$$

$$l = 1$$

$$l = 1$$

$$\begin{pmatrix} \eta2\_fit \\ h2\_fit \\ A2\_fit \end{pmatrix} = \text{Minerr}(\eta2\_start, h2\_start, A2\_start)$$

-----  
The result of the Solve Block,  $\eta2\_fit$ ,  $h2\_fit$  and  $A2\_fit$  is.

$$\eta2\_fit = 0.2345 \cdot \text{newton} \frac{\text{sec}}{\text{m}^2}$$

$$h2\_fit = 183.979 \cdot \mu\text{m}$$

$$A2\_fit = 0.2575 \cdot \text{cm}^2$$

Compute the residual error, ERR, given by  $ERR = SSE2\_3(e1\_fit, \eta2\_start, h2\_start, A2\_start)$ .

$$ERR = 0.057$$

Compute  $|Z|$  and  $\theta_Z$  for the hydrophilic sensor in air.

$$MZA1\_fit_i = MZA(c1\_fit, \eta1\_fit, h1\_fit, A1\_fit, \omega h c A r_i)$$

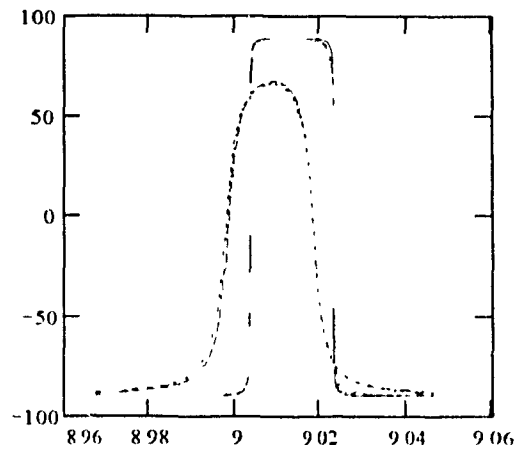
$$\theta Za1\_fit_i = \theta Za(c1\_fit, \eta1\_fit, h1\_fit, \omega h c A r_i)$$

Compute  $|Z|$  and  $\theta_Z$  for the hydrophobic sensor in air.

$$MZA2\_fit_i = MZA(c1\_fit, \eta2\_fit, h2\_fit, A2\_fit, \omega h c A r_i)$$

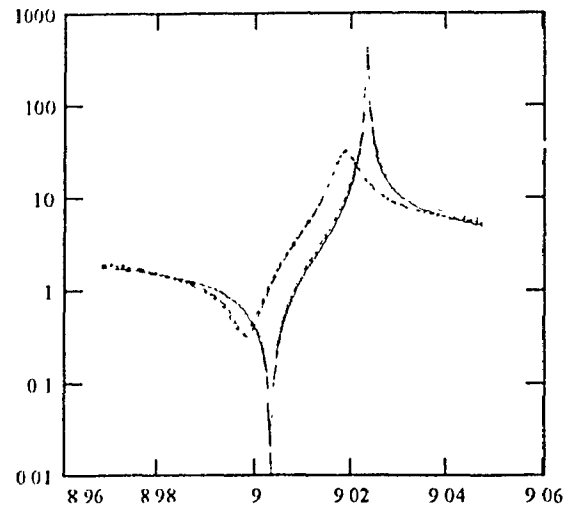
$$\theta Za2\_fit_i = \theta Za(c1\_fit, \eta2\_fit, h2\_fit, \omega h c A r_i)$$

Plot of  $\theta_Z$  versus  $f$  for the hydrophilic and hydrophobic sensor in air.



- Hydrophilic Sensor (Fitted Curve)
- Hydrophilic Sensor (Experimental Curve)
- - - Hydrophobic Sensor (Fitted Curve)
- - - Hydrophobic Sensor (Experimental Curve)

Plot of  $|Z|$  versus  $f$  for the hydrophilic and hydrophobic sensor in air.



-- Hydrophilic Sensor (Fitted Curve)  
 — Hydrophilic Sensor (Experimental Curve)  
 - · - Hydrophobic Sensor (Fitted Curve)  
 ··· Hydrophobic Sensor (Experimental Curve)

Summary of results for hydrophilic sensor

$$e1\_fit = 0.0798 \cdot \frac{\text{coul}}{\text{m}^2}$$

$$\eta1\_fit = 0.0084 \cdot \frac{\text{newton} \cdot \text{sec}}{\text{m}^2}$$

$$h1\_fit = 183.879 \cdot \mu\text{m}$$

$$A1\_fit = 0.2985 \cdot \text{cm}^2$$

Summary of results for hydrophobic sensor

$$e2\_fit = 0.0798 \cdot \frac{\text{coul}}{\text{m}^2}$$

$$\eta2\_fit = 0.2345 \cdot \frac{\text{newton} \cdot \text{sec}}{\text{m}^2}$$

$$h2\_fit = 183.979 \cdot \mu\text{m}$$

$$A2\_fit = 0.2575 \cdot \text{cm}^2$$

Store data for the hydrophilic and hydrophobic sensor in air.

$$\text{SENSOR1} = \begin{pmatrix} \frac{e1\_fit}{\left(\frac{\text{coul}}{\text{m}^2}\right)} \\ \eta1\_fit \\ \left(\frac{\text{newton} \cdot \text{sec}}{\text{m}^2}\right) \\ \frac{h1\_fit}{\mu\text{m}} \\ \frac{\Lambda1\_fit}{\text{cm}^2} \end{pmatrix} \quad \text{SENSOR1} = \begin{pmatrix} -0.08 \\ 0.008 \\ 183.879 \\ 0.298 \end{pmatrix} \quad \text{WRITEPRN}(\text{SENSOR1}) \quad \text{SENSOR1}$$

$$\text{SENSOR2} = \begin{pmatrix} \frac{e1\_fit}{\left(\frac{\text{coul}}{\text{m}^2}\right)} \\ \eta2\_fit \\ \left(\frac{\text{newton} \cdot \text{sec}}{\text{m}^2}\right) \\ \frac{h2\_fit}{\mu\text{m}} \\ \frac{\Lambda2\_fit}{\text{cm}^2} \end{pmatrix} \quad \text{SENSOR2} = \begin{pmatrix} 0.08 \\ 0.231 \\ 183.979 \\ 0.257 \end{pmatrix} \quad \text{WRITEPRN}(\text{SENSOR2}) \quad \text{SENSOR2}$$

Store fitted and experimental data of  $|Z|$  and  $\theta_z$  for the hydrophilic and hydrophobic sensor in air.

$$\text{WRITEPRN}(\text{TZLCAIR}) = \text{augment}\left(\frac{f_{lcAir}}{\text{MHz}}, \text{augment}\left(\frac{\theta Z a1\_fit}{\text{deg}}, \theta Z_{lcAir}\right)\right)$$

$$\text{WRITEPRN}(\text{MZLCAIR}) = \text{augment}\left(\frac{f_{lcAir}}{\text{MHz}}, \text{augment}\left(\frac{M Z a1\_fit}{\text{k}\Omega}, \frac{M Z_{lcAir}}{\text{k}\Omega}\right)\right)$$

$$\text{WRITEPRN}(\text{TZBCAIR}) = \text{augment}\left(\frac{f_{bcAir}}{\text{MHz}}, \text{augment}\left(\frac{\theta Z a2\_fit}{\text{deg}}, \theta Z_{bcAir}\right)\right)$$

$$\text{WRITEPRN}(\text{MZBCAIR}) = \text{augment}\left(\frac{f_{bcAir}}{\text{MHz}}, \text{augment}\left(\frac{M Z a2\_fit}{\text{k}\Omega}, \frac{M Z_{bcAir}}{\text{k}\Omega}\right)\right)$$

**APPENDIX 6 Non-linear Regression Analysis of Sensor in Liquid, Mathcad Program DOC3.MCD**

Non-Linear regression analysis of the theoretical complex-valued expression of the impedance for the hydrophilic and hydrophobic sensor in water-glycerol solution.

The best-fit values for the interfacial slip parameter,  $\alpha$ , and the effective surface area,  $A$ , will be determined by fitting the theoretical complex-valued expression of  $Z$  to the experimental data for the hydrophilic and hydrophobic sensors in water-glycerol solutions of varying concentrations ranging from pure water to pure glycerol in steps of 0.1 mole fraction. The fitting of theory to experiment will be done by minimizing the appropriate Sum of Squares Of Errors, SSE, by using Mathcad's Minerr function.

The theoretical complex-valued expression of the impedance,  $Z$ , for the liquid loaded AT-cut quartz sensor in terms of the sixteen expressions is:

$$cbar = c + \frac{c^2}{\epsilon}$$

$$\delta(\eta, \omega) = \eta \omega \sqrt{cbar}$$

$$kq(\eta, \omega) = \omega \sqrt{\frac{\rho q}{cbar + j \omega \eta}}$$

$$kl(v, \omega) = \sqrt{\frac{\omega}{j v}}$$

$$\gamma1(\eta, h, \omega) = \exp(-h kq(\eta, \omega))$$

$$\gamma2(v, h, \omega) = \exp(-h kl(v, \omega))$$

$$\lambda1(\eta, h, \omega) = \gamma1(\eta, h, \omega) - 1$$

$$\lambda2(\eta, h, \omega) = \gamma1(\eta, h, \omega) + 1$$

$$\lambda3(\eta, h, \omega) = \gamma1(\eta, h, \omega)^2 + 1$$

$$b31(\eta, h, \omega) = 2 \delta(\eta, \omega)^2 \epsilon \lambda1(\eta, h, \omega) \lambda2(\eta, h, \omega) kq(\eta, \omega)^2$$

$$B31(\eta, h, \omega) = \omega \epsilon b31(\eta, h, \omega)$$

$$b32(\eta, v, \rho l, h, \omega) = 2 \delta(\eta, \omega) \epsilon \lambda3(\eta, h, \omega) kl(v, \omega) kq(\eta, \omega) v \rho l \omega$$

$$B32(\eta, v, \rho l, h, \omega) = \omega \epsilon b32(\eta, v, \rho l, h, \omega)$$

$$b_{33}(\eta, h, \omega) = \delta(\eta, \omega) \lambda_1(\eta, h, \omega) k_q(\eta, \omega) \left( \frac{\delta(\eta, \omega) \varepsilon \lambda_2(\eta, h, \omega) h k_q(\eta, \omega)}{+ 2 e^2 \lambda_1(\eta, h, \omega)} \right) \quad \text{A6-2}$$

$$b_{34}(\eta, v, \rho l, h, \omega) = k_l(v, \omega) \left( \frac{\delta(\eta, \omega) \varepsilon \lambda_3(\eta, h, \omega) h k_q(\eta, \omega)}{+ e^2 \lambda_1(\eta, h, \omega) \lambda_2(\eta, h, \omega)} \right) v \omega \rho l$$

$$\zeta_l(\eta, v, \rho l, \alpha, h, \omega) = -2j \left( \frac{\alpha b_{34}(\eta, v, \rho l, h, \omega) + b_{33}(\eta, h, \omega)}{\alpha B_{32}(\eta, v, \rho l, h, \omega) + B_{31}(\eta, h, \omega)} \right)$$

The expression of the impedance,  $Z_l$ , is

$$Z_l(\eta, v, \rho l, \alpha, h, \Lambda, \omega) = \frac{1}{\Lambda} \zeta_l(\eta, v, \rho l, \alpha, h, \omega)$$

The expression of the magnitude of  $Z_l$ ,  $|Z_l|$ , is

$$M_{Z_l}(\eta, v, \rho l, \alpha, h, \Lambda, \omega) = |Z_l(\eta, v, \rho l, \alpha, h, \Lambda, \omega)|$$

The expression of the phase of  $Z_l$ ,  $\theta_{Z_l}$ , is

$$\theta_{Z_l}(\eta, v, \rho l, \alpha, h, \omega) = \text{atan} \left( \frac{\text{Im}(\zeta_l(\eta, v, \rho l, \alpha, h, \omega))}{\text{Re}(\zeta_l(\eta, v, \rho l, \alpha, h, \omega))} \right)$$

Enter the number of experimental data points  $N$ .  $N = 401$

The range variable,  $i$ , iterates through the  $N$  experimental data points.

$$i = 1 \text{ N}$$

### Experimental Data for Hydrophilic Sensor in Water-Glycerol Solution

Read in data array `flicAir` for frequency,  $f$ , an array of 401 values of  $f$ .

$$flic = \text{READPRN}(FLIC) \text{ MHz}$$

Read in data array `MZlicAir` for the magnitude of  $Z$ ,  $|Z|$ , an array of 401 values of  $|Z|$ .

$$MZlic = \text{READPRN}(ZLIC) \text{ k}\Omega$$

Read in data array `thetaZlicAir` for the phase of  $Z$ ,  $\theta_Z$ , an array of 401 values of  $\theta_Z$ .

$$\theta Zlic = \text{READPRN}(THLIC)$$

Experimental Data for Hydrophobic Sensor in Water-Glycerol Solution

A6-3

Read in data array flicAir for frequency,  $f$ , an array of 401 values of  $f$ .

$$fbic = \text{READPRN}(\text{FBIC}) \text{ MHz}$$

Read in data array MZlicAir for the magnitude of  $Z$ ,  $|Z|$ , an array of 401 values of  $|Z|$ .

$$MZbic = \text{READPRN}(\text{ZBIC}) \text{ k}\Omega$$

Read in data array  $\theta ZlicAir$  for the phase of  $Z$ ,  $\theta_Z$ , an array of 401 values of  $\theta_Z$ .

$$\theta Zbic = \text{READPRN}(\text{THBIC})$$

Using the above frequency data flic and fbic, compute the corresponding angular frequency data  $\omega lic$  and  $\omega bic$ .

$$\omega lic = 2 \pi flic$$

$$\omega bic = 2 \pi \cdot fbic$$

For each  $i = 1, \dots, 401$  and  $klic = 1, \dots, 11$  compute the experimental data of the impedance,  $Z$ , using the exponential form for the complex number  $Z = |Z| \exp(j\theta_Z)$  for the hydrophilic sensor in water-glycerol solution.

$$klic = 1 \dots 11$$

$$Zlic_{i,klic} = MZlic_{i,klic} \exp(j \theta Zlic_{i,klic} \text{ deg})$$

For each  $i = 1, \dots, 401$  and  $kbic = 1, \dots, 7$  compute the experimental data of the impedance,  $Z$ , using the exponential form for the complex number  $Z = |Z| \exp(j\theta_Z)$  for the hydrophobic sensor in water-glycerol solution.

$$kbic = 1 \dots 7$$

$$Zbic_{i,kbic} = MZbic_{i,kbic} \exp(j \theta Zbic_{i,kbic} \text{ deg})$$

For each water-glycerol concentration, the above experimental data for  $|Z|$  and  $\theta_Z$  consists of 401 points measured at 401 equally spaced frequencies. At each concentration level, the resonant region of the quartz sensor was modified so as to achieve a full characterization of the quartz sensor.

Data for Hydrophilic and Hydrophobic Sensor

Enter numerical value for the mass density of quartz.

$$\rho_q = 2649 \frac{\text{kg}}{\text{m}^3}$$

Enter numerical value for the elastic coefficient of quartz.

$$c = 29.01 \cdot 10^9 \frac{\text{newton}}{\text{m}^2}$$

Enter numerical value for the best-fit piezoelectric stress coefficient of quartz.

$$e = 0.0798007 \frac{\text{coul}}{\text{m}^2}$$

Enter numerical values for the best-fit viscoelastic coefficient of quartz.

$$\eta_{lic\_fit} = 0.0083762 \frac{\text{newton} \cdot \text{sec}}{\text{m}^2}$$

$$\eta_{bic\_fit} = 0.2344606 \frac{\text{newton} \cdot \text{sec}}{\text{m}^2}$$

Enter numerical values for the best-fit thickness.

$$h_{lic\_fit} = 183.8790101 \mu\text{m}$$

$$h_{bic\_fit} = 183.9794329 \mu\text{m}$$

Enter numerical value for the dielectric constant of quartz.

$$\epsilon = 39.82 \cdot 10^{12} \frac{\text{coul}}{\text{volt} \cdot \text{m}}$$

Water-Glycerol Solution for Hydrophilic Sensor

Read in data array v<sub>lic</sub> for kinematic viscosity,  $\nu$ , an array of eleven values of  $\nu$ .

v<sub>lic</sub> READPRN(NULIC) cS

Read in data array  $\rho_{lic}$  for kinematic viscosity,  $\rho$ , an array of eleven values of  $\rho$ .

$\rho_{lic}$  READPRN(RHOLIC)  $\frac{\text{kg}}{\text{liter}}$



Water-Glycerol Solution for Hydrophobic Sensor

Read in data array vbic for kinematic viscosity,  $\nu$ , an array of eleven values of  $\nu$ .

$$vbic = \text{READPRN}(\text{NUBIC}) \text{ cS}$$

Read in data array pbic for kinematic viscosity,  $\rho$ , an array of eleven values of  $\rho$ .

$$pbic = \text{READPRN}(\text{RHOBIC}) \cdot \frac{\text{kg}}{\text{liter}}$$

Hydrophilic Sensor

For each  $i = 1, \dots, 401$  and  $klic = 1, \dots, 11$  compute the four complex-valued functions B31, B32, b33 and b34. The two-dimensional arrays B31\_lic, B32\_lic, b33\_lic and b34\_lic store the 401x11 values of the complex-valued functions B31, B32, b33 and b34 respectively.

$$B31_{lic,i,klic} = B31 \left[ \eta_{lic\_fit}, h_{lic\_fit}, (\omega_{lic}^{\langle klic \rangle})_i \right]$$

$$B32_{lic,i,klic} = B32 \left[ \eta_{lic\_fit}, \nu_{lic\_klic}, \rho_{lic\_klic}, h_{lic\_fit}, (\omega_{lic}^{\langle klic \rangle})_i \right]$$

$$b33_{lic,i,klic} = b33 \left[ \eta_{lic\_fit}, h_{lic\_fit}, (\omega_{lic}^{\langle klic \rangle})_i \right]$$

$$b34_{lic,i,klic} = b34 \left[ \eta_{lic\_fit}, \nu_{lic\_klic}, \rho_{lic\_klic}, h_{lic\_fit}, (\omega_{lic}^{\langle klic \rangle})_i \right]$$

$$\zeta_{lic}(\alpha, k, i) = -2j \left( \frac{\alpha b34_{lic,i,k} + b33_{lic,i,k}}{\alpha B32_{lic,i,k} + B31_{lic,i,k}} \right)$$

From the above expression for  $\zeta_{lic}$ , the expression for the impedance,  $fz_{lic}$ , is.

$$fz_{lic}(\alpha, A, k, i) = \frac{1}{A} \zeta_{lic}(\alpha, k, i)$$

The expressions for the magnitude of  $fz_{lic}$ ,  $|fz_{lic}|$ , and the phase of  $fz_{lic}$ ,  $\theta_{z_{lic}}$ , are.

$$Mfz_{lic}(\alpha, A, k, i) = |fz_{lic}(\alpha, A, k, i)|$$

$$\theta_{z_{lic}}(\alpha, k, i) = \text{atan} \left( \frac{\text{Im}(\zeta_{lic}(\alpha, k, i))}{\text{Re}(\zeta_{lic}(\alpha, k, i))} \right)$$

Hydrophobic Sensor

For each  $i = 1, \dots, 401$  and  $kbic = 1, \dots, 7$  compute the four complex-valued functions  $B31$ ,  $B32$ ,  $b33$  and  $b34$ . The two-dimensional arrays  $B31\_bic$ ,  $B32\_bic$ ,  $b33\_bic$  and  $b34\_bic$  store the  $401 \times 7$  values of the complex-valued functions  $B31$ ,  $B32$ ,  $b33$  and  $b34$  respectively.

$$B31\_bic_{i,kbic} = B31 \left[ \eta_{bic\_fit}, h_{bic\_fit}, (\omega_{bic} \langle kbic \rangle)_i \right]$$

$$B32\_bic_{i,kbic} = B32 \left[ \eta_{bic\_fit}, v_{bic\_kbic}, \rho_{bic\_kbic}, h_{bic\_fit}, (\omega_{bic} \langle kbic \rangle)_i \right]$$

$$b33\_bic_{i,kbic} = b33 \left[ \eta_{bic\_fit}, h_{bic\_fit}, (\omega_{bic} \langle kbic \rangle)_i \right]$$

$$b34\_bic_{i,kbic} = b34 \left[ \eta_{bic\_fit}, v_{bic\_kbic}, \rho_{bic\_kbic}, h_{bic\_fit}, (\omega_{bic} \langle kbic \rangle)_i \right]$$

$$\zeta_{bic}(\alpha, k, i) = -2j \left( \frac{\alpha b34\_bic_{i,k} + b33\_bic_{i,k}}{\alpha B32\_bic_{i,k} + B31\_bic_{i,k}} \right)$$

From the above expression for  $\zeta_{bic}$ , the expression for the impedance,  $fZ_{bic}$ , is.

$$fZ_{bic}(\alpha, A, k, i) = \frac{1}{A} \zeta_{bic}(\alpha, k, i)$$

The expressions for the magnitude of  $fZ_{bic}$ ,  $|fZ_{bic}|$ , and the phase of  $fZ_{bic}$ ,  $f\theta_{Z_{bic}}$ , are.

$$MfZ_{bic}(\alpha, A, k, i) = |fZ_{bic}(\alpha, A, k, i)|$$

$$f\theta_{Z_{bic}}(\alpha, k, i) = \text{atan} \left( \frac{\text{Im}(\zeta_{bic}(\alpha, k, i))}{\text{Re}(\zeta_{bic}(\alpha, k, i))} \right)$$

Hydrophilic Sensor

The following Sum Of Squares Of Errors,  $SSE_{lic}(\alpha, A, k)$ , will be used in the fitting of the experimental data to the theoretical complex-valued expression of the impedance,  $Z$ , given by the function  $fZ_{lic}$ . The results from the fitting procedure will consist of eleven best-fit values for  $\alpha$  and  $A$ , one value of  $\alpha$  and  $A$  for each concentration of glycerol in water.

$$SSE_{lic}(\alpha, A, k) = \frac{1}{N} \sum_i \left| \left( \frac{Z_{lic} \langle k \rangle}{k\Omega} \right)_i - \frac{fZ_{lic}(\alpha, A, k, i)}{k\Omega} \right|^2$$

Hydrophobic Sensor

The following Sum Of Squares Of Errors,  $SSE_{bic}(\alpha, A, k)$ , will be used in the fitting of the experimental data to the theoretical complex-valued expression of the impedance,  $Z$ , given by the function  $fz_{bic}$ . The results from the fitting procedure will consist of seven values best-fit for  $\alpha$  and  $A$ , one value of  $\alpha$  and  $A$  for each concentration of glycerol in water.

$$SSE_{bic}(\alpha, A, k) = \frac{1}{N} \sum_i \left| \left| \frac{(Z_{bic}^{<k>})_i}{k\Omega} - \frac{fz_{bic}(\alpha, A, k, i)}{k\Omega} \right| \right|^2$$

Hydrophilic Sensor

Determination of  $\alpha$  in pure water.

Enter guess values for  $\alpha$  and  $A$ .

$\alpha1\_guess = 3.76 + 2.30j$

$A1\_guess = 0.4 \text{ cm}^2$

----- Mathcad Solve Block -----

Given

$$SSE_{bic}(\alpha1\_guess, A1\_guess, 1) = 0$$

$$1 = 1$$

$$\begin{pmatrix} \alpha1\_fit \\ A1\_fit \end{pmatrix} = \text{Minerr}(\alpha1\_guess, A1\_guess)$$

-----

The result of the solve block,  $\alpha1\_fit$  and  $A1\_fit$ , is.

$$\alpha1\_fit = 3.774 + 2.299i$$

$$A1\_fit = 0.4115 \cdot \text{cm}^2$$

Compute the residual error,  $ERR$ , given by  $ERR = SSE_{bic}(\alpha1\_fit, A1\_fit, 1)$ .

$$ERR = 0.131$$

Hydrophilic Sensor

Determination of  $\alpha$  in 0.1 molar water-glycerol solution.

Enter guess values for  $\alpha$  and  $A$ .

$$\alpha_{2\_guess} = 2.6 + 1.3j$$

$$A_{2\_guess} = 0.39 \text{ cm}^2$$

----- Mathcad Solve Block -----

Given

$$\text{SSElc}(\alpha_{2\_guess}, A_{2\_guess}, 2) = 0$$

$$l = 1$$

$$\begin{pmatrix} \alpha_{2\_fit} \\ A_{2\_fit} \end{pmatrix} = \text{Minerr}(\alpha_{2\_guess}, A_{2\_guess})$$

-----

The result of the solve block,  $\alpha_{2\_fit}$  and  $A_{2\_fit}$ , is.

$$\alpha_{2\_fit} = 2.631 + 1.246j$$

$$A_{2\_fit} = 0.3911 \text{ cm}^2$$

Compute the residual error, ERR, given by  $\text{ERR} = \text{SSElc}(\alpha_{2\_fit}, A_{2\_fit}, 2)$ .

$$\text{ERR} = 0.088$$

Hydrophilic Sensor

Determination of  $\alpha$  in 0.2 molar water-glycerol solution.

Enter guess values for  $\alpha$  and A.

$$\alpha_{3\_guess} = 1.9 + 0.6j$$

$$A_{3\_guess} = 0.34 \text{ cm}^2$$

----- Mathcad Solve Block -----

Given

$$\text{SSElc}(\alpha_{3\_guess}, A_{3\_guess}, 3) = 0$$

$$l = 1$$

$$\begin{pmatrix} \alpha_{3\_fit} \\ A_{3\_fit} \end{pmatrix} = \text{Minerr}(\alpha_{3\_guess}, A_{3\_guess})$$

-----

The result of the solve block,  $\alpha_{3\_fit}$  and  $A_{3\_fit}$ , is.

$$\alpha_{3\_fit} = 1.9145 + 0.6513j$$

$$A_{3\_fit} = 0.3494 \cdot \text{cm}^2$$

Compute the residual error, ERR, given by  $\text{ERR} = \text{SSElc}(\alpha_{3\_fit}, A_{3\_fit}, 3)$ .

$$\text{ERR} = 0.043$$

Hydrophilic Sensor

Determination of  $\alpha$  in 0.3 molar water-glycerol solution.

Enter guess values for  $\alpha$  and A.

$$\alpha_{4\_guess} = 16 + 0.4j$$

$$A_{4\_guess} = 0.34 \text{ cm}^2$$

----- Mathcad Solve Block -----

Given

$$\text{SSE}_{lc}(\alpha_{4\_guess}, A_{4\_guess}, 4) = 0$$

$$1 = 1$$

$$\begin{pmatrix} \alpha_{4\_fit} \\ A_{4\_fit} \end{pmatrix} = \text{Minerr}(\alpha_{4\_guess}, A_{4\_guess})$$

-----

The result of the solve block,  $\alpha_{4\_fit}$  and  $A_{4\_fit}$ , is.

$$\alpha_{4\_fit} = 1.68 + 0.3999i$$

$$A_{4\_fit} = 0.3509 \text{ cm}^2$$

Compute the residual error, ERR, given by  $\text{ERR} = \text{SSE}_{lc}(\alpha_{4\_fit}, A_{4\_fit}, 4)$ .

$$\text{ERR} = 0.036$$

Hydrophilic Sensor

A6-11

Determination of  $\alpha$  in 0.4 molar water-glycerol solution.

Enter guess values for  $\alpha$  and A.

$$\alpha5\_guess = 14 + 0.2j$$

$$A5\_guess = 0.34 \text{ cm}^2$$

----- Mathcad Solve Block -----

Given

$$\text{SSE1ic}(\alpha5\_guess, A5\_guess, 5) = 0$$

$$i = 1$$

$$\begin{pmatrix} \alpha5\_fit \\ A5\_fit \end{pmatrix} = \text{Minerr}(\alpha5\_guess, A5\_guess)$$

-----

The result of the solve block,  $\alpha5\_fit$  and  $A5\_fit$ , is.

$$\alpha5\_fit = 1.432 + 0.213j$$

$$A5\_fit = 0.3433 \cdot \text{cm}^2$$

Compute the residual error, ERR, given by  $\text{ERR} = \text{SSE1ic}(\alpha5\_fit, A5\_fit, 5)$ .

$$\text{ERR} = 0.012$$

Hydrophilic Sensor

Determination of  $\alpha$  in 0.5 molar water-glycerol solution.

Enter guess values for  $\alpha$  and A.

$$\alpha_{\text{guess}} = 13 + 0.1j$$

$$A_{\text{guess}} = 0.33 \text{ cm}^2$$

----- Mathcad Solve Block -----

Given

$$\text{SSElic}(\alpha_{\text{guess}}, A_{\text{guess}}, 6) = 0$$

$$1 = 1$$

$$\begin{pmatrix} \alpha_{\text{fit}} \\ A_{\text{fit}} \end{pmatrix} = \text{Minerr}(\alpha_{\text{guess}}, A_{\text{guess}})$$

-----

The result of the solve block,  $\alpha_{\text{fit}}$  and  $A_{\text{fit}}$ , is.

$$\alpha_{\text{fit}} = 13.16 + 0.118j$$

$$A_{\text{fit}} = 0.3316 \cdot \text{cm}^2$$

Compute the residual error, ERR, given by  $\text{ERR} = \text{SSElic}(\alpha_{\text{fit}}, A_{\text{fit}}, 6)$ .

$$\text{ERR} = 0.003$$



Hydrophilic Sensor

Determination of  $\alpha$  in 0.6 molar water-glycerol solution.

Enter guess values for  $\alpha$  and A.

$$\alpha_{7\_guess} = 1.1 + 0.07i$$

$$A_{7\_guess} = 0.32 \text{ cm}^2$$

----- Mathcad Solve Block -----

Given

$$\text{SSE}_{lc}(\alpha_{7\_guess}, A_{7\_guess}, 7) = 0$$

$$1 = 1$$

$$\begin{pmatrix} \alpha_{7\_fit} \\ A_{7\_fit} \end{pmatrix} = \text{MinErr}(\alpha_{7\_guess}, A_{7\_guess})$$

-----

The result of the solve block,  $\alpha_{7\_fit}$  and  $A_{7\_fit}$ , is.

$$\alpha_{7\_fit} = 1.172 + 0.069i$$

$$A_{7\_fit} = 0.3271 \cdot \text{cm}^2$$

Compute the residual error, ERR, given by  $\text{ERR} = \text{SSE}_{lc}(\alpha_{7\_fit}, A_{7\_fit}, 7)$ .

$$\text{ERR} = 0.001$$

Hydrophilic Sensor

Determination of  $\alpha$  in 0.7 molar water-glycerol solution.

Enter guess values for  $\alpha$  and A.

$$\alpha_{8\_guess} = 0.92 + 0.01j$$

$$A_{8\_guess} = 0.33 \text{ cm}^2$$

----- Mathcad Solve Block -----

Given

$$\text{SSElic}(\alpha_{8\_guess}, A_{8\_guess}, 8) = 0$$

$$l = 1$$

$$\begin{pmatrix} \alpha_{8\_fit} \\ A_{8\_fit} \end{pmatrix} = \text{Minerr}(\alpha_{8\_guess}, A_{8\_guess})$$

-----

The result of the solve block,  $\alpha_{8\_fit}$  and  $A_{8\_fit}$ , is.

$$\alpha_{8\_fit} = 0.937 + 0.016j$$

$$A_{8\_fit} = 0.3255 \text{ cm}^2$$

Compute the residual error, ERR, given by  $\text{ERR} = \text{SSElic}(\alpha_{8\_fit}, A_{8\_fit}, 8)$ .

$$\text{ERR} = 0.002$$

Hydrophilic Sensor

Determination of  $\alpha$  in 0.8 molar water-glycerol solution.

Enter guess values for  $\alpha$  and A.

$$\alpha_0_{\text{guess}} = 0.8 - 0.003j$$

$$A_0_{\text{guess}} = 0.32 \text{ cm}^2$$

----- Mathcad Solve Block -----

Given

$$\text{SSElic}(\alpha_0_{\text{guess}}, A_0_{\text{guess}}, 9) = 0$$

$$1 = 1$$

$$\begin{pmatrix} \alpha_0_{\text{fit}} \\ A_0_{\text{fit}} \end{pmatrix} = \text{Minerr}(\alpha_0_{\text{guess}}, A_0_{\text{guess}})$$

-----

The result of the solve block,  $\alpha_0_{\text{fit}}$  and  $A_0_{\text{fit}}$ , is.

$$\alpha_0_{\text{fit}} = 0.8935 - 0.0044j$$

$$A_0_{\text{fit}} = 0.3242 \text{ cm}^2$$

Compute the residual error, ERR, given by  $\text{ERR} = \text{SSElic}(\alpha_0_{\text{fit}}, A_0_{\text{fit}}, 9)$ .

$$\text{ERR} = 0.002$$

Hydrophilic Sensor

Determination of  $\alpha$  in 0.9 molar water-glycerol solution.

Enter guess values for  $\alpha$  and A.

$$\alpha_{10\_guess} = 0.8 - 0.04j$$

$$A_{10\_guess} = 0.32 \text{ cm}^2$$

----- Mathcad Solve Block -----

Given

$$\text{SSEhc}(\alpha_{10\_guess}, A_{10\_guess}, 10) = 0$$

$$i = 1$$

$$\begin{pmatrix} \alpha_{10\_fit} \\ A_{10\_fit} \end{pmatrix} = \text{Minerr}(\alpha_{10\_guess}, A_{10\_guess})$$

-----

The result of the solve block,  $\alpha_{10\_fit}$  and  $A_{10\_fit}$ , is.

$$\alpha_{10\_fit} = 0.842 - 0.048j$$

$$A_{10\_fit} = 0.3236 \cdot \text{cm}^2$$

Compute the residual error, ERR, given by  $\text{ERR} = \text{SSEhc}(\alpha_{10\_fit}, A_{10\_fit}, 10)$ .

$$\text{ERR} = 0.003$$

Hydrophilic Sensor

Determination of  $\alpha$  in pure glycerol.

Enter guess values for  $\alpha$  and A.

$\alpha_{11\_guess} = 0.8 - 0.06j$

$A_{11\_guess} = 0.32 \text{ cm}^2$

----- Mathcad Solve Block -----

Given

$$\text{SSElc}(\alpha_{11\_guess}, A_{11\_guess}, l1) = 0$$

$l1 = 1$

$$\begin{pmatrix} \alpha_{11\_fit} \\ A_{11\_fit} \end{pmatrix} = \text{Minerr}(\alpha_{11\_guess}, A_{11\_guess})$$

-----

The result of the solve block,  $\alpha_{11\_fit}$  and  $A_{11\_fit}$ , is.

$$\alpha_{11\_fit} = 0.83 - 0.066j$$

$$A_{11\_fit} = 0.3221 \text{ cm}^2$$

Compute the residual error, ERR, given by  $\text{ERR} = \text{SSElc}(\alpha_{11\_fit}, A_{11\_fit}, l1)$ .

$$\text{ERR} = 0.001$$

Hydrophobic Sensor

Determination of  $\alpha$  in pure water.

Enter guess values for  $\alpha$  and  $A$ .

$$\alpha\alpha1\_guess = 4.9 \cdot 23j$$

$$AA1\_guess = 0.36 \text{ cm}^2$$

----- Mathcad Solve Block -----

Given

$$\text{SSEbic}(\alpha\alpha1\_guess, AA1\_guess, 1) = 0$$

$$l = 1$$

$$\begin{pmatrix} \alpha\alpha1\_fit \\ AA1\_fit \end{pmatrix} = \text{Minerr}(\alpha\alpha1\_guess, AA1\_guess)$$

-----

The result of the solve block,  $\alpha\alpha1\_fit$  and  $AA1\_fit$ , is.

$$\alpha\alpha1\_fit = 3.02 + 1.446i$$

$$AA1\_fit = 0.368 \cdot \text{cm}^2$$

Compute the residual error, ERR, given by  $\text{ERR} = \text{SSEbic}(\alpha\alpha1\_fit, AA1\_fit, 1)$ .

$$\text{ERR} = 0.056$$

Hydrophobic Sensor

Determination of  $\alpha$  in 0.1 molar water-glycerol solution.

Enter guess values for  $\alpha$  and A.

$$\alpha\alpha_2\_guess = 3.2 + 1.2j$$

$$\Lambda\Lambda_2\_guess = 0.37 \text{ cm}^2$$

----- Mathcad Solve Block -----

Given

$$\text{SSEbic}(\alpha\alpha_2\_guess, \Lambda\Lambda_2\_guess, 2) = 0$$

$$i = 1$$

$$\begin{pmatrix} \alpha\alpha_2\_fit \\ \Lambda\Lambda_2\_fit \end{pmatrix} = \text{Minerr}(\alpha\alpha_2\_guess, \Lambda\Lambda_2\_guess)$$

-----

The result of the solve block,  $\alpha\alpha_2\_fit$  and  $\Lambda\Lambda_2\_fit$ , is.

$$\alpha\alpha_2\_fit = 2.192 + 0.795i$$

$$\Lambda\Lambda_2\_fit = 0.3728 \cdot \text{cm}^2$$

Compute the residual error, ERR, given by  $\text{ERR} = \text{SSEbic}(\alpha\alpha_2\_fit, \Lambda\Lambda_2\_fit, 2)$ .

$$\text{ERR} = 0.048$$

Hydrophobic Sensor

Determination of  $\alpha$  in 0.2 molar water-glycerol solution.

Enter guess values for  $\alpha$  and A.

$$\alpha\alpha3\_guess = 2.3 + 0.7j$$

$$AA3\_guess = 0.35 \text{ cm}^2$$

----- Mathcad Solve Block -----

Given

$$\text{SSEbic}(\alpha\alpha3\_guess, AA3\_guess, 3) = 0$$

$$l = 1$$

$$\begin{pmatrix} \alpha\alpha3\_fit \\ AA3\_fit \end{pmatrix} = \text{Minerr}(\alpha\alpha3\_guess, AA3\_guess)$$

-----

The result of the solve block,  $\alpha\alpha3\_fit$  and  $AA3\_fit$ , is.

$$\alpha\alpha3\_fit = 1.707 + 0.417i$$

$$AA3\_fit = 0.3581 \cdot \text{cm}^2$$

Compute the residual error, ERR, given by  $\text{ERR} = \text{SSEbic}(\alpha\alpha3\_fit, AA3\_fit, 3)$ .

$$\text{ERR} = 0.026$$



Hydrophobic Sensor

Determination of  $\alpha$  in 0.4 molar water-glycerol solution.

Enter guess values for  $\alpha$  and A.

$$\alpha_{\text{guess}} = 1.3 + 0.1j$$

$$AA_{\text{guess}} = 0.34 \text{ cm}^2$$

----- Mathcad Solve Block -----

Given

$$\text{SSEbic}(\alpha_{\text{guess}}, AA_{\text{guess}}, 4) = 0$$

$$l = 1$$

$$\begin{pmatrix} \alpha_{\text{fit}} \\ AA_{\text{fit}} \end{pmatrix} = \text{Minerr}(\alpha_{\text{guess}}, AA_{\text{guess}})$$

-----

The result of the solve block,  $\alpha_{\text{fit}}$  and  $AA_{\text{fit}}$ , is.

$$\alpha_{\text{fit}} = 1.135 + 0.037j$$

$$AA_{\text{fit}} = 0.341 \cdot \text{cm}^2$$

Compute the residual error, ERR, given by  $\text{ERR} = \text{SSEbic}(\alpha_{\text{fit}}, AA_{\text{fit}}, 4)$ .

$$\text{ERR} = 0.005$$

Hydrophobic Sensor

Determination of  $\alpha$  in 0.6 molar water-glycerol solution.

Enter guess values for  $\alpha$  and A.

$$\alpha\alpha5\_guess = 11.93 \cdot 10^{-4}$$

$$AA5\_guess = 0.35 \text{ cm}^2$$

----- Mathcad Solve Block -----

Given

$$\text{SSEbic}(\alpha\alpha5\_guess, AA5\_guess, 5) = 0$$

$$1 = 1$$

$$\begin{pmatrix} \alpha\alpha5\_fit \\ AA5\_fit \end{pmatrix} = \text{Minerr}(\alpha\alpha5\_guess, AA5\_guess)$$

-----

The result of the solve block,  $\alpha\alpha5\_fit$  and  $AA5\_fit$ , is.

$$\alpha\alpha5\_fit = 1.043 - 0.053i$$

$$AA5\_fit = 0.3529 \cdot \text{cm}^2$$

Compute the residual error, ERR, given by  $\text{ERR} = \text{SSEbic}(\alpha\alpha5\_fit, AA5\_fit, 5)$ .

$$\text{ERR} = 0.011$$

Hydrophobic Sensor

Determination of  $\alpha$  in 0.8 molar water-glycerol solution.

Enter guess values for  $\alpha$  and A.

$$\alpha\alpha6\_guess = 0.8 - 0.05$$

$$AA6\_guess = 0.33 \text{ cm}^2$$

----- Mathcad Solve Block -----

Given

$$\text{SSEbic}(\alpha\alpha6\_guess, AA6\_guess, 6) = 0$$

$$I = 1$$

$$\begin{pmatrix} \alpha\alpha6\_fit \\ AA6\_fit \end{pmatrix} = \text{Minerr}(\alpha\alpha6\_guess, AA6\_guess)$$

-----

The result of the solve block,  $\alpha\alpha6\_fit$  and  $AA6\_fit$ , is.

$$\alpha\alpha6\_fit = 0.801 - 0.073$$

$$AA6\_fit = 0.3345 \cdot \text{cm}^2$$

Compute the residual error, ERR, given by  $\text{ERR} = \text{SSEbic}(\alpha\alpha6\_fit, AA6\_fit, 6)$ .

$$\text{ERR} = 0.013$$

Hydrophobic Sensor

Determination of  $\theta$  in pure glycerol.

Enter guess values for  $\alpha$  and A.

$$\alpha\alpha7\_guess = 0.7 \text{ } 0.11$$

$$AA7\_guess = 0.32 \text{ cm}^2$$

----- Mathcad Solve Block -----

Given

$$SSEbic(\alpha\alpha7\_guess, AA7\_guess, 7) = 0$$

$$1 = 1$$

$$\begin{pmatrix} \alpha\alpha7\_fit \\ AA7\_fit \end{pmatrix} = \text{Minerr}(\alpha\alpha7\_guess, AA7\_guess)$$

The result of the solve block,  $\alpha\alpha7\_fit$  and  $AA7\_fit$ , is.

$$\alpha\alpha7\_fit = 0.7703 \text{ } 0.1344$$

$$AA7\_fit = 0.3399 \text{ cm}^2$$

Compute the residual error, ERR, given by  $ERR = SSEbic(\alpha\alpha7\_fit, AA7\_fit, 7)$ .

$$ERR = 0.03$$

Data for Hydrophilic and Hydrophobic Sensor

$\alpha1\_fit$	$\Lambda\_hydrophilic =$	$A1\_fit$
$\alpha2\_fit$		$A2\_fit$
$\alpha3\_fit$		$A3\_fit$
$\alpha4\_fit$		$A4\_fit$
$\alpha5\_fit$		$A5\_fit$
$\alpha\_hydrophilic - \alpha6\_fit$		$A6\_fit$
$\alpha7\_fit$		$A7\_fit$
$\alpha8\_fit$		$A8\_fit$
$\alpha9\_fit$		$A9\_fit$
$\alpha10\_fit$		$A10\_fit$
$\alpha11\_fit$		$A11\_fit$

Store the data for  $\alpha_{\text{hydrophilic}}$  and  $\Lambda_{\text{hydrophilic}}$  in the data files ALPLIC.PRN and ALIC.PRN.

WRITEPRN(ALPLIC)  $\alpha_{\text{hydrophilic}}$

WRITEPRN(ALIC)  $\Lambda_{\text{hydrophilic}}$   
cm<sup>2</sup>

For each  $i = 1, \dots, 401$  and  $k_{lic} = 1, \dots, 11$  compute the magnitude and phase of  $Z$ .

$$MZ_{lic\_fit_{i,k_{lic}}} = MZl \left[ \eta_{lic\_fit}, v_{lic_{k_{lic}}}, \rho_{lic_{k_{lic}}}, \alpha_{\text{hydrophilic}_{k_{lic}}}, h_{lic\_fit}, \Lambda_{\text{hydrophilic}_{k_{lic}}}, (\omega_{lic}^{k_{lic}})^{-1} \right]$$

$$\theta Z_{lic\_fit_{i,k_{lic}}} = \theta Zl \left[ \eta_{lic\_fit}, v_{lic_{k_{lic}}}, \rho_{lic_{k_{lic}}}, \alpha_{\text{hydrophilic}_{k_{lic}}}, h_{lic\_fit}, (\omega_{lic}^{k_{lic}})^{-1} \right]$$

Store the data for  $MZ_{lic\_fit}$  and  $\theta Z_{lic\_fit}$  in the data files MZLICFIT.PRN and TZLICFIT.PRN

WRITEPRN(MZLICFIT)  $MZ_{lic\_fit}$   
k $\Omega$

WRITEPRN(TZLICFIT)  $\theta Z_{lic\_fit}$   
deg

$\alpha_{\text{hydrophobic}}$	$\begin{bmatrix} \alpha\alpha1\_fit \\ \alpha\alpha2\_fit \\ \alpha\alpha3\_fit \\ \alpha\alpha4\_fit \\ \alpha\alpha5\_fit \\ \alpha\alpha6\_fit \\ \alpha\alpha7\_fit \end{bmatrix}$	$\Lambda_{\text{hydrophobic}}$	$\begin{bmatrix} \Lambda\Lambda1\_fit \\ \Lambda\Lambda2\_fit \\ \Lambda\Lambda3\_fit \\ \Lambda\Lambda4\_fit \\ \Lambda\Lambda5\_fit \\ \Lambda\Lambda6\_fit \\ \Lambda\Lambda7\_fit \end{bmatrix}$
-------------------------------	--	--------------------------------	--

Store the data for  $\alpha_{\text{hydrophobic}}$  and  $\Lambda_{\text{hydrophobic}}$  in the data files ALPBIC.PRN and ABIC.PRN.

WRITEPRN(ALPBIC)  $\alpha_{\text{hydrophobic}}$

WRITEPRN(ABIC)  $\Lambda_{\text{hydrophobic}}$   
cm<sup>2</sup>

For each  $i = 1, \dots, 401$  and  $k_{bic} = 1, \dots, 7$  compute the magnitude and phase of  $Z$ .

$$MZ_{bic\_fit_{i,k_{bic}}} = MZl \left[ \eta_{bic\_fit}, v_{bic_{k_{bic}}}, \rho_{bic_{k_{bic}}}, \alpha_{\text{hydrophobic}_{k_{bic}}}, h_{bic\_fit}, \Lambda_{\text{hydrophobic}_{k_{bic}}}, (\omega_{bic}^{k_{bic}})^{-1} \right]$$

$$\theta Z_{bic\_fit_{i,k_{bic}}} = \theta Zl \left[ \eta_{bic\_fit}, v_{bic_{k_{bic}}}, \rho_{bic_{k_{bic}}}, \alpha_{\text{hydrophobic}_{k_{bic}}}, h_{bic\_fit}, (\omega_{bic}^{k_{bic}})^{-1} \right]$$

APPENDIX 7      Plots of Interfacial Slip Parameter,  
Mathcad Program DOC4.MCD

Data Analysis of Interfacial Slip Parameter,  $\alpha$ , Versus Kinematic  
Viscosity,  $\nu$ , and Mole Fraction,  $M_f$ .

The power law model given by  $F(a,b,c,x)=ax^{b+c}$  will be fitted to the  
experimental data consisting of the real part of  $\alpha$ ,  $\alpha_{Re}$ , imaginary part  
of  $\alpha$ ,  $\alpha_{Im}$ , the magnitude of  $\alpha$ ,  $|\alpha|$ , and the phase of  $\alpha$ ,  $\theta_\alpha$  versus  
kinematic viscosity,  $\nu$ .

The exponential law model given by  $G(a,b,c,x)=ae^{bx+c}$  will be fitted to  
the experimental data consisting of the real part of  $\alpha$ ,  $\alpha_{Re}$ , imaginary  
part of  $\alpha$ ,  $\alpha_{Im}$ , the magnitude of  $\alpha$ ,  $|\alpha|$ , and the phase of  $\alpha$ ,  $\theta_\alpha$  versus  
mole fraction,  $M_f$ .

Hydrophilic Sensor

Read in data array  $\alpha_{lic}$  for interfacial slip parameter,  $\alpha$ , an array of eleven  
values of  $\alpha$ .

$\alpha_{lic}$  READPRN(ALPLIC)

$\alpha_{lic} \left\langle \begin{matrix} <1> \\ <2> \end{matrix} \right\rangle$

Read in data array  $\nu_{lic}$  for kinematic viscosity,  $\nu$ , an array of eleven  
values of  $\nu$ .

$\nu_{lic}$  READPRN(NULIC) cS

Read in data array  $M_{flic}$  for mole fraction,  $M_f$ , an array of eleven  
values of  $M_f$ .

$M_{flic}$  READPRN(MOLLIC)

Hydrophobic Sensor

Read in data array  $\alpha_{bic}$  for interfacial slip parameter,  $\alpha$ , an array of seven values of  $\alpha$ .

$\alpha_{bic} = \text{READPRN}(\text{ALPBIC})$

$\alpha_{bic} = \alpha_{bic}^{<1>} + j \alpha_{bic}^{<2>}$

Read in data array  $v_{bic}$  for kinematic viscosity,  $v$ , an array of seven values of  $v$ .

$v_{bic} = \text{READPRN}(\text{NUBIC}) \cdot \text{cS}$

Read in data array  $M_{Fbic}$  for mole fraction,  $M_f$ , an array of seven values of  $M_f$ .

$M_{Fbic} = \text{READPRN}(\text{MOLBIC})$

Hydrophilic Sensor

The arrays  $\alpha_{Relic}$ ,  $\alpha_{Imlic}$ ,  $\alpha_{Maglic}$  and  $\theta_{\alpha lic}$  store respectively  $\alpha_{Re}$ ,  $\alpha_{Im}$ ,  $|\alpha|$  and  $\theta_{\alpha}$ . Compute  $\alpha_{Re}$ ,  $\alpha_{Im}$ ,  $|\alpha|$  and  $\theta_{\alpha}$ .

$$\alpha_{Relic} = \text{Re}(\alpha_{lic})$$

$$\alpha_{Imlic} = \text{Im}(\alpha_{lic})$$

$$\alpha_{Maglic} = |\alpha_{lic}|$$

$$\theta_{\alpha lic} = \text{atan} \left( \frac{\alpha_{Imlic}}{\alpha_{Relic}} \right) \text{deg}$$

The subscript  $klic$  takes on integral values from 1 through 11 inclusive. Each value of  $klic$  corresponds to a different concentration of glycerol in water.

Hydrophilic Sensor

$k_{lic} = 1$  corresponds to pure water.  
 $k_{lic} = 2$  corresponds to 0.1 molar water-glycerol solution.  
 $k_{lic} = 3$  corresponds to 0.2 molar water-glycerol solution.  
 $k_{lic} = 4$  corresponds to 0.3 molar water-glycerol solution.  
 $k_{lic} = 5$  corresponds to 0.4 molar water-glycerol solution.  
 $k_{lic} = 6$  corresponds to 0.5 molar water-glycerol solution.  
 $k_{lic} = 7$  corresponds to 0.6 molar water-glycerol solution.  
 $k_{lic} = 8$  corresponds to 0.7 molar water-glycerol solution.  
 $k_{lic} = 9$  corresponds to 0.8 molar water-glycerol solution.  
 $k_{lic} = 10$  corresponds to 0.9 molar water-glycerol solution.  
 $k_{lic} = 11$  corresponds to pure glycerol.

$N_{lic}$  corresponds to the number of experimental data points given by

$$N_{lic} = 11$$

$$k_{lic} = 1 \cdot N_{lic}$$

Hydrophobic Sensor

The arrays  $\alpha_{Re_{lic}}$ ,  $\alpha_{Im_{lic}}$ ,  $\alpha_{Mag_{lic}}$  and  $\theta_{\alpha_{lic}}$  store respectively  $\alpha_{Re}$ ,  $\alpha_{Im}$ ,  $|\alpha|$  and  $\theta_{\alpha}$ . Compute  $\alpha_{Re}$ ,  $\alpha_{Im}$ ,  $|\alpha|$  and  $\theta_{\alpha}$ .

$$\alpha_{Re_{lic}} = \text{Re}(\alpha_{lic})$$

$$\alpha_{Im_{lic}} = \text{Im}(\alpha_{lic})$$

$$\alpha_{Mag_{lic}} = |\alpha_{lic}|$$

$$\theta_{\alpha_{lic}} = \frac{\text{atan}\left(\frac{\alpha_{Im_{lic}}}{\alpha_{Re_{lic}}}\right)}{\text{deg}}$$

The subscript  $k_{bic}$  takes on integral values from 1 through 7 inclusive. Each value of  $k_{bic}$  corresponds to a different concentration of glycerol in water.



Hydrophobic Sensor

kbic = 1 corresponds to pure water.  
 kbic = 2 corresponds to 0.1 molar water-glycerol solution.  
 kbic = 3 corresponds to 0.2 molar water-glycerol solution.  
 kbic = 4 corresponds to 0.4 molar water-glycerol solution.  
 kbic = 5 corresponds to 0.6 molar water-glycerol solution.  
 kbic = 6 corresponds to 0.8 molar water-glycerol solution.  
 klbc = 7 corresponds to pure glycerol.

Nbic corresponds to the number of experimental data points given by

$$Nbic = 7$$

$$kbic = 1 Nbic$$

For the hydrophilic and hydrophobic sensors, the mathematical model  $F(a,b,c,x) = ax^b+c$  will be used to fit the experimental data consisting of  $\alpha_{Re}$ ,  $\alpha_{Im}$ ,  $|\alpha|$  and  $\theta_\alpha$  versus kinematic viscosity,  $\nu$ . For the experimental data consisting of  $\alpha_{Re}$ ,  $\alpha_{Im}$ ,  $|\alpha|$  and  $\theta_\alpha$  versus mole fraction,  $M_f$ , the mathematical model  $G(a,b,c,x) = ae^{bx}+c$  will be used.

The following Sum Of Squares Of Errors will be used in the non-linear curve-fitting process  $SSE1ic(a,b,c), \dots, SSE81ic(a,b,c)$  and  $SSE1bic(a,b,c), \dots, SSE8bic(a,b,c)$ .

Power Law Model

$$F(a,b,c,x) = ax^b+c$$

Exponential Law Model

$$G(a,b,c,x) = ae^{bx}+c$$

Hydrophilic SensorNon-Linear Regression Analysis of  $\alpha_{Re}$  vs  $v$ 

$$SSE_{Ilic}(a,b,c) = \frac{1}{N_{Ilic}} \sum_{k_{Ilic}} \left( \alpha_{Re_{Ilic}_{k_{Ilic}}} - F\left(a,b,c, \frac{v_{Ilic_{k_{Ilic}}}}{cS}\right) \right)^2$$

Enter guess values for a,b and c.

aIlic\_guess = 1

bIlic\_guess = 0.1

cIlic\_guess = 1

----- Mathcad Solve Block -----

Given

$$SSE_{Ilic}(a_{Ilic\_guess}, b_{Ilic\_guess}, c_{Ilic\_guess}) = 0$$

$$1 = 1$$

$$1 = 1$$

$$\begin{pmatrix} a_{Ilic\_fit} \\ b_{Ilic\_fit} \\ c_{Ilic\_fit} \end{pmatrix} = \text{Minerr}(a_{Ilic\_guess}, b_{Ilic\_guess}, c_{Ilic\_guess})$$

-----

$$a_{Ilic\_fit} = 3.0298$$

$$b_{Ilic\_fit} = -0.4182$$

$$c_{Ilic\_fit} = 0.7142$$

Compute the residual error, ERR, given by  $ERR = SSE_{Ilic}(a_{Ilic\_fit}, b_{Ilic\_fit}, c_{Ilic\_fit})$ .

$$ERR = 0.0036$$

Hydrophilic SensorNon-Linear Regression Analysis of  $\alpha_{Im}$  vs  $v$ 

$$SSE_{2lc}(a,b,c) = \frac{1}{N_{lc}} \sum_{k_{lc}} \left( \alpha_{Im_{k_{lc}}} - F\left(a,b,c, \frac{v_{lc_{k_{lc}}}}{cS}\right) \right)^2$$

Enter guess values for a,b and c.

$$a_{2lc\_guess} = 1$$

$$b_{2lc\_guess} = -0.1$$

$$c_{2lc\_guess} = 1$$

----- Mathcad Solve Block -----

Given

$$SSE_{2lc}(a_{2lc\_guess}, b_{2lc\_guess}, c_{2lc\_guess}) = 0$$

$$1 = 1$$

$$1 = 1$$

$$\begin{pmatrix} a_{2lc\_fit} \\ b_{2lc\_fit} \\ c_{2lc\_fit} \end{pmatrix} = \text{Minerr}(a_{2lc\_guess}, b_{2lc\_guess}, c_{2lc\_guess})$$

$$a_{2lc\_fit} = 2.3904$$

$$b_{2lc\_fit} = -0.5718$$

$$c_{2lc\_fit} = 0.0838$$

Compute the residual error, ERR, given by  $ERR = SSE_{2lc}(a_{2lc\_fit}, b_{2lc\_fit}, c_{2lc\_fit})$ .

$$ERR = 2.4244 \cdot 10^{-4}$$

Hydrophilic SensorNon-Linear Regression Analysis of  $|\alpha|$  vs  $v$ 

$$SSE_{3lic}(a, b, c) = \frac{1}{N_{lic}} \sum_{k_{lic}} \left( \alpha_{Maglic_{k_{lic}}} - F\left(a, b, c, \frac{v_{lic_{k_{lic}}}}{cS}\right) \right)^2$$

Enter guess values for a, b and c.

a3lic\_guess = 1

b3lic\_guess = 0.1

c3lic\_guess = 1

----- Mathcad Solve Block -----

Given

$$SSE_{3lic}(a3lic\_guess, b3lic\_guess, c3lic\_guess) = 0$$

$$1 = 1$$

$$1 = 1$$

$$\begin{pmatrix} a3lic\_fit \\ b3lic\_fit \\ c3lic\_fit \end{pmatrix} = \text{Minerr}(a3lic\_guess, b3lic\_guess, c3lic\_guess)$$

$$a3lic\_fit = 3.6292$$

$$b3lic\_fit = -0.484$$

$$c3lic\_fit = 0.7619$$

Compute the residual error, ERR, given by  $ERR = SSE_{3lic}(a3lic\_fit, b3lic\_fit, c3lic\_fit)$ .

$$ERR = 0.0041$$

Hydrophilic SensorNon-Linear Regression Analysis of  $\theta_{\alpha}$  vs  $v$ 

$$SSE_{4lc}(a,b,c) = \frac{1}{N_{4lc}} \sum_{k_{4lc}} \left( \theta_{4lc,k_{4lc}} \cdot \text{deg} - F \left( a, b, c, -\frac{v_{4lc,k_{4lc}}}{cS} \right) \right)^2$$

Enter guess values for a,b and c.

$$a_{4lc\_guess} = 1$$

$$b_{4lc\_guess} = -0.01$$

$$c_{4lc\_guess} = 1$$

----- Mathcad Solve Block -----

Given

$$SSE_{4lc}(a_{4lc\_guess}, b_{4lc\_guess}, c_{4lc\_guess}) = 0$$

$$| = 1$$

$$| = 1$$

$$\begin{pmatrix} a_{4lc\_fit} \\ b_{4lc\_fit} \\ c_{4lc\_fit} \end{pmatrix} = \text{Minerr}(a_{4lc\_guess}, b_{4lc\_guess}, c_{4lc\_guess})$$

-----

$$a_{4lc\_fit} = 0.8113$$

$$b_{4lc\_fit} = -0.2101$$

$$c_{4lc\_fit} = 0.2303$$

Compute the residual error, ERR, given by  $ERR = SSE_{4lc}(a_{4lc\_fit}, b_{4lc\_fit}, c_{4lc\_fit})$ .

$$ERR = 3.5861 \cdot 10^{-4}$$

Hydrophobic SensorNon-Linear Regression Analysis of  $\alpha_{Re}$  vs  $v$ 

$$SSE1bic(a,b,c) = \frac{1}{Nbic} \sum_{kbic} \left( \alpha_{Rebic_{kbic}} - F\left(a,b,c, \frac{vbic_{kbic}}{cS}\right) \right)^2$$

Enter guess values for a,b and c.

albic\_guess = 1

blbic\_guess = 0.1

clbic\_guess = 1

----- Mathcad Solve Block -----

Given

$$SSE1bic(albic\_guess, blbic\_guess, clbic\_guess) = 0$$

$$l = 1$$

$$l = 1$$

$$\begin{pmatrix} albic\_fit \\ blbic\_fit \\ clbic\_fit \end{pmatrix} = \text{Minerr}(albic\_guess, blbic\_guess, clbic\_guess)$$

$$albic\_fit = 2.3621$$

$$blbic\_fit = -0.4143$$

$$clbic\_fit = 0.663$$

Compute the residual error, EPR, given by  $ERR = SSE1bic(albic\_fit, blbic\_fit, clbic\_fit)$ .

$$ERR = 0.0013$$

Hydrophobic SensorNon-Linear Regression Analysis of  $\alpha_{Im}$  vs  $v$ 

$$SSE2bic(a,b,c) = \frac{1}{Nbic} \sum_{kbic} \left( \alpha_{Imbic_{kbic}} - F\left(a,b,c, \frac{vbic_{kbic}}{cS}\right) \right)^2$$

Enter guess values for a,b and c.

a2bic\_guess = 1

b2bic\_guess = -0.1

c2bic\_guess = 1

----- Mathcad Solve Block -----  
Given

$$SSE2bic(a2bic\_guess, b2bic\_guess, c2bic\_guess) = 0$$

$$1 = 1$$

$$1 = 1$$

$$\begin{pmatrix} a2bic\_fit \\ b2bic\_fit \\ c2bic\_fit \end{pmatrix} = \text{Minerr}(a2bic\_guess, b2bic\_guess, c2bic\_guess)$$

-----  
a2bic\_fit = 1.6247  
b2bic\_fit = 0.5201  
c2bic\_fit = -0.1664

Compute the residual error, ERR, given by  $ERR = SSE2bic(a2bic\_fit, b2bic\_fit, c2bic\_fit)$ .

$$ERR = 4.9071 \cdot 10^{-4}$$

Hydrophobic SensorNon-Linear Regression Analysis of  $|a|$  vs  $v$ 

$$SSE3bic(a,b,c) = \frac{1}{N_{bic}} \sum_{kbic} \left( \alpha_{Magbic_{kbic}} - F\left(a,b,c, \frac{vbic_{kbic}}{cS}\right) \right)^2$$

Enter guess values for a,b and c.

a3bic\_guess = 1

b3bic\_guess = 0.1

c3bic\_guess = 1

----- Mathcad Solve Block -----  
Given

$$SSE3bic(a3bic\_guess, b3bic\_guess, c3bic\_guess) = 0$$

$$1 = 1$$

$$1 = 1$$

$$\begin{pmatrix} a3bic\_fit \\ b3bic\_fit \\ c3bic\_fit \end{pmatrix} = \text{Minerr}(a3bic\_guess, b3bic\_guess, c3bic\_guess)$$

$$a3bic\_fit = 2.6548$$

$$b3bic\_fit = -0.4648$$

$$c3bic\_fit = 0.6995$$

Compute the residual error, ERR, given by  $ERR = SSE3bic(a3bic\_fit, b3bic\_fit, c3bic\_fit)$ .

$$ERR = 0.0014$$



Hydrophobic SensorNon-Linear Regression Analysis of  $\theta_\alpha$  vs  $v$ 

$$SSE_{4bic}(a,b,c) = \frac{1}{N_{bic}} \sum_{k_{bic}} \left( \theta_{\alpha_{k_{bic}}} \text{ deg} - F\left(a, b, c, \frac{v_{k_{bic}}}{cS}\right) \right)^2$$

Enter guess values for a, b and c.

$$a_{4bic\_guess} = 1$$

$$b_{4bic\_guess} = -0.1$$

$$c_{4bic\_guess} = 1$$

----- Mathcad Solve Block -----  
Given

$$SSE_{4bic}(a_{4bic\_guess}, b_{4bic\_guess}, c_{4bic\_guess}) = 0$$

$$1 = 1$$

$$1 = 1$$

$$\begin{pmatrix} a_{4bic\_fit} \\ b_{4bic\_fit} \\ c_{4bic\_fit} \end{pmatrix} = \text{Minerr}(a_{4bic\_guess}, b_{4bic\_guess}, c_{4bic\_guess})$$

-----

$$a_{4bic\_fit} = 0.8075$$

$$b_{4bic\_fit} = 0.2057$$

$$c_{4bic\_fit} = -0.3292$$

Compute the residual error, ERR, given by  $ERR = SSE_{4bic}(a_{4bic\_fit}, b_{4bic\_fit}, c_{4bic\_fit})$ .

$$ERR = 6.272 \cdot 10^{-4}$$

Hydrophilic SensorNon-Linear Regression Analysis of  $\alpha_{Re}$  vs  $M_f$ 

$$SSE_{5lic}(a,b,c) = \frac{1}{N_{lic}} \sum_{k_{lic}} (\alpha_{Relic_{k_{lic}}} - G(a,b,c, MF_{lic_{k_{lic}}}))^2$$

Enter guess values for a,b and c.

a5lic\_guess 1

b5lic\_guess - 2

c5lic\_guess 1

----- Mathcad Solve Block -----

Given

$$SSE_{5lic}(a5lic\_guess, b5lic\_guess, c5lic\_guess) = 0$$

$$1 = 1$$

$$1 = 1$$

$$\begin{pmatrix} a5lic\_fit \\ b5lic\_fit \\ c5lic\_fit \end{pmatrix} = \text{Minerr}(a5lic\_guess, b5lic\_guess, c5lic\_guess)$$

-----

$$a5lic\_fit = 2.8631$$

$$b5lic\_fit = -4.2491$$

$$c5lic\_fit = 0.8387$$

Compute the residual error, ERR, given by  $ERR = SSE_{5lic}(a5lic\_fit, b5lic\_fit, c5lic\_fit)$ .

$$ERR = 0.0073$$

Hydrophilic SensorNon-Linear Regression Analysis of  $\alpha_{Im}$  vs  $M_f$ 

$$SSE_{6hc}(a,b,c) = \frac{1}{N_{6hc}} \sum_{k_{6hc}} (\alpha_{Im_{k_{6hc}}} - G(a,b,c, M_{f_{6hc}}))^2$$

Enter guess values for a,b and c.

a<sub>6hc</sub>\_guess = 1

b<sub>6hc</sub>\_guess = -0.1

c<sub>6hc</sub>\_guess = 1

----- Mathcad Solve Block -----

Given

$$SSE_{6hc}(a_{6hc\_guess}, b_{6hc\_guess}, c_{6hc\_guess}) = 0$$

$$1 = 1$$

$$1 = 1$$

$$\begin{pmatrix} a_{6hc\_fit} \\ b_{6hc\_fit} \\ c_{6hc\_fit} \end{pmatrix} = \text{Minerr}(a_{6hc\_guess}, b_{6hc\_guess}, c_{6hc\_guess})$$

-----

$$a_{6hc\_fit} = 2.3159$$

$$b_{6hc\_fit} = -5.7621$$

$$c_{6hc\_fit} = 0.0354$$

Compute the residual error, ERR, given by  $ERR = SSE_{6hc}(a_{6hc\_fit}, b_{6hc\_fit}, c_{6hc\_fit})$ .

$$ERR = 6.7774 \cdot 10^{-4}$$

Hydrophilic SensorNon-Linear Regression Analysis of  $|\alpha|$  vs  $M_F$ 

$$SSE_{7hc}(a,b,c) = \frac{1}{N_{7hc}} \sum_{k_{7hc}} (\alpha_{Mag_{7hc}_{k_{7hc}}} - G(a,b,c, MF_{7hc}_{k_{7hc}}))^2$$

Enter guess values for a, b and c.

a<sub>7hc\_guess</sub> = 1

b<sub>7hc\_guess</sub> = 0.1

c<sub>7hc\_guess</sub> = 1

----- Mathcad Solve Block -----  
Given

$$SSE_{7hc}(a_{7hc\_guess}, b_{7hc\_guess}, c_{7hc\_guess}) = 0$$

$$1 = 1$$

$$1 = 1$$

$$\begin{pmatrix} a_{7hc\_fit} \\ b_{7hc\_fit} \\ c_{7hc\_fit} \end{pmatrix} = \text{Minerr}(a_{7hc\_guess}, b_{7hc\_guess}, c_{7hc\_guess})$$

-----

$$a_{7hc\_fit} = 3.473$$

$$b_{7hc\_fit} = -4.8874$$

$$c_{7hc\_fit} = 0.8714$$

Compute the residual error, ERR, given by  $ERR = SSE_{7hc}(a_{7hc\_fit}, b_{7hc\_fit}, c_{7hc\_fit})$ .

$$ERR = 0.0089$$

Hydrophilic SensorNon-Linear Regression Analysis of  $\theta_{\alpha}$  vs  $M_f$ 

$$SSE_{8hc}(a,b,c) = \frac{1}{N_{8hc}} \sum_{k_{8hc}} (\theta_{8hc_{k_{8hc}}} - \text{deg}(a,b,c, M_{8hc_{k_{8hc}}}))^2$$

Enter guess values for a,b and c.

a8hc\_guess = 1

b8hc\_guess = -0.1

c8hc\_guess = 1

----- Mathcad Solve Block -----  
Given

$$SSE_{8hc}(a8hc\_guess, b8hc\_guess, c8hc\_guess) = 0$$

$$1 = 1$$

$$1 = 1$$

$$\begin{pmatrix} a8hc\_fit \\ b8hc\_fit \\ c8hc\_fit \end{pmatrix} = \text{Minerr}(a8hc\_guess, b8hc\_guess, c8hc\_guess)$$

$$a8hc\_fit = 1.0236$$

$$b8hc\_fit = 0.9586$$

$$c8hc\_fit = 0.5074$$

Compute the residual error, ERR, given by  $ERR = SSE_{8hc}(a8hc\_fit, b8hc\_fit, c8hc\_fit)$ .

$$ERR = 7.0692 \cdot 10^{-4}$$

Hydrophobic SensorNon-Linear Regression Analysis of  $\alpha_{Re}$  vs  $M_F$ 

$$SSE5bic(a,b,c) = \frac{1}{N_{bic}} \sum_{kbic} \left( \alpha_{Rebic_{kbic}} - G(a,b,c, MFbic_{kbic}) \right)^2$$

Enter guess values for a,b and c.

a5bic\_guess = 1

b5bic\_guess = 2

c5bic\_guess = 1

----- Mathcad Solve Block -----

Given

$$SSE5bic(a5bic\_guess, b5bic\_guess, c5bic\_guess) = 0$$

$$1 = 1$$

$$1 = 1$$

$$\begin{pmatrix} a5bic\_fit \\ b5bic\_fit \\ c5bic\_fit \end{pmatrix} = \text{Minerr}(a5bic\_guess, b5bic\_guess, c5bic\_guess)$$

$$a5bic\_fit = 2.2309$$

$$b5bic\_fit = -4.378$$

$$c5bic\_fit = 0.7751$$

Compute the residual error, ERR, given by  $ERR = SSE5bic(a5bic\_fit, b5bic\_fit, c5bic\_fit)$ .

$$ERR = 0.0022$$

Hydrophobic SensorNon-Linear Regression Analysis of  $\alpha_{Im}$  vs  $M_f$ 

$$SSE_{6bic}(a,b,c) = \frac{1}{N_{bic}} \sum_{k_{bic}} \left( \alpha_{Im_{k_{bic}}} - G(a,b,c, M_{f_{k_{bic}}}) \right)^2$$

Enter guess values for a,b and c.

a6bic\_guess = 1

b6bic\_guess = -0.1

c6bic\_guess = 1

----- Mathcad Solve Block -----  
Given

$$SSE_{6bic}(a6bic\_guess, b6bic\_guess, c6bic\_guess) = 0$$

$$1 = 1$$

$$1 = 1$$

$$\begin{pmatrix} a6bic\_fit \\ b6bic\_fit \\ c6bic\_fit \end{pmatrix} = \text{Minerr}(a6bic\_guess, b6bic\_guess, c6bic\_guess)$$

-----  
a6bic\_fit = 1.5698  
b6bic\_fit = -5.2243  
c6bic\_fit = 0.1297

Compute the residual error, ERR, given by ERR =  
SSE<sub>6bic</sub>(a6bic\_fit, b6bic\_fit, c6bic\_fit).

$$ERR = 3.1137 \cdot 10^{-4}$$

Hydrophobic SensorNon-Linear Regression Analysis of  $|\alpha|$  vs  $M_F$ 

$$SSE7bic(a,b,c) = \frac{1}{N_{bic}} \sum_{kbic} \left( \alpha_{Magbic_{kbic}} - G(a,b,c, MF_{bic_{kbic}}) \right)^2$$

Enter guess values for a, b and c.

a7bic\_guess 1

b7bic\_guess 2

c7bic\_guess 1

----- Mathcad Solve Block -----  
Given

$$SSE7bic(a7bic\_guess, b7bic\_guess, c7bic\_guess) = 0$$

$$l = 1$$

$$l = 1$$

$$\begin{pmatrix} a7bic\_fit \\ b7bic\_fit \\ c7bic\_fit \end{pmatrix} = \text{Minerr}(a7bic\_guess, b7bic\_guess, c7bic\_guess)$$

-----

$$a7bic\_fit = 2.5396$$

$$b7bic\_fit = -4.8354$$

$$c7bic\_fit = 0.793$$

Compute the residual error, ERR, given by  $ERR = SSE7bic(a7bic\_fit, b7bic\_fit, c7bic\_fit)$ .

$$ERR = 0.0024$$



Hydrophobic SensorNon-Linear Regression Analysis of  $\theta_{\alpha}$  vs  $M_f$ 

$$SSE8bic(a,b,c) = \frac{1}{N_{bic}} \sum_{kbic} (\theta_{\alpha bic_{kbic}} \cdot deg - G(a,b,c, Mf_{bic_{kbic}}))^2$$

Enter guess values for a,b and c.

a8bic\_guess = 1

b8bic\_guess = 2

c8bic\_guess = 1

----- Mathcad Solve Block -----

Given

$$SSE8bic(a8bic\_guess, b8bic\_guess, c8bic\_guess) = 0$$

$$| = 1$$

$$| = 1$$

$$\begin{pmatrix} a8bic\_fit \\ b8bic\_fit \\ c8bic\_fit \end{pmatrix} = \text{Minerr}(a8bic\_guess, b8bic\_guess, c8bic\_guess)$$

-----

$$a8bic\_fit = 0.7646$$

$$b8bic\_fit = -1.7386$$

$$c8bic\_fit = 0.3113$$

Compute the residual error, ERR, given by  $ERR = SSE8bic(a8bic\_fit, b8bic\_fit, c8bic\_fit)$ .

$$ERR = 4.1297 \cdot 10^{-4}$$

Plot the fitted and experimental data for  $\alpha_{Re}$ ,  $\alpha_{Im}$ ,  $|\alpha|$  and  $\theta_{\alpha}$  versus  $v$  and  $M_f$ .

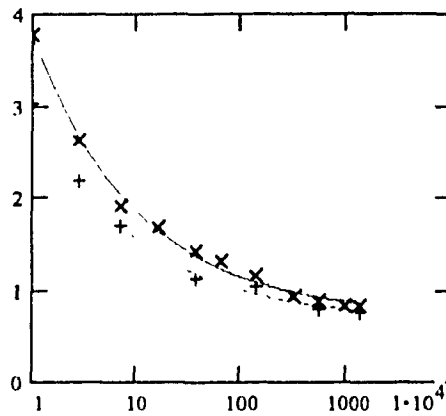
Plot  $\alpha_{pe}$ ,  $\alpha_{Im}$ ,  $|\alpha|$  and  $\theta_{\alpha}$  versus  $v$  and  $M_f$  for the hydrophilic and hydrophobic sensor.

$v$  10 cS, 20 cS 1400 cS

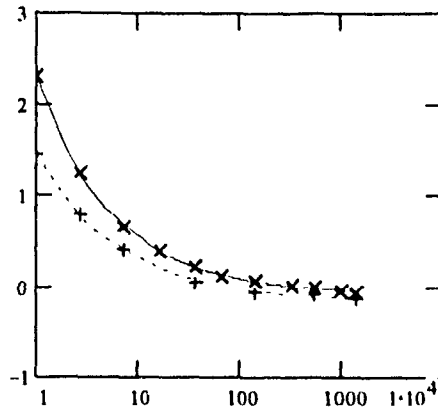
$M_f$  0,001 1

Hydrophilic and Hydrophobic Sensor

Plot of  $\alpha_{Re}$  versus  $v$  (Hydrophilic and Hydrophobic Sensor)

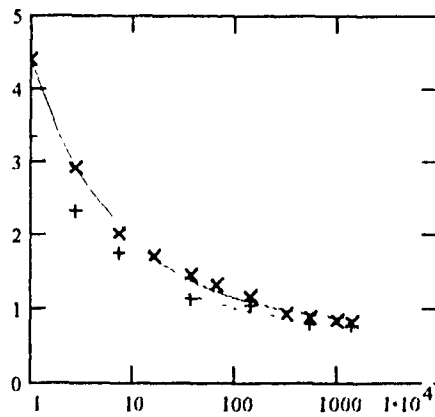


- × Hydrophilic Sensor (Experimental Curve)
- Hydrophilic Sensor (Fitted Curve)
- + Hydrophobic Sensor (Experimental Curve)
- - Hydrophobic Sensor (Fitted Curve)

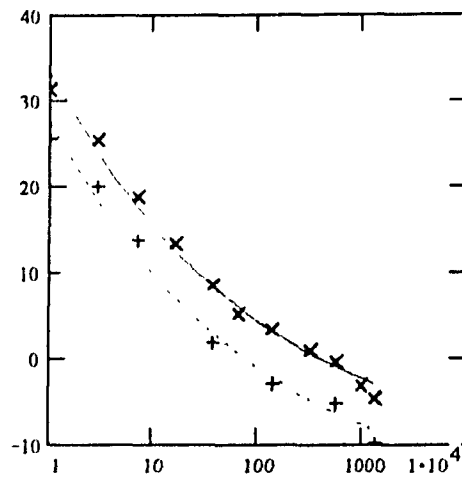


- x Hydrophilic Sensor (Experimental Curve)
- Hydrophilic Sensor (Fitted Curve)
- + Hydrophobic Sensor (Experimental Curve)
- - Hydrophobic Sensor (Fitted Curve)

Plot of  $|\alpha|$  versus  $v$  (Hydrophilic and Hydrophobic Sensor)

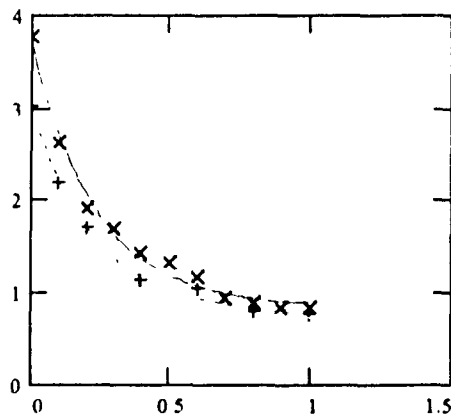


- x Hydrophilic Sensor (Experimental Curve)
- Hydrophilic Sensor (Fitted Curve)
- + Hydrophobic Sensor (Experimental Curve)
- - Hydrophobic Sensor (Fitted Curve)

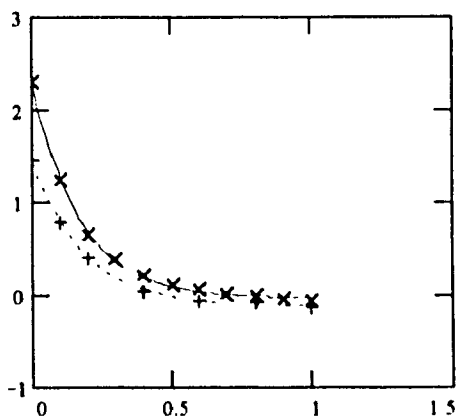


- × Hydrophilic Sensor (Experimental Curve)
- Hydrophilic Sensor (Fitted Curve)
- + Hydrophobic Sensor (Experimental Curve)
- - Hydrophobic Sensor (Fitted Curve)

Plot of  $\alpha_{Re}$  versus  $M_f$  (Hydrophilic and Hydrophobic Sensor)

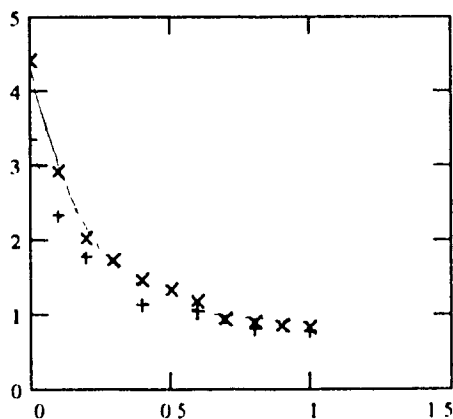


- × Hydrophilic Sensor (Experimental Curve)
- Hydrophilic Sensor (Fitted Curve)
- + Hydrophobic Sensor (Experimental Curve)
- - Hydrophobic Sensor (Fitted Curve)

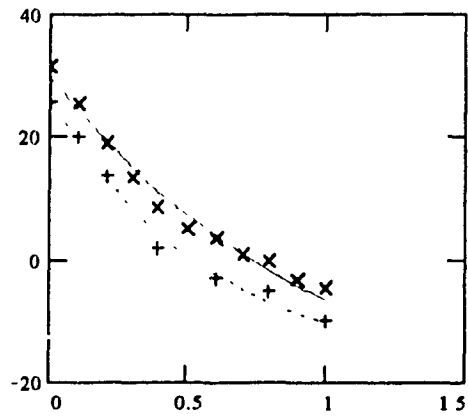


- × Hydrophilic Sensor (Experimental Curve)
- Hydrophilic Sensor (Fitted Curve)
- + Hydrophobic Sensor (Experimental Curve)
- - Hydrophobic Sensor (Fitted Curve)

Plot of  $|\alpha|$  versus  $M_f$  (Hydrophilic and Hydrophobic Sensor)



- × Hydrophilic Sensor (Experimental Curve)
- Hydrophilic Sensor (Fitted Curve)
- + Hydrophobic Sensor (Experimental Curve)
- - Hydrophobic Sensor (Fitted Curve)

Plot of  $\theta_{\alpha}$  versus  $M_F$  (Hydrophilic and Hydrophobic Sensor)

- × Hydrophilic Sensor (Experimental Curve)
- Hydrophilic Sensor (Fitted Curve)
- + Hydrophobic Sensor (Experimental Curve)
- Hydrophobic Sensor (Fitted Curve)

**APPENDIX 8 Particle Displacement of Sensor in Liquid,  
Mathcad Program DOC5.MCD**

**Numerical Solution of the Maximum Values of the Real Part of  $u_x$  and  $u_{(1)x}$  Versus Kinematic Viscosity,  $\nu$ , for the Hydrophilic and Hydrophobic Sensor in Water-Glycerol Solution**

The maximum value of the real part of the liquid particle displacement,  $u_{(1)x}$ , and the quartz particle displacement,  $u_x$ , will be computed at the interface over the time interval,  $I=[0,5/f_0]$  for the hydrophilic and hydrophobic sensor.

The following seventeen complex-valued expressions constitute the expression for the particle displacement,  $u_x$ , of the quartz sensor.

$$cbar = c + \frac{c^2}{\epsilon}$$

$$\delta(\eta, \omega) = \eta \cdot \omega - j \cdot cbar$$

$$kq(\eta, \omega) = \omega \sqrt{\frac{\rho q}{cbar + j \omega \eta}}$$

$$kl(\nu, \omega) = \sqrt{\frac{\omega}{j \nu}}$$

$$\gamma_1(\eta, h, \omega) = \exp(j \cdot h \cdot kq(\eta, \omega))$$

$$\gamma_2(\nu, h, \omega) = \exp(j \cdot h \cdot kl(\nu, \omega))$$

$$\lambda_1(\eta, h, \omega) = \gamma_1(\eta, h, \omega) - 1$$

$$\lambda_2(\eta, h, \omega) = \gamma_1(\eta, h, \omega) + 1$$

$$\lambda_3(\eta, h, \omega) = \gamma_1(\eta, h, \omega)^2 + 1$$

$$b_{11}(\eta, h, \omega) = -2 \cdot \delta(\eta, \omega) \cdot \epsilon \cdot \lambda_1(\eta, h, \omega) \cdot \gamma_1(\eta, h, \omega) \cdot kq(\eta, \omega) \cdot \phi_0$$

$$b_{12}(\eta, \nu, \rho l, h, \omega) = -2 \cdot \epsilon \cdot \epsilon \cdot \gamma_1(\eta, h, \omega)^2 \cdot kl(\nu, \omega) \cdot \nu \cdot \omega \cdot \phi_0 \cdot \rho l$$

$$b_{13}(\eta, h, \omega) = \delta(\eta, \omega) \cdot \lambda_1(\eta, h, \omega) \cdot kq(\eta, \omega) \left( \begin{array}{l} \delta(\eta, \omega) \cdot \epsilon \cdot \lambda_2(\eta, h, \omega) \cdot h \cdot kq(\eta, \omega) \\ + 2 \cdot \epsilon^2 \cdot \lambda_1(\eta, h, \omega) \end{array} \right)$$

$$b_{14}(\eta, \nu, \rho l, h, \omega) = kl(\nu, \omega) \left( \begin{array}{l} \delta(\eta, \omega) \cdot \epsilon \cdot \lambda_3(\eta, h, \omega) \cdot h \cdot kq(\eta, \omega) \\ + \epsilon^2 \cdot \lambda_1(\eta, h, \omega) \cdot \lambda_2(\eta, h, \omega) \end{array} \right) \cdot \nu \cdot \omega \cdot \rho l$$

$$b_{21}(\eta, h, \omega) = 2 \cdot \delta(\eta, \omega) \cdot e \cdot \epsilon \lambda_1(\eta, h, \omega) k_q(\eta, \omega) \cdot \phi_0$$

$$b_{22}(\eta, v, \rho_l, h, \omega) = 2 e \epsilon k_l(v, \omega) \cdot v \cdot \omega \cdot \rho_l \cdot \phi_0$$

$$a_1(\eta, v, \rho_l, \alpha, h, \omega) = \left( \frac{\alpha b_{12}(\eta, v, \rho_l, h, \omega) + b_{11}(\eta, h, \omega)}{\alpha b_{14}(\eta, v, \rho_l, h, \omega) + b_{13}(\eta, h, \omega)} \right)$$

$$a_2(\eta, v, \rho_l, \alpha, h, \omega) = \left( \frac{\alpha b_{22}(\eta, v, \rho_l, h, \omega) + b_{21}(\eta, h, \omega)}{\alpha b_{14}(\eta, v, \rho_l, h, \omega) + b_{13}(\eta, h, \omega)} \right)$$

The particle displacement,  $u_x$ , of the quartz sensor at the solid-liquid interface is.

$$u_x(\eta, v, \rho_l, \alpha, h, \omega, t) = \left( a_1(\eta, v, \rho_l, \alpha, h, \omega) \cdot \exp(-j \cdot k_q(\eta, \omega) \cdot h) \dots \right) \cdot \exp(j \cdot \omega \cdot t) \\ + a_2(\eta, v, \rho_l, \alpha, h, \omega) \cdot \exp(j \cdot k_q(\eta, \omega) \cdot h)$$

From the slip boundary condition, the liquid particle displacement,  $u_{(l)x}$ , at the solid-liquid interface is.

$$u_{lx}(\eta, v, \rho_l, \alpha, h, \omega, t) = \alpha u_x(\eta, v, \rho_l, \alpha, h, \omega, t)$$

#### Data for Hydrophilic and Hydrophobic Sensor

Enter numerical value for the mass density of quartz.

$$\rho_q = 2649 \frac{\text{kg}}{\text{m}^3}$$

Enter numerical value for the elastic coefficient of quartz.

$$c = 2901 \cdot 10^9 \frac{\text{newton}}{\text{m}^2}$$

Enter numerical value for the best-fit piezoelectric stress coefficient of quartz.

$$e = -0.0798007 \frac{\text{coul}}{\text{m}^2}$$

Enter numerical values for the best-fit viscoelastic coefficient of quartz.

$$\eta_{lic\_fit} = 0.0083762 \text{ newton} \frac{\text{sec}}{\text{m}^2}$$

$$\eta_{bic\_fit} = 0.2344606 \text{ newton} \frac{\text{sec}}{\text{m}^2}$$



Enter numerical values for the best-fit thickness.

$$h_{lc\_fit} = 183.8790101 \mu\text{m}$$

$$h_{bc\_fit} = 183.9794329 \mu\text{m}$$

Enter numerical value for the dielectric constant of quartz.

$$\epsilon = 39.8210 \frac{12 \text{ coul}}{\text{volt m}}$$

#### Water-Glycerol Solution for Hydrophilic Sensor

Read in data array  $v_{lc}$  for kinematic viscosity,  $\nu$ , an array of eleven values of  $\nu$ .

$$v_{lc} = \text{READPRN}(\text{NULIC}) \text{ cS}$$

Read in data array  $\rho_{lc}$  for kinematic viscosity,  $\rho$ , an array of eleven values of  $\rho$ .

$$\rho_{lc} = \text{READPRN}(\text{RHOLIC}) \frac{\text{kg}}{\text{liter}}$$

Read in data array  $\alpha_{lc}$  for interfacial slip parameter,  $\alpha$ , an array of eleven values of  $\alpha$ .

$$\alpha_{lc} = \text{READPRN}(\text{ALPLIC})$$

$$\alpha_{lc} = \alpha_{lc}^{<1>} \cdot j \alpha_{lc}^{<2>}$$

#### Water-Glycerol Solution for Hydrophobic Sensor

Read in data array  $v_{bc}$  for kinematic viscosity,  $\nu$ , an array of eleven values of  $\nu$ .

$$v_{bc} = \text{READPRN}(\text{NUBIC}) \text{ cS}$$

Read in data array  $\rho_{bc}$  for kinematic viscosity,  $\rho$ , an array of eleven values of  $\rho$ .

$$\rho_{bc} = \text{READPRN}(\text{RHOBIC}) \frac{\text{kg}}{\text{liter}}$$

Read in data array  $\alpha_{bc}$  for interfacial slip parameter,  $\alpha$ , an array of seven values of  $\alpha$ .

$$\alpha_{bc} = \text{READPRN}(\text{ALPBIC})$$

$$\alpha_{bc} = \alpha_{bc}^{<1>} \cdot j \alpha_{bc}^{<2>}$$

Using the nominal resonant frequency,  $f_0$ , of the quartz sensor, compute  $u_x(h,t)$  and  $u_{(1)x}(h,t)$  over the time interval  $[0, 5/f_0]$ .

Enter numerical value for nominal resonant frequency,  $f_0$ .  $f_0 = 90 \text{ MHz}$

The corresponding angular frequency,  $\omega_0$ , is given by.  $\omega_0 = 2\pi \cdot f_0$

Enter starting value for the time  $t$ ,  $t_s$ .  $t_s = 0 \text{ sec}$

Enter terminal value for the time  $t$ ,  $t_f$ .  $t_f = \frac{5}{f_0}$   $t_f = 0.556 \cdot \mu\text{sec}$

Enter numerical value for the time step  $\Delta t$ .  $\Delta t = 0.001 \cdot \mu\text{sec}$

The number of data points,  $N$ , is.  $N = \text{floor}\left(\frac{t_f - t_s}{\Delta t}\right)$   $N = 555$

In the above expression for  $N$ , Mathcad's floor function, converts a real number into the smallest integer corresponding to that real number.

The range variable,  $i$ , takes on integral values from 1 to  $N$  inclusive.

$$i = 1 \text{ } N$$

Generate a partition of  $N$  equally spaced time points,  $t_i$ , each of width  $\Delta t$ .

$$t_1 = t_s$$

$$t_{i+1} = t_i + \Delta t$$

$$t_N = t_f$$

Hydrophilic Sensor

Compute the real part of  $u_x$  and  $u_{(1)x}$  over the time interval  $[0, 5/f_0]$  for each  $i=1, \dots, N$  and  $klic=1, \dots, 11$ .

$klic = 1 \ 11$

$$uxRe\_hydrophilic_{i,klic} = \text{Re}\left(ux\left(\eta_{lic\_fit}, v_{lic\_klic}, \rho_{lic\_klic}, \alpha_{lic\_klic}, h_{lic\_fit}, \omega, t_i\right)\right)$$

$$ulxRe\_hydrophilic_{i,klic} = \text{Re}\left(ulx\left(\eta_{lic\_fit}, v_{lic\_klic}, \rho_{lic\_klic}, \alpha_{lic\_klic}, h_{lic\_fit}, \omega, t_i\right)\right)$$

Using Mathcad's max function, compute the maximum values of the real parts of  $u_x$  and  $u_{(1)x}$  over the time interval  $[0, 5/f_0]$  for each  $klic=1, \dots, 11$ .

$$uxmax\_lic_{klic} = \max(uxRe\_hydrophilic^{<klic>})$$

$$ulxmax\_lic_{klic} = \max(ulxRe\_hydrophilic^{<klic>})$$

Store the one-dimensional arrays  $uxmax\_lic$  and  $ulxmax\_lic$  in the respective data files  $UXMAXLIC.PRN$  and  $ULMAXLIC.PRN$ .

$$\text{WRITEPRN}(UXMAXLIC) = \text{augment}\left(\begin{array}{l} v_{lic} \ uxmax\_lic \\ cS \ ' \ \text{angstrom} \end{array}\right)$$

$$\text{WRITEPRN}(ULMAXLIC) = \text{augment}\left(\begin{array}{l} v_{lic} \ ulxmax\_lic \\ cS \ ' \ \text{angstrom} \end{array}\right)$$

Hydrophobic Sensor

Compute the real part of  $u_x$  and  $u_{(1)x}$  over the time interval  $[0, 5/f_0]$  for each  $i=1, \dots, N$  and  $kbic=1, \dots, 7$ .

$kbic = 1..7$

$$uxRe\_hydrophobic_{i,kbic} = \text{Re}\left(ux\left(\eta_{bic\_fit}, vbic_{kbic}, \rho_{bic_{kbic}}, \alpha_{bic_{kbic}}, h_{bic\_fit}, \omega, t_i\right)\right)$$

$$ulxRe\_hydrophobic_{i,kbic} = \text{Re}\left(ulx\left(\eta_{bic\_fit}, vbic_{kbic}, \rho_{bic_{kbic}}, \alpha_{bic_{kbic}}, h_{bic\_fit}, \omega, t_i\right)\right)$$

Using Mathcad's max function, compute the maximum values of the real parts of  $u_x$  and  $u_{(1)x}$  over the time interval  $[0, 5/f_0]$  for each  $kbic=1, \dots, 7$ .

$$uxmax\_bic_{kbic} = \max\left(uxRe\_hydrophobic^{<kbic>}\right)$$

$$ulxmax\_bic_{kbic} = \max\left(ulxRe\_hydrophobic^{<kbic>}\right)$$

Store the one-dimensional arrays  $uxmax\_bic$  and  $ulxmax\_bic$  in the respective data files UXMAXBIC.PRN and ULMAXBIC.PRN.

$$\text{WRITEPRN}(UXMAXBIC) = \text{augment}\left(\frac{vbic}{cS}, \frac{uxmax\_bic}{\text{angstrom}}\right)$$

$$\text{WRITEPRN}(ULMAXBIC) = \text{augment}\left(\frac{vbic}{cS}, \frac{ulxmax\_bic}{\text{angstrom}}\right)$$

For the case of the hydrophilic and hydrophobic sensors immersed in pure water, store the data for the real part of  $u_x$  and  $u_{(1)x}$  versus the time  $t$  in the respective data files UXRELIC.PRN, UXREBIC.PRN, ULRELIC.PRN and ULREBIC.PRN.

$$\text{WRITEPRN}(UXRELIC) = \text{augment}\left(\frac{tt}{\mu\text{sec}}, \frac{uxRe\_hydrophilic^{<1>}}{\text{angstrom}}\right)$$

$$\text{WRITEPRN}(UXREBIC) = \text{augment}\left(\frac{tt}{\mu\text{sec}}, \frac{uxRe\_hydrophobic^{<1>}}{\text{angstrom}}\right)$$

$$\text{WRITEPRN}(ULRELIC) = \text{augment}\left(\frac{tt}{\mu\text{sec}}, \frac{ulxRe\_hydrophilic^{<1>}}{\text{angstrom}}\right)$$

$$\text{WRITEPRN}(ULREBIC) = \text{augment}\left(\frac{tt}{\mu\text{sec}}, \frac{ulxRe\_hydrophobic^{<1>}}{\text{angstrom}}\right)$$

Use the power law model  $F(a,b,c,x) = ax^b + c$  to fit the data consisting of  $uxmax\_lic$ ,  $uxmax\_bic$ ,  $ulxmax\_lic$  and  $ulxmax\_bic$ .

$$F(a,b,c,x) = ax^b + c$$

The following Sum Of Squares Of Errors,  $SSEUXLIC(a,b,c)$ ,  $SSEULXLIC(a,b,c)$ ,  $SSEUXBIC(a,b,c)$  and  $SSEULXBIC(a,b,c)$  will be used in the following non-linear curve-fitting procedure.

$$SSEUXLIC(a,b,c) = \frac{1}{11} \sum_{klic} \left( \frac{uxmax\_lic_{klic}}{angstrom} - F\left(a, b, c, \frac{vlic_{klic}}{cS}\right) \right)^2$$

$$SSEULXLIC(a,b,c) = \frac{1}{11} \sum_{klic} \left( \frac{ulxmax\_lic_{klic}}{angstrom} - F\left(a, b, c, \frac{vlic_{klic}}{cS}\right) \right)^2$$

$$SSEUXBIC(a,b,c) = \frac{1}{7} \sum_{kbic} \left( \frac{uxmax\_bic_{kbic}}{angstrom} - F\left(a, b, c, \frac{vbic_{kbic}}{cS}\right) \right)^2$$

$$SSEULXBIC(a,b,c) = \frac{1}{7} \sum_{kbic} \left( \frac{ulxmax\_bic_{kbic}}{angstrom} - F\left(a, b, c, \frac{vbic_{kbic}}{cS}\right) \right)^2$$

To start the non-linear curve-fitting procedure, enter guess values for a, b and c.

Enter guess value for a.      `aguessux_lic = 14`

Enter guess value for b.      `bguessux_lic = -0.2`

Enter guess value for c.      `cguessux_lic = -1.4`

----- Mathcad Solve Block -----

Given

$$\text{SSEUXLIC}(\text{aguessux\_lic}, \text{bguessux\_lic}, \text{cguessux\_lic}) = 0$$

$$1 = 1$$

$$1 = 1$$

$$\begin{pmatrix} \text{afitux\_lic} \\ \text{bfitux\_lic} \\ \text{cfitux\_lic} \end{pmatrix} = \text{Minerr}(\text{aguessux\_lic}, \text{bguessux\_lic}, \text{cguessux\_lic})$$

-----

The result of the Solve Block, `afitux_lic`, `bfitux_lic` and `cfitux_lic` is.

$$\text{afitux\_lic} = 14.523$$

$$\text{bfitux\_lic} = -0.246$$

$$\text{cfitux\_lic} = -1.529$$

Compute the residual error, `ERR`, given by `ERR = SSEUXLIC(afitux_lic, bfitux_lic, cfitux_lic)`.

$$\text{ERR} = 0.057$$

To start the non-linear curve-fitting procedure, enter guess values for a, b and c.

Enter guess value for a.      `aguessulx_lic = 56`

Enter guess value for b.      `bguessulx_lic = -0.6`

Enter guess value for c.      `cguessulx_lic = 0.5`

----- Mathcad Solve Block -----

Given

$$\text{SSEULXLIC}(\text{aguessulx\_lic}, \text{bguessulx\_lic}, \text{cguessulx\_lic}) = 0$$

$$1 = 1$$

$$1 = 1$$

$$\begin{pmatrix} \text{afitulx\_lic} \\ \text{bfitulx\_lic} \\ \text{cfitulx\_lic} \end{pmatrix} = \text{Minerr}(\text{aguessulx\_lic}, \text{bguessulx\_lic}, \text{cguessulx\_lic})$$

-----

The result of the Solve Block, `afitulx_lic`, `bfitulx_lic` and `cfitulx_lic` is.

$$\text{afitulx\_lic} = 56.032$$

$$\text{bfitulx\_lic} = 0.649$$

$$\text{cfitulx\_lic} = 0.577$$

Compute the residual error, ERR, given by  $\text{ERR} = \text{SSEULXLIC}(\text{afitulx\_lic}, \text{bfitulx\_lic}, \text{cfitulx\_lic})$ .

$$\text{ERR} = 0.036$$

To start the non-linear curve-fitting procedure, enter guess values for a, b and c.

Enter guess value for a.      `aguessux_bic = 18`

Enter guess value for b.      `bguessux_bic = -0.04`

Enter guess value for c.      `cguessux_bic = -11`

----- Mathcad Solve Block -----

Given

$$\text{SSEUXBIC}(\text{aguessux\_bic}, \text{bguessux\_bic}, \text{cguessux\_bic}) = 0$$

$$| = |$$

$$| = |$$

$$\begin{pmatrix} \text{afitux\_bic} \\ \text{bfitux\_bic} \\ \text{cfitux\_bic} \end{pmatrix} = \text{Minerr}(\text{aguessux\_bic}, \text{bguessux\_bic}, \text{cguessux\_bic})$$

-----  
The result of the Solve Block, `afitux_bic`, `bfitux_bic` and `cfitux_bic` is.

$$\text{afitux\_bic} = 19.311$$

$$\text{bfitux\_bic} = -0.081$$

$$\text{cfitux\_bic} = -10.043$$

Compute the residual error, ERR, given by  $\text{ERR} = \text{SSEUXBIC}(\text{afitux\_bic}, \text{bfitux\_bic}, \text{cfitux\_bic})$ .

$$\text{ERR} = 0.051$$



To start the non-linear curve-fitting procedure, enter guess values for a, b and c.

Enter guess value for a.       $aguess_{x\_bic} = 34$

Enter guess value for b.       $bguess_{x\_bic} = -0.5$

Enter guess value for c.       $cguess_{x\_bic} = 0.3$

----- Mathcad Solve Block -----

Given

$$SSEULXBIC(aguess_{x\_bic}, bguess_{x\_bic}, cguess_{x\_bic}) = 0$$

$$1 = 1$$

$$1 = 1$$

$$\begin{pmatrix} afitulx\_bic \\ bfitulx\_bic \\ cfitulx\_bic \end{pmatrix} = \text{Minerr}(aguess_{x\_bic}, bguess_{x\_bic}, cguess_{x\_bic})$$

-----

The result of the Solve Block,  $afitulx\_bic$ ,  $bfitulx\_bic$  and  $cfitulx\_bic$  is.

$$afitulx\_bic = 31.284$$

$$bfitulx\_bic = 0.536$$

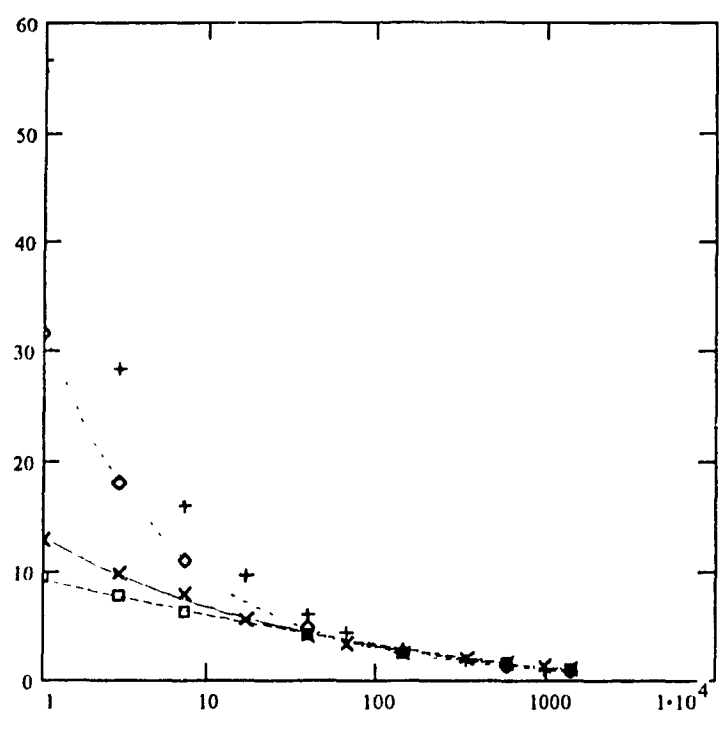
$$cfitulx\_bic = 0.308$$

Compute the residual error, ERR, given by  $ERR = SSEULXBIC(afitulx\_bic, bfitulx\_bic, cfitulx\_bic)$ .

$$ERR = 0.01$$

Plot of the maximum displacement of the real part of  $u_x$  and  $u_{(1)x}$  versus  $n$  for the hydrophilic and hydrophobic sensor.

$\times 10, 2.1400$



- × Maximum displacement of the real part of  $u_x$ , hydrophilic
- Fitted Curve
- + Maximum displacement of the real part of  $u_{(1)x}$ , hydrophilic
- Fitted Curve
- Maximum displacement of the real part of  $u_x$ , hydrophobic
- Fitted Curve
- ◇ Maximum displacement of the real part of  $u_{(1)x}$ , hydrophobic
- Fitted Curve

**APPENDIX 9          Numerical Solution of Interfacial Slip Model,  
Mathcad Program DOC6.MCD**

**Numerical Solution of the Equation of Motion of Mass  $m_1$  using  
Runge-Kutta's Fourth Order Method.**

The numerical computation of the displacement,  $x_1$ , of mass  $m_1$  will be performed by using a fourth-order Runge-Kutta method. Using a semi-interactive method, the displacement  $x_1$ , will be computed over the time interval  $[0, 5/f]$ , for several values of the ratio of spring constant and mass of liquid particle,  $k/m_1$ , starting with  $10^2$  and ending with  $10^9$ . Using the above data for  $x_1$ , the maximum displacement of  $x_{1\max}$  will be computed for each value of  $k/m_1$ . The maximum displacement  $x_{1\max}$  is defined as the largest displacement of mass  $m_1$  in the time interval  $[0, 5/f]$ .

**Implementation of Runge-Kutta's Method Using Mathcad**

Let  $x_1(t)$  denote the displacement of the liquid particle of mass  $m_1$  from its equilibrium position at time  $t$ .

Let  $x_2(t)$  denote the displacement of the solid particle of mass  $m_2$  from its equilibrium position at time  $t$ .

Let  $v_1(t)$  denote the velocity of mass  $m_1$  at time  $t$ .

Let  $v_2(t)$  denote the velocity of mass  $m_2$  at time  $t$ .

Let  $l$  denote the length of the spring connecting masses  $m_1$  and  $m_2$ .

Let  $k$  denote the force constant of the spring.

Let  $A$  denote the amplitude of the displacement of mass  $m_2$ .

Let  $\phi$  denote the phase angle of the displacement of mass  $m_2$ .

STATEMENT OF PROBLEM

Given that  $x_2 = x_2(t) = A \cos(\omega t + \phi)$ , determine  $x_1 = x_1(t)$  numerically over the closed time interval  $[t_i, t_f]$ .

$x_1 = x_1(t)$  satisfies the following non-linear second-order differential equation.

$$\frac{d^2}{dt^2} x_1(t) = \frac{k}{m_1} \frac{\left[ \sqrt{(\Lambda \cos(\omega t + \phi) - x_1(t))^2 + l^2 - 1} \right] (\Lambda \cos(\omega t + \phi) - x_1(t))}{\sqrt{(\Lambda \cos(\omega t + \phi) - x_1(t))^2 + l^2}}$$

To determine  $x_1 = x_1(t)$  numerically, a Runge-Kutta method of stepsize  $\Delta t$  will be used.

Enter numerical value for the amplitude A of the displacement of mass  $m_2$ .

$$A = 1$$

Enter numerical value for the phase angle  $\phi$  of the displacement of mass  $m_2$ .

$$\phi = -\frac{\pi}{2}$$

Enter numerical value for the driving frequency f of mass  $m_2$ .

$$f = 9$$

The corresponding angular frequency  $\omega$  of mass  $m_2$  is given by.

$$\omega = 2\pi f$$

Enter initial value for the time t.  $t_i = 0$

Enter terminal value for the time t.  $t_f = \frac{5}{f}$

Enter time increment dt.  $dt = 0.001$

The number of time increments N is given by.  $N = \text{floor}\left(\frac{t_f - t_i}{dt}\right) \quad N = 555$

Enter initial values for the displacement and velocity of mass  $m_1$ .

Initial values...  $u^{<0>} = \begin{pmatrix} 0 \\ 0 \end{pmatrix}$  ...Initial displacement of mass  $m_1$ .  
 ...Initial velocity of mass  $m_1$ .

The derivative vector  $\mathbf{F}(t, \mathbf{u})$  is given by.

$$\mathbf{F}(t, \mathbf{u}) = \begin{pmatrix} u_1 \\ \frac{k}{m l} \frac{\left[ \sqrt{(A \cos(\omega t + \phi) - u_0)^2 + l^2} - l \right] (A \cos(\omega t + \phi) - u_0)}{\sqrt{(A \cos(\omega t + \phi) - u_0)^2 + l^2}} \end{pmatrix}$$

The four functions  $K_1, K_2, K_3,$  and  $K_4$  implement the Runge-Kutta method.

$$K_1(t, \mathbf{u}, F, dt) = F(t, \mathbf{u})$$

$$K_2(t, \mathbf{u}, F, dt) = F\left(t + \frac{dt}{2}, \mathbf{u} + \frac{dt}{2} K_1(t, \mathbf{u}, F, dt)\right)$$

$$K_3(t, \mathbf{u}, F, dt) = F\left(t + \frac{dt}{2}, \mathbf{u} + \frac{dt}{2} K_2(t, \mathbf{u}, F, dt)\right)$$

$$K_4(t, \mathbf{u}, F, dt) = F(t + dt, \mathbf{u} + dt K_3(t, \mathbf{u}, F, dt))$$

The function RK computes the weighted average of the above four functions.

$$RK(t, \mathbf{u}, F, dt) = \frac{dt}{6} (K_1(t, \mathbf{u}, F, dt) + 2 K_2(t, \mathbf{u}, F, dt) + 2 K_3(t, \mathbf{u}, F, dt) + K_4(t, \mathbf{u}, F, dt))$$

For each  $i = 1, \dots, N$  compute the displacement,  $x_1$ , and velocity,  $v_1$ , of mass  $m_1$  at each time  $t_1$  using the recurrence relation given below.

$i = 1 \dots N$

$$t_i = t + (i - 1) \cdot dt$$

$$\mathbf{u}^{<i>} = \mathbf{u}^{<i-1>} + RK(t_{i-1}, \mathbf{u}^{<i-1>}, F, dt)$$

From the above recurrence relation,  $u_{(0,1)}$  and  $u_{(1,1)}$  correspond to  $x_1 = x_1(t_1)$  and  $v_1 = v_1(t_1)$  respectively.

The displacement of mass  $m_1$  at each  $t = t_1$  is given by.

$$x1_i = u_{0,i}$$

Compute the displacement of mass  $m_2$  at each  $t = t_1$ .

$$x2_i = A \cdot \cos(\omega t_i + \phi)$$

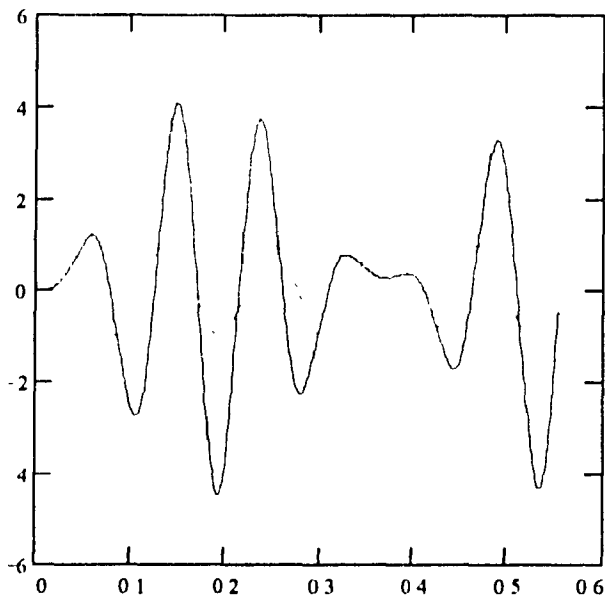
To initiate the numerical computation of  $x_1(t_i)$ , enter appropriate numerical values for the mass  $m_1$ , the length of the spring  $l$  and the force constant,  $k$ , of the spring.

Enter numerical value for mass  $m_1$ .  $m1=1$

Enter numerical value for the length  $l$  of the spring.  $l=1$

Enter numerical value for the force constant  $k$  of the spring.  $k=10^4$

Plot the displacements of masses  $m_1$  and  $m_2$  versus the time  $t$ .



— displacement of mass  $m_1$  versus time  
 - - - displacement of mass  $m_2$  versus time

### Numerical Computation Of $x_{1\max}$

The above mentioned semi-interactive method is described below.

Mathcad's **max** function will be used to compute  $x_{1\max}$  for each value of  $k$  in the interval  $[10^2, 10^9]$ . For  $k/m_1 = 10^2$  Mathcad's **WRITEPRN** function will store the first pair  $(\log(k/m_1), x_{1\max})$  in the data file X1MAX.PRN. Disabling the function **WRITEPRN**, Mathcad's function **APPENDPRN** will then append succeeding pairs  $(\log(k/m_1), x_{1\max})$  to the data file X1MAX.PRN for each value of  $k/m_1$ .

$$\text{WRITEPRN(X1MAX)} \begin{pmatrix} \log\left(\frac{k}{m_1}\right) \\ \max(x_1) \end{pmatrix}^T$$

$$\text{APPENDPRN(X1MAX)} \begin{pmatrix} \log\left(\frac{k}{m_1}\right) \\ \max(x_1) \end{pmatrix}^T$$

## REFERENCES

- Auld, B.A., *Acoustic Fields and Waves in Solids, Volume I*, Wiley, New York (1973).
- Auld, B.A., *Acoustic Fields and Waves in Solids, Volume II*, Wiley, New York (1973).
- Bottom, V.E., *Introduction to Quartz Crystal Unit Design*, Van Nostrand Reinhold, New York (1982).
- Cady, W.G., *Piezoelectricity*, Dover, New York (1964).
- Duncan-Hewitt, W.C. and Thompson, M., *Anal. Chem.*, **64**, 94-105, (1992).
- Eringen, A.C., *Mechanics of Continua*, Wiley, New York (1967).
- Eringen, A.C. and Maugin G.A., *Electrodynamics of Continua I (Foundations and Solid Media)*, Springer-Verlag, New York (1990).
- Hughes, W.F. Brighton, J.A., *Fluid Dynamics*, McGraw-Hill Schaum's Outline Series, New York (1967).
- Kipling, A.L. and Thompson, M., *Anal. Chem.*, **62**, 1514-1519, (1990).
- Kinsler, L.E., Frey, A.R., Coppens, A.B. and Sanders, J.V., *Fundamentals of Acoustics*, Wiley, New York, third edition (1982).
- Landau, L.D. and Lifshitz, E.M., *Fluid Mechanics*, Pergamon, New York, second edition (1987).
- Lide, D.R., *CRC Handbook of Chemistry and Physics*, CRC Press, Boca Raton, 71st edition (1990-1991).
- Lorrain, P., Corson, D.R. and Lorrain, F., *Electromagnetic Fields and Waves*, Freeman, New York, third edition (1988).
- Rajaković, L.V., Čavić-Vlasak, B.A., Ghaemmaghami, V., Kallury, K.M.R., Kipling, A.L. and Thompson, M., *Anal. Chem.*, **63**, 615-621, (1991).
- Schoenberg, M., *J. Acoust. Soc. Am.*, **68**(5), 1516-1521, (1980).
- Thompson, M., Kipling, A.L., Duncan-Hewitt, W.C., Rajaković, L.V. and Čavić-Vlasak, B.A., *Analyst*, **116**, 881-890, (1991).



Tiersten, H.F., *Linear Piezoelectric Plate Vibrations (Elements of the Linear Theory of Piezoelectricity and the Vibrations of Piezoelectric Plates)*, Plenum, New York (1969).

Reed, C.E., Kanazawa, K.K. and Kaufman, J.H., *J. Appl. Phys.*, **68**(5), 1993-2001, (1990).

Sauerbrey, G., *Z. Phys.*, **155**, 206-212, (1959).

Yuan, S.W., *Foundations of Fluid Mechanics*, Prentice-Hall, New Jersey (1967).